A conserved signalling network regulates *Epichloë festucae* cell-cell fusion and the mutualistic symbiotic interaction between *E. festucae* and *Lolium perenne.*

A thesis presented in partial fulfilment of the requirements for the degree of

Doctor of Philosophy (PhD) in

Genetics

at Massey University, Manawatu,

New Zealand.

Kimberly Anne Green

2016

Abstract

Epichloë festucae is a filamentous fungus that forms a mutually beneficial symbiotic association with *Lolium perenne*. The NADPH oxidase complex components *noxA, noxR* and *racA*, the transcription factor *proA*, and the cell wall integrity (CWI) MAP kinases, *mkkA* and *mpkA*, are required for mutualistic *E. festucae-L. perenne* associations and cell-cell fusion. Homologues of these genes in *Neurospora crassa, Sordaria macrospora* and *Podospora anserina* are required for cell-cell fusion and sexual fruiting body maturation, thereby establishing a link between self signalling and hyphal network formation in the *E. festucae-L. perenne* symbiosis. In *Podospora anserina,* IDC2 and IDC3 are required for cell-cell fusion, crippled growth and fruiting body formation. In *S. macrospora* and *N. crassa,* components of the STRIPAK complex regulate cell-cell fusion and fruiting body formation. The aim of this project was to test if *E. festucae* homologues of IDC2 and IDC3, and the STRIPAK complex protein MOB3, named SymB, SymC and MobC, respectively, are also required for cell-cell fusion and plant symbiosis. Gel shift assays showed the promoters of *symB* and *symC* are targets for the transcription factor ProA. In culture, the frequency of cell-cell fusion of Δ*mobC* was reduced, but in Δ*symB* and Δ*symC* mutants, totally abolished. All three mutants hyperconidiated and formed intra-hyphal hyphae. Plants infected with these mutants were severely stunted and hyphae exhibited proliferative growth and increased colonisation of the intercellular spaces and vascular bundles. Expressoria formation, structures allowing colonisation of the leaf surface, was reduced in Δ*mobC,* and abolished in Δ*symB* and Δ*symC* mutants. Microscopy analyses showed SymB-GFP and SymC-mRFP1 co-localise to the plasma membrane and septa. SymC also localised to highly dynamic punctate structures. Although Δ*symB* and Δ*symC* phenotypes are identical to Δ*mpkA,* and the *E. festucae* pheromone response pathway scaffold Δ*idcA* mutants, MpkA and MpkB phosphorylation and cellular localisation was unchanged compared to wild-type. Using yeast-two-hybrid assays, an interaction between SymC and the STRIPAK complex associated protein GPI1 was demonstrated. Collectively these results show that MobC, SymB and SymC are required for *E. festucae* cell-cell fusion and host symbiosis. It is proposed that SymB and SymC interact to form a sensor complex at the cell wall which regulates cell-cell fusion in culture and hyphal network development *in planta*.

Acknowledgements

To my supervisor, Professor Barry Scott, thanks for investing the time to create this project and for always providing invaluable feedback on every aspect of my research. I have learnt so much from you and have received every possible opportunity that I could have imagined. To my co-supervisor, Dr Yvonne Becker, thanks for putting up with my constant supply of questions and teaching me absolutely everything. You have shaped the researcher I am today. I consider myself lucky to have learnt from someone who has an endless supply of patience and willingness to teach. Also thanks to you and your family, Matthias, Finja and Mia, for hosting me in Germany. I really appreciated my time spent there and I am fortunate to have met you. To my co-supervisor, Dr Helen Fitzimons, thanks for being an integral part of this project. Your comments, suggestions and knowledge have significantly enhanced the progression of this research.

To Dr Philippe Silar and Dr Hervé Lalucque, thank you for providing the sequences of IDC2 and IDC3. Without these, this project would not have been possible. To Dr Aiko Tanaka and Dr Daigo Takemoto, thank you for your inputs on the SymB and SymC manuscript. To Dr Stephan Seiler, Dr Anne Dettmann and Dr Yvonne Heilig, thank you for hosting me in Germany. To Ulrike Brandt, thank you for doing the *N. crassa* C-terminal Yeast-2-hybrid library screen work. To Dr André Fleißner, thank you for your invaluable discussions on the SymB and SymC manuscript. To the past and present MMIC members, Doug, Jianyu, Jordan, Niki and Matthew, thanks for always producing the highest level of quality help, sample preparation and advice. To Ann, Cynthia, Debbie and Paul, your administrative input has not gone unnoticed.

To Arvina, the heart, soul and magical hands of the laboratory, thank you for everything that you have done, not only for me but for every one else in the lab. Without you, the lab would be very empty (especially of chocolate) and probably fall apart. To the past lab members, Carla, Conni, Tetsuya, Leonie, Pip and Will, present lab members, Nazanin, Berit, Taryn, Dan, Yonathan and Alex, and honorary lab members, Asli, Benjamin, Ellie and Alyesha, thanks for the laughs, feedback and countless amounts of good advice that you have given me. I couldn't have asked for a better group of people to share this experience with. I wish each of you well in your own personal journeys to come.

To my family and friends, immediate and extended, you know who you are, the amount of support you have given me, and how much it has meant to me. Thanks for your unconditional love and patience.

This research was supported by a Massey University Doctoral Scholarship and a short term DAAD Research Scholarship.

Table of Contents

List of Figures

List of Tables

Abbreviations

aa	Amino acid
Amp	Ampicillin
Amp^R	Ampicillin resistant
Ao	*Aspergillus oryzae*
asc	Ascogonia mutant
Bc	*Botrytis cinerea*
BLAST	Basic local alignment search tool
BLASTn	Nucleotide database search using a nucleotide query
BLASTp	Protein database search using a protein query
bp	Base pair(s)
CAT(s)	Conidial anastomosis germ tube(s)
cDNA	Complementary DNA
CFW	Calcofluor white
CG	Crippled growth
CIAP	Calf intestinal phosphatase
CLSM	Confocal Laser Scanning Microscopy
Cp	*Claviceps purpurea*
CW	Cell wall
CWI	Cell wall integrity
Cys	Cysteine
DIC	Differential interference contrast
DIG	Digoxigenin
DNA	Deoxyribonucleic acid
dNTP	Deoxynucleotide triphosphate
EDTA	Ethylene diamine tetra-acetic acid

eGFP	Enhanced green fluorescent protein
EMSA	Electrophoretic mobility shift assay
FB	Fruiting body
Fg	*Fusarium graminearum*
Fo	*Fusarium oxysporum*
g	Gram
gDNA	Genomic DNA
GEF	Guanine nucleotide exchange factor
Gen	Geneticin
Gen^R	Geneticin resistant
GFP	Green fluorescent protein
GPI	Glycosylphosphatidylinositol
h	Hour(s)
ham	Hyphal anastomosis mutant
H_2O_2	Hydrogen peroxide
Hph	Hygromycin
Hyg^R	Hygromycin resistant
IDC	Impaired development of crippled growth
kb	Kilobase(s)
KO	Knock-out
L	Litre
LB	Luria-Bertani broth
M	Molar
MAPK(K/K)	Mitogen activated protein kinase (kinase/kinase)
mg	Milligram
Mg	*Magnaporthe grisea*
µg	Microgram
min	Minute(s)
µL	Microlitre

mL	Millilitre
µm	Micrometre
µM	Micromolar
mm	Millimeter
mM	Millimolar
Mo	*Magnaporthe oryzae*
MOB	Monopolar spindle-one-binder
mRFP1	Monomeric red fluorescent protein
mRNA	Messenger ribonucleic acid
NADH	Nicotinamide adenine dinucleotide (reduced form)
NADPH	Nicotinamide adenine dinucleotide phosphate (reduced form)
Nc	*Neurospora crassa*
NCBI	National Centre for Biotechnology Information
ng	Nanogram
Nox	NADPH oxidase
Pa	*Podospora anserina*
PB1	Protein binding domain 1
PC	Plant cell
PCR	Polymerase chain reaction
PD	Potato dextrose
PEG	Polyethylene glycol
per	Perithicia mutant
pile	Perithicia placement mutant
pg	Picogram
pmol	Picomole
PMSF	Phenylmethylsulfonyl fluoride
PP2A	Protein phosphatase 2A
PR	Pheromone response
pro	Protoperithicia mutant

RG	Regeneration
RNA	Ribonucleic acid
RNase	Ribonuclease
RNA-seq	Ribonuclease sequencing
ROS	Reactive oxygen species
rpm	Revolutions per minute
RT	Reverse transcriptase
RT-PCR	Reverse transcriptase-polymerase chain reaction
SAK	Stress-activated kinase
SAM	Shoot apical meristem
Sc	*Saccharomyces cerevisiae*
SC	Synthetic complete
SD	Synthetic defined
SDS	Sodium dodecyl sulfate
SDS-PAGE	Sodium dodecyl sulfate-polyacrylamide gel electrophoresis
SEM	Scanning electron microscopy
STRIPAK	Striatin interacting phosphatase and kinase
sym	Symbiosis mutant
TBE	Tris-boric acid-EDTA
tBLASTn	Translated nucleotide database search using a protein query
T-DNA	Transfer-deoxyribonucleic acid
TEM	Transmission electron microscopy
TMD	Transmembrane domain
Um	*Ustilago maydis*
UV	Ultraviolet
V	Volts
v/v	Volume/volume ratio
WT	Wild-type

w/v	Weight/volume ratio
YE	Yeast extract
°C	Degrees Celsius

1 Introduction

1.1 Plant-fungal interactions

Many different fungi are capable of colonising the surface and intercellular spaces of a host plant. The nature of these interactions can either be pathogenic, where the host is adversely affected by the fungus, or mutualistic, where both fungus and host benefit from the association (reviewed, Kogel *et al.,* 2006). The signalling that occurs within and between a fungus and its host is often highly complex, involving many different genes, which are constantly evolving (reviewed, Chisholm *et al.,* 2006). Pathogenic relationships can therefore be thought of as an "arms race" where the host evolves genes involved in pathogen perception, cell strengthening and programmed cell-death for protection against invasion, while the pathogen evolves methods to evade detection and suppress the host immune-system to survive (reviewed, Anderson *et al.,* 2010). In contrast, mutualistic relationships often involve the co-evolution of genes and signalling pathways that allow both organisms to sense each other and undergo cellular changes that accommodate and promote a beneficial relationship (reviewed, Kogel *et al.,* 2006). The complex contribution of multiple genes and signalling pathways, both within and between two organisms, makes fungal-plant interactions an exciting research area and leads to the intriguing question, "what tips the balance between fungal parasitism and mutualism?"

1.2 *Epichloë festucae:* a model organism for studying mutualistic interactions

The Clavicipitaceae family of fungi contains both pathogenic and mutualistic species that colonise a range of different Arthropod (insect) and Poaceae and Cyperaceae (plant) hosts (Schardl, 2002). Of interest to this study are the *Epichloë* endophytes, which form symbiotic relationships with Poöideae grasses within the Poaceae family. Two major clades of *Epichloë* exist; the first contains *E. amarillans, E. baconii, E. brachyelytri, E. bromicola, E. elymi, E. festucae, E. glyceriae*, *E. yangzii,* and the second (the *E. typhina* complex) contains *E. clarkia*, *E. sylvatica* and *E. typhina* (Clay & Shardl, 2002). Depending on the endophyte, which can either be a hybrid or non-hybrid species, or an asexual or sexual species (Gentile *et al.,* 2005; Shoji *et al.,* 2015), *Epichloë* endophytes can exhibit diverse host specificity and *Epichloë*-host associations can range from mutualistic to antagonistic (Schardl 1996; Schardl & Clay 1997). *Epichloë* endophytes are of particular agricultural importance as *in planta,* most species synthesize a variety of different bio-protective secondary metabolites. Examples of these are ergot alkaloids and indolediterpenes (lolitrems) which are known for antimammalian toxicity, peramine which is an insect deterrent, and lolines which can be both deterrent and insecticidal compounds (Clay & Schardl, 2002; Schardl *et al.,* 2007, 2013a & 2013b). The presence of *Epichloë* endophytes also helps confer drought tolerance increasing host fitness and survival (Clay & Schardl, 2002; Kuldua & Bacon, 2008). Thus, understanding how *Epichloë* associations are regulated or how they can be enhanced has positive implications for agriculture

where perennial ryegrass is commonly used. Currently the most well studied *Epichloë* endophyte, in terms of molecular genetics, is *E. festucae* (Scott *et al.,* 2012) which has a limited host range, compared to *E. typhina*, and forms mutualistic symbiotic relationships within the aerial tissues of species of cool-season grasses within the *Festuca* and *Lolium* genera (Christensen *et al.,* 2002). The genome sequences of several *E. festucae* strains are available online (http://www.endophyte.uky.edu/) and *E. festucae* Fl1, which is a sexual non-hybrid species, can be easily manipulated using molecular techniques, moreover host associations are easily induced in *L. perenne* in the laboratory (reviewed, Schardl, 2001; Scott *et al.,* 2012). Given its ease of use, *E. festucae* Fl1 is an ideal model organism for studying mutualistic aerial symbiotic interactions.

1.3 Life cycle of *E. festucae*

1.3.1 The asexual cycle

The development of *E. festucae* within its host can be characterised by two different life cycles, asexual and sexual (**Figure 1.1 A**). The asexual cycle occurs when hyphae within the intercellular spaces of host plant cells expand out of the vegetative tissue apex and colonise the host inflorescences, developing ovules and developing seeds (**Figure 1.1 B-D**). This colonisation provides a means of propagation for *E. festucae*, as hyphae can be transmitted vertically through host seed, and provides hyphae with a source of nutrients from the host apoplastic fluid (Schardl 1996; Clay & Schardl 2002). Following seed germination hyphae colonise the shoot apical meristem and leaf primordia by hyphal tip growth and become aligned parallel to the longitudinal developing leaf axis and adhere to plant cells (**Figure 1.1 E**). Subsequent lateral branching and hyphal fusion result in the formation of a highly structured hyphal network within the aerial tissue of the host plant (Christensen *et al.,* 2002; Scott *et al.,* 2012). Intercalary growth preserves this network. As host cells expand, hyphae attached to plant cells avoid mechanical shearing by undergoing subapical extension and division (Christensen *et al.,* 2008; **Figure 1.1 F**). The hyphal network is thought to not only restrict *Epichloë* growth, so that it continues to be mutualistic, but to also synchronise *Epichloë*-host development (Christensen *et al.,* 2008). When leaf expansion ceases, growth of the hyphae also ceases, but the hyphae remain metabolically active (Tan *et al.*, 2001).

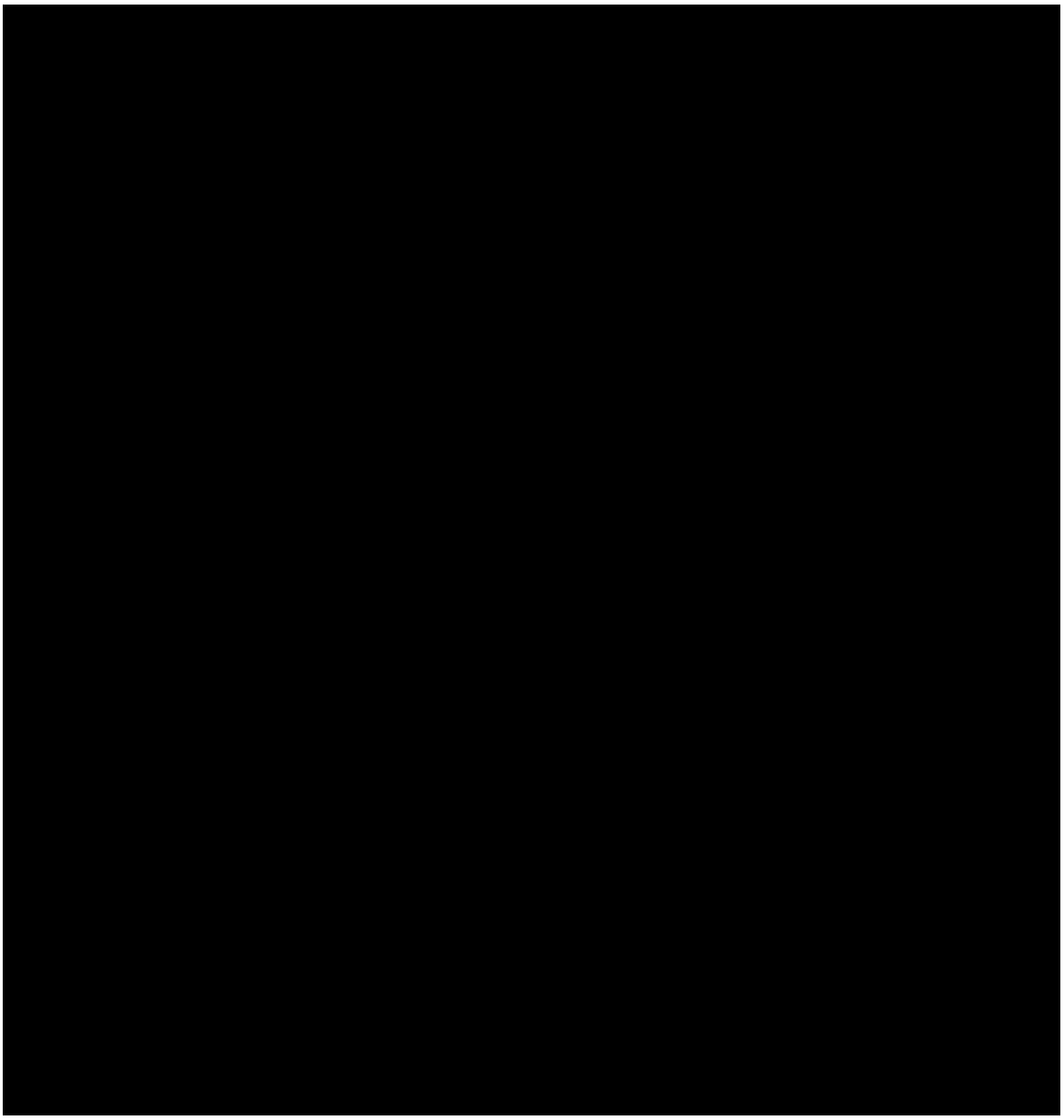

Figure 1.1 Life cycles of *E. festucae.* A) *E. festucae* asexual and sexual life cycles. Image adapted from Schardl, 2001. Hyphae expressing cyan-fluorescent protein colonising the developing host **B)** ovules **C)** seed and **D)** shoot apical meristem. Images reproduced from Schardl *et al.,* 2013b. **E)** Confocal *z*-stack images of hyphal network formation (green pseudocolour) within the host blade and sheath tissue. Image reproduced from Christensen *et al.,* 2008. **F)** Confocal images of intercalary growth between joined hyphae (arrows) expressing GFP within a 190 minute period *in planta*. Image reproduced from Christensen *et al.,* 2008. **G)** Stromata formation on a host inflorescence, image reproduced from Schardl *et al.,* 2013b. Confocal *z*-stacks of infected leaf tissue stained with aniline blue and WGA-AF488 showing **H)** endophytic hyphae (en; red pseudocolour) exiting the host cuticle layer (green pseudocolour) via an **I)** expressorium (*) to form **J)** epiphyllous (ep) hyphae which exhibit changes in WGA-AF488 (blue psuedocolour) fluorescence. **K)** Scanning Electron Microscopy showing the epiphyllous hyphal network on the host. **H-K)** Images reproduced from Becker *et al.,* 2016.

1.3.2 The sexual cycle

In contrast to the asexual cycle, the *E. festucae* sexual cycle is pathogenic. Hyphae within the host enter a highly proliferative growth phase and rapidly colonise the developing inflorescence to form reproductive structures known as stromata on the host inflorescence. This prevents the host inflorescences from fully developing and causes "choke disease" (Clay & Schardl, 2002; **Figure 1.1A & G**). Stromata produce conidia, which are transported horizontally via *Botanophila* flies to neighbouring host inflorescences. Transferred conidia fuse with an ascogonium of the opposite mating type, resulting in the formation of ascospores which are dispersed following seed dissemination, thereby completing the sexual cycle. This method of transmission is rare during *E. festucae-Festuca* associations and has never been documented within perennial ryegrass to date. Asexual *E. festucae* derivatives, which lack the ability to form stromata, can only be transmitted vertically (Clay & Schardl, 2002; Schardl *et al.,* 2013a). Furthermore only one documented hybrid species, *E. liyangensis,* is known to form stromata (Yan *et al.,* 2011). The *E. festucae*-host association that is of importance to this study is therefore considered mutually beneficial and rarely antagonistic.

1.3.3 Formation of an epiphyllous hyphal network

Although *E. festucae* is considered to be an endophyte, it also an epiphyte as endophytic hyphae have been observed to emerge from within the host leaf expansion zone to form an epiphyllous network on the surface of the host grass leaves (Moy *et al.,* 2000; Christensen *et al.,* 1997 & 2002). Here hyphae remain connected to the endophytic hyphal network and are thought to increase the resistance of the host to fungal pathogens through 'niche exclusion' (Moy *et al.,* 2000). It is only recently that the structure which allows hyphae to exit the host plant has been characterised in *E. festucae,* and it resembles an inverted appressorium-like swelling, coined an "expressorium" (Becker *et al.,* 2016). Upon exiting the host cuticle layer hyphae undergo major changes to their cell-wall structure, as noted in differences in WGA-AF488 chitin staining (**Figure 1.1 J**). These changes, where chitin is "masked" *in planta*, are proposed to facilitate mutualistic associations by suppressing the activation of host-defence mechanisms (Becker *et al.,* 2016).

1.4 Identification and characterisation of *E. festucae* mutants

Many genes essential for maintaining mutualistic *E. festucae-L. perenne* symbiotic relationships have been characterised within the *E. festucae* Fl1 (E894) strain through mutagenesis and targeted gene deletions (Scott *et al.,* 2012; Eaton *et al.,* 2012). Those of importance to this study are associated with the nicotinamide adenine dinucleotide phosphate (NADPH) oxidase complex (the Nox complex), as well as the cell wall integrity (CWI), stress

activated (SAK) and pheromone response (PR) mitogen-activated protein kinase (MAPK) pathways. These pathways are highlighted in more detail below.

1.4.1 The Nox complex

Nox complexes are involved in the production of reactive oxygen species (ROS) through conversion of O_2 to O•. ROS are important signalling molecules and the conversion of O• to H_2O_2 by superoxide dismutases is proposed to activate signal transduction cascades that are required for multi-cellular development and cell-cell communication, via the sensing of ROS bursts (reviewed, Breitenbach *et al*., 2015). In human neutrophils, the Nox complex consists of the membrane catalytic subunit, $gp91^{phox}$, the membrane bound adaptor protein $p22^{phox}$, the regulator of $gp91^{phox}$, $p67^{phox}$, the GTPase Rac1/2 which activates $p67^{phox}$ by binding GTP, and the organiser components $p47^{phox}$ and $p40^{phox}$ (**Figure 1.2**). Homologues of the Nox complex components in fungi were first identified in *Aspergillus nidulans* (Lara-Ortiz *et al.,* 2003) and *Podospora anserina* (Lalucque & Silar, 2003). Several fungi have been shown to contain two proteins, NoxA and NoxB, with homology to $gp91^{phox}$ (Aguirre *et al.,* 2005; Takemoto *et al.,* 2007), a protein with homology to $p67^{phox}$, NoxR (Takemoto *et al.,* 2006; Cano-Domınguez *et al.,* 2008; Brun *et al.,* 2009), and proteins which share homology to Rac1/2 (Weinzierl *et al.,* 2002; Boyce *et al.,* 2003; Mahlet *et.*, 2006; Rolke *et al.,* 2008; Chen & Dickman, 2004; Chen *et al.,* 2008), and the organiser components $p47^{phox}$ and $p40^{phox}$, BemA and Cdc24 (Takemoto *et al.,* 2011; Schürg *et al.,* 2012; Giesbert *et al.,* 2014; Herrmann *et al.,* 2014). A protein suggested to perform a similar function to human $p22^{phox}$, NoxD, which interacts with NoxA, has also been identified (Siegmund *et al.,* 2014; Lacaze *et al.,* 2014) (**Figure 1.2**). In fungi, NoxA and NoxD are required for cell-cell fusion, pathogenicity and fruiting body formation, whereas NoxB and Pls1 have separate functions, in that they are required for ascospore germination and appressorium development (reviewed, Scott, 2015). Although direct NoxB-Pls1 interactions have not been shown in fungi, phenotypic evidence suggests they act in the same pathway (reviewed, Scott, 2015). Nox homologues in other fungi will be highlighted in Section 1.7.1 and those in *E. festucae* highlighted below.

The first evidence that the Nox complex was involved in regulating *E. festucae* symbiosis came from the use of a forward genetics pAN7-1 plasmid insertion mutagenesis screen (Tanaka *et al.,* 2006). From 220 potential mutants inoculated into perennial ryegrass, one mutant, FR2, exhibited altered symbiosis, host stunting and premature senescence *in planta*. Sequence analysis of the region containing the pAN7-1 insert revealed that the gene disrupted in the FR2 mutant shared homology to *P. anserina nox1*, *A. nidulans noxA* and human $gp91^{Phox}$. The identification of *noxA* prompted the analysis of a second Nox homologue, *noxB*, which was reported to have no host-association phenotype when deleted. However new results, using plants grown under a controlled environment, showed that Δ*noxB* does have a symbiosis interaction phenotype, which is characterised by stunting of the host plant (Becker *et al.,* 2016). Given that NoxA is required for the mutualistic *E. festucae* association a bioinformatical approach was used to identify the homologues of human $p67^{phox}$ (NoxR) and Rac1/2 (RacA) in *E. festucae*. Gene deletion and yeast-two-hybrid experiments showed that NoxR and RacA interact and are required for mutualistic interactions, with *noxR* deletions being less severe than *noxA* (Takemoto *et al.,* 2006; Tanaka *et al.,* 2008). Takemoto *et al.,* (2011) identified a PB1 domain within NoxR, and PB1 binding domains in Cdc24, BemA and a previously uncharacterised protein. Yeast-2-hybrid experiments validated NoxR-BemA and NoxR-Cdc24 interactions, and GFP fusion experiments showed that NoxR, BemA and Cdc24 co-localise at actively growing hyphal tips. Furthermore, deletion analysis showed that *bemA* is required for mutualistic associations while Δ*cdc24* strains were not recovered, suggesting *cdc24* is an essential gene in *E. festucae*. The *E. festucae* NoxD homologue is also required for mutualistic associations (Ozaki *et al.,* 2015). Nox mediated ROS production has previously been shown by many studies to be required for correct temporal and spatial cellular differentiation, fruiting body formation, ascospore germination, appressorium development and polarized tip growth (reviewed, Scott & Eaton, 2008). It is also required for hyphal tip homing and cell fusion during the formation of conidial anastomosis germ tubes (CATs) in *Neurospora crassa* (Read *et al.,* 2012). Given these reports, *E. festucae* Δ*noxA*, Δ*noxR*, Δ*racA* (Kayano *et al.,* 2013) and Δ*noxD* (Ozaki *et al.,* 2015) mutants were analysed for cell-cell fusion defects and found to be fusion negative in culture, while Δ*bemA* mutants exhibited a marked reduction in fusion compared to Fl1 (Kayano *et al.*, 2013). Additionally, Δ*noxA*, Δ*noxB* and Δ*noxR* mutants are defective in expressorium formation (Becker *et al.,* 2016), indicating that components of the Nox complex are required for mutualistic *E. festucae* associations, expressorium formation and cell-cell fusion.

1.4.2 MAP kinase pathways

Budding yeast contain five mitogen-activated protein kinase (MAPK) pathways which are involved in mating and pheromone response, filamentous and invasive growth, cell wall

integrity and abiotic stress response, hyperosmolarity responses, and ascospore formation (**Figure 1.3**; Hamel *et al.,* 2012; Saito & Tatebayashi, 2004). In comparison, filamentous fungi contain only three main MAPK pathways (Rispail *et al.,* 2009), which in *E. festucae* are known as the Stress Activated MAPK pathway (SAK), the Pheromone Response pathway (PR) and the Cell Wall Integrity pathway (CWI) (**Figure 1.4**; Eaton *et al.,* 2012). Each of these pathways are collectively involved in perceiving a wide range of stimuli that are subsequently fed into complex signalling cascades that alter gene expression. This allows the fungus to undergo cellular changes to respond to environmental stress or to alter hyphal growth. Several MAPK pathway genes are involved in regulating *E. festucae* symbiosis and will be outlined in the following sections below. Homologues of these genes in other filamentous fungi will be outlined in Section 1.7.3.

1.4.2.1 The Stress Activated MAPK pathway

In yeast, the High Osmolarity pathway involves the membrane osmolarity sensors Sho1/Msb2, the GTPase Cdc42, the p21-activated kinase Ste20, the MAPKKK Ste11, MAPKK Pbs2, MAPK Hog1 and downstream transcription factors Hot1, Msn2 and Sko1 (**Figure 1.3**; Hamel *et al.,* 2012; Saito & Tatebayashi, 2004). Several homologues of these proteins have been identified in *E. festucae* (**Figure 1.4**; Eaton *et al.,* 2012). The homologue of Hog1 in *E. festucae*, SakA, is required for mutualistic associations (Eaton *et al.,* 2010). Interestingly, while Δ*cdc42* associations are not pathogenic, Cdc42 is required for intercalary growth, as Δ*cdc42* hyphae exhibit hyphal breakage within the expanding host tissues *in planta* and are unable to colonise into fully developed leaf tissue (Takemoto *et al.,* 2015). Collectively these results suggest that the core components of the SAK pathway are required for *E. festucae* mutualism and regulated growth *in planta*.

1.4.2.2 The Cell Wall Integrity pathway

In yeast, the CWI pathway stress sensors Mid2/Mlt2 and Wsc1/2/3 bind to the guanyl nucleotide exchange factor (GEF) Rom2 when activated. This binding activates the GTPase Rho1, which subsequently activates PKC1. PKC1 then activates the CWI MAP kinase cascade involving the MAPKKK Bck1, MAPKK Mkk1/2 and MAPK Slt2/Mpk1. Activation of the MAPK pathway then activates the downstream transcription factors Rlm1, Sbf1 and Swi4/6, which induce changes in gene expression (**Figure 1.3**; Hamel *et al.,* 2012). Homologues of the CWI scaffold Ste5 (So) (Charlton *et al.,* 2012; Teichert *et al.,* 2014) and MAP kinases Mkk1/2 (MkkA) and Slt2/Mpk1 (MpkA) (Becker *et al.,* 2015) have been identified in *E. festucae* (**Figure 1.4**) Targeted deletion of *so*, *mkkA* and *mpkA* results in a stunted host phenotype *in planta* and additionally Δ*so*, Δ*mkkA* and Δ*mpkA* mutants are defective in cell-cell fusion and

Δ*mkkA* and Δ*mpkA* mutants hyperconidiate in culture. Collectively these results show that the CWI MAPK pathway is crucial for cell-cell fusion and mutualistic *E. festucae*-host interactions.

Figure 1.3 *S. cerevisiae* MAPK pathways. Image reproduced from Saito & Tatebayashi, 2004.

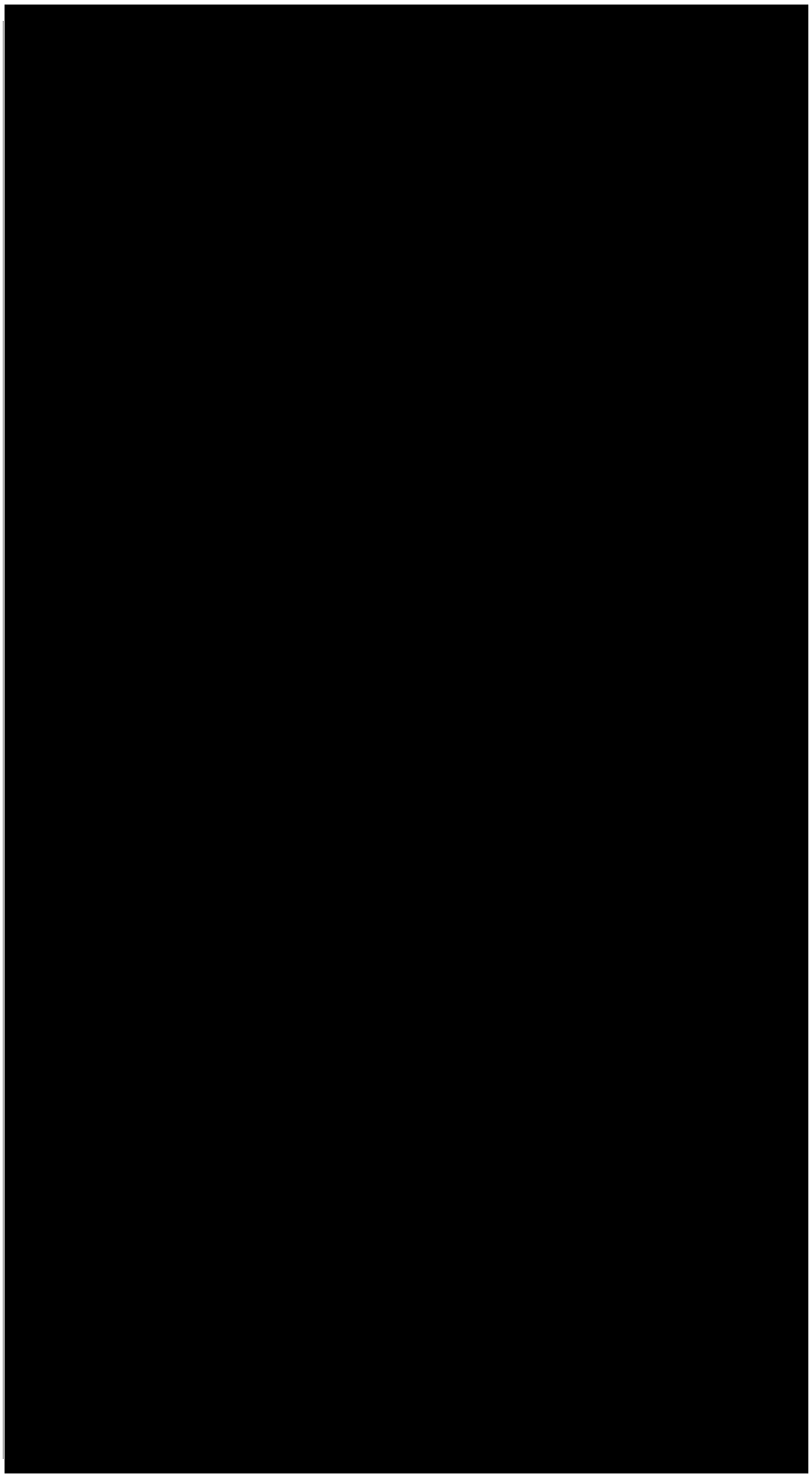

Figure 1.4 *E. festucae* Fl1 MAPK pathways. Images modified from Eaton *et al.,* 2012. Membrane sensors are in orange, phosphatases in red, kinases in purple, cyan and blue, transcription factors in pink, guanine nucleotide exchange factors in light green and additional proteins in dark green. Dashed grey boxes indicate the putative scaffold proteins for the CWI (So) and PR pathway (IdcA).

1.4.2.3 Pheromone Response MAPK pathway

The yeast mating and PR pathway involves the pheromone receptors Ste2/3, the GTPase Cdc42, Bem1, the protein activated kinase Ste20, the MAPKKK Ste11, MAPKK Ste7, MAPKs Fus3 and Kss1, the MAPK protein scaffold Ste5 and the downstream transcription factor Ste12 (**Figure 1.3**; Hamel *et al.,* 2012). Homologues of several of these proteins have been identified in *E. festucae* (**Figure 1.4**). The homologue of the yeast scaffold protein Ste5 is known as IdcA in *E. festucae,* and is required for cell-cell fusion and symbiosis (Eaton *et al.,* 2013). IdcA shares homology to *P. anserina* IDC1 (Jamet-Vierny *et al.,* 2007) and *N. crassa* HAM-5 (Jonkers *et al.,* 2014; Dettman *et al.,* 2014). The *E. festucae* nuclear localised protein NsiA, shows positive yeast-2-hybrid interactions with the homologue of the transcription factor Ste12 (Ozaki *et al.,* 2015). Furthermore, Δ*nsiA* mutants exhibit prolific growth *in planta* and a loss of cell-cell fusion. Interestingly, *noxD* and the transcription factor *proA* (further mentioned in Section 1.4.3) are down-regulated in Δ*nsiA* mutants, suggesting these genes are regulated by the transcription factor NsiA. *nsiA, proA* and *noxD* are all required for *E. festucae* cell-cell fusion and symbiosis (Tanaka *et al.,* 2013; Ozaki *et al.,* 2015). Collectively these results suggest that components of the PR MAPK pathway are required for *E. festucae* cell-cell fusion and mutualism.

1.4.3 The transcription factor ProA

In *Sordaria macrospora*, the C6 Zinc finger transcription factor, PRO1 (further mentioned in Section 1.7.2), is essential for fruiting body development and cell-cell fusion (Masloff *et al.,* 1999 & 2002). The *E. festucae* homologue of *pro1*, *proA*, was identified via an *Agrobacterium tumefaciens* T-DNA screen where Δ*proA* mutants exhibited proliferative growth in *planta*, and a loss of cell-cell fusion and a hyperconidiation phenotype in culture (Tanaka *et al.,* 2013). Although these phenotypes were similar to Δ*noxA* mutants, *proA* deletion had no effect on *noxA* expression, indicating ProA is unlikely to regulate *noxA*. ProA did however regulate the expression of two divergently transcribed genes, *EF320* and *esdC*. Although the deletion of *EF320* or *esdC* had no effect on *E. festucae* growth *in planta* or in culture, the analysis of *EF320* and *esdC* promoter regions, using electrophoretic mobility shift assays, identified two motifs, A2 motif = GGCGC and A5 motif = GCGCCG, to which ProA binds. When used in conjunction with the recently published RNA-seq data (Eaton *et al.,* 2015), which identified a number of genes differentially expressed in *proA* mutants compared to WT, these motifs can be used to further predict whether a promoter may be targeted by ProA.

1.4.4 Additional signalling pathways

Additionally, iron acquisition, pH sensing and histone modifications are required for mutualistic symbiotic interactions. Deletion of the siderophore synthesis gene *sidN* (Johnson *et al.,* 2007 & 2013), the H3K9 and H3K27 methyltransferases *clrD* and *ezhB* (Chujo & Scott, 2014), the heterochromatin remodelling protein, HepA (unpublished results Chujo *et al.,*), and constitutive expression of the pH regulated transcription factor, PacC (Lukito *et al.,* 2015), result in altered host interaction phenotypes. The involvement of these pathways and those prior mentioned, highlights the complexity of *E. festucae* associations with the host plant and how finely tuned it is, both genetically and epigenetically. Interestingly *E. festucae* not only regulates its own growth *in planta* but also induces a major reprogramming of the host transcriptome, with genes involved in drought and biotic-related stress, pathogenesis, DNA synthesis and repair and primary metabolism reported as being down-regulated, and genes associated with trichome development, stomatal closure and secondary metabolite production reported as being up-regulated (Dupont *et al.,* 2015). Thus, complex signalling not only occurs within *E. festucae,* which regulates hyphal growth *in planta,* but also between *E. festucae* and the host that synchronises fungal-plant development.

The impact *E. festucae* has on the host transcriptome and the variety of pathways required for mutualism has led to the intriguing questions, what tips the balance between pathogenicity and mutualism and which genes are required for *E. festucae*-host associations? Eaton *et al.,* (2015) have recently published a 3-way RNAseq analysis involving the combined analysis of genes differentially regulated in Δ*noxA,* Δ*sakA* and Δ*proA* associations, which complements an original Δ*sakA* RNA study (Eaton *et al.,* 2010). This study identified 182 genes that exhibit common expression patterns present in all three associations. Most notably an upregulation of primary metabolic genes, membrane transporters and genes potentially involved in host cell-wall degradation, suggesting mutant associations are pathogenic. A further study performed in Δ*hepA* mutants has since reduced this set to 111 genes (unpublished results Chujo *et al.,*). These transcriptome studies have substantially expanded current understanding on which genes and signalling pathways may be required for mutualistic associations, and provide an opportunity to identify novel genes in *E. festucae* that may be involved in regulating *E. festucae* symbiosis**.**

1.5 Cell-cell fusion: required for mutualistic *E. festucae* associations?

In summary, the identification of several mutants, Δ*noxA*, Δ*noxR* (Tanaka *et al.,* 2006 & 2008; Takemoto *et al.,* 2006 & 2011; Kayano *et al.,* 2013), Δ*proA* (Tanaka *et al.,* 2013), Δ*idcA* (Eaton *et al.,* 2013), Δ*so* (Charlton *et al.,* 2012), Δ*noxD* (Ozaki *et al.,* 2015), Δ*mkkA* and Δ*mpkA*

(Becker *et al.,* 2015), which exhibit a loss of cell-cell fusion and deregulated symbiosis, has led to the hypothesis that cell-cell fusion is required for hyphal network formation *in planta* and mutualistic *E. festucae* associations. Although these components have been identified and the majority of them have been functionally placed into signalling pathways, such as the Nox complex or CWI or PR pathway, how the signals required for cell-cell fusion and mutualism are transmitted and how they are perceived between hyphae, has not been fully elucidated in *E. festucae*. Additionally, relatively little is known as to how these signals are integrated between these different pathways, indicating that further research is required if we are to advance our understanding of the *E. festucae- L. perenne* system.

Interestingly, several homologues of the above mentioned genes are also required for cell-cell fusion and sexual fruiting body development in the organisms *Sordaria macrospora, Neurospora crassa* and *Podospora anserina*, suggesting common regulatory pathways exist within these two different developmental pathways and between these different fungi (Haedens *et al.,* 2005; Lord & Read, 2011; Read *et al.,* 2012). As a result of mutagenesis screening several candidate proteins that are potentially involved in signal perception or signal integration have been identified. In the following sections, sexual development and cell-cell fusion in *S. macrospora, N. crassa* and *P. anserina* will be discussed and based on these research findings, candidate genes of importance to this study highlighted.

1.6 *Sordaria macrospora, Neurospora crassa* and *Podospora anserina* sexual development and mutant screening

1.6.1 *Sordaria macrospora* life cycle and mutant screening

Sordaria macrospora is a homothallic self-fertile fungus that begins its life cycle as a single spore that germinates sending out new hyphae (**Figure 1.5**). This phase of growth is known as the vegetative phase. Hyphal fusion and polarised growth later cause these hyphae to come together to create a branched interconnected mycelial network that extends outwards from the initial spore. Hyphal development then transitions to a sexual cycle, which can be divided into three distinct phases known as the ascogonial, protoperithecial, and perithecial stages. During the ascogonial stage, newly emerging lateral hyphae begin to curl creating coiled hyphae known as ascogonial hyphae, the first structures to develop during fruiting body formation. During the protoperithecial stage, ascogonial hyphal are enveloped in five-six layers of pseudoparenchymatous cells that arise from neighboring lateral hyphae to form protoperithica. Basal ascogonial hyphae then cluster together while the upper hyphal layers form a loose network that is removed during the perithecial stage. Several asci, each containing eight spores, develop up from the basal coiled ascogonium and mature within fully formed perithecia. Ascospores are then ejected through the upper opening of the perithecium, the ostiole,

completing the *Sordaria* sexual cycle stages (Hock *et al.,* 1978; Lord & Read, 2011).

Several mutants, known as the *asc*, *pro*, *per* and *pile* mutants (**Figure 1.5**), which develop defects in the formation of sexual fruiting bodies, have been identified in *S. macrospora* (Engh *et al.,* 2010). *asc* mutants are characterised by malformed ascogonia that do not form or curl properly causing arrested protoperithicium/perithecium development. In *pro* mutants, ascogonia appear normal and it is the development of protoperithicia from ascogonia that are affected. Mutant *pro* protoperithicia become rounded and stunted, unable to develop further to form elevated perithecia. In contrast to *asc* and *pro* mutants, *per* mutants are capable of forming normal ascogonia, protoperithicia and perithecia, but are unable to generate viable ascospores or asci, which causes sterility. *pile* mutants are the only mutants out of the four characterised groups which produce viable spores. They are not defective in the development of sexual structures but rather in their spatial order, and are characterised by overlapping perithecia. Of importance to this study are the *Sordaria pro* mutants, several of which were generated through an initial UV mutagenesis screen and a second EMS mutagenesis screen (Masslof *et al.,* 1999; Pöggeler & Kück, 2004). Once identified, mutant *pro* phenotypes can be confirmed by targeted *pro* gene deletions to obtain "clean" deletion mutants (Engh *et al.,* 2010).

Figure 1.5 Life cycle of *Sordaria macrospora* and associated fruiting body mutants. Image modified from Kück *et al.,* 2009.

1.6.2 *Podospora anserina* and *Neurospora crassa* life cycles

P. anserina and *N. crassa* life cycles are similar to that observed in *S. macrospora*, with the exception that their sexual cycles involve the differentiation of female (ascogonia) and male (conidia) hyphae (**Figure 1.6 A**). Which structures form is dependent on whether hyphae express the *a* (female) or *A* (male) mating type locus. During the ascogonial stage, female ascogonia are fertilised by male conidia. Fertilised ascogonia are then enclosed by nearby hyphae (similar to *Sordaria* protoperithecia development) and proliferate to create multinucleate cells that contain both male and female mating type nuclei. Pairs of male and female nuclei later migrate together to form specialised cells known as multi-nucleated croziers. Mitosis later occurs within these croziers in order to form two uni-nucleate cells and a single bi-nucleate cell. During the perithecia stage, bi-nucleated cells differentiate and undergo meiosis to form asci that contain 8 haploid spores. Ascospores are then ejected from perithecia as they mature, completing *P. anserina* and *N. crassa* sexual cycles (Coppin *et al.,* 1997).

1.6.3 *Neurospora crassa* and *Podospora anserina* mutant screening

In *N. crassa*, the development and fusion of specialised hyphal tubes known as conidial anastomosis tubes (CATs), which arise from asexual conidia, facilitates the initiation of new colonies by creating interconnected hyphal networks between germinating spores (Roca *et al.,* 2005). CAT induction typically begins with the formation of small tubes that protrude outward from isolated spores and fuse when they come into contact. Several mutants known as hyphal anastomosis mutants (*ham*), which are defective in CAT fusion and the formation of protoperithecia, have been characterised in *N. crassa* (**Figure 1.6 B**; Read *et al.,* 2009 & 2012; Lichius, 2010; Fu *et al.,* 2011; Lichius *et al.,* 2014). Additionally, *ham* mutants are also often defective in vegetative cell-cell fusion.

In *P. anserina,* a cell degenerative phenomenon known as crippled growth (CG) arises following prolonged periods of stationary hyphal growth (Silar *et al.,* 1999). The appearance of CG acts to slow colony expansion and arrests the development of aerial hyphae and perithecia and is thought to be caused by a cytoplasmic and infectious element (C) that is transmitted exclusively during mitosis in a non-mendelian fashion as a result of abnormal activation of the CWI pathway (Silar *et al.,* 1999 & 2001; Jamet-Vierny *et al.,* 2007). Several mutants that exhibit impaired development of CG (IDC) (**Figure 1.6 C**) were identified in genetic suppressor screen. The majority of these mutants are also defective in vegetative cell-cell fusion and sexual fruiting body development, in that they do not generate protoperithecia or viable spores (Haedens *et al.,* 2005).

Figure 1.6 *Neurospora crassa* and *Podospora anserina* life cycles and mutant screening. A) *P. anserina* and *N. crassa* life cycles. Image taken from Coppin *et al.,* 1997. **B)** *N. crassa* wild-type CAT fusion (left image arrows) and hyphal anastomosis (*ham*) mutant (right image) phenotypes. Images taken from Aldabbous *et al.,* 2010. Scale bar = 10 μm. **C)** *P. anserina* crippled growth (CG) and impaired development of crippled growth (IDC) phenotypes. Example of WT CG (left) and mutant *IDC* and loss of fruiting body (FB) phenotypes in *IDC*^{1} mutants compared to WT. Images taken from Silar *et al.,* 2001 and Jamet-Vierny *et al.,* 2007.

1.7 Identification and characterisation of *pro, ham* and *IDC* mutants.

Several *N. crassa ham*, *S. macrospora pro* and *P. anserina IDC* mutants have been functionally characterised and found to be associated with a conserved signalling network.

1.7.1 The Nox complex

The first evidence that the Nox complex was present in filamentous fungi was found by Lara-Ortíz *et al.,* (2003) in *A. nidulans*, and Lalucque & Silar (2003) in *P. anserina* (*Pa*). Targeted deletion of *noxA* showed that *A. nidulans* NoxA is required for sexual development while cloning and bioinformatics showed that *PaNox1* homologues are found in several fungi capable of sexual development, suggesting the Nox complex is involved in fungal multi-cellular development. Targeted deletions of *P. anserina PaNox1* and *PaNox2* showed that *PaNox1* is required for fruiting body development and *PaNox2* is required for ascospore germination (Malagnac *et al.,* 2004). The filamentous fungal NoxR homologue was characterised in *E. festucae* by Takemoto *et al.,* (2006). In *B. cinerea*, Δ*noxA* and Δ*noxR* mutants are defective in pathogenicity and infection progression and Δ*noxB* mutants are impaired in the formation of host penetration structures (Segmüller *et al.,* 2008). Similar to *B. cinerea*, *P. anserina* Δ*Nox1*/*IDC*^{343} and Δ*NoxR/IDC*^{524} mutants are unable to penetrate cellulose (Haedens *et al.,* 2005; Brun *et al.,* 2009). In *N. crassa*, Nox complex homologues were identified by Cano-Dominguez *et al.,* (2008) where targeted *nox-1* and *nor-1* (NoxR homologue) deletions produced defects in vegetative growth, conidiation, protoperitheium and aerial hyphae development, and *nox*-2 deletions produced defects in spore germination. *N. crassa* Δ*nox-1* and Δ*nor-1* (Lichius, 2010; Fu *et al.,* 2011; Read *et al.,* 2012) and *B. cinerea* Δ*noxA* and Δ*noxR* mutants (Roca *et al.,* 2012) were also defective in CAT fusion, and *P. anserina PaNoxA* and *PaNoxR* mutants, defective in vegetative cell-cell fusion (Tong *et al.,* 2014). Targeted gene deletions showed that *S. macrospora nox1* and *nor1* homologues are required for fruiting body formation and cell-cell fusion (Dirschnabel *et al.,* 2014). In *N. crassa, rac-1* and *bemA* homologues were shown to be required for CAT fusion (Lichius, 2010; Fu *et al.,* 2011; Schürg *et al.,* 2012; Lichius & Lord, 2014). In *B. cinerea,* heterokaryon Δ*cdc24* mutants showed reduced virulence and Δ*bem1* mutants displayed a loss of CAT fusion (Giesbert *et al.,* 2014). In *S. macrospora,* PRO41 (NoxD homologue) was identified in an EMS mutagenesis screen for *pro* mutants (Pöggeler & Kück, 2004), and has been characterised as an ER localised protein that is required for fruiting body formation (Nowrousian *et al.,* 2007). In *N. crassa*, the homologue of PRO41, HAM-6, was shown to be required for cell-cell fusion and fruiting body development and correct MAK-1 (CWI MAP kinase) phosphorylation (Lichius, 2010; Fu *et al.,* 2011; Fu *et al.,* 2014). Homologues of PRO41/HAM-6 were identified in *B. cinerea* and *P. anserina* and subsequently named NoxD (Siegmund *et al.,* 2014; Lacaze *et al.,* 2014). In *B.*

cinerea, NoxA and NoxD interacted, suggesting NoxD was part of the NoxA associated Nox complex (Siegmund *et al.*, 2014). In *B. cinerea,* NoxD is required for pathogenicity and CAT fusion (Siegmund *et al.*, 2014) and in *P. anserina*, NoxD is required for CG and fruiting body development, cellulose penetration and cell-cell fusion (Haedens *et al.,* 2005; Lacaze *et al.,* 2014). Similar to *Pa*Nox2 and *Bc*NoxB (Haedens *et al.,* 2005; Brun *et al.,* 2009; Segmüller *et al.,* 2008), *P. anserina Pa*Pls1 (Lambou *et al.,* 2008; Brun *et al.,* 2009) is required for ascospore germination and cellulose penetration and *B. cinerea* Pls1 is required for pathogenicity (Siegmund *et al.,* 2013). Collectively these results suggest that two Nox complexes exist in filamentous fungi, where Nox2/B and Pls1 are required for ascospore germination and NoxA and NoxD are required for cell-cell fusion.

1.7.2 The transcription factor PRO1

The homologue of *E. festucae* ProA, PRO1, was identified in *S. macrospora* in a UV mutagenesis screen and identified as being a C6 Zinc finger transcription factor, essential for fruiting body development (Masloff *et al.,* 1999). Interestingly cDNA from the predicted *N. crassa adv-1* homologue complemented mutant *pro1 S. macrospora* defects, suggesting PRO1 functions are conserved among fungi (Masloff *et al.,* 2002). Furthermore, ADV-1 is required for *N. crassa* CAT fusion and sexual development (Colot *et al.,* 2006; Fu *et al.,* 2011; Lichius & Lord, 2014).

1.7.3 Cell-cell fusion: a PR and CWI pathway ping-pong mechanism

1.7.3.1 MAK2 and the PR pathway

Components of the PR pathway have been well characterised in *N. crassa*. In *N. crassa*, the PR pathway MAPKKK NCR-1, MAPKK MEK-2 and MAPK MAK-2 (Pandey *et al.,* 2004; Fu *et al.,* 2011; Lichius *et al.,* 2012), the pheromone receptor PRE-1 (Kim & Borkovich, 2004), and predicted downstream transcription factor PP-1 (Li *et al.,* 2005*;* Leeder *et al.,* 2013), are required for female fertility and cell-cell fusion (Fu *et al.,* 2011; Read *et al.,* 2012). In addition to regulating the PR pathway, MAK-2 interacts with the PR pathway scaffold protein HAM-5 (Dettmann *et al.,* 2014; Jonkers *et al.,* 2014) and the nuclear Dbf2-related (NDR) scaffolding protein HYM-1 (Dettmann *et al.,* 2012). HYM-1 is essential for normal MAK-2 activity, cell-cell fusion and protoperithecia development, and interacts with the COT-1 NDR kinase complex, COT1-MOB-2-POD-6, to regulate COT-1 associations with POD-6 (Seiler *et al.,* 2006; Maerz *et al.,* 2008; Dettmann *et al.,* 2012). HAM-5 is essential for cell-cell fusion and sexual fruiting body development (Aldabbous *et al.,* 2010), contains a MAPK consensus phosphorylation site, and interacts with and co-localises with NRC-1, MEK-2 and MAK-2 during CAT tip homing (Jonkers *et al.,* 2014; Dettmann *et al.,* 2014), suggesting HAM-5 is the

scaffold for the PR pathway. In *P. anserina,* homologues of the PR Pathway MAPK kinases Tkl2 (NCR-1), Mkk2 (MEK-2) and Mpk2 (MAK-2) (Lalucque *et al.,* 2012; Tong *et al.,* 2014), and the scaffold protein IDC1 (HAM-5) (Jamet-Vierny *et al.,* 2007; Tong *et al.,* 2014), are required for the development of protoperithecia, CG and cell-cell fusion, and additionally the PR MAP kinases are required for cellulose penetration. In *Sordaria,* double deletions of the pheromone-precursors and associated pheromone receptors, Δ*pre2*/Δ*ppg2* and Δ*pre1*/Δ*ppg1* and double Δ*ppg1*/Δ*ppg2*, alters perithecia development (Mayrhofer *et al.,* 2006). Collectively these results suggest that the PR pathway is required for cell-cell fusion and sexual fruiting body development in fungi.

1.7.3.2 SO and the CWI pathway

N. crassa Δ*so*/*ham-1* mutants are female sterile, defective in CAT fusion and exhibit altered growth and conidiation (Fleißner *et al.,* 2005). In response to injury SO localises to septal plugs (Fleißner *et al.,* 2007), and during CAT homing MAK-2, and SO oscillate and show a "ping-pong" localisation pattern, suggesting they are involved in a signalling communication feedback loop which regulates cell-cell communication (**Figure 1.7**; Read *et al.,* 2009; Fleißner *et al.,* 2009; Goryachev *et al.,* 2012). The PR pathway kinases NCR-1 and MEK-2 (Dettmann *et al.,* 2012) and the scaffold protein HAM-5, all co-localise and oscillate with MAK-2 during this hyphal homing (Jonkers *et al.,* 2014; Dettmann *et al.,* 2014). Similar to SO, components of the *N. crassa* CWI pathway, MIK-1, MEK-1 and MAK-1, are required for perithecia development and cell-cell fusion (Lichius, 2010; Fu *et al.,* 2011; Read *et al.,* 2012; Lichius & Lord, 2012). However unlike MAK-2, the CWI MAPK MAK-1 does not show oscillatory recruitment to the plasma membrane during hyphal homing (Dettmann *et al.,* 2013). The homologue of SO in *S. macrospora*, PRO40, was identified in a UV mutagenesis screen as being required for fruiting body formation and cell-cell fusion (Masloff *et al.,* 1999). Similar to SO (Fleißner *et al.,* 2007), PRO40 localises to septal pores (Engh *et al.,* 2007). Affinity purification, mass spectrometry and yeast-2-hybrid experiments showed PRO40 binds to the CWI MAP kinases MIK1, MEK1 and MAK1, and the upstream activator, PKC1 (Teichert *et al.,* 2014), suggesting PRO40/SO acts as a scaffold for the CWI pathway. Furthermore, *S. macrospora* Δ*pro40,* Δ*mik1/pro30*, Δ*mek1* and Δ*mak1* mutants exhibit a loss of cell-cell fusion and altered sexual development, indicating the CWI pathway is essential for these two processes. The oscillation of SO and MAK-2 in homing hyphal tips (Read *et al.,* 2009, Goryachev *et al.,* 2009; Fleißner *et al.,* 2009) and SO/PRO40–MAK1 interactions (Teichert *et al.,* 2014), has suggested crosstalk occurs between the PR and CWI pathways that regulates hyphal homing and cell-cell fusion. *P. anserina* homologues of the CWI MAPKs, ASK1 (MIK-1), MPK1 (MAK-1) and MKK1 (MEK-1), and the CWI MAPK scaffold SO, are required for CG and sexual development (Kicka, & Silar, 2004; Haedens *et al.,* 2005; Kicka *et al.* 2006; Lalucque *et al.,* 2012) and cell-

cell fusion (Tong *et al.,* 2014). In *P. anserina*, the homologue of *N. crassa* PR pathway scaffold HAM-5, IDC1 (Jamet-Vierny *et al.* 2007), and the PR MAPK kinase Mpk2 (MAK-2) (Lalucque *et al.,* 2012), are required for the correct Mpk1 (MAK-1) nuclear localisation during the stationary growth phase, further suggesting crosstalk occurs between the PR and CWI MAP kinase pathways. Until recently it was unclear how cross talk between these pathways occurred within filamentous fungi, but recently it was shown that the Striatin-Interacting-Phosphatase-And-Kinase (STRIPAK) complex (discussed in the section below) may facilitate such cross talk (Bloemendal *et al.,* 2012; Dettmann *et al.,* 2013).

Figure 1.7 Oscillation of GFP labelled MAK-2 and dsRED labelled SO in homing *Neurospora crassa* tips. Images from Fleiβner *et al.,* 2009.

1.7.3.3 PR and CWI signal integration: the STRIPAK complex

The STRIPAK complex in filamentous fungi was identified in *Sordaria* and consists of several proteins, the Striatin scaffold protein, PRO11; Striatin-interacting protein, PRO22; kinase activator, MOB3; GPI anchored protein, GPI1; serine/threonine phosphatase PP2A subunits A and C; germinal centre kinases, KIN3 and KIN23; the sarcolemmal membrane-associated protein, PRO45; as well as several other accessory proteins (**Figure 1.8**; reviewed, Kück *et al.,* 2016). PRO11 was the first component characterised and was found during an EMS mutant screen directed at identifying mutants that were defective in protoperithecia-perithecia development (Pöggeler & Kück, 2004). The gene defective in Δ*pro11* strains was identified as the homologue of mammalian STRIPAK component Striatin as mouse Striatin complemented Δ*pro11* defects. PRO22 was identified in the same mutagenesis screen as PRO11 (Pöggeler & Kück, 2004), and was characterised as being a transmembrane domain protein required for sexual fruiting body development, cell-cell fusion and correct septation, which localised to the vesicular-vacuolar network and shared homology to the human Striatin-interacting protein (Bloemendal *et al.,* 2010). These findings prompted the analysis of a third STRIPAK complex component known as monopolar-spindle-binder 3 (MOB3), which in mammals was shown to interact with three rat striatin proteins (Baillat *et al*. 2001). Targeted *mob3* deletions showed that *S. macrospora* Δ*pro11* and Δ*mob3* mutants exhibited similar phenotypes and were defective in fruiting body development and cell-cell fusion (Bernhards & Pöggeler, 2011). To determine whether other STRIPAK complex components could be found in *S. macrospora*, tandem

affinity purification (TAP) and mass spectrometry, using multidimensional protein identification technology (MudPIT), was used to identify components that associated with PRO22 (Bloemendal *et al.,* 2012). This study identified that PRO11, PP2Aa, PP2Ac1 and MOB3 are associated with PRO22, and that direct PRO22-PRO11, PRO22-PP2AA, PRO22-PP2Ac1 and PRO11-MOB3 interactions occur (Bloemendal *et al.,* 2012). Additional Yeast-2-hybrid and CoIP experiments have shown that MOB3 interacts with PRO45 and GPI and PRO11 interacts with KIN3 and KIN24 (**Figure 1.8**; Nordzieke *et al.,* 2015; Frey *et al.,* 2015a & 2015b).

Mutant analysis of *Sordaria* STRIPAK components (reviewed, Kück *et al.,* 2016) and their respective homologues HAM-3 (PRO11) and HAM-2 (PRO22) (Simonin *et al.,* 2010), MOB-3 (MOB3) (Maerz *et al.,* 2009), HAM-4 (PRO45) and PP2A-A & PPG-1 (PP2A subunits) (Fu *et al.,* 2011; Read *et al.,* 2012) in *N. crassa*, has collectively shown that components of the STRIPAK complex are required for cell-cell fusion and sexual fruiting body development in filamentous fungi. Additionally, *S. macrospora* PRO22 (Bloemendal *et al.,* 2010) and KIN3 and KIN24 (Frey *et al.,* 2015b) are associated with septation, GPI1 acts as a repressor of fruiting body development (Frey *et al.,* 2015a), and homologues of PRO11 in *Fusarium verticillioides* (Fsr1) (Yamamura & Shim, 2008), *Aspergillus nidulans* (StrA) (Wang *et al.,* 2010) and *Colletotrichum graminicola* (Str1) (Wang *et al.,* 2016), are associated with altered radial growth, ascosporogenesis and virulence. Furthermore, localisation studies have shown that GPI1 localises to the plasma membrane and mitochondria (Frey *et al.,* 2015a), PRO45 localises to the nuclear envelope, mitochondria and endoplasmic reticulum (Nordzieke *et al.,* 2015) and KIN3 and KIN24 localise to septal pores (Frey *et al.,* 2015b). In *N. crassa*, HAM2, HAM3, HAM4, PP2A and MOB3 additionally localise to the nuclear envelope (Dettmann *et al.,* 2013). Interestingly in *N. crassa*, MAK-2 (PR kinase) mediated phosphorylation of MOB-3 is required for HAM-2 (PRO11) and HAM-3 (PRO22) nuclear envelope localisation, and this localisation pattern is required for the nuclear accumulation of the CWI kinase MAK-1 (Dettmann *et al.,* 2013). Specifically MAK-2 interacts with and phosphorylates the N terminal MOB3 kinase domain, with loss of this domain shown to result in a loss of MAK-1 nuclear localisation. Collectively these results have demonstrated that the STRIPAK complex components exhibit multiple temporal and spatial localisation patterns and are involved in transmitting and relaying signals from both the CWI and PR MAPK pathways, via MOB3, which then regulate multiple downstream developmental signalling pathways such as cell-cell fusion, septation, pathogenicity and sexual development (Kück *et al.,* 2016).

Figure 1.8 Diagram of the *Sordaria* STRIPAK complex components with their predicted interaction partners, transmembrane domains and cellular localisation patterns shown. Image from Kück *et al.,* 2016.

Interestingly, disruption of the PR pathway transcription factor *pp-1,* homologous to *S. cerevisiae* STE12 (Li *et al.,* 2005), abolishes CAT fusion in *N. crassa* (Read *et al.,* 2012) and RNA-seq data have shown that *adv-1*, *ham-7, ham-6, nox-1, nor-1, so, mek-1, mak-1, pp2A* and *mob-3* are differentially expressed in Δ*pp-1* mutants compared to WT (Leeder *et al.,* 2013). Taken together, the oscillation of MAK-2 and SO in homing CAT tips, the requirement for MAK-2 phosphorylation of MOB3 for nuclear MAK-1 accumulation, and the RNA-seq data collected from Δ*pp-1* mutants suggests complex cross talk occurs within and between the PR and CWI pathway (Read *et al.,* 2009, Goryachev *et al.,* 2009; Fleiβner *et al.,* 2009; Teichert *et al.,* 2014; Dettman *et al.,* 2013; Leeder *et al.,* 2013).

1.7.4 *Podospora* IDC2 and IDC3: a receptor complex for cell-cell fusion?

Podospora IDC[2] and *IDC*[3] mutants are defective in cell-cell fusion and CG (Haedens *et al.,* 2005) and the proteins encoded by *IDC2* and *IDC3* are proposed to interact and form a membrane-associated receptor complex (personal communication, P. Silar). *IDC2* is the homologue of *N. crassa ham-7*, and Δ*ham-7* strains are defective in cell-cell fusion, fruiting body development and normal MAK-1 phosphorylation under stress conditions, results suggesting HAM-7 feeds into the CWI pathway (Maddi *et al.,* 2012). Analysis of RNA-seq data showed that *E. festucae IDC2* and *IDC3* homologues, *symB* and *symC,* are down regulated 6.92

and 3.29 fold in Δ*proA* host association (Eaton *et al.,* 2015), results suggesting *symB* and *symC* are regulated by ProA. As ProA and the CWI kinases MpkA and MkkA are essential for cell-cell fusion and symbiosis in *E. festucae* (Tanaka *et al.,* 2013; Becker *et al.,* 2015), *symB* and *symC* were selected as candidates for further analysis.

1.8 Cell-cell fusion a signalling network: candidate genes in *E. festucae*

A summary of the genes characterised as being involved in cell-cell fusion, fruiting body development, crippled growth and symbiosis across *E. festucae, N. crassa, S. macrospora* and *P. anserina* that are of importance to this study are listed in **Table 1.1**. Based on the research performed in these organisms a signalling pathway depicting how each homologue potentially interacts has been generated and is shown in **Figure 1.9**. This model served as a working hypothesis for this project and was used to identify candidate genes that may be required for cell fusion and symbiosis. Based on this model *E. festucae* MobC, SymB and SymC were selected for further analysis.

Table 1: Genes involved in *E. festucae* symbiosis and *S. macrospora*, *P. anserina* and *N. crassa* CAT, protoperithicium and CG formation.

E. festucae	*N. crassa*	*S. macrospora*	*P. anserina*	*S. cerevisiae*
Nox complex				
noxR [a, b, c]	*nor-1* [b, d]	*nor1* [b, d]	*IDC524/Nor1* [b-e]	-
noxA [a, b, c]	*nox-1* [b, d]	*nox1* [b, d]	*IDC384/Nox1* [b-e]	-
noxB [a, c]	*nox-2*	-	*Nox2* [c, e]	-
ham-6 [a, b]	*ham-6* [b, d]	*pro41* [b, d]	*IDC509/NoxD* [b-e]	-
racA [a, b]	*rac-1* [b, d]	-	-	-
bemA [a]	*bem1* [b]	-	-	-
cdc24[?]	*cdc24* [b]	-	-	-
Pro1 signalling				
proA [a, b]	*adv-1* [b, d]	*pro1* [b, d]	-	-
Stress MAPK signalling				
sakA [a]	*os-2*	-	-	*Hog1*
PR signalling				
mpkB[?]	*mak-2* [b, d]	-	*Mpk2* [b-e]	*Fus3*
mkkB[?]	*mek-2* [b, d]	-	*Mkk* [b-e]	*Ste7*
-	*ncr-1* [b, d]	-	*Tlk2* [b-e]	*Ste11*
idcA [a, b]	*ham-5* [b, d]	-	*IDC1* [b-e]	*Ste5*
-	*pp1* [b, d]	-	-	*Ste12*
nsiA [a, b]	-	-	-	-
CWI signalling				
so [a, b]	*so/ham-1* [b, d]	*pro40* [b, d]	*IDC821/so* [b, d, e]	*Spa2*
mpkA [a, b]	*mak-1* [b, d]	*mak1* [b, d]	*Mpk1* [b, d, e]	*Slt2*
mkkA [a, b]	*mek-1* [b, d]	*mek1* [b, d]	*IDC404/Mkk1* [b, d, e]	*Mkk1/2*
-	*mik-1* [b, d]	*pro30/mik1* [b, d]	*IDC118/Ask1* [b, d, e]	*Bck1*
STRIPAK complex				
-	*ham-2* [b, d]	*pro22* [b, d]	-	*Far11*
-	*ham-3* [b, d]	*pro11* [b, d]	-	*Far8*
mobC[?]	*mob3* [b, d]	*mob3* [b, d]	-	-
-	*pp2A* [b, d]	*pp2Ac1* [b, d]	-	*Pph21/22, Ppg1*
	pp2aa [b, d]	*pp2aa* [b, d]	-	*Tpd3*
-	*ham-4* [b, d]	*pro45* [b, d]	-	*Far9/10*
Candidate genes				
symB[?]	*ham-7* [b, d]	-	*IDC2* [b, d, e]	-
symC[?]	-	-	*IDC3* [b, d, e]	-

a Symbiosis defect
b Cell-cell fusion defect
c Expressoria/cellulose penetration defect
d Fruiting body defect
e Crippled growth defect
- Not known or not named
? Not characterised

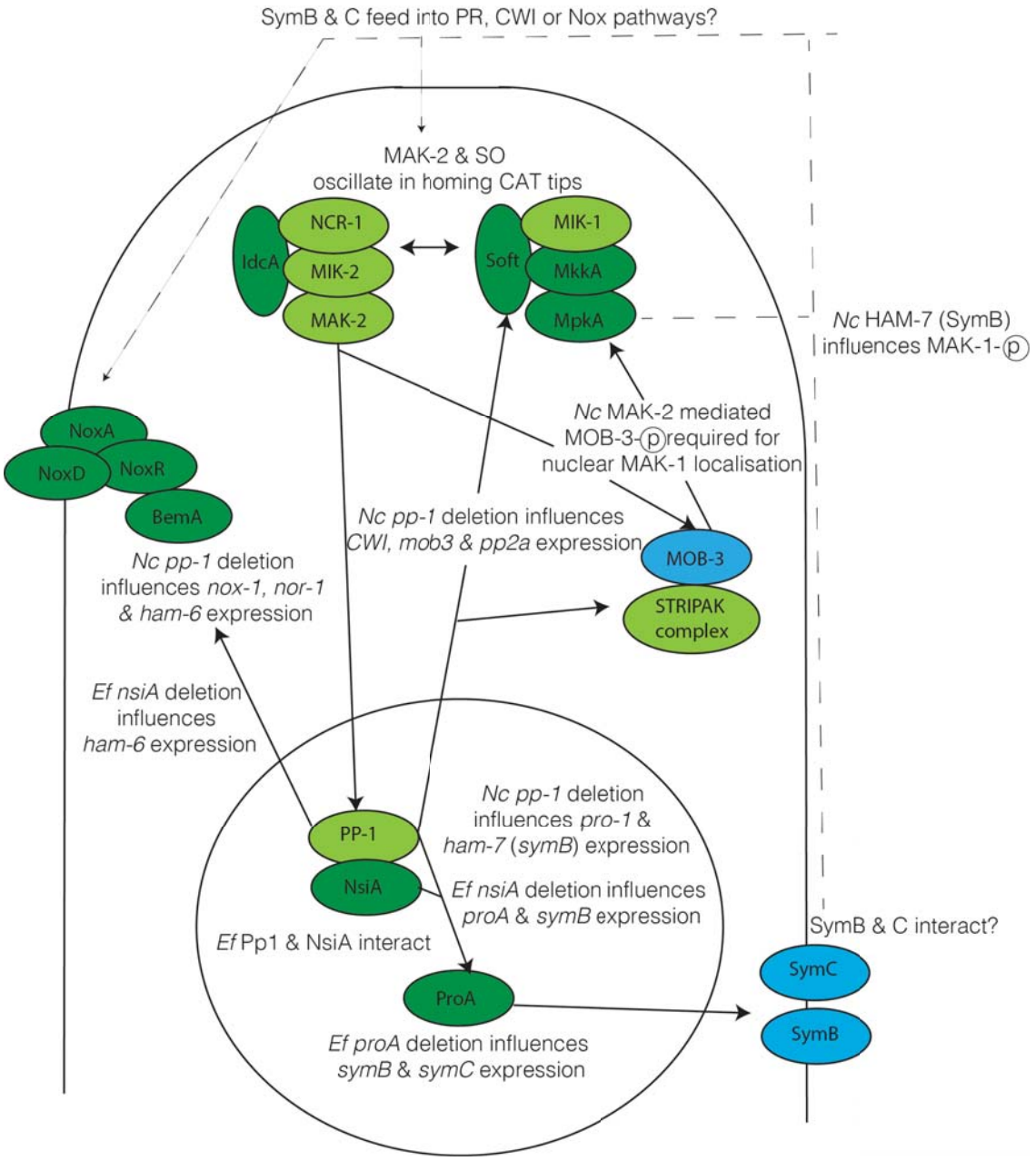

Figure 1.9 Proposed signalling network for cell-cell fusion. Proteins of interest to this study are shown in blue, homologues characterised in *E. festucae* (*Ef*) in dark green and *N. crassa* (*Nc)* homologues in light green.

1.9 Aims and Objectives

Given *E. festucae proA, noxA, noxR, mkkA, mpkA, racA* and *so* mutants all exhibit symbiosis and hyphal fusion defects, it was hypothesised that hyphal fusion is necessary for the formation of hyphal networks and regulated and restricted hyphal growth *in planta*. The aim of this study was to identify candidate proteins which may form a receptor complex or be involved in signal integration, and test their role in *E. festucae* cell-cell fusion and mutualistic symbiotic

interactions. To address this, the following objectives in relation to the STRIPAK complex and *idc2* and *idc3* homologues were pursued.

The first aim of this research was to characterise the homologue of MOB3, MobC, in *E. festucae*. This was achieved by addressing the following objectives:

1. **Identify STRIPAK complex homologues in *E. festucae* using bioinformatics tools.**
2. **Generate Δ*mobC* deletion mutants by homologous recombination.**
3. **Determine Δ*mobC* phenotypes in culture.**
   This was achieved by analysing overall colony morphology, hyphal morphology, cell-cell fusion and conidiation phenotypes in culture. Additionally the level of MpkA phosphorylation was determined by Western analysis.
4. **Determine Δ*mobC* phenotypes *in planta***.
   This was achieved by inoculating ryegrass seedlings with Δ*mobC* mycelium and analysing the host plant phenotype, and Δ*mobC* colonisation and hyphal morphology *in planta* by Confocal and Transmission Election Microscopy.
5. **Complement Δ*mobC* strains to confirm phenotypes are due to gene deletion.**
   This was achieved by transforming the *mobC* gene into Δ*mobC* protoplasts and analysing Δ*mobC*/*mobC* phenotypes in culture and *in planta.*

The second aim of this research was to characterise the homologues of IDC2 and IDC3, SymB and SymC, in *E. festucae*. This was achieved by addressing the following objectives:

1-5. **As per Δ*mobC* strains, generate and characterise Δ*symB* and Δ*symC* strains.**
6. **Determine where SymB and SymC localise.**
   This was achieved by analysing the localisation patterns of GFP-tagged SymB and mRFP1-tagged SymC proteins in culture.
7. **Determine which pathway SymB and SymC activate.**
   This was pursued using culture stress tests, Western analysis to determine the levels of MpkA and MpkB phosphorylation, and GFP tagged MpkA and MpkB localisation assays. Deletion experiments were used to determine if the C-terminus of SymC is essential for cell-cell fusion, and yeast-2-hybrid experiments used to identify proteins that interacted with this C-terminus.

2 MobC manuscript

MASSEY UNIVERSITY
GRADUATE RESEARCH SCHOOL

STATEMENT OF CONTRIBUTION
TO DOCTORAL THESIS CONTAINING PUBLICATIONS

(To appear at the end of each thesis chapter/section/appendix submitted as an article/paper or collected as an appendix at the end of the thesis)

We, the candidate and the candidate's Principal Supervisor, certify that all co-authors have consented to their work being included in the thesis and they have accepted the candidate's contribution as indicated below in the *Statement of Originality*.

Name of Candidate: Kimberly Anne Green

Name/Title of Principal Supervisor: Professor Barry Scott

Name of Published Research Output and full reference:

Green, K. A., Becker, Y., Fitzsimons, H. L., Scott, B. (2016). An Epichloë festucae homolog of MOB3, a component of the STRIPAK complex, is required for establishment of a mutualistic symbiotic interaction with Lolium perenne. Mol Plant Pathol. doi: 10.1111/mpp.12443. [Epub ahead of print]

In which Chapter is the Published Work: 2

Please indicate either:

- The percentage of the Published Work that was contributed by the candidate 80

  and / or

- Describe the contribution that the candidate has made to the Published Work:

  All experiments were performed by the candidate. The candidate prepared all figures and co-wrote the manuscript text.

Green, Kim — Digitally signed by Green, Kim Date: 2016.07.04 13:02:42 +12'00'
Candidate's Signature

15.07.16
Date

Barry Scott — Digitally signed by Barry Scott DN: cn=Barry Scott, o=Massey University, ou=PTS, email=d.b.scott@massey.ac.nz, c=NZ Date: 2016.07.15 16:50:39 +12'00'
Principal Supervisor's signature

15.07.16
Date

All methods, results and the discussion pertaining to this chapter have been included within the manuscript below, accepted for publication in Molecular Plant Pathology. The text sections included are the summary, introduction, results, figures and figure legends (embedded within the results section), discussion, experimental procedures, acknowledgements and references. The supplementary primer and biological lists and supplementary figures have been inserted directly after the references. All plasmid maps associated with this manuscript have been deposited within Chapter 7. Specific plasmid maps can be located using the list of figures found within the beginning pages of this thesis.

An *Epichloë festucae* homolog of MOB3, a component of the STRIPAK complex, is required for establishment of a mutualistic symbiotic interaction with *Lolium perenne*

KIMBERLY A GREEN, YVONNE BECKER, HELEN L FITZSIMONS and BARRY SCOTT*

Institute of Fundamental Sciences, Massey University, Palmerston North, New Zealand

*Corresponding author: Barry Scott

SUMMARY

In both *Sordaria macrospora* and *Neurospora crassa* components of the conserved STRIPAK complex regulate cell-cell fusion, hyphal network development and fruiting body formation. Interestingly, a number of *Epichloë festucae* genes that are required for hyphal cell-cell fusion, such as *noxA, noxR, proA, mpkA* and *mkkA,* are also required for establishment of a mutualistic symbiotic interaction with *Lolium perenne*. To determine whether MobC, a homolog of the STRIPAK complex component MOB3 in *S. macrospora* and *N. crassa*, is required for *E. festucae* hyphal fusion and symbiosis a *mobC* deletion strain was generated. The Δ*mobC* mutant had reduced rates of hyphal cell-cell fusion, formed intra-hyphal hyphae and had enhanced conidiation. Plants infected with Δ*mobC* were severely stunted. Hyphae of Δ*mobC* had a proliferative pattern of growth within the leaves of *Lolium perenne* with increased colonisation of the intercellular spaces and vascular bundles. While hyphae were still able to form expressoria, structures allowing colonisation of the leaf surface, the frequency of formation was significantly reduced. Collectively these results show that the STRIPAK component MobC is required for establishing a mutualistic symbiotic association between *E. festucae* and *L. perenne* and has an accessory role in regulating hyphal cell-cell fusion and expressorium development in *E. festucae*.

INTRODUCTION

Filamentous fungi exhibit complex life cycles. Numerous temporal and spatial cellular changes are required for progressive spore germination, septation, cell-cell fusion and the development of sexual and pathogenic structures such as fruiting bodies and appressoria. The characterisation of several protoperithecia (*pro*) mutants in *Sordaria macrospora*, and *pro* homologues in other fungi, has revealed that components of the fungal Striatin-interacting phosphatase and kinase (STRIPAK) complex are required for multiple developmental processes and appear to coordinate cross-talk between different signalling pathways, indicating that they have evolved diverse regulatory functions (Kück *et al.*, 2016).

The STRIPAK complex in *Sordaria* consists of several proteins, the Striatin scaffold protein, PRO11; Striatin-interacting protein, PRO22; kinase activator MOB3; GPI anchored protein GPI1; serine/threonine phosphatase PP2A subunits A and C; germinal centre kinases, KIN3 and KIN23; the sarcolemmal membrane-associated protein, PRO45; as well as several other accessory proteins (Bloemendal *et al.*, 2012, Frey *et al.*, 2015a, Frey *et al.*, 2015b, Nordzieke *et al.*, 2015). Mutant analysis of these components and their respective homologues HAM-3 (PRO11), HAM-2 (PRO22), MOB-3 (MOB3), HAM-4 (PRO45) and PP2A-A & PPG-1 (PP2A subunits) in *Neurospora crassa* has shown that components of the STRIPAK complex are required for cell-cell fusion and sexual fruiting body development (Pöggeler & Kück, 2004, Maerz *et al.*, 2009, Simonin *et al.*, 2010, Fu *et al.*, 2011, Bloemendal *et al.*, 2010, Bloemendal *et al*., 2012, Read *et al.*, 2012, Frey *et al*., 2015a, Frey *et al*., 2015b, Bernhards & Pöggeler, 2011, Nordzieke *et al*., 2015, Dettmann *et al.*, 2013). Additionally PRO22, KIN3 and KIN24 are associated with septation (Bloemendal et al., 2010, Frey *et al*., 2015b) and homologues of PRO11 in *Fusarium verticillioides* (Fsr1), *Aspergillus nidulans* (StrA) and *Colletotrichum graminicola* (Str1), are associated with altered radial growth, ascosporogenesis and virulence (Wang *et al.*, 2010, Wang *et al.*, 2016, Yamamura & Shim, 2008).

In *Sordaria*, GPI1 localises to the plasma membrane, PRO45 to the nuclear membrane, PRO45/GPI1 to mitochondria and KIN3 and KIN24 to septal pores, while in *N. crassa,* HAM-2 and HAM-3 localise to the nuclear envelope (Bloemendal *et al*., 2010, Dettmann *et al*., 2013, Frey *et al*., 2015a, Frey *et al*., 2015b, Nordzieke *et al*., 2015). A correct localisation pattern of HAM-2 and HAM-3 is required for MAK-1 (cell wall integrity (CWI) pathway MAP kinase) nuclear accumulation in a MAK-2 (pheromone response (PR) pathway MAP kinase) dependent manner, as MAK-2 is required for phosphorylation of the STRIPAK component MOB3 (Dettman *et al.,* 2013). These results demonstrate that the STRIPAK complex components exhibit multiple temporal and spatial localisation patterns, and play integral roles in transmitting

signals from both the CWI- and PR-MAP kinase pathways, which in turn regulate multiple downstream developmental signalling pathways.

Epichloë festucae forms mutualistic symbiotic relationships with species of cool-season grasses such as *Festuca* and *Lolium*, by both systemic colonisation of the intercellular spaces within the host leaves and by colonisation of the leaf surface via epiphyllous growth (Christensen *et al.*, 2008, Schardl, 1996, Clay & Schardl, 2002). Mutations in genes encoding components of the Nox complex (*noxA* or *noxR)*, cell wall integrity (CWI) MAP kinases and scaffold (*mpkA*, *mkkA* and *so*), as well as the transcription factor *proA*, abolish cell-cell fusion in culture and trigger proliferative pathogenic-like hyphal growth *in planta* (Tanaka *et al.*, 2006, Tanaka *et al.*, 2008, Tanaka *et al.*, 2013, Takemoto *et al.*, 2006, Takemoto *et al.*, 2011, Charlton *et al.*, 2012, Becker *et al.*, 2015). The co-association of these phenotypes leads to the hypothesis that cell-cell fusion is required for the maintenance of a mutualistic symbiotic interaction between this fungal endophyte and the host grass.

Given the STRIPAK complex is important for cell-cell fusion in *N. crassa* and *S. macrospora* (Bloemendal *et al*., 2012, Dettmann *et al*., 2013), but has not been investigated in *E. festucae*, we set out to first identify if the STRIPAK complex members were conserved in *E. festucae* and then to test whether the homologue of the STRIPAK complex component MOB3 has a role in *E. festucae* hyphal cell-cell fusion and maintenance of a mutualistic symbiotic interaction with the plant host *Lolium perenne*.

RESULTS

E. festucae contains homologues of the STRIPAK complex

To determine whether *E. festucae* contains components of the STRIPAK complex a tBLASTn search of the genome sequence was carried out using *S. macrospora* PRO11, PRO22, PRO45 and MOB3 as the query sequences. The *E. festucae* homologues identified were aligned with the *S. macrospora* sequences as well as the corresponding polypeptide sequences from *Fusarium graminearum, Magnaporthe oryzae, Neurospora crassa* and *Podospora anserina* (**Figs. S1-4**). The *E. festucae* homologues share 70% and 69% identity to *S. macrospora* and *N. crassa* PRO11 and HAM-3, 61% and 62% identity to PRO22 and HAM-2, 57 and 51% identity to PRO45 and HAM-4, and 48% and 51% identity to MOB3 and MOB-3, respectively. In addition they contain all of the conserved domains found in these proteins suggesting that *E. festucae* contains a functional STRIPAK complex. In particular MobC contains a MOB domain, serine and threonine phosphorylation domains, a Cys2-His2 Zn^{2+} binding domain and a SH3 binding domain, suggesting MobC participates in protein phosphorylation and protein-protein interactions. In *S. macrospora* re-introduction of the N-terminal MOB3 domain complements

the *mob3* mutant defects while introduction of the C-terminal domain does not (Bernhards & Pöggeler, 2011). These findings may explain the variability in the sequence of the C-terminus observed between MOB3 homologues.

To investigate the role of the STRIPAK complex in regulating *E. festucae* hyphal cell-cell fusion and the interaction of this endophyte with its host *L. perenne* we deleted the homologue of *mob3*, which we have named *mobC*, by transforming protoplasts of *E. festucae* with a restriction enzyme-generated linear fragment of pKG4 (**Fig. S5a**). PCR screening of fifty geneticin-resistant (Gen^R) transformants identified six (Δ*mobC*#21, 28, 31, 37, 38 & 40) that produced banding patterns consistent with targeted replacement events (**Fig. S5b**). Southern analysis of genomic DNA digests from these transformants confirmed that just two (Δ*mobC*#21 and #37) were single copy 'clean' replacements at the *mobC* locus (**Fig. S5c**). Based on these results these two strains were selected for further experiments.

Culture phenotype of Δ*mobC*

The culture morphology and radial growth of Δ*mobC* mutants on PD agar was indistinguishable from wild-type (WT) (**Fig. 1a**), however, light microscopy revealed that the Δ*mobC* mutants produced intra-hyphal hyphae (IHH) (**Fig. 1b**), a phenotype that has never been observed in WT cultures. In addition Δ*mobC* mutants had significantly more conidia than WT (**Figs. 2a & 2c**), a phenotype complemented by the reintroduction of the wild-type gene (**Fig. 2c**). Surprisingly, whereas *mob3* deletion mutants in *S. macrospora* and *N. crassa* are completely defective in cell-cell fusion (Kück *et al*., 2016, Bernhards & Pöggeler, 2011, Maerz *et al*., 2009), the *E. festucae* Δ*mobC* strains were still capable of undergoing hyphal cell-cell fusion, albeit at a 2-3 fold lower frequency than that of WT (**Figs. 2b & d**). Introduction of a wild-type copy of *mobC* into Δ*mobC* restored the wild-type fusion phenotype confirming complementation of this mutant (**Figs. 2d & S5**). These results suggest that MobC plays an accessory role in negatively regulating conidiation and positively regulating hyphal fusion in *E. festucae.*

To test whether deletion of *mobC* affected basal level phosphorylation of the MpkA (cell wall integrity) and MpkB (pheromone response) MAP kinases, the phosphorylation status of each was analysed by western analysis (**Fig. S6**). Two bands were detected in wild-type, corresponding to phosphorylated MpkA at 47 kDa and phosphorylated MpkB, the Fus3 homolog, at 41 kDa. While MpkA phosphorylation was not detected in the Δ*mpkA* and Δ*mkkA* cell wall integrity kinase mutants (Becker *et al*., 2015), both MpkA and MpkB phosphorylation still occurred in the Δ*mobC*#21 and Δ*mobC*#37 mutants, with bands of similar intensity to wild-type.

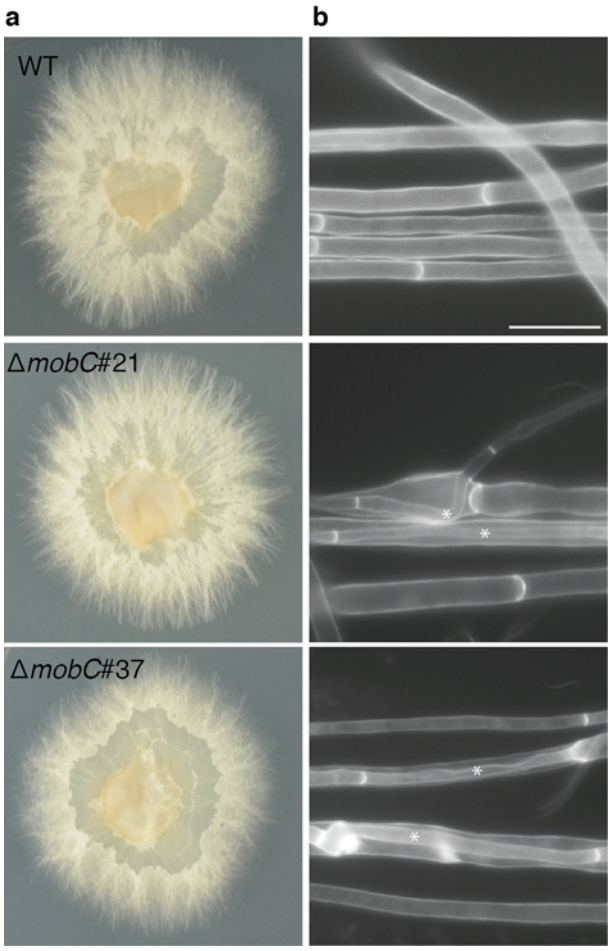

Fig. 1 Culture phenotype of Δ*mobC* and wild-type strains. (a) Colony morphology of cultures grown on PD agar for 7 days. (b) Fluorescent images of hyphae grown for 7 days on water agar and stained with Calcofluor white. An asterisk indicates intra-hyphal-hyphae (IHH) in Δ*mobC* mutants. Bar = 10 μm.

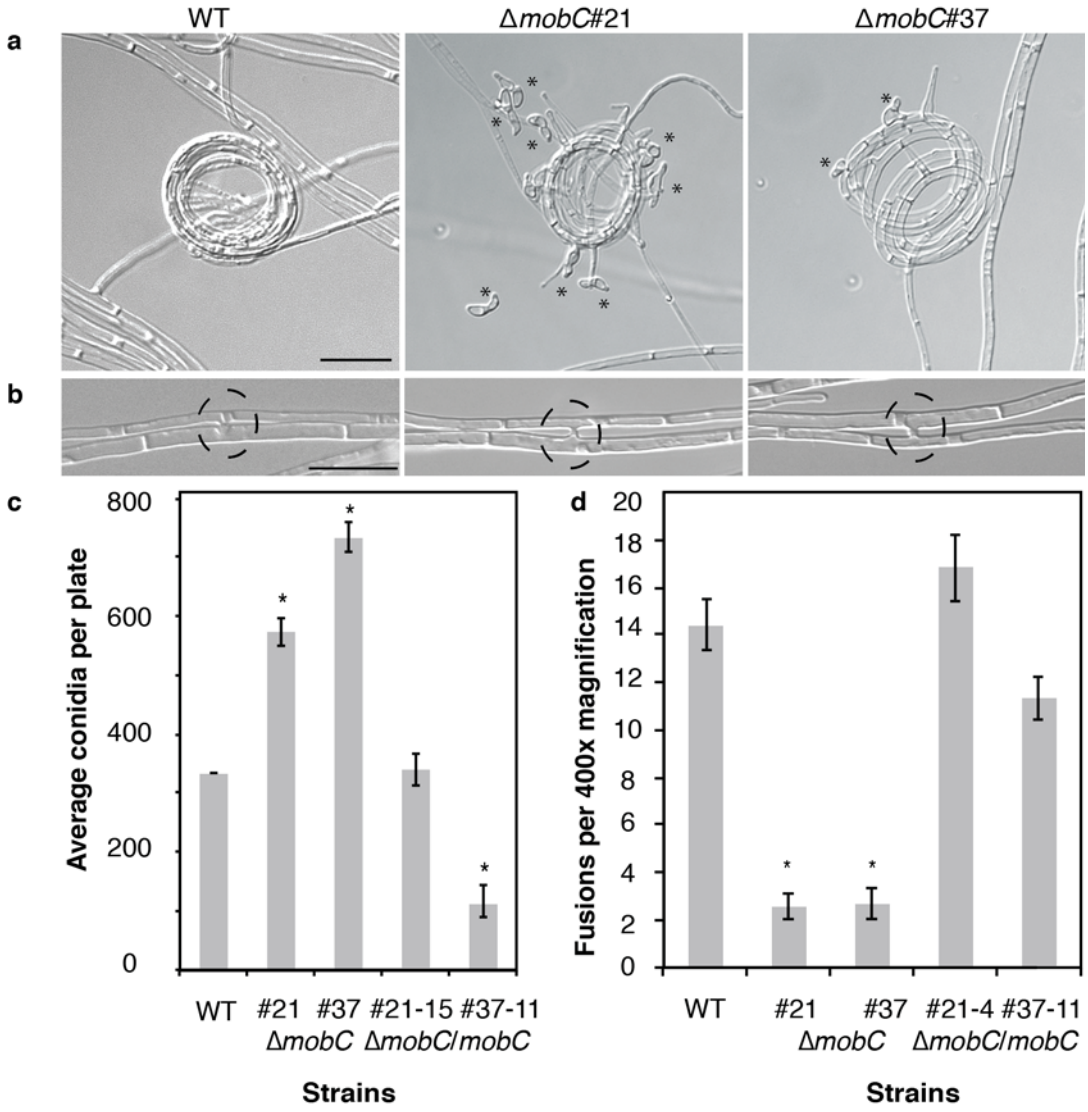

Fig. 2 Conidiation and cell-cell fusion phenotype of Δ*mobC*. (a) DIC images of Δ*mobC* cultures undergoing hyper-conidiation on 1.5% water agar after 7 days. Conidia are marked with an asterisk. Bar = 20 µm. (b) DIC images of cell-cell fusions in culture as indicated by the circles. Bar = 10 µm. (c) Quantification of single colonies recovered from 300 µL wild-type, Δ*mob*C and Δ*mob*C/*mobC* complemented conidia suspensions recovered from a total of 15 cultures grown on PD plates for 7 days. Bars represent ± standard error (*n*=3). An asterisk indicates significant differences from WT as determine by Welch's *t* test. (d) Average cell-cell fusions observed per ×40 objective lens magnification field. Bars represent mean ± standard error (*n*=10). An asterisk indicates significant differences from WT as determined by Welch's *t* test.

Symbiotic interaction phenotype of Δ*mobC*

Given IHH formation and hyperconidiation are phenotypes shared among many *E. festucae* symbiosis mutants (Becker *et al.*, 2015, Tanaka *et al.*, 2013), we next tested whether *mobC* is required for the symbiotic interaction of *E. festucae* with *L. perenne*. Plants infected with Δ*mobC* were severely stunted compared to wild-type infected plants (**Fig. 3a & Supplementary Table 3**). While there were no significant differences in the number of tillers per plant between wild-type and Δ*mobC* infected plants, both tiller length and root length were significantly reduced (**Fig. S7**). Introduction of a wild-type copy of *mobC* into the Δ*mobC* background rescued the wild-type symbiotic interaction phenotype (**Fig. 3a & Fig. S7**). To evaluate the cellular phenotype of plants infected with Δ*mobC*, we harvested leaf sheath tissue samples and examined a range of phenotype parameters by transmission electron microscopy (TEM) (**Fig. 4**) and confocal laser scanning microscopy (CLSM) (**Fig. 5**). We observed extensive hyphal colonisation in Δ*mobC*-infected plants, with up to six hyphae per intercellular space in the mesophyll tissue. In contrast, wild-type associations contained mostly one to two hyphae per intercellular space (**Fig. 3b & Fig. 4a**). In addition, the Δ*mobC* hyphae were frequently vacuolated (**Fig. 4c**), a subset of hyphae contained IHH (**Fig. 4d**), with the outer cell walls appearing less electron dense (**Fig. 4e**). Hyphae of Δ*mobC* were also very abundant in the vascular bundle tissue (**Fig. 4b**), which is seldom, if ever, colonised by wild-type hyphae. Hyphae in these tissues were electron dense presumably reflecting the abundant supply of nutrients in these tissues for growth.

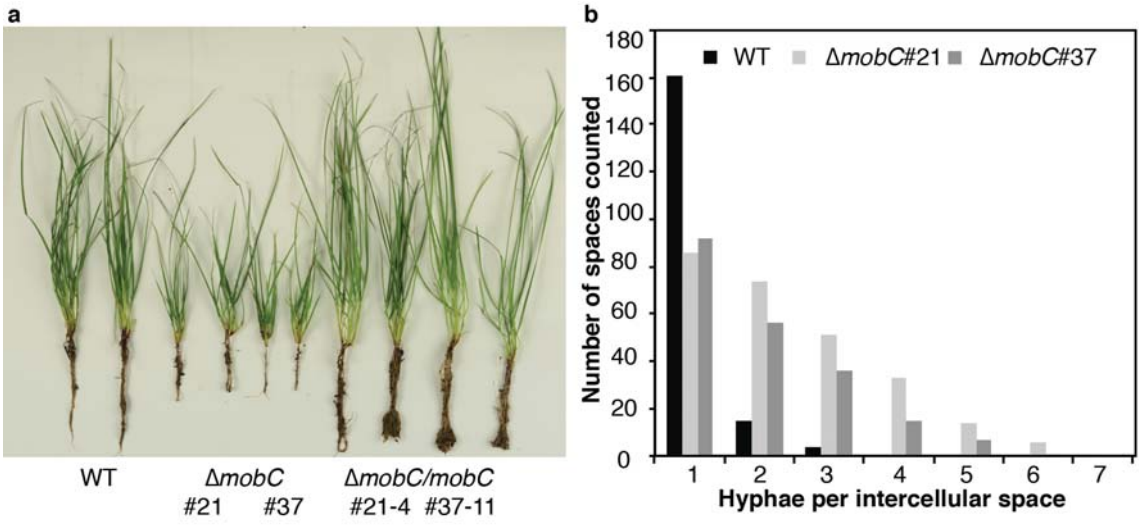

Fig. 3 Plant interaction phenotype of Δ*mobC*. (a) Phenotype of infected *Lolium perenne* plants at 10 weeks post inoculation. (b) Number of hyphae within the intercellular spaces of the outer most leaf of 10 leaf sheath cross sections fields observed at ×100 objective lens magnification using light microscopy.

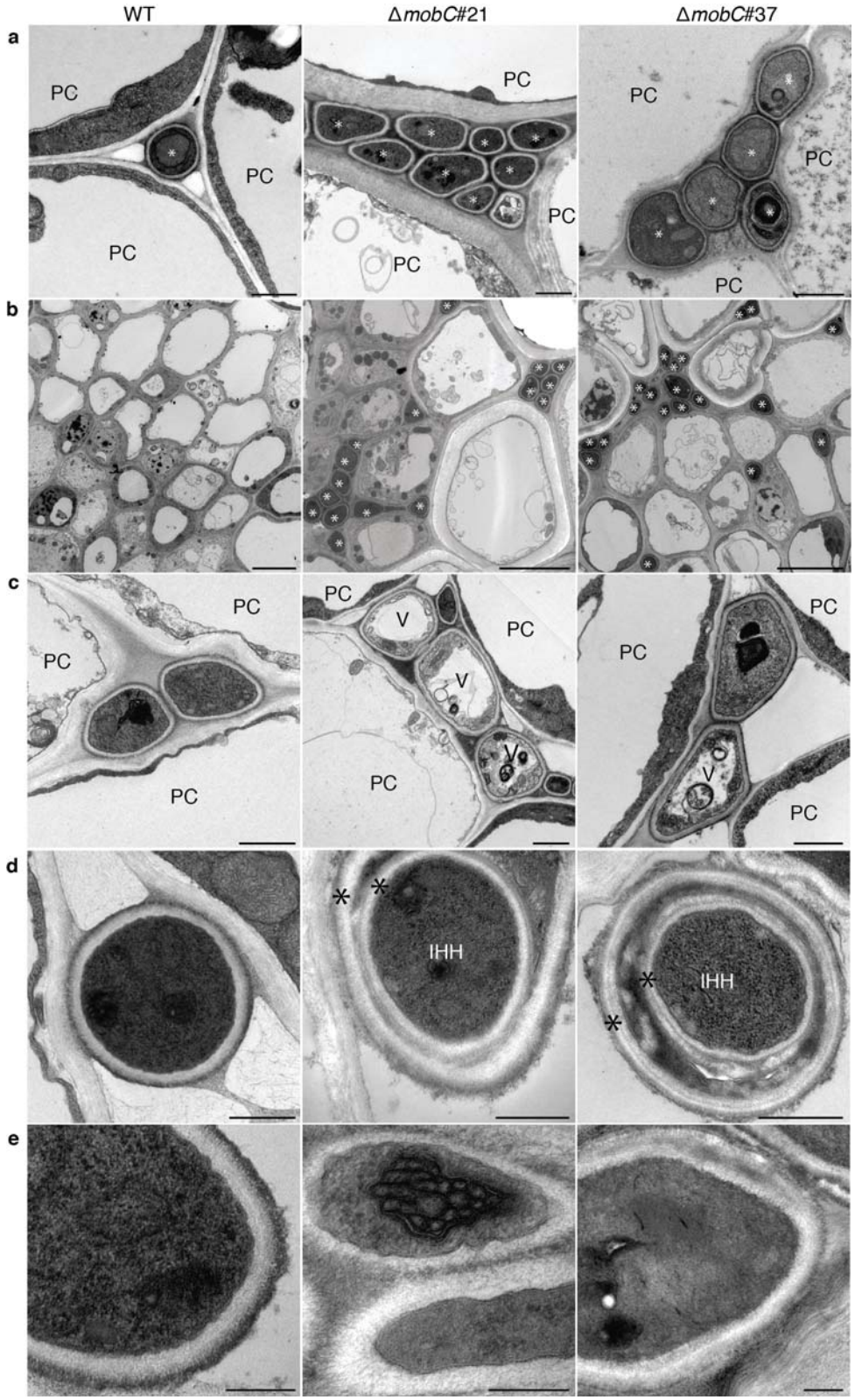

Fig. 4 Transmission electron micrographs of *L. perenne* leaf sheath cross sections infected with wild-type and Δ*mobC* strains. (a) Hyphae growing within the intercellular spaces between plant cells (PC). Hyphae are marked with an asterisk. Bar = 1 µm. (b) Vascular bundle colonisation. Bar = 5 µm. (c) Highly vacuolated (V) mutant hyphae within the intercellular spaces. Bar = 1 µm. (d) Mutant intra-hyphal hyphae (IHH) formation. Bar = 500 nm. (e) Altered mutant hyphal cell wall. Bar = 200 nm.

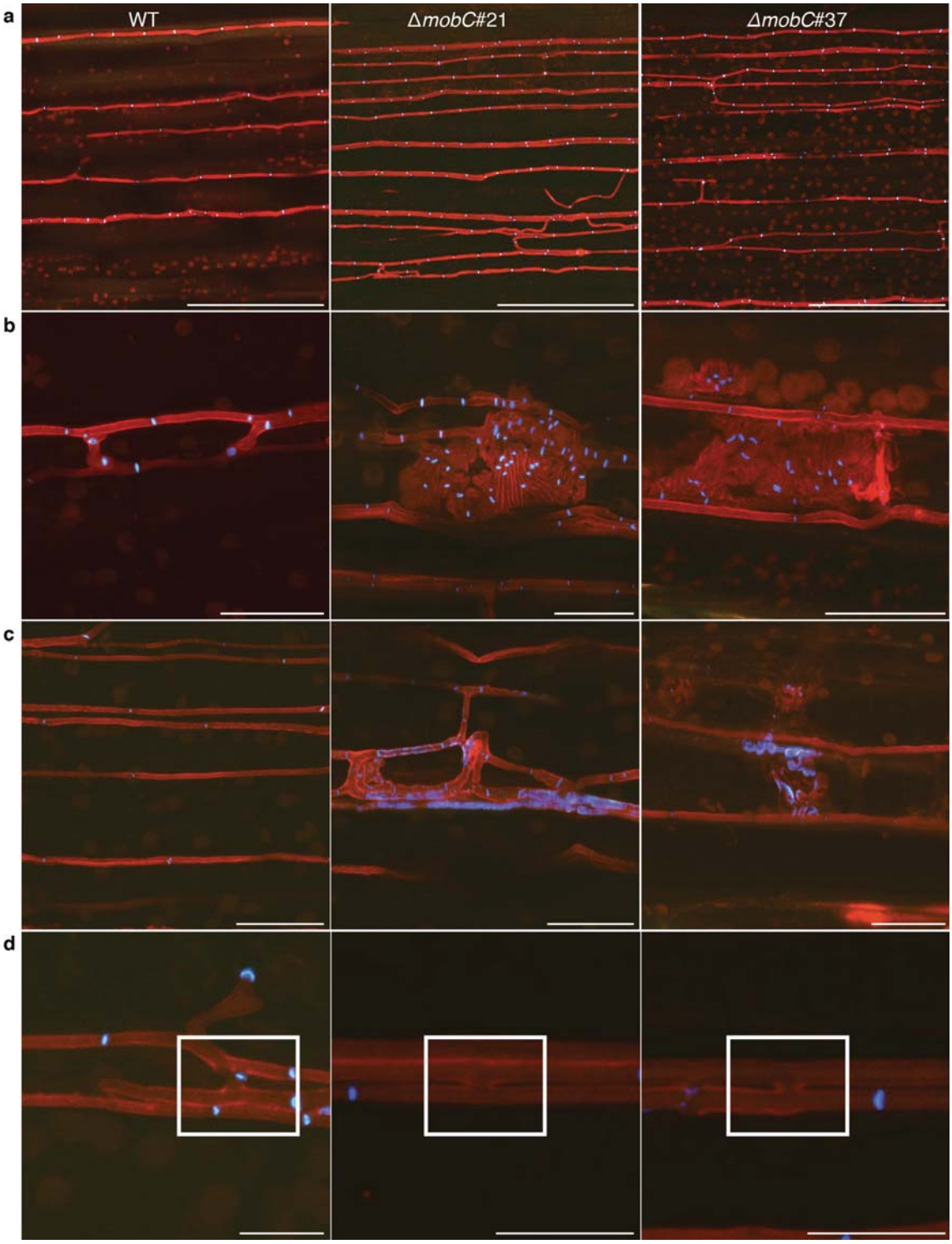

Fig. 5 Confocal depth series images of aniline blue/WGA-AF488 stained *L. perenne* leaf sheaths infected with wild-type and Δ*mobC* strains. (a) Maximun projection of compressed z-stacks (10 μm) showing increased Δ*mobC* hyphal biomass. Endophytic hyphae show aniline blue fluorescence of β-glucans captured with red pseudocolour and chitin staining of septa captured by WGA-AF488 fluorescence in blue pseudocolour. Bar = 100 μm. (b) Aberrant hyphal structures observed in Δ*mobC* associations. Bar = 25 μm. (c) Delocalised WGA-AF488 fluorescence in Δ*mobC* hyphae. Bar = 25 μm. (d) Hyphal fusions *in planta* as indicated in boxes. Bar = 10 μm.

The prolific growth of the Δ*mobC* mutant in leaf sheath tissue compared to the more restrictive growth of the wild-type was also evident from CLSM analysis of leaf sheath tissue stained with aniline blue (orange/red pseudocolour) and WGA-AF488 (blue pseudocolour), which stain β-glucan and chitin, respectively (**Fig. 5a**). Not only were the Δ*mobC* hyphae more abundant than wild-type hyphae but they also formed aberrant convoluted hyphal structures comprised of many cells as evident from the many fluorescent septa (**Fig. 5b**) and exhibited patchy chitin staining (**Fig. 5c**). Despite these dramatic changes in growth within the plant, Δ*mobC* hyphae were still capable of forming cell-cell fusions *in planta* (**Fig. 5d**).

mobC has an accessory role in regulating _E. festucae_ expressorium formation

Endophytic *E. festucae* hyphae exit the host cuticle layer, via an expressorium, to form an epiphyllous hyphal network on the surface of the host plant. Formation of these structures requires functional NADPH oxidase NoxA and NoxB complexes (Becker *et al.*, 2016). The inability of *nox* mutants to develop expressoria results in the formation of extensive sub-cuticular growth of hyphae, which eventually breach the surface of the leaves. Given the role of NoxA and NoxB in the development of expressoria in *E. festucae – L. perenne* associations, leaf sheath tissues infected with the Δ*mobC* mutant were examined by CLSM for the formation of these structures (**Fig. 6**). Although a few expressoria were identified (**Fig. 6b & e**), the more common phenotype was extensive sub-cuticular growth of Δ*mobC* (**Fig. 6c & f**), suggesting these strains were not fully competent to develop expressoria (**Fig. 6**). The frequency of expressoria formation in leaf tissue infected with Δ*mobC* was significantly lower than in wild-type (**Fig. S8a**). Instead mutant associations had a much greater frequency of sub-cuticular hyphae (**Fig. S8b**) that were found to eventually rupture the cuticle of the leaf (**Fig. S8c**). These results suggest MobC has an accessory role in regulating the differentiation of *E. festucae* expressoria. An additional observation was the occasional emergence of hyphae through stomata (**Fig. 6i**). However, once on the cell surface the cell walls of mutant hyphae, like wild-type hyphae, are remodeled with both cell wall and septa binding WGA-AF488 (captured in blue pseudocolour), whereas just septa of endophytic hyphae bind WGA-AF488 *in planta* (Becker *et al.*, 2016).

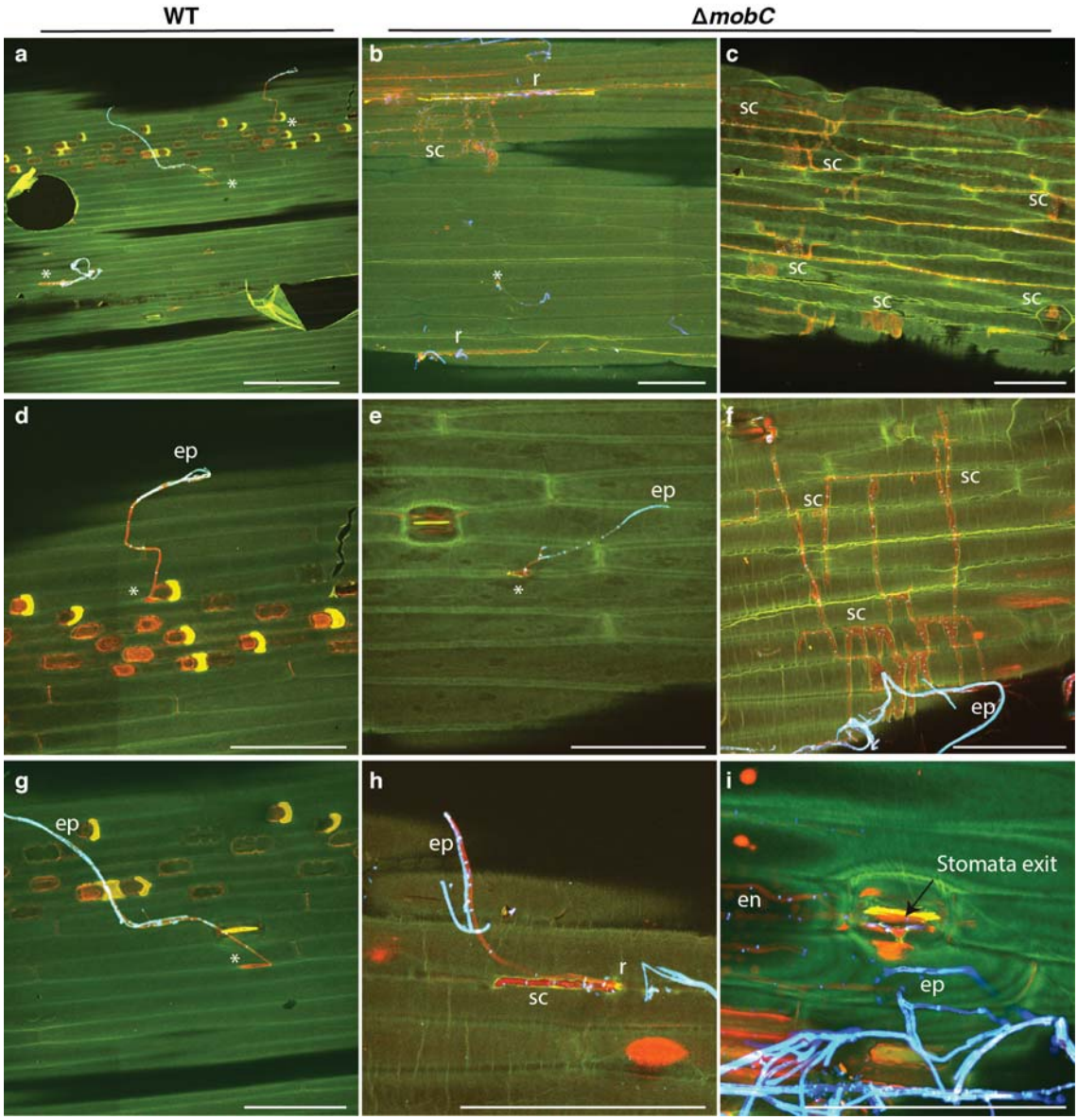

Fig. 6 Confocal depth series images of wild-type and Δ*mobC* expressoria and sub-cuticular hyphae within *L. perenne* associations. Representative images of the surface of the host leaf sheath infected with (a, d & g) WT and (b, c, e, f, h & i) Δ*mobC* strains. Representative images demonstrating the diversity of Δ*mobC* infection phenotypes where either (b) sub-cuticular hyphae (sc), expressoria (*) and rupture (r) points can be observed or (c) only sc hyphae compared to (a) WT. Bar = 200 µm. Zoomed in images of expressoria formation in (d & g) WT and (e) Δ*mobC* strains and (f) sc aberrant hyphal structures in Δ*mobC* , (h) points of rupture (r) and (i) stomata exit (se) in Δ*mobC* Bar = 100 µm. Fluorescence of endophytic hyphae captured by aniline blue fluorescence of stained β-glucans in red pseudocolour. Septa and epiphyllous hyphae (ep) captured by WGA-AF488 fluorescence in blue pseudocolour, soon after exiting the host cuticle layer captured with green pseudocolour.

DISCUSSION

E. festucae, NoxA, NoxR, So, ProA, MpkA and MkkA, are required for cell-cell fusion in culture and hyphal network formation *in planta*. These findings gave rise to the hypothesis that cell-cell fusion regulates and restricts hyphal growth in *planta* and is required for establishment of a mutualistic association (Takemoto *et al*., 2006, Takemoto *et al*., 2011, Tanaka *et al*., 2006, Tanaka *et al*., 2013, Tanaka *et al*., 2008, Becker *et al*., 2015, Charlton *et al*., 2012). Here we show that *E. festucae* MobC, the homologue of the *S. macrospora* STRIPAK complex component MOB3, is essential for maintaining a mutualistic symbiotic interaction between *E. festucae* and *L. perenne* and has an accessory role in regulating cell-cell fusion and expressoria formation.

In culture *E. festucae* hyphal strands adhere to one another to form cables, which extend outwards from the colony centre. Cell-cell fusion within these cables occurs by tip-to-side fusion events that are easy to observe and quantify using light microscopy (Becker *et al*., 2015). To date we have not been able to test whether cell-cell fusion mutants of *E. festucae* are also defective in fruiting body development as the sexual cycle of *E. festucae* is highly complex and only occurs on the plant host and requires a third symbiont, a *Botanophila* fly, to transfer spermatia from a stroma of one mating type to a stroma of the opposite mating type (Bultman & Leuchtmann, 2009). In contrast, *S. macrospora* and *N. crassa* readily form fruiting bodies in culture enabling phenotype analysis of cell communication mutants in both the vegetative and reproductive stages of development (Roca *et al*., 2005, Fleißner *et al*., 2009, Kück *et al*., 2009, Teichert *et al*., 2014, Engh *et al*., 2010). In *E. festucae* deletion of *mobC* results in a reduction in cell-cell fusion but does not completely abolish it as is the case in *S. macrospora* and *N. crassa* (Bernhards & Pöggeler, 2011, Maerz *et al*., 2009), suggesting MobC may be less tightly regulated in *E. festucae* than in *S. macrospora* and *N. crassa* which have different life cycles.

In culture, *E. festucae* conidiation is sparse whereas Δ*proA,* Δ*noxA,* Δ*mpkA* and Δ*mkkA* mutants have a hyper-conidiation phenotype and a loss of cell-cell fusion suggesting that the regulatory circuits controlling these two phenotypes are linked (Tanaka *et al*., 2013). Additionally, Δ*mpkA* and Δ*mkkA* mutants form IHH, structures that have not been observed in the wild-type strain (Becker *et al*., 2015). Deletion of *mobC* in *E. festucae* also results in an increase in conidiation and IHH formation. In contrast, deletion of *mek-1* and *mak-1* and the STRIPAK complex genes *ham-3* and *mob3* in *N. crassa* and *ham-3* homologues *strA* in *Aspergillus nidulans* and *str1* in *Colletotrichum graminicola* reduces both conidiation and cell-cell fusion indicating that the regulatory circuits for these developmental processes are 'wired' differently in these fungi (Park *et al*., 2008, Maerz *et al*., 2009, Simonin *et al*., 2010, Wang *et al*., 2010, Wang *et al*., 2016). In addition, no change was observed in the basal phosphorylation

levels of MpkA (cell wall integrity) and MpkB (pheromone response) kinases in the Δ*mobC* mutant. Given the pleiotropic nature of the Δ*mobC* mutation, it is difficult to determine whether the Δ*mobC* hyperconidiation and IHH formation phenotypes observed are a direct effect of the *mobC* deletion or an indirect effect. Cell-cell fusion is important for colony nutrient transfer and the reduction or loss of fusion may induce starvation and impair the transport of nutrients to isolated hyphae.

In the grass host, *E. festucae* hyphae absorb nutrients directly from the inter-cellular spaces of the leaves. Mutations that result in prolific growth *in planta* or disrupt the formation of the hyphal network are likely to trigger a starvation response. This is most likely due to multiple hyphae per inter-cellular space requiring and absorbing an excess of nutrients from the apoplast or from the loss of the hyphal network, impairing nutrient transfer between hyphae. Analysis of the genes up- and down-regulated in the Δ*proA,* Δ*noxA* and Δ*sakA* associations is consistent with this hypothesis (Eaton *et al.*, 2015). The genes that are significantly up-regulated in all three mutant associations include those involved in primary metabolism, peptide and sugar transport, and host cell wall degradation. Key genes that are down-regulated in this core gene set include genes involved in secondary metabolism and some genes that encode small secreted proteins.

As previously reported for the Δ*proA,* Δ*noxA,* Δ*sakA,* and Δ*sidN* mutants (Johnson *et al.*, 2013, Tanaka *et al*., 2013, Tanaka *et al*., 2006, Eaton *et al.*, 2010), Δ*mobC* also forms a pathogenic-like interaction with *L. perenne*; IHH are frequently observed, as is vascular bundle colonisation and breakdown of the hyphal network in the leaves. Although some cell-cell fusions were observed *in planta* the presence of highly convoluted hyphal structures in the intercellular spaces of Δ*mobC*-infected plants suggests that cell-cell fusion may also be impaired within the host. Interestingly, Δ*mobC* hyphae within the vascular bundles are electron dense, suggesting they are much healthier than the mutant hyphae growing in the intercellular spaces. This location-specific phenotype observed for the Δ*mobC* mutant is consistent with the hypothesis that prolific growth together with impaired hyphal fusion triggers a starvation response in hyphae located outside of the nutrient rich vascular bundles (Eaton *et al*., 2015, Becker *et al*., 2015).

The homologue of PRO11, *str1,* in *Colletotrichum graminicola* is required for full virulence in maize and although Δ*str1* strains produce functional appressoria, infection and further colonisation are attenuated (Wang *et al*., 2016). Unlike pathogens, *E. festucae* is not known to colonise leaves by formation of appressoria-like structures on the leaf surface. However, a recent study has shown that *E. festucae* does form appressoria-like structures, named expressoria, that allow endophytic hyphae to breach the cuticle from the inside of the

leaf to form a net of epiphyllous hyphae on the surface of the leaf. Deletion of *noxA* and *noxR* abolishes expressoria formation in *E. festucae*, and instead, the mutant hyphae form convoluted branched structures under the surface of the leaf cuticle (Becker *et al*., 2016). Although some wild-type-like expressoria structures were observed on the adaxial surface of *L. perenne* leaves infected with the Δ*mobC* mutant, more commonly sub-cuticular, highly convoluted structures were observed, suggesting that MobC is important but not absolutely required for expressoria development. In this regard the Δ*mobC* mutant of *E. festucae* is very similar to the *str1* mutant of *Colletotrichum graminicola* (Wang *et al*., 2016).

In conclusion, *E. festucae* contains highly conserved PRO11, PRO22, PRO45 and MOB3 homologues suggesting that this fungal endophyte has a functional STRIPAK complex. A phenotype analysis of the *E. festucae* Δ*mobC* mutant showed that MobC is essential for maintaining a mutualistic symbiotic interaction between *E. festucae* and *L. perenne* and has an accessory role in regulating cell-cell fusion and expressorium development. The Δ*mobC* mutant phenotypes observed are similar to those previously reported for mutants, Δ*mpkA* and Δ*mkkA*, in the cell wall integrity MAP kinase signalling pathway (Becker *et al*., 2015), suggesting MobC, MpkA and MkkA are involved in the same signalling pathway. Whether, *E. festucae* MobC is directly linked to the CWI MAP kinase pathway, as proposed for *N. crassa* (Dettmann *et al*., 2013), remains to be tested.

EXPERIMENTAL PROCEDURES

Strains and growth conditions

Cultures of *Escherichia coli* were grown overnight in LB (Luria-Bertani) broth or on 1.5% LB agar containing 100 μg/mL ampicillin as previously described (Miller, 1972). Cultures of *E. festucae* were grown on either 2.4% (w/v) potato dextrose (PD), 1.5% water agar plates or in PD broth as previously described (Moon *et al.*, 1999, Moon *et al.*, 2000).

Plant growth and endophyte inoculation conditions

Endophyte-free seedlings of perennial ryegrass (*Lolium perenne* cv. Samson) were inoculated with *E. festucae* (Latch & Christensen, 1985). Plants were grown in root trainers in an environmentally controlled growth room at 22°C with a photoperiod of 16 h of light (~100 $\mu E/m^2$ per sec) and at 8 weeks post inoculation, tested for the presence of the endophyte by immunoblotting (Tanaka *et al.,* 2005).

DNA isolation, PCR and sequencing

Plasmid DNA from *E. coli* cultures was extracted using the High Pure Plasmid Isolation Kit (Roche) according to the manufacturer's instructions. Fungal genomic DNA used for

Southern analysis was extracted from freeze-dried mycelium as previously described (Byrd *et al.,* 1990). Standard PCR amplification was performed with *Taq* DNA polymerase (Roche) as per the manufacturer's instructions in a 50 µL volume. Where proofreading activity was required Phusion High-Fidelity DNA Polymerase (Thermo Scientific) was used as per the manufacturer's instructions in a 50 µL volume. Sequencing reactions were performed using the dideoxynucleotide chain termination method with the Big-Dye™ Terminator Version 3.1 Ready Reaction Cycle Sequencing Kit (Applied BioSystems) and separated using an ABI3730 genetic analyzer (Applied BioSystems). Sequence data was then assembled and analyzed using the MacVector sequence assembly software, Version 12.0.5.

Preparation of deletion and complementation constructs

Lists of all plasmids and the primer sequences used to prepare constructs can be found in Tables S1 and S2.

The *mobC* replacement construct pKG4 was prepared by Gibson Assembly (Gibson *et al.*, 2009) using PCR amplified pRS426 vector (primers pRS426F and R), 1.2-kb 5' (primers KG45 and 46) and 1.5-kb 3' (primers KG47 and 48) *mobC* flanking sequences amplified from *E. festucae* genomic Fl1 DNA, and a 1.7-kb geneticin resistance cassette (primers genF and R), amplified from pII99 plasmid DNA. The *in vitro* recombined DNA mixture was transformed into chemically competent *E. coli* DH5α cells and ampicillin-resistant transformants screened using Clonechecker for plasmids with restriction enzyme digest patterns predicted from *in silico* construction of pKG4. The order of the fragments within these clones was verified by DNA sequencing. The *mobC* replacement fragment contained within pKG4 was excised by *Xho*I digestion, gel purified and then transformed into *E. festucae* protoplasts as described below using Gen^R selection.

The *mobC* complementation construct pKG8 was prepared by Gibson Assembly (Gibson *et al*., 2009) using PCR amplified pRS426 vector (primers pRS426F and R) and a 2.7-kb fragment containing the *mobC* gene (primers KG66 and 67) amplified from *E. festucae* genomic Fl1 DNA. This DNA mixture was transformed into *E. coli* DH5α and pKG8 identified and verified as described above. Plasmid pKG8 was co-transformed with pSF15.15 into *E. festucae* Δ*mobC* protoplasts as described below using Hyg^R selection.

Fungal transformations

E. festucae protoplasts were prepared as previously described by (Young *et al.*, 2005). Protoplasts were transformed with 2-3 µg of linear (restriction enzyme excised) or circular plasmid DNA using the method described (Itoh *et al.*, 1994). Transformants were selected on

RG media containing either hygromycin (150 μg/ml) or geneticin (200 μg/ml) and nuclear purified by three rounds of sub-culturing on selection medium.

DNA hybridization

Following restriction digestion, *E. festucae* genomic DNA was separated by agarose gel electrophoresis, transferred to positively-charged nylon membranes (Roche)(Southern, 1975) and fixed by UV light cross-linking in a Cex-800 UV light cross-linker (Ultra-Lum) at 254 nm for 2 min. Labeling of DNA probes with digoxigenin-dUTP (DIG), hybridization, and visualization with nitro blue tetrazolium chloride and 5-bromo-4-chloro-3-indolyl-phosphate (NBT/BCIP) were performed using the DIG High Prime DNA Labelling and Detection Starter Kit I (Roche) according to the manusfacturer's instructions.

Western blot analysis

E. festucae cultures were grown for 4 days in 50 ml of PD and 1.5 g aliquots weighed into fresh duplicate 50 mL PD flasks and incubated with shaking (200 rpm) overnight. Samples were washed, flash-frozen in liquid nitrogen and freeze-dried overnight. Protein was then extracted from ground mycelia samples in 1 ml of Lysis Buffer [50 mM Tris-HCl pH 8, 100 mM NaCl, 10 mM EDTA, 1μl/ml IGEPAL CA-630 (Sigma-Aldrich, Germany), 0.5 mM PMSF, 2 mM DTT, and 10 μl/ml Phosphatase Inhibitor (Sigma-P5726)] and centrifuged at 14,000 rpm for 15 min at 4°C. Protein samples (70 μg) were separated by SDS-PAGE [10% (w/v) (Bio-Rad)] and transferred to PVDF membranes (Roche). The phosphorylation of MpkA and MpkB was detected using anti-phospho-p44/42 MAPK (Erk1/2) antibody (Number 9102; Cell Signalling Technology). To check sample loading the membrane was reprobed with 12G10 anti-α-tubulin (Developmental Studies Hybridoma Bank, University of Iowa). Primary antibodies were detected using HPR-conjugated secondary antibodies and ECL Prime Western Blotting Detection Reagent (GE Healthcare Amersham).

Microscopy

Cultures to be analyzed by microscopy were inoculated at the edge of a thin layer of water agar (1.5%), layered on top of a glass microscope slide embedded in a layer of water agar (1.5%) and grown for 5-7 days. Square blocks were then extracted and placed onto new slides, covered with a cover slip, and analyzed using an Olympus IX71 inverted fluorescence microscope using filters set for capturing DIC or Calcofluor (Fluorescent brightener 28, Sigma, concentration 3 mg/ml) staining. For quantifying hyphal fusions, 10 fields were examined at 400x magnification from three independent colonies. For quantifying conidiation, three PD agar plates, each containing 5 colonies were grown at 22°C for 7 days. Conidia were then harvested by scrubbing colonies with 2 ml of sterile water, which was then filtered through glass wool

packed tips. Suspensions of 300 µL were then spread onto PD agar plates for imaging and quantification.

Growth and morphology of hyphae *in planta* was determined by staining leaf sheaths with aniline blue diammonium salt (Sigma) and WGA AlexaFluor-488 (Molecular Probes/Invitrogen) as follows. Infected leaf sheaths were sequentially incubated at 4°C in 95% (v/v) ethanol overnight, then treated with 10% potassium hydroxide for three hours. The tissue was washed three times in PBS (pH 7.4) and incubated in staining solution (0.02% aniline blue, 10 ng/ml WGA-AF488, and 0.02% Tween 20 in PBS [pH 7.4]) for five minutes, followed by a 30-min vacuum infiltration step. Images were captured by Confocal Laser Scanning Microscopy (CLSM) using a Leica SP5 DM6000B confocal microscope (488 nm argon and 561 nm DPSS laser, ×20 or ×40 oil immersion objective, NA=1.3)(Leica Microsystems). Three photomultiplier tubes (PMTs) were used to capture the emission fluorescence from the dyes, as well as plant autofluorescence. Blue pseudocolour (PMT1: 498-551 nm) was assigned to emission fluorescence from WGA-AF488 excited with the 488 nm argon ion laser. Two pseudocolours were assigned to emission fluorescence from aniline blue and plant autofluorescence (PMT2: 571-633 nm, green and PMT3: 661-800 nm red) as the result of excitation with the 561 nm DPSS laser (Becker *et al*., 2016). For TEM, pseudostem sections were fixed in 3% glutaraldehyde and 2% formaldehyde in 0.1 M phosphate buffer, pH7.2 for 1 h as previously described (Spiers & Hopcroft, 1993). A Philips CM10 TEM was used to examine the fixed samples and the images were acquired using a SIS Morada digital camera.

Bioinformatic analysis

E. festucae mobC was identified by tBLASTn analysis of the *E. festucae* Fl1 (E894) genome (http://csbio-l.csr.uky.edu/ef894-2011) with homologous protein sequences obtained from either NCBI GenBank database (http://www.ncbi.nlm.nih.gov/) or the Broad Institute (http://www.broad.mit.edu). Identity and similarity scores were calculated after ClustalW pairwise alignments of sequences (Thompson *et al.*, 1994), using MacVector Version 12.0.5. The *E. festucae* genome sequence data, as curated by C.L. Schardl at the University of Kentucky is available at http://www.endophyte.uky.edu (Schardl *et al.*, 2013). Sequences for each of the genes analysed in this study are available from that site.

ACKNOWLEDGEMENTS

Kimberly Green was supported by a Massey University PhD scholarship and Barry Scott by an Alexander von Humboldt Research Award. The authors thank Matthew Savoian, Jordan Taylor and Niki Murray (Manawatu Microscopy and Imaging Centre, Massey University), Arvina Ram for technical assistance and Tetsuya Chujo for advice on the statistics. We thank Chris Schardl for provision of *Clavicipitaceae* genome sequences, made available through funding from the

U.S. National Science Foundation (grant no. EF-0523661), the U.S. Department of Agriculture National Research initiative (grant no. 2005-35319-16141), and the National Institutes of Health (grant no. 2 P20 RR-16481).

REFERENCES

Becker, M., Becker, Y., Green, K. and Scott, B. (2016) The endophytic symbiont *Epichloë festucae* establishes an epiphyllous net on the surface of *Lolium perenne* leaves by development of an expressorium, an appressorium-like leaf exit structure. *New Phytol.,* **211,** 240-254.

Becker, Y., Eaton, C. J., Brasell, E., May, K. J., Becker, M., Hassing, B., *et al.* (2015) The fungal cell wall integrity MAPK cascade is crucial for hyphal network formation and maintenance of restrictive growth of *Epichloë festucae* in symbiosis with *Lolium perenne*. *Mol. Plant-Microbe Interact,* **28,** 69-85.

Bernhards, Y. and Pöggeler, S. (2011) The phocein homologue SmMOB3 is essential for vegetative cell fusion and sexual development in the filamentous ascomycete *Sordaria macrospora*. *Curr. Genet.,* **57,** 133-149.

Bloemendal, S., Bernhards, Y., Bartho, K., Dettmann, A., Voigt, O., Teichert, I., *et al.* (2012) A homologue of the human STRIPAK complex controls sexual development in fungi. *Mol. Microbiol.,* **84,** 310-323.

Bloemendal, S., Lord, K. M., Rech, C., Hoff, B., Engh, I., Read, N. D., *et al.* (2010) A mutant defective in sexual development produces aseptate ascogonia. *Eukaryot. Cell,* **9,** 1856-1866.

Charlton, N. D., Shoji, J. Y., Ghimire, S. R., Nakashima, J. and Craven, K. D. (2012) Deletion of the fungal gene *soft* disrupts mutualistic symbiosis between the grass endophyte *Epichloë festucae* and the host plant. *Eukaryot. Cell,* **11,** 1463-1471.

Christensen, M. J., Bennett, R. J., Ansari, H. A., Koga, H., Johnson, R. D., Bryan, G. T., *et al.* (2008) *Epichloë* endophytes grow by intercalary hyphal extension in elongating grass leaves. *Fungal Genet. Biol.,* **45,** 84-93.

Clay, K. and Schardl, C. (2002) Evolutionary origins and ecological consequences of endophyte symbiosis with grasses. *Amer. Naturalist,* **160,** S99-S127.

Dettmann, A., Heilig, Y., Ludwig, S., Schmitt, K., Illgen, J., Fleißner, A., *et al.* (2013) HAM-2 and HAM-3 are central for the assembly of the *Neurospora* STRIPAK complex at the nuclear envelope and regulate nuclear accumulation of the MAP kinase MAK-1 in a MAK-2-dependent manner. *Mol. Microbiol.,* **90,** 796-812.

Eaton, C. J., Cox, M. P., Ambrose, B., Becker, M., Hesse, U., Schardl, C. L., *et al.* (2010) Disruption of signaling in a fungal-grass symbiosis leads to pathogenesis. *Plant Physiol.,* **153,** 1780-1794.

Eaton, C. J., Dupont, P.-Y., Solomon, P. S., Clayton, W., Scott, B. and Cox, M. P. (2015) A core gene set describes the molecular basis of mutualism and antagonism in *Epichloë* species. *Mol. Plant-Microbe Interact,* **28,** 218-231.

Engh, I., Nowrousian, M. and Kück, U. (2010) *Sordaria macrospora*, a model organism to study fungal cellular development. *Eur J Cell Biol,* **89,** 864-872.

Fleißner, A., Leeder, A. C., Roca, M. G., Read, N. D. and Glass, N. L. (2009) Oscillatory recruitment of signaling proteins to cell tips promotes coordinated behavior during cell fusion. *Proc. Natl. Acad. Sci. USA,* **106,** 19387-19392.

Frey, S., Lahmann, Y., Hartmann, T., Seiler, S. and Pöggeler, S. (2015a) Deletion of Smgpi1 encoding a GPI-anchored protein suppresses sterility of the STRIPAK mutant Δ*Smmob3* in the filamentous ascomycete *Sordaria macrospora*. *Mol. Microbiol.,* **97,** 676-697.

Frey, S., Reschka, E. J. and Pöggeler, S. (2015b) Germinal center kinases SmKIN3 and SmKIN24 are associated with the *Sordaria macrospora* Striatin-Interacting Phosphatase and Kinase (STRIPAK) complex. *PLoS One,* **10,** e0139163.

Fu, C., Iyer, P., Herkal, A., Abdullah, J., Stout, A. and Free, S. J. (2011) Identification and characterization of genes required for cell-to-cell fusion in *Neurospora crassa*. *Eukaryot. Cell,* **10,** 1100-1109.

Gibson, D. G., Young, L., Chuang, R. Y., Venter, J. C., Hutchison, C. A., III and Smith, H. O. (2009) Enzymatic assembly of DNA molecules up to several hundred kilobases. *Nat Methods,* **6,** 343-345.

Itoh, Y., Johnson, R. and Scott, B. (1994) Integrative transformation of the mycotoxin-producing fungus, *Penicillium paxilli*. *Curr. Genet.,* **25,** 508-513.

Johnson, L. J., Koulman, A., Christensen, M., Lane, G. A., Fraser, K., Forester, N., *et al.* (2013) An extracellular siderophore is required to maintain the mutualistic interaction of *Epichloë festucae* with *Lolium perenne*. *PLoS Pathog,* **9,** e1003332.

Kück, U., Beier, A. M. and Teichert, I. (2016) The composition and function of the striatin-interacting phosphatases and kinases (STRIPAK) complex in fungi. *Fungal Genet. Biol.,* **90,** 31-38.

Kück, U., Pöggeler, S., Nowrousian, M., Nolting, N. and Engh, I. (2009) *Sordaria macrospora*, a model system for fungal development. In: *The Mycota.* (Anke, T., ed.). Heidelberg, New York, Tokyo: Springer, pp. 17-39.

Latch, G. C. M. and Christensen, M. J. (1985) Artificial infection of grasses with endophytes. *Ann. Appl. Biol.,* **107,** 17-24.

Maerz, S., Dettmann, A., Ziv, C., Liu, Y., Valerius, O., Yarden, O., *et al.* (2009) Two NDR kinase-MOB complexes function as distinct modules during septum formation and tip extension in *Neurospora crassa*. *Mol. Microbiol.,* **74,** 707-723.

Miller, J. H. (1972) *Experiments in Molecular Genetics.* New York: Cold Spring Harbor Laboratory Press.

Moon, C. D., Scott, B., Schardl, C. L. and Christensen, M. J. (2000) The evolutionary origins of *Epichloë* endophytes from annual ryegrasses. *Mycologia,* **92,** 1103-1118.

Moon, C. D., Tapper, B. A. and Scott, B. (1999) Identification of *Epichloë* endophytes *in planta* by a microsatellite-based PCR fingerprinting assay with automated analysis. *Appl. Environ. Microbiol.,* **65,** 1268-1279.

Nordzieke, S., Zobel, T., Fränzel, B., Wolters, D. A., Kück, U. and Teichert, I. (2015) A fungal sarcolemmal membrane-associated protein (SLMAP) homolog plays a fundamental role in

development and localizes to the nuclear envelope, endoplasmic reticulum, and mitochondria. *Eukaryot. Cell,* **14,** 345-358.

Park, G., Pan, S. and Borkovich, K. A. (2008) Mitogen-activated protein kinase cascade required for regulation of development and secondary metabolism in *Neurospora crassa*. *Eukaryot. Cell,* **7,** 2113-2122.

Pöggeler, S. and Kück, U. (2004) A WD40 repeat protein regulates fungal cell differentiation and can be replaced functionally by the mammalian homologue striatin. *Eukaryot. Cell,* **3,** 232-240.

Read, N. D., Goryachev, A. B. and Lichius, A. (2012) The mechanistic basis of self-fusion between conidial anastomosis tubes during fungal colony initiation. *Fungal Biolog Reviews,* **26,** 1-11.

Roca, M. G., Arlt, J., Jeffree, C. E. and Read, N. D. (2005) Cell biology of conidial anastomosis tubes in *Neurospora crassa*. *Eukaryot. Cell,* **4,** 911-919.

Schardl, C. L. (1996) *Epichloë* species: fungal symbionts of grasses. *Annu. Rev. Phytopathol.,* **34,** 109-130.

Schardl, C. L., Young, C. A., Hesse, U., Amyotte, S. G., Andreeva, K., Calie, P. J., *et al.* (2013) Plant-symbiotic fungi as chemical engineers: multi-genome analysis of the Clavicipitaceae reveals dynamics of alkaloid loci. *PLoS Genetics,* **9,** e1003323.

Simonin, A. R., Rasmussen, C. G., Yang, M. and Glass, N. L. (2010) Genes encoding a striatin-like protein (*ham-3*) and a forkhead associated protein (*ham-4*) are required for hyphal fusion in *Neurospora crassa*. *Fungal Genet. Biol.,* **47,** 855-868.

Southern, E. M. (1975) Detection of specific sequences among DNA fragments separated by gel electrophoresis. *J. Mol. Biol.,* **98,** 503-517.

Spiers, A. G. and Hopcroft, D. H. (1993) Black canker and leaf spot of Salix in New Zealand caused by *Glomerella miyabeana* (*Colletotrichum gloeosporioides*). *Eur. J. Forest Pathol.,* **23,** 92-102.

Takemoto, D., Kamakura, S., Saikia, S., Becker, Y., Wrenn, R., Tanaka, A., *et al.* (2011) Polarity proteins Bem1 and Cdc24 are components of the filamentous fungal NADPH oxidase complex. *Proc. Natl. Acad. Sci. USA,* **108,** 2861-2866.

Takemoto, D., Tanaka, A. and Scott, B. (2006) A $p67^{Phox}$-like regulator is recruited to control hyphal branching in a fungal-grass mutualistic symbiosis. *Plant Cell,* **18,** 2807-2821.

Tanaka, A., Cartwright, G. M., Saikia, S., Kayano, Y., Takemoto, D., Kato, M., *et al.* (2013) ProA, a transcriptional regulator of fungal fruiting body development, regulates leaf hyphal network development in the *Epichloë festucae-Lolium perenne* symbiosis. *Mol. Microbiol.,* **90,** 551-568.

Tanaka, A., Christensen, M. J., Takemoto, D., Park, P. and Scott, B. (2006) Reactive oxygen species play a role in regulating a fungus-perennial ryegrass mutualistic association. *Plant Cell,* **18,** 1052-1066.

Tanaka, A., Takemoto, D., Hyon, G. S., Park, P. and Scott, B. (2008) NoxA activation by the small GTPase RacA is required to maintain a mutualistic symbiotic association between *Epichloë festucae* and perennial ryegrass. *Mol. Microbiol.,* **68,** 1165-1178.

Teichert, I., Nowrousian, M., Pöggeler, S. and Kück, U. (2014) The filamentous fungus *Sordaria macrospora* as a genetic model to study fruiting body development. *Adv Genet,* **87,** 199-244.

Thompson, J. D., Higgins, D. G. and Gibson, T. J. (1994) CLUSTAL W: improving the sensitivity of progressive multiple sequence alignment through sequence weighting, position-specific gap penalties and weight matrix choice. *Nucleic Acids Res.,* **22,** 4673-4680.

Wang, C.-L., Shim, W.-B. and Shaw, B. D. (2010) *Aspergillus nidulans* striatin (StrA) mediates sexual development and localizes to the endoplasmic reticulum. *Fungal Genet. Biol.,* **47,** 789-799.

Wang, C.-L., Shim, W.-B. and Shaw, B. D. (2016) The *Colletotrichum graminicola* striatin ortholog Str1 is necessary for anastomosis and is a virulence factor. *Mol Plant Pathol,* DOI: 10.1111/mpp.12339.

Yamamura, Y. and Shim, W. B. (2008) The coiled-coil protein-binding motif in *Fusarium verticillioides* Fsr1 is essential for maize stalk rot virulence. *Microbiology*, **154,** 1637-1645.

Young, C. A., Bryant, M. K., Christensen, M. J., Tapper, B. A., Bryan, G. T. and Scott, B. (2005) Molecular cloning and genetic analysis of a symbiosis-expressed gene cluster for lolitrem biosynthesis from a mutualistic endophyte of perennial ryegrass. *Mol. Gen. Genomics,* **274,** 13-29.

SUPPORTING INFORMATION

Supplementary Table 1: Biological Material

Biological material	Relevant characteristics	Reference
Fungal strains		
Epichloë festucae		
PN2278 (WT)	Fl1	Young *et al*., 2005
PN3020 (*ΔmobC*#37)	Fl1/*ΔmobC*::*gen* (pKG4); Gen^R	This study
PN3021 (*ΔmobC*#21)	Fl1/*ΔmobC*::*gen* (pKG4); Gen^R	This study
PN3069 (*ΔmobC*#21/*mobC #4)*	Δ*mobC*#21/P*mobC-mobC-TmobC* (pKG8) & pSF15.15; Gen^R, Hyg^R	This study
PN3071 (*ΔmobC*#37/*mobC #11)*	Δ*mobC*#37/P*mobC-mobC-TmobC* (pKG8) & pSF15.15; Gen^R, Hyg^R	This study
PN3070 (*Δ*mobC#21/*mob3* #15)	Δ*mobC*#21/P*mobC-mobC-TmobC* (pKG8) & pSF15.15; Gen^R, Hyg^R	This study
Bacterial strains		
E.coli		
PN1687	Source of pII99; Amp^R, Gen^R	Namiki et al., 2001
PN1862	Source of pSF15.15; Amp^R, Hyg^R	S. Foster
PN413	Source of pRS426; Amp^R	Christianson et al., 1992
PN4251	Source of pKG4; Amp^R	This study
PN4268	Source of pKG8; Amp^R	This study
Plasmids		
pII99	P*trpC-nptII*-T*trpC*; Amp^R, Gen^R	Namiki et al., 2001
pSF15.15	P*trpC*-hph-T*trpC*; Amp^R, Hyg^R	S. Foster
pRS426	ori(f1)-lacZ-T7 promoter-MCS (KpnI-SacI)-T3 promoter-lacI-ori(pMB1)-ampR-ori (2 micron), URA3, Amp^R	Winston et al, 1995
pKG4	pRS426 containing 5'*mobC*-P*trpC-gen*-3'*mobC*; Amp^R, Gen^R	This study

pKG8	pRS426 containing 2.8kb P*mob-mobC*-T*mobC* complementation construct; Amp^R	This study

Supplementary Table 2: Primers used in this study.

Primer	Sequence
genF	GATATTGAAGGAGCACTTTTTG
genR	CTACCCATCTTAGTAGGAATG
pRS426F	GTAACGCCAGGGTTTTCCCAGTCACGAC
pRS426R	GCGGATAACAATTTCACACAGGAAACAGC
KG33	CGGTAATATGCAGTTTCGC
KG34	TTGACCTCCACTAGCTCC
KG35	GCCTACAGGACACACATT
KG36	CTTTGCAGAATCCCAACG
KG37	GAACACGATAGGTCAGAAACTC
KG38	TGATGACCCTTGATGCACC
KG39	GGCTCTGGCACCGAGAT
KG40	TCACTCTGGATCCGTAACCTG
KG45	GTAACGCCAGGGTTTTCCCAGTCACGACTGAACTCGAGCCTTGACTAGC
KG46	CCAAGCCCAAAAAGTGCTCCTTCAATATCAGGGGGAATTCGAATCCACC
KG47	GAAAATCATTCCTACTAAGATGGGTAGCAGCTCTCGCCGATGTCA
KG48	GCGGATAACAATTTCACACAGGAAACAGCCTTCTCGAGTCGATCAAAACC
KG66	GTAACGCCAGGGTTTTCCCAGTCACGACGTCGACCAGCTCTGGAGG
KG67	GCGGATAACAATTTCACACAGGAAACAGCTGATGACCCTTGATGCACC

Supplementary Table 3: Analysis of plant survival rates.

	Planted	Survived (S)	Infected (I)	% S	% I
Experiment 1					
WT	48	20	14	0.42	0.70
21	52	3	0	0.06	0.00
37	52	11	6	0.21	0.55
Experiment 2					
WT	56	33	21	0.59	0.64
21	36	15	5	0.42	0.33
37	60	25	6	0.42	0.24
Experiment 3					
WT	40	25	21	0.63	0.84
21	52	16	7	0.31	0.44
37	52	19	10	0.37	0.53

Fig. S1 *Epichloë festucae mobC* gene structure and amino acid sequence alignment. (a) Gene structure showing three exons and two introns of 216, 978 and 309 and 145 32 bp respectively. Bar = 200 bp. (b) ClustalW alignment of amino acid sequences with the degree of conserved amino acids as indicated by dark-light shading and missing amino acids by dashed lines. Gene ID's with associated GenBank protein accession are as shown. *Ef*, *Epichloë festucae* MobC EfM3.028150; *Fg*, *Fusarium graminearum* FGSG_05101.3 (XP_011323597.1); *Nc*, *Neurospora crassa* NCU07674.7/*mob-3* (XM_957223.3); *Pa*, *Podospora anserina* Pa_6_3550 (XM_001910099.1); *Mo*, *Magnaporthe oryzae* MGG_07095.6 (XM_003715237.1) and *Sm*, *Sordaria macrospora mob3* (FN995002.1). Predicted Mob domain (green), serine and threonine phosphorylation sites (orange), Cys^2-His^2 Zn^{2+} (pink) and SH3 (blue) binding domains are as shown.

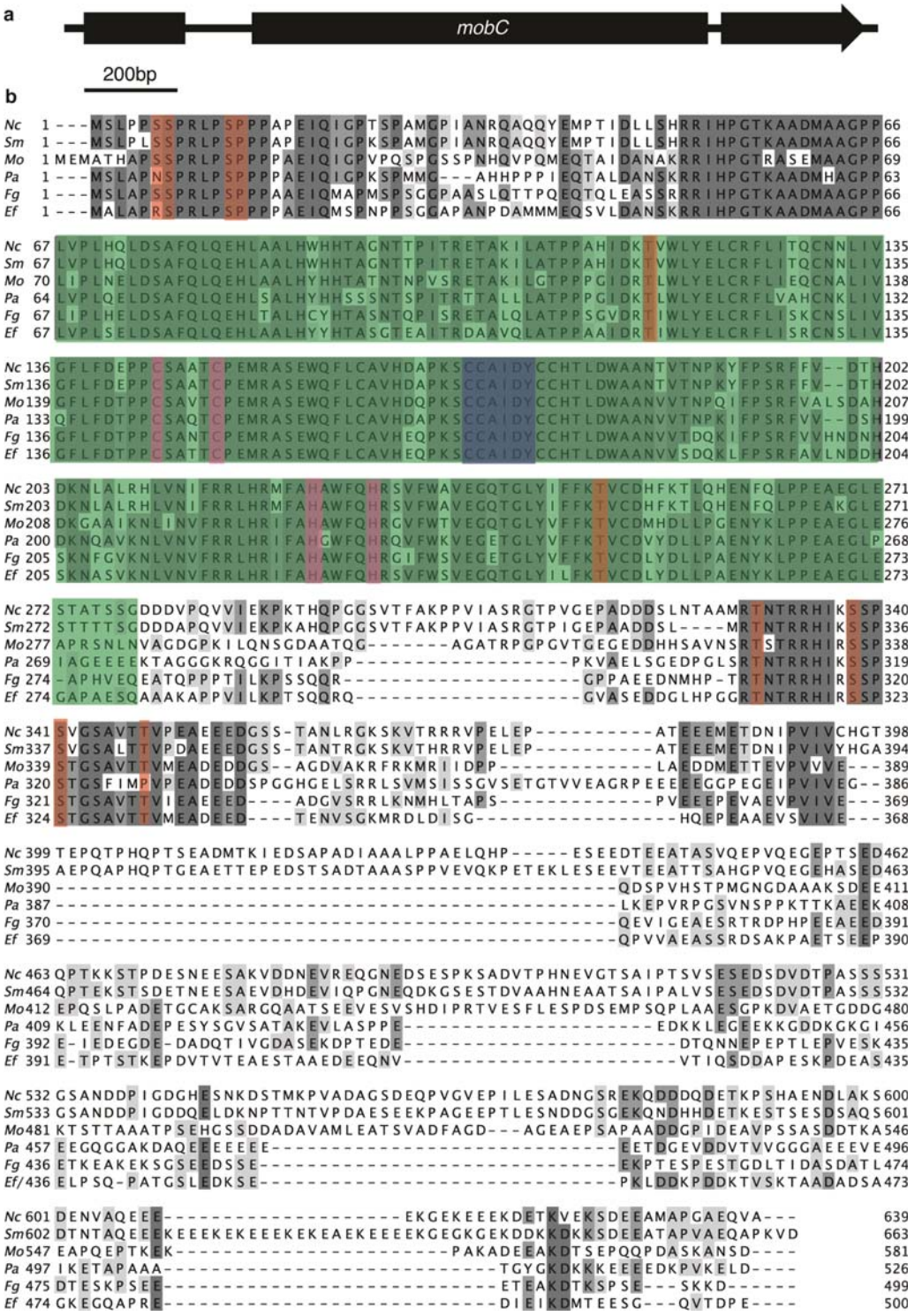

Fig. S2 ***Epichloë festucae pro11*** **homologue gene structure and amino acid sequence alignment.** (a) Gene structure showing three exons and two introns of 376, 1871 and 258 and 84 and 63 bp respectively. Bar = 200 bp. (b) ClustalW alignment of amino acid sequences with the degree of conserved amino acids as indicated by dark-light shading and missing amino acids by dashed lines. Gene ID's with associated GenBank protein accession are as shown. *Ef*, *E. festucae* EfM3.057840; *Fg*, *Fusarium graminearum* FGSG_01665.3 (XM_011319188.1); *Nc*, *Neurospora crassa* NCU08741.7/*ham-3* (XM_958509.2) *Pa*, *Podospora anserina* Pa_6_11770 (XM_001906817.1) and *Sm*, *Sordaria*

macrospora SMAC_08794/*pro11* (XM_003345392.1) protein homologues. Predicted striatin (red), coiled-coil (green) and conserved WD40 binding domains (blue) are as shown.

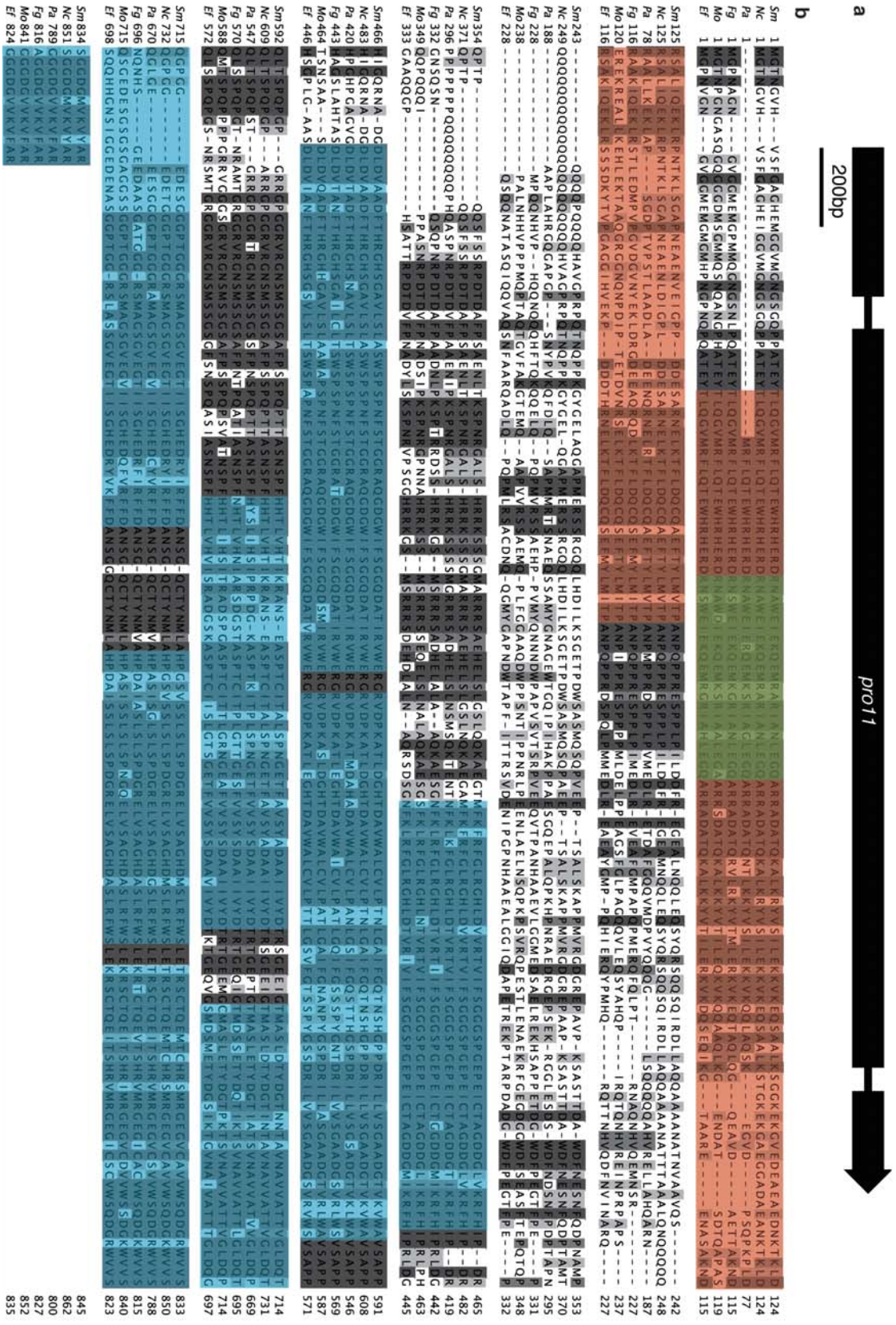

Fig. S3 *Epichloë festucae pro22* homologue gene structure and amino acid sequence alignment. (a) Gene structure showing six exons and five introns of 755, 146, 89, 1192, 130 and 886 and 100, 59, 80, 121 and 67 bp respectively. Bar = 500 bp. (b) ClustalW alignment of amino acid sequences with the degree of conserved amino acids as indicated by dark-light shading and missing amino acids by dashed lines. Gene ID's with associated GenBank protein accession are as shown. *Ef*, *Epichloë festucae* EfM3.000170; *Fg, Fusarium graminearum* FGSG_07159.3 (XM_011328574.1); *Nc, Neurospora crassa* NCU03727.7/*ham-2* (XM_011396271.1); *Pa, Podospora anserina* Pa_2_9440 (XM_001911717.1); *Mo, Magnaporthe oryzae* MGG_00731.6 (XM_003718223.1) and *Sm, Sordaria macrospora* SMAC_02580/*pro22* (XM_003352097.1) protein homologues.

Fig. S4 *Epichloë festucae pro45* homologue gene structure and amino acid sequence alignment. (a) Gene structure showing two exons and one intron of 1029 and 1164 and 65 bp respectively. Bar = 500 bp. (b) ClustalW alignment of amino acid sequences with the degree of conserved amino acids as indicated by dark-light shading and missing amino acids by dashed lines. Gene ID's with associated GenBank protein accession are as shown. *Ef*, *Epichloë festucae* EfM3.037520; *Fg, Fusarium graminearum* FGSG_09221.3 (XM_011330252.1); *Nc*, *Neurospora crassa* NCU00528/*ham-4* (XM_958987.2); *Pa*, *Podospora anserina* Pa_1_15490 (XM_001906952.1); *Mo*, *Magnaporthe oryzae* MGG_02878.6 (XM_003720805.1) and *Sm*, *Sordaria macrospora* SMAC_01224/*pro45* (XM_003352342.1) protein homologues. Predicted forkhead associated domain (green) and trans-membrane helix (blue) are as shown.

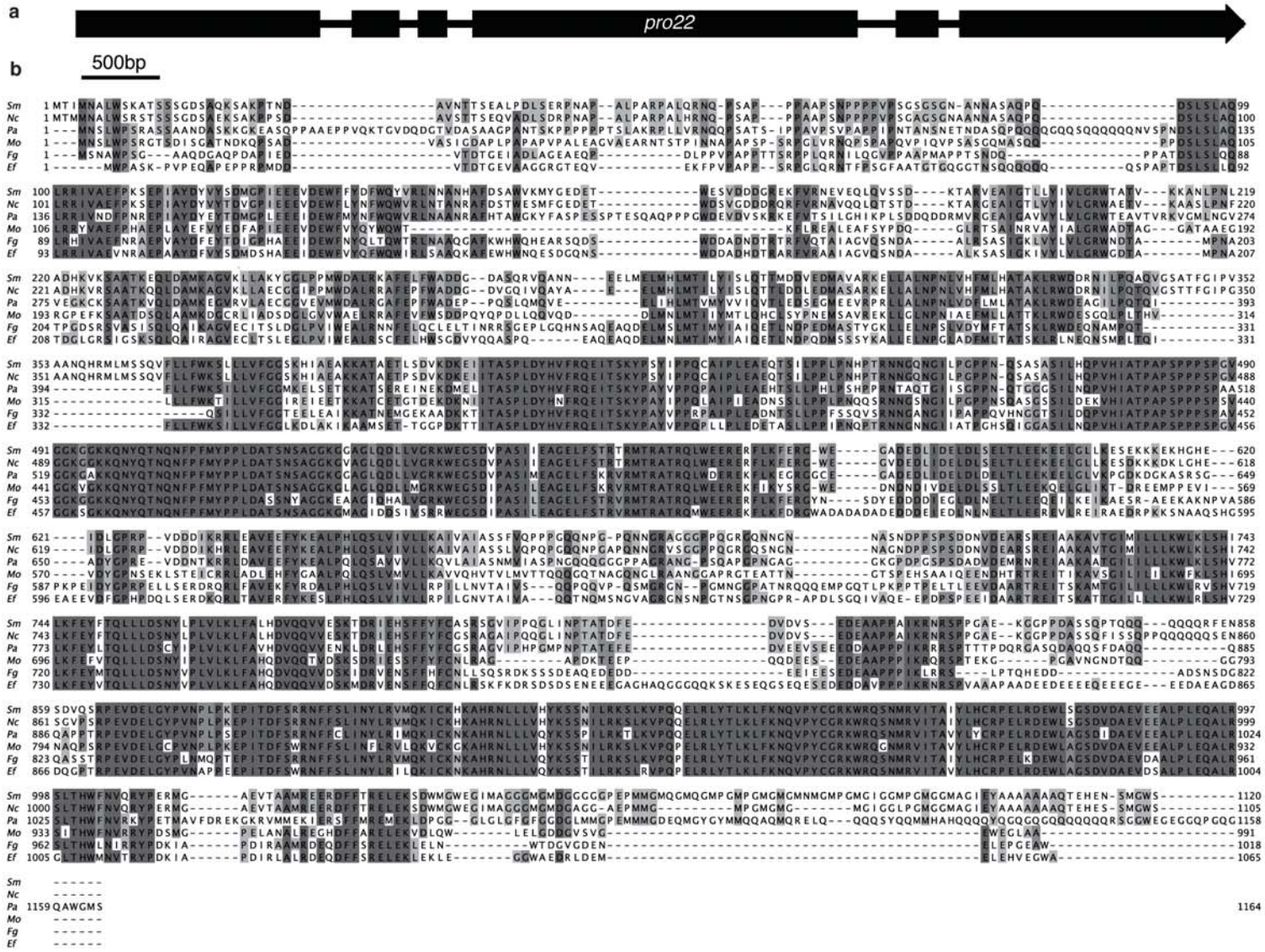
a
pro22
b
500bp
Sm
Nc
Pa
Mo
Fg
Ef

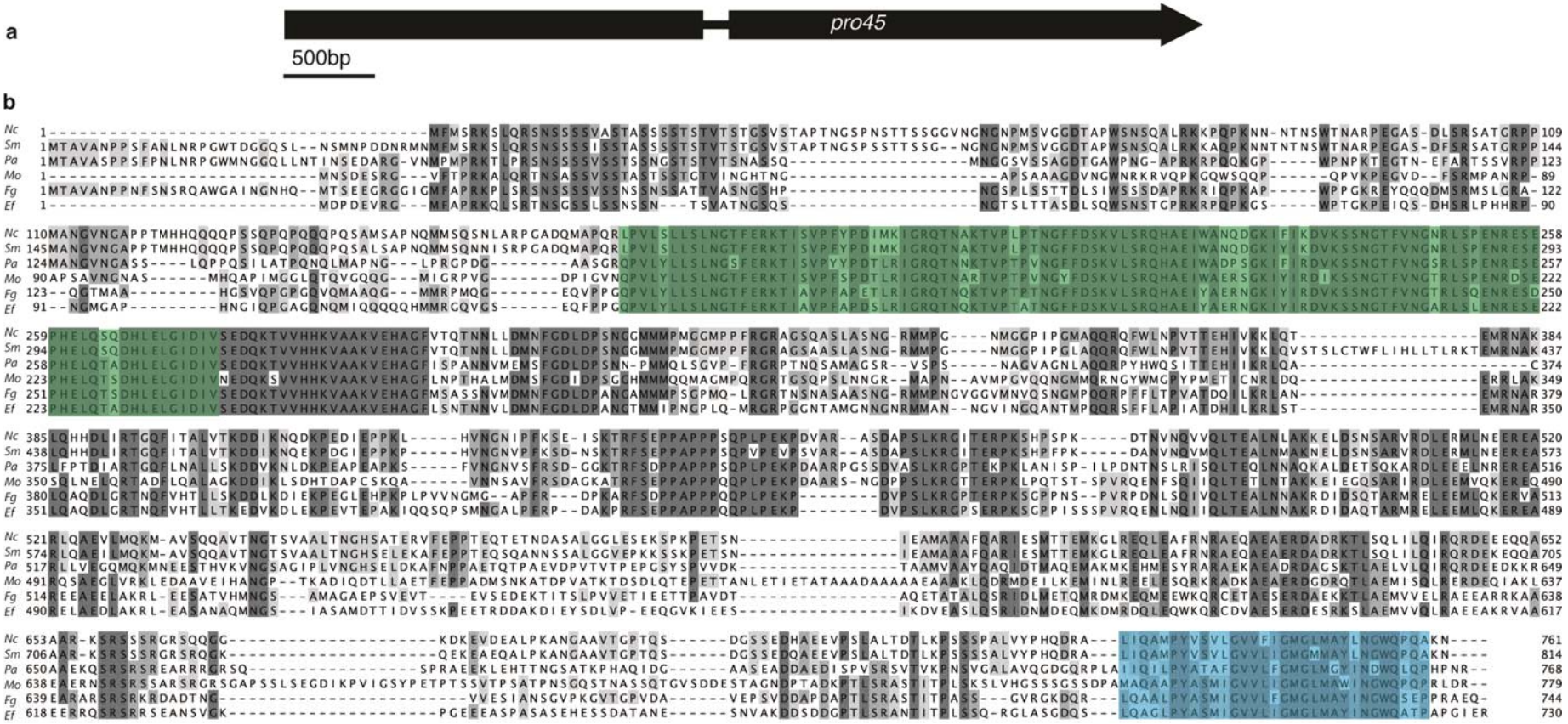
a
pro45
500bp
b
Nc
Sm
Pa
Mo
Fg
Ef

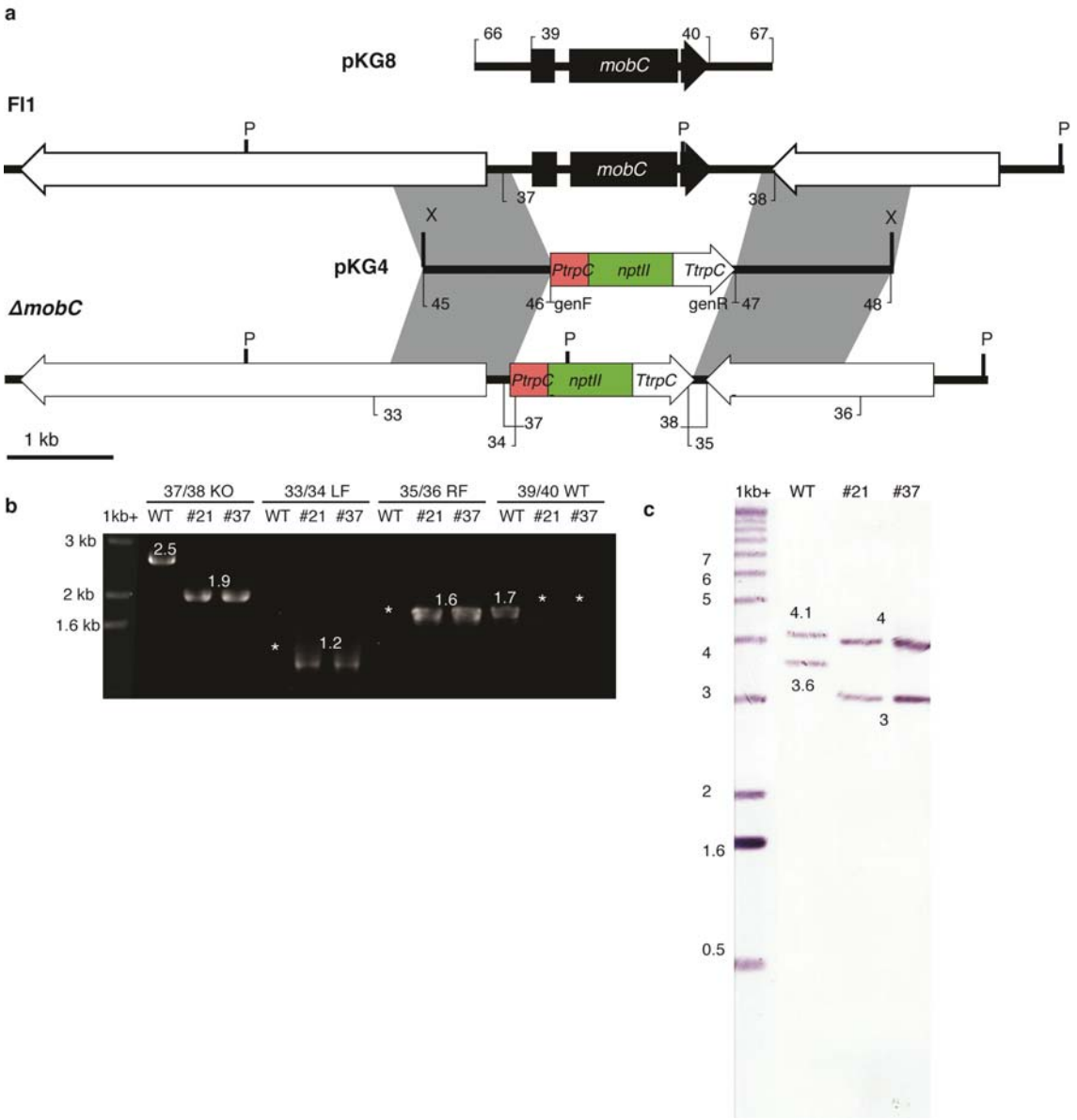

Fig. S5 *mobC* deletion and complementation construct design, screening primers and Southern analysis. (a) Schematic of the wild type (Fl1) *mobC* genomic locus and linear inserts of *mobC* deletion construct pKG4 and *mobC* complementation construct pKG8. Regions of recombination are indicated by grey shading. *Pst*I (P) restriction enzyme sites used for Southern analysis and PCR primers used for Gibson assembly and knock-out screening are as shown. (b) PCR products of the expected size generated from primary screen with primers KG37/38 and secondary screen with primers KG33/34, KG35/36 and KG39/40. **C,** NBT/BCIP-stained Southern blot of *Pst*I (P) genomic DNA digests (1.5 µg) probed with (DIG)-11-dUTP-labeled linear pKG4 fragment purified from an *Xho*I restriction enzyme digest of the plasmid. Fragments of the expected size are as shown.

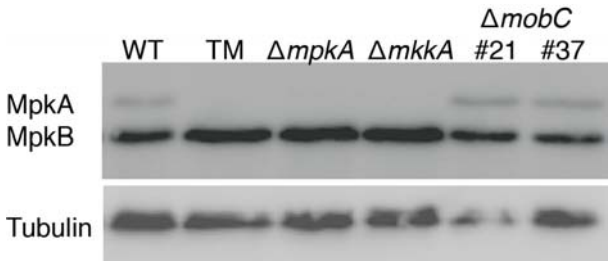

Fig. S6 Analysis of MpkA and MpkB phosphorylation in Δ*mobC*. Western blot analysis of MpkA and MpkB phosphorylation in wild type (WT), TM1066 (TM; a Δ*mkkA* mutant described in Becker *et al.* 2015), Δ*mpkA*, Δ*mkkA* (Becker *et al.* 2015), Δ*mobC#21* and Δ*mobC#37* mutants. Phosphorylated MpkA (47 kDa) and MpkB (41 kDa) were detected using anti-phospho p42/p44 MAPK antibodies. Tubulin (54 kDa) was used as a loading control and detected using an anti-α-tubulin antibody.

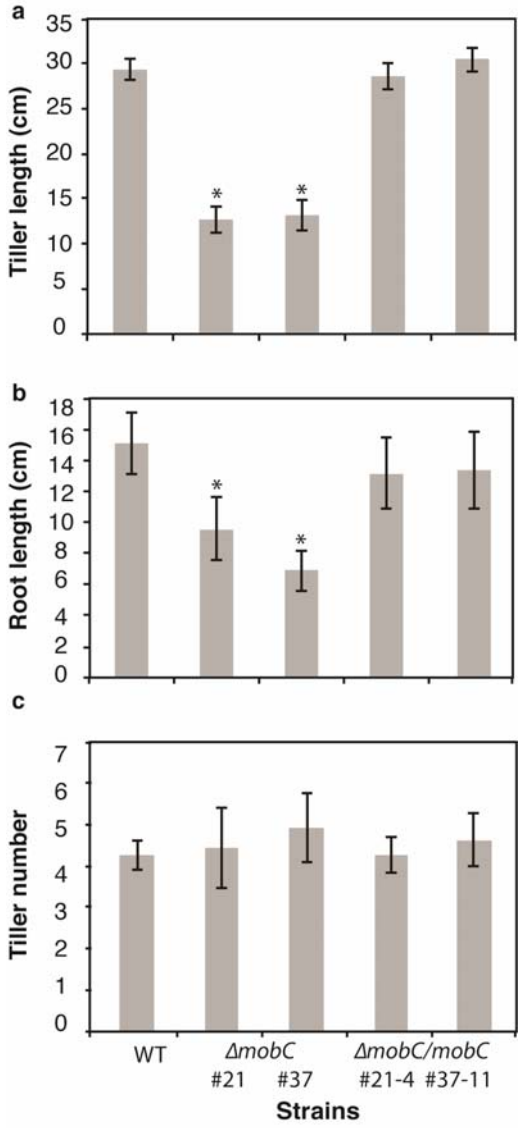

Fig. S7 Quantification of the whole plant phenotype of *Lolium perenne* inoculated with wild-type, Δ*mobC* and complemented Δ*mobC/mobC* strains. Average (a) tiller length (b) root length and (c) tiller number observed. Bars represent the ± standard error (n=7-16). An asterisk indicates significant differences from WT as determined by Welch's *t* test.

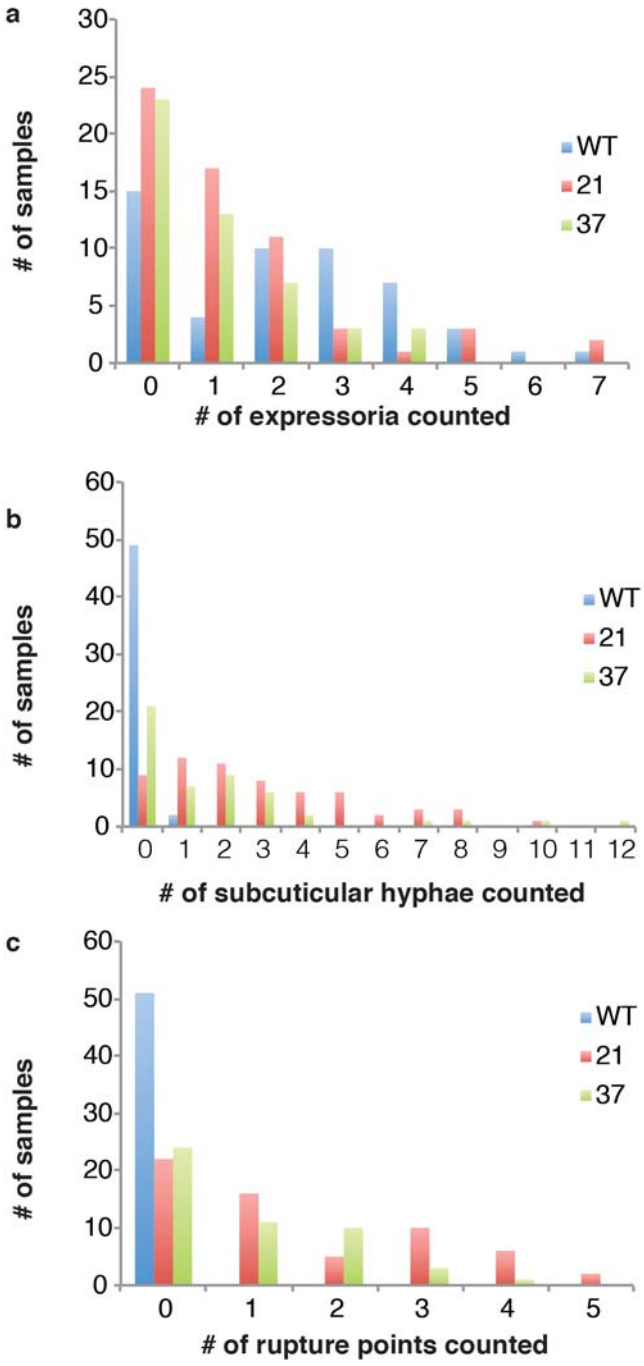

Fig. S8 Expressoria phenotype of Δ*mobC*. Frequency of (a) expressoria (b) sub-cuticular hyphae and (c) cuticle rupture points observed during associations per leaf sample at ×200 magnification. All two mutant phenotypes were significantly different to wild-type as determined by a Kruskal-Wallis test and Dunn's multiple comparison test with *P* values of $P<0.05$ (#21) and $P<0.01$ (#37) for the expressoria phenotype, $P<0.0001$ (#21 & #37) for the sub-cuticular hyphae phenotype and $P<0.0001$ (#21 & #37) for the cuticle rupture phenotype.

3 SymB and SymC manuscript

MASSEY UNIVERSITY
GRADUATE RESEARCH SCHOOL

STATEMENT OF CONTRIBUTION TO DOCTORAL THESIS CONTAINING PUBLICATIONS

(To appear at the end of each thesis chapter/section/appendix submitted as an article/paper or collected as an appendix at the end of the thesis)

We, the candidate and the candidate's Principal Supervisor, certify that all co-authors have consented to their work being included in the thesis and they have accepted the candidate's contribution as indicated below in the *Statement of Originality*.

Name of Candidate: Kimberly Anne Green

Name/Title of Principal Supervisor: Professor Barry Scott

Name of Published Research Output and full reference:

Green, K. A., Becker, Y., Tanaka, A., Takemoto, D., Fitzsimons, H. L., Seiler, S., Lalucque, H., Silar, P., and Scott, B., (2016) SymB and SymC, two membrane associated proteins, are required for Epichloë festucae hyphal cell-cell fusion and establishment of a mutualistic interaction with Lolium perenne. Manuscript in preparation.

In which Chapter is the Published Work: 3

Please indicate either:

- The percentage of the Published Work that was contributed by the candidate: 70

  and / or

- Describe the contribution that the candidate has made to the Published Work:

  All constructs with the exception of MpkA-eGFP and MpkB-eGFP plasmids, and experiments with the exception of the Gel Shift Assay (Figure 1.B, Aiko Tanaka), were prepared and performed by the candidate. The candidate co-wrote the maunscript text and prepared all manuscript figures.

Green, Kim — Digitally signed by Green, Kim Date: 2016.07.04 13:25:06 +12'00'

Candidate's Signature — 15.07.16 — Date

Barry Scott — Digitally signed by Barry Scott DN: cn=Barry Scott, o=Massey University, ou=IFS, email=d.b.scott@massey.ac.nz, c=NZ Date: 2016.07.15 16:51:45 +12'00'

Principal Supervisor's signature — 15.07.16 — Date

All methods, results and the discussion pertaining to this chapter have been included within the draft manuscript below, which is to be submitted to the Molecular Plant-Microbe Interactions Journal. The text sections included are the summary, introduction, results (figures and figure legends embedded), experimental procedures, acknowledgements and references. The supplementary primer and biological lists and supplementary figures have been inserted directly after the references. All plasmid maps associated with this manuscript have been deposited within Chapter 7. Specific plasmid maps can be located using the list of figures within the beginning pages of this thesis.

SymB and SymC, two membrane-associated proteins, are required for *Epichloë festucae* hyphal cell-cell fusion and establishment of a mutualistic interaction with *Lolium perenne*

Kimberly A Green,[1,2] Yvonne Becker,[1] Aiko Tanaka,[3] Daigo Takemoto,[3] Helen L Fitzsimons,[1] Stephan Seiler,[4] Hervé Lalucque,[5] Philippe Silar,[5] and Barry Scott[1,2]

[1]Institue of Fundamental Sciences and [2]Bioprotection Research Centre, Massey University, Palmerston North 4442, New Zealand; [3]Graduate School of Bioagricultural Sciences, Nagoya University, Nagoya 464-8601, Japan; [4]Freiburg Institute for Advanced Studies, Albert-Ludwigs Universität Freiburg, Freiburg, Germany; [5]Institut de Génétique et Microbiologie, Université Paris Diderot, France.

[*] Corresponding Author: Telephone: (+64) 6-951 7705; Fax (+64) 6-350 5682; E-mail d.b.scott@massey.ac.nz;

Hyphal cell-cell fusion in fungi is required for colony formation, nutrient transfer and signal transduction. Disruption of genes required for hyphal fusion in *Epichloë festucae*, a mutualistic symbiont of *Lolium* and *Festuca* grasses, severely disrupts the host interaction phenotype. To test if *symB* and *symC*, homologs of genes in *Podospora anserina* (*IDC2* and *IDC3*) that suppress a cell growth defect, are required for *E. festucae* hyphal fusion and host symbiosis, targeted deletions of each gene were generated. In culture, both mutants were defective in hyphal cell-cell fusion, formed intra-hyphal hyphae, and had enhanced conidiation. Inverted microscopy analysis revealed that SymB-GFP and SymC-mRFP1 localise to the plasma membrane, septa and points of hyphal cell-cell fusion associated with septa. SymC also localised to highly dynamic punctate structures. Plants infected with Δ*symB* and Δ*symC* strains were severely stunted. Hyphae of the mutants colonised the vascular bundles, were more abundant than wild type in the intercellular spaces and frequently formed intra-hyphal hyphae. Hyphal branches failed to fuse but instead formed convoluted bundles. Although these culture and plant phenotypes are identical to those previously observed for the cell wall integrity MAP kinase mutants, Δ*mkkA* and Δ*mpkA*, no difference was observed in the basal level of MpkA phosphorylation or its cellular localisation in the mutant backgrounds. Collectively these results show that SymB and SymC are key components of a conserved signalling network for *E. festucae* to establish a mutualistic symbiotic interaction within *L. perenne*.

The fungal endophyte *Epichloë festucae* is a mutualistic symbiont of *Festuca* and *Lolium* temperate grasses (Christensen *et al.,* 2002, Leuchtmann *et al.,* 1994, Schardl, 2001). In these associations *E. festucae* systemically colonises the intercellular regions of all aerial tissues to form a tightly connected symbiotic hyphal network (Takemoto *et al.,* 2006, Tanaka *et al.,* 2006). Within the meristematic tissues of the true stem, hyphae grow by tip growth, from where they ramify into the leaf primordia that give rise to new leaves (Christensen *et al.,* 2008). Hyphae within the leaf blade and leaf sheath cell division zones initially grow by tip growth but once they enter the cell expansion zone they switch to intercalary growth (Christensen *et al.,* 2008), a pattern of growth that synchronises their growth with that of the plant host, thereby avoiding mechanical shear as the leaf expands. When leaf expansion ceases, growth of the hyphae also ceases, but the hyphae remain metabolically active (Tan *et al.,* 2001).

E. festucae is also an epiphyte, forming a restricted hyphal network on the leaf surface (Christensen *et al.,* 1997, Tanaka *et al.,* 2006, Eaton *et al.,* 2010, Scott *et al.,* 2012). Recent work has shown that an appressorium-like structure, called an expressorium, mediates exit of endophytic hyphae from the epidermal cells in the lower part of the leaf expansion zone to the leaf surface (Becker *et al.,* 2016). Differentiation of the expressorium and repolarization of growth from the point of contact of this structure with the cuticle requires functional NoxA and

NoxB NADPH oxidase complexes (Becker *et al.,* 2016) as well as MobC (Green *et al.,* 2016), a component of the STRIPAK complex (Bloemendal *et al.,* 2012, Dettmann *et al.,* 2013, Bernhards & Pöggeler, 2011).

The isolation of *Epichloë festucae* mutants that have a severe host interaction phenotype including components of the NoxA NADPH oxidase complex (Tanaka *et al.,* 2006, Tanaka *et al.,* 2008, Takemoto *et al.,* 2006); the transcription factor ProA (Tanaka *et al.,* 2013); the cell wall integrity MAP kinases, MpkA and MkkA (Becker *et al.,* 2015), and associated scaffold protein Soft (Pro40) (Charlton *et al.,* 2012); has provided important insights into the signalling pathways that control the symbiotic interaction. Interestingly, all these mutants were also defective in hyphal cell-cell fusion (Kayano *et al.,* 2013, Becker *et al.,* 2015, Charlton *et al.,* 2012, Tanaka *et al.,* 2013), leading to the hypothesis that hyphal fusion *in planta* is crucial for *E. festucae* hyphal network formation and maintenance of the mutualistic symbiotic interaction with *L. perenne*.

Homologues of a subset of these genes, namely *noxA*, *so*, *mpkA* and *mkkA*, are required in *Podospora anserina* for the development of the cell degenerative phenomenon known as crippled growth (CG; Silar *et al.,* 1999). Mutations in these genes cause impaired development of CG (IDC). Crippled growth occurs as a result of abnormal activation of the cell wall integrity (CWI) MAP kinase pathway and is characterised by slow colony expansion, loss of pigmentation, and arrest of aerial hyphae and perithecia development (Haedens *et al.,* 2005, Kicka *et al.,* 2006, Lalucque *et al.,* 2012, Malagnac *et al.,* 2004, Silar *et al.,* 1999, Tong *et al.,* 2014). Interestingly, in addition to their *IDC* phenotype, Δ*Mkk11/IDC*^{404}, Δ*Mpk1*, Δ*Nox1/IDC*^{343}, Δ*So/IDC*^{821} and Δ*IDC*^{1} mutants are defective in both cell-cell fusion and sexual fruiting body development (Haedens *et al.,* 2005, Jamet-Vierny *et al.,* 2007, Malagnac *et al.,* 2004, Kicka & Silar, 2004, Kicka *et al.,* 2006, Tong *et al.,* 2014). In *Neurospora crassa* and *Sordaria macrospora*, cell-cell fusion and sexual fruiting body development have been extensively studied and several hyphal anastomosis (*ham*) and protoperithecia (*pro*) mutants identified that are defective in both developmental processes cell-cell fusion and sexual fruiting body development (Teichert *et al.,* 2014a, Kück *et al.,* 2009, Fu *et al.,* 2011, Aldabbous *et al.,* 2010, Simonin *et al.,* 2010, Bloemendal *et al.,* 2012).

In *Sordaria,* PRO1 (*N. crassa* ADV-1, *E. festucae* ProA) is a transcription factor which regulates sexual development, PRO30 (*N. crassa* MIK-1, *P. anserina* Ask1) is the CWI pathway MAP kinase kinase kinase, and PRO11 (*N. crassa* HAM-3), PRO22 (*N. crassa* HAM-2) and PRO45 (*N. crassa* HAM-4), are core components of the STRIPAK complex, which in *N. crassa* is proposed to transduce signals from and between the Pheromone Response (PR) MAP kinase pathway and the CWI MAP kinase pathway (Colot *et al.,* 2006, Becker *et al.,* 2015, Bloemendal *et al.,* 2010, Bloemendal *et al.,* 2012, Fu *et al.,* 2011, Masloff *et al.,* 1999, Tanaka *et al.,* 2013, Park *et al.,* 2008, Pöggeler & Kück, 2004, Simonin *et al.,* 2010, Dettmann *et al.,*

2013, Nordzieke *et al.,* 2015, Teichert *et al.,* 2014b, Kück *et al.,* 2016). In *N. crassa*, HAM-5 (*P. anserina* IDC1) functions as the PR pathway scaffold and MAK-2 (PR pathway MAP kinase) oscillates with the CWI pathway scaffold SO (*S. macrospora* PRO40, *E. festucae* So, *P. anserina* So) during pre-fusion hyphae homing (Teichert *et al.,* 2014b, Fleiβner & Glass, 2007, Fleiβner *et al.,* 2008, Charlton *et al.,* 2012, Jamet-Vierny *et al.,* 2007, Jonkers *et al.,* 2014, Fleiβner *et al.,* 2009a). Additionally, HAM-6 (*S. macrospora* PRO41, *P. anserina* and *Botrytis cinerea* NoxD), HAM-7 (*P. anserina* IDC2 homologue) and HAM-8 are proposed to be part of a peripheral membrane-associated signalling complex in *N. crassa* which regulates cell-cell fusion (Fu *et al.,* 2014, Nowrousian *et al.,* 2007, Lacaze *et al.,* 2015, Siegmund *et al.,* 2015, Haedens *et al.,* 2005, Maddi *et al.,* 2012).

Although these and many other proteins required for cell-cell fusion have been characterised in *P. anserina, N. crassa*, *S. macrospora* and *E. festucae,* a defined receptor-signalling complex, which regulates the perception and initiation of cell-cell fusion has yet to be identified. The objective of this study was to test if *E. festucae* homologues of two *P. anserina* self-signalling genes, *IDC2* (*N. crassa Ham-7*) and *IDC3* (Haedens *et al.,* 2005), which we have named *symB* and *symC,* are required for hyphal network formation and establishment of a mutualistic interaction with the host *Lolium perenne*. *IDC2* (*N. crassa Ham-7*) and *IDC3* encode putative membrane-associated proteins with glycosylphosphatidylinositol (GPI)-anchored and four transmembrane domains, respectively. They are therefore candidate proteins for receptor signalling and regulation of cell-cell fusion in *E. festucae* and other filamentous fungi.

RESULTS

E. festucae symB and *symC* encode membrane-associated proteins

A tBLASTn search of the *E. festucae* Fl1 (E894) genome sequence, using *P. anserina* IDC2 and IDC3 as the query sequences, identified gene models EfM3.029010 and EfM3.029020 (Schardl *et al.,* 2013), which we have named SymB and SymC respectively, as the *E. festucae* homologues. To confirm the gene structure, each of these sequences was aligned with the *P. anserina* homologue as well as the corresponding polypeptide sequences from *Fusarium graminearum, Magnaporthe oryzae, N. crassa* HAM-7 (Maddi *et al.,* 2012) and *S. macrospora* (**Figs. S1 & S2**). The proposed exon-intron structure of each gene was verified by cDNA sequencing. *E. festucae* SymB, is a 230 amino acid protein that shares 76% identity to *P. anserina* IDC2 and 75% identity to *N. crassa* HAM-7 (Maddi *et al.,* 2012). The presence of an 18 amino acid N-terminal signal peptide (Signal P; Petersen *et al.,* 2011, Nielsen *et al.,* 1997) and a post-translation C-terminal GPI anchor (big-PI Fungal Predictor; Eisenhaber *et al.,* 2004) suggests that SymB is a secreted membrane-anchored protein (**Fig. S1**).

E. festucae SymC, is a 274 amino acid protein and shares 56% identity to *P. anserina* IDC3 and 51% identity to *N. crassa* NCU00938. Analysis of SymC using TMHMM (Krogh *et al.,* 2001, Sonnhammer *et al.,* 1998) predicts four trans-membrane domains (TMDs), with extracellular domains between TMDs 1-2 and 3-4, and intracellular domains between TMDs 2-3 and downstream of TMD4, suggesting that SymC is likely to be a membrane bound protein (**Fig. S2**).

***symB* and *symC* promoters contain putative binding sites for the transcription factor ProA.**

To gain some insight into whether *symB* and *symC* were important for the symbiosis we examined RNA-seq data sets generated by sequencing mRNA from plants infected with three different symbiotic mutants (Eaton *et al.,* 2015) including, Δ*noxA* (NADPH oxidase; Tanaka *et al.,* 2006), Δ*proA* (C6-Zn transcription factor; Tanaka *et al.,* 2013) and Δ*sakA* (stress-activated MAP kinase; Eaton *et al.,* 2008, Eaton *et al.,* 2010). Both genes were up-regulated in the Δ*noxA* and Δ*sakA* data sets (**Fig. S3**) but the expression changes were only significant in the latter [based on statistically significant differences (corrected $P < 0.05$) and a 2-fold change cut off]. Both genes were significantly down-regulated in the Δ*proA* data set. Given we had previously identified a ProA binding site consensus sequence of GGCGCTTA (Tanaka *et al.,* 2013), we analysed the promoter sequences of both *symB* and *symC* and their homologs in other Clavicipitaceae for the presence of this motif. In both cases a single motif identical to the consensus sequence was identified (**Figs. S4 & S5**). We therefore tested whether the promoter sequences containing this motif were ProA binding sites *in vitro* using electrophoretic mobility shift assays (EMSA). Various *symB* and *symC* promoter fragments were incubated with a fusion protein of the N-terminal 120 amino acid residues of ProA containing the zinc cluster domain fused to the maltose binding protein (MalE-ProA 1-120; pMal-ProA3)(Tanaka *et al.,* 2013). Mobility shifts were observed for the fragments containing the sequence of GGCGCTTAA (P*symB*: F1 and P*symC*: F2) (**Fig. 1A-C**). No extra bases on the 5'side of GGCGCTTAA were required for ProA binding in the *symB* promoter (P*symB*: R2) while a few more bases were required for ProA binding in the *symC* promoter (P*symC*: R1 and R2) (**Fig. 1C-D**). Replacement of CTT to AAA on the 3' side of GGCGCTTAA in the *symB* promoter (P*symB*: R4 and R5) did not prevent ProA binding (**Fig. 1C-D**). This analysis confirmed that these motifs are specific binding sites for ProA (**Fig. 1**). Given we have previously shown that ProA is a transcription factor critical for cell-cell fusion and symbiosis (Tanaka *et al.,* 2013), we propose that *symB* and *symC* are downstream targets of ProA in the molecular pathway required for cell-cell fusion and symbiosis.

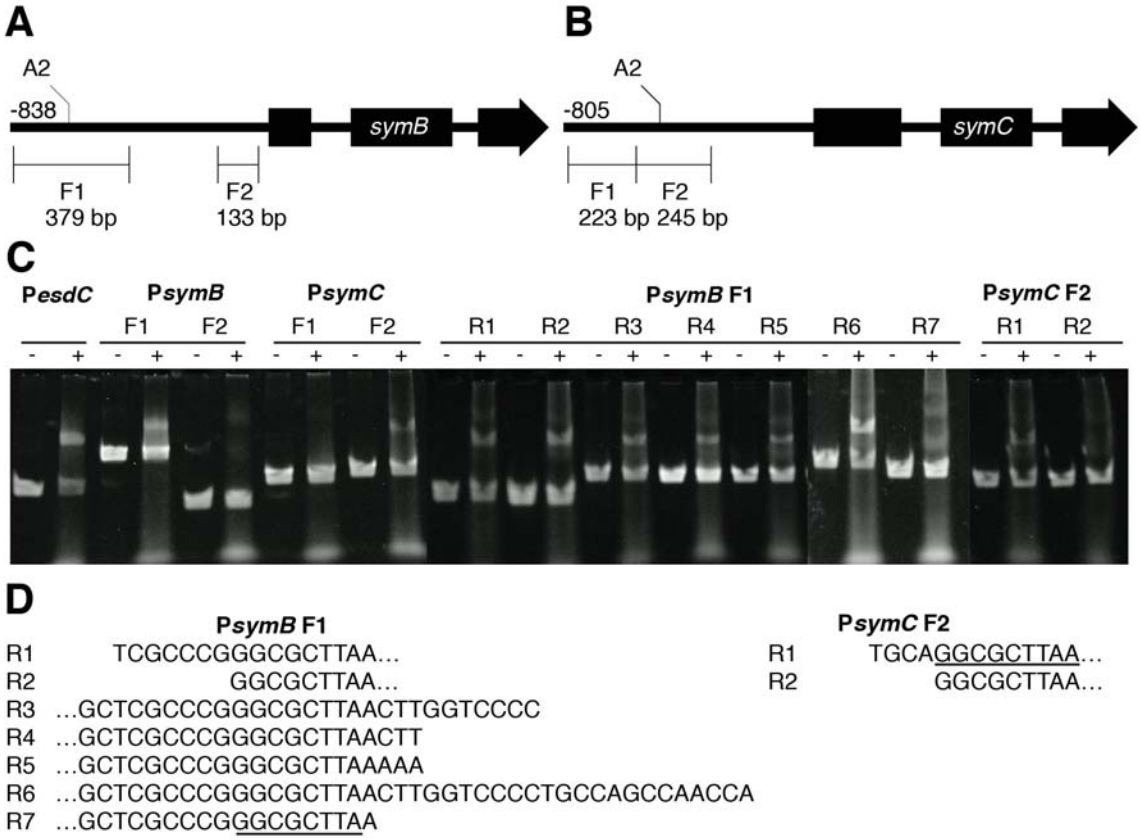

Fig. 1. Electrophoretic mobility shift assays of *symB* and *symC* promoter fragments bound to ProA. Physical map of the **A,** *symB* and **B,** *symC* promoter regions with the A2 GGCGCTTAA regions and gel shift target regions, F1 and F2 shown. **C,** EMSA with (+) and without (-) ProA incubation using the corresponding fragment regions as indicated in A, B, and D, and a positive P*esdC* control fragment as per Tanaka *et al.* (2013). **D,** DNA sequence of binding regions with the A2 GGCGCTTAA region indicated.

Deletion of *symB* and *symC* genes

To determine whether SymB and SymC are required for hyphal cell-cell fusion in *E. festucae* and establishment of a mutualistic symbiotic interaction with *L. perenne*, *symB* and *symC* genes were individually deleted in the Fl1 wild-type background using a gene replacement approach. Linear fragments containing replacement cassettes for *symB* and *symC* were purified from restriction enzyme-digested pKG1 and pKG2 plasmid DNA, transformed into protoplasts of wild-type, and plated on either hygromycin (pKG1) or geneticin (pKG2) containing solid media (**Fig. S6**). PCR screening of an arbitrary selection of these transformants identified 7 putative Δ*symB* (#3, #6, #8, #9, #11, #14 and #17) and 6 putative Δ*symC* (#2, #7, #8, #20, #25 and #28) mutants. Southern blot analysis of genomic DNA digests obtained from these candidates confirmed that all were 'clean knock-outs'. Δ*symB*#3 and #6 and Δ*symC*#7 and #8 strains were subsequently selected for all further experiments (**Fig. S6**).

Culture phenotype of Δ*symB* and Δ*symC* strains

In axenic culture the colony size and morphology of Δ*symB* and Δ*symC* strains were indistinguishable from wild-type (**Fig. 2A**). However, closer analysis revealed that Δ*symB* and Δ*symC* strains formed intra-hyphal hyphae and had increased rates of conidiation (**Figs. 2B-C & S7A**). Most of the conidia appeared to arise from conidiophores associated with hyphal coils. Microscopic examination of the germination of isolated conidia revealed no noticeable morphological differences between mutants and wild-type (**Fig. S7B**). Hyphae of Δ*symB* and Δ*symC* strains were also defective in the ability to form the tip-to-side hyphal fusions observed in wild-type (**Fig. 2D**). To validate this cell-cell fusion phenotype, cultures of Δ*symB* and Δ*symC* expressing either eGFP or mRFP1 were co-inoculated in close proximity to one another and hyphae examined for evidence of cytoplasmic mixing. Whereas wild-type co-inoculations showed co-expression of the two reporter genes, Δ*symB* and Δ*symC* hyphae were either red or green indicating they were unable to fuse (**Fig. 2D**). The introduction of wild-type *symB* and *symC* genes into the mutant backgrounds restored this fusion defect, demonstrating that deletion of *symB* or *symC* was responsible for the cell-cell fusion defect (**Figs. 2E & S6**).

Given the culture phenotypes of Δ*symB* and Δ*symC* described above were identical to Δ*mkkA* and Δ*mpkA* (Becker *et al.*, 2015), we also tested whether these mutants were sensitive to cell-wall stress agents and conditions. *E. festucae* Δ*symB* and Δ*symC* mutants grew as well as the wild-type strain on media containing Congo red or Calcofluor white. In addition, radial growth of the mutants was the same as wild-type on media buffered to pH 5, pH 6.5 or pH 8 (**Fig. S8**).

Fig. 2. Culture phenotype of wild-type, Δ*symB* and Δ*symC* strains. A, Colony morphology of wild-type (WT), Δ*symB* and Δ*symC* mutants cultures grown on PD agar for 5 days. **B,** DIC images of mutant hyphae forming intra-hyphal hyphae as indicated by an arrow. Bar = 10 µm. **C,** DIC images of coil-like structures and conidiophore formation in cultures grown on water agar for 7 days. Conidia are marked with an asterisk. Bar = 20 µm. **D,** DIC and fluorescent images of eGFP and mRFP1 expressing strains co-cultivated onto water agar for 5 days. Sites of cell-cell fusion are indicated by boxes. Bar = 10 µm. **E,** DIC images of wild-type and complemented strains grown on water agar for 5 days showing restoration of cell-cell fusion. Bar = 10 µm.

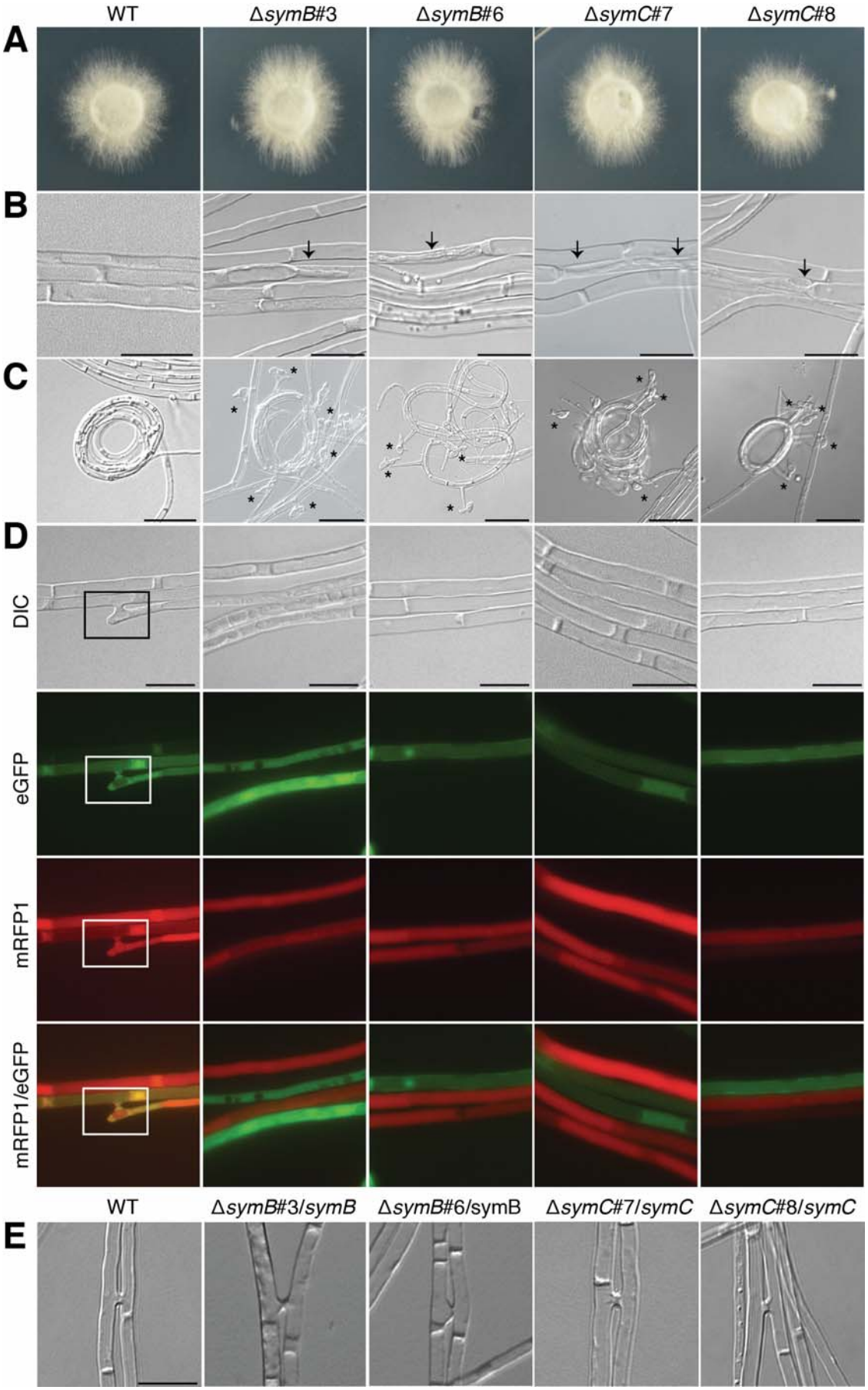
WT
ΔsymB#3
ΔsymB#6
ΔsymC#7
ΔsymC#8
A
B
C
D
DIC
eGFP
mRFP1
mRFP1/eGFP
WT
ΔsymB#3/symB
ΔsymB#6/symB
ΔsymC#7/symC
ΔsymC#8/symC
E

***In planta* phenotype of Δ*symB* and Δ*symC* strains**

We next examined the role of *symB* and *symC* in regulating the symbiotic interaction of *E. festucae* with *L. perenne*. Δ*symB* and Δ*symC* cultures were inoculated into seedlings and the phenotype analysed at 10 weeks post-inoculation. A large number of mutant-infected plants died at around three to five weeks post-planting (**Supplementary Table 3**). Those that survived, and were subsequently used for microscopy, were severely stunted compared to wild-type infected plants (**Fig. 3A**). Introduction of wild-type copies of *symB* and *symC* genes into the mutant backgrounds rescued the wild-type symbiotic interaction phenotype demonstrating that *symB* and *symC* are essential for *E. festucae* mutualistic associations (**Figs. 3B & C, S6**).

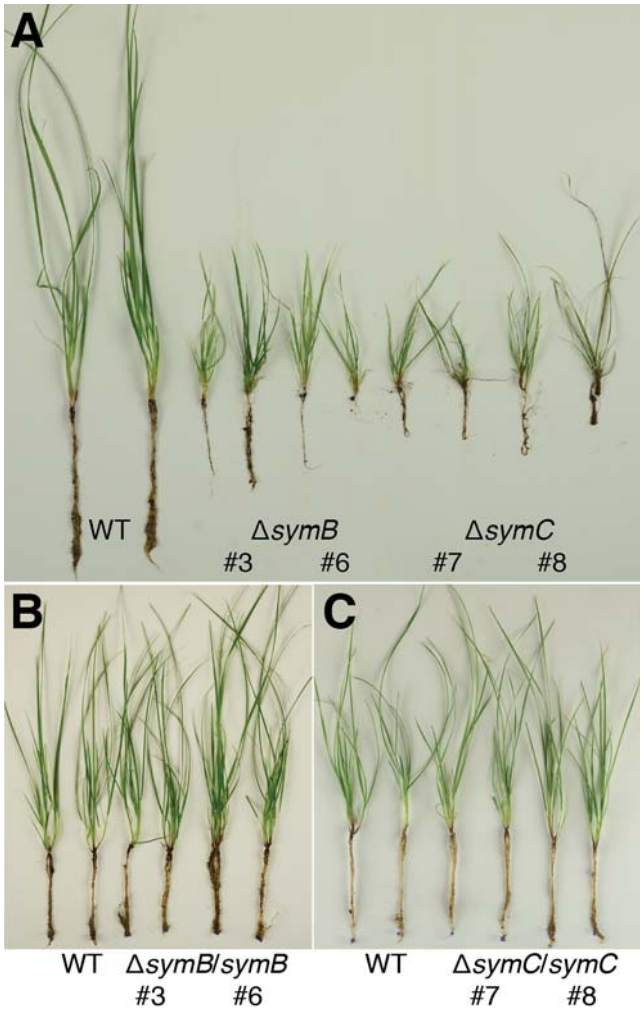

Fig. 3. Plant phenotype of *Lolium perenne* infected with wild-type, Δ*symB*, Δ*symC* and complemented strains. Whole plant interaction phenotype of *L. perenne* infected with **A,** wild-type (WT), Δ*symB* and Δ*symC* strains, **B,** wild-type and Δ*symB* complemented strains, and **C,** wild-type and Δ*symC* complemented strains, 10 weeks after infection.

To evaluate the cellular phenotype of Δ*symB* and Δ*symC* in infected plants, we harvested leaf sheath tissue samples and examined the hyphal phenotype by transmission electron microscopy (TEM) (**Fig. 4**) and confocal laser scanning microscopy (CLSM) (**Fig. 5**). While wild-type associations contained mostly one to two hyphae per intercellular space, Δ*symB* and Δ*symC* mutant associations contained up to nine hyphae per intercellular space (**Figs. 4A & S9**). These mutant hyphae were frequently vacuolated (**Fig. 4A**), a subset of hyphae contained intra-hyphal hyphae (**Fig. 4D**), and the outer cell walls appeared to be less electron-dense (**Fig. 4C**). Hyphae of Δ*symB* and Δ*symC* were also very abundant in the vascular bundle tissue (**Fig. 4B**), which is seldom, if ever, colonised by wild-type hyphae. Hyphae in these tissues were electron dense presumably reflecting the abundant supply of nutrients in these tissues for growth.

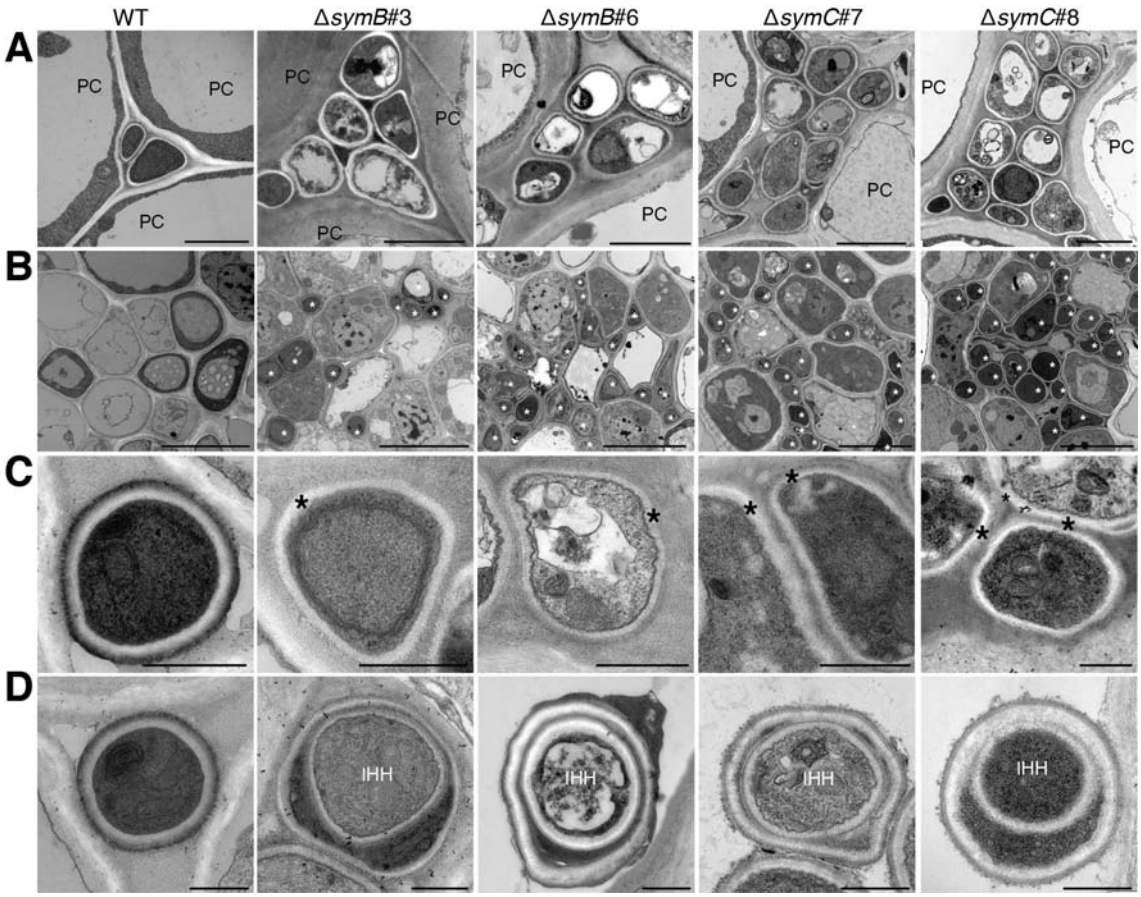

Fig. 4. *In planta* cellular phenotype of Δ*symB* and Δ*symC* mutants. Transmission electron micrographs of *L. perenne* leaf sheath cross-sections infected with wild-type, Δ*symB* and Δ*symC* strains. **A,** Hyphae growing within the intercellular spaces of plant cells (PC). Bar = 1 µm. **B,** Vascular bundle colonisation in Δ*symB* and Δ*symC* associations. Hyphae are marked with a white asterisk. Bar = 5 µm. **C,** Altered mutant hyphal cell wall staining. Hyphal cell wall is indicated with an asterisk. Bar = 500 nm. **D,** Mutant intra-hyphal hyphae (IHH) formation. Bar = 500 nm.

The prolific growth of the Δ*symB* and Δ*symC* mutants in leaf tissue compared to the more restrictive growth of the wild-type was also evident from CLSM analysis of leaf sheath tissue stained with aniline blue and WGA-AF488, which stain β-glucan and chitin, respectively (**Fig. 5**). In wild-type associations, lateral hyphae were observed to undergo tip-to-tip cell fusion to form a restricted hyphal network throughout the host plant (**Fig. 5**). Although qPCR was not performed to qauntify hyphal biomass *in planta,* microscopy showed that the hyphae of Δ*symB* and Δ*symC* were much more prolific within the leaf sheath tissue (**Fig. 5A**), had an irregular pattern of growth, and frequently formed highly convoluted structures comprised of many cells as evident from the many fluorescent septa (**Fig. 5B & C**). These structures were never observed in wild-type tissue. Whereas just the septa of wild-type hyphae stained with AF488-WGA, in the mutant hyphae, large patches of WGA-AF488 fluorescence were visible (**Fig. 5C**), suggesting a change in the structure and/or composition of the cell wall resulting in greater accessibility of the cell wall chitin to the fluorophore-labelled lectin.

Expressorium formation in Δ*symB* and Δ*symC* strains

Expressoria allow *E. festucae* hyphae to exit the host plant and form an epiphyllous hyphal net on the leaf surface of the host plant. As we have previously shown, deletion of *noxA* and *noxR* disrupts expressoria formation and mutant hyphae form sub-cuticular hyphal bundles (Becker *et al.,* 2016). Given the very similar plant interaction phenotypes of Δ*symB* and Δ*symC* strains to Δ*noxA* and Δ*noxR* (Takemoto *et al.,* 2006, Tanaka *et al.,* 2006), we examined expressoria development in these mutants. In contrast to wild-type hyphae, which formed expressoria and induced a thinning of the cuticle layer at the contact point (**Fig. 6**), Δ*symB* and Δ*symC* strains were unable to differentiate expressoria but instead developed highly reticulate hyphal structures immediately beneath the surface of the cuticle (**Figs. 6A & B**). Examination of this tissue by TEM revealed the presence of swollen hyphae that appeared unable to degrade the cuticle (**Fig. 6C**). These results demonstrate that both SymB and SymC are necessary for expressorium differentiation.

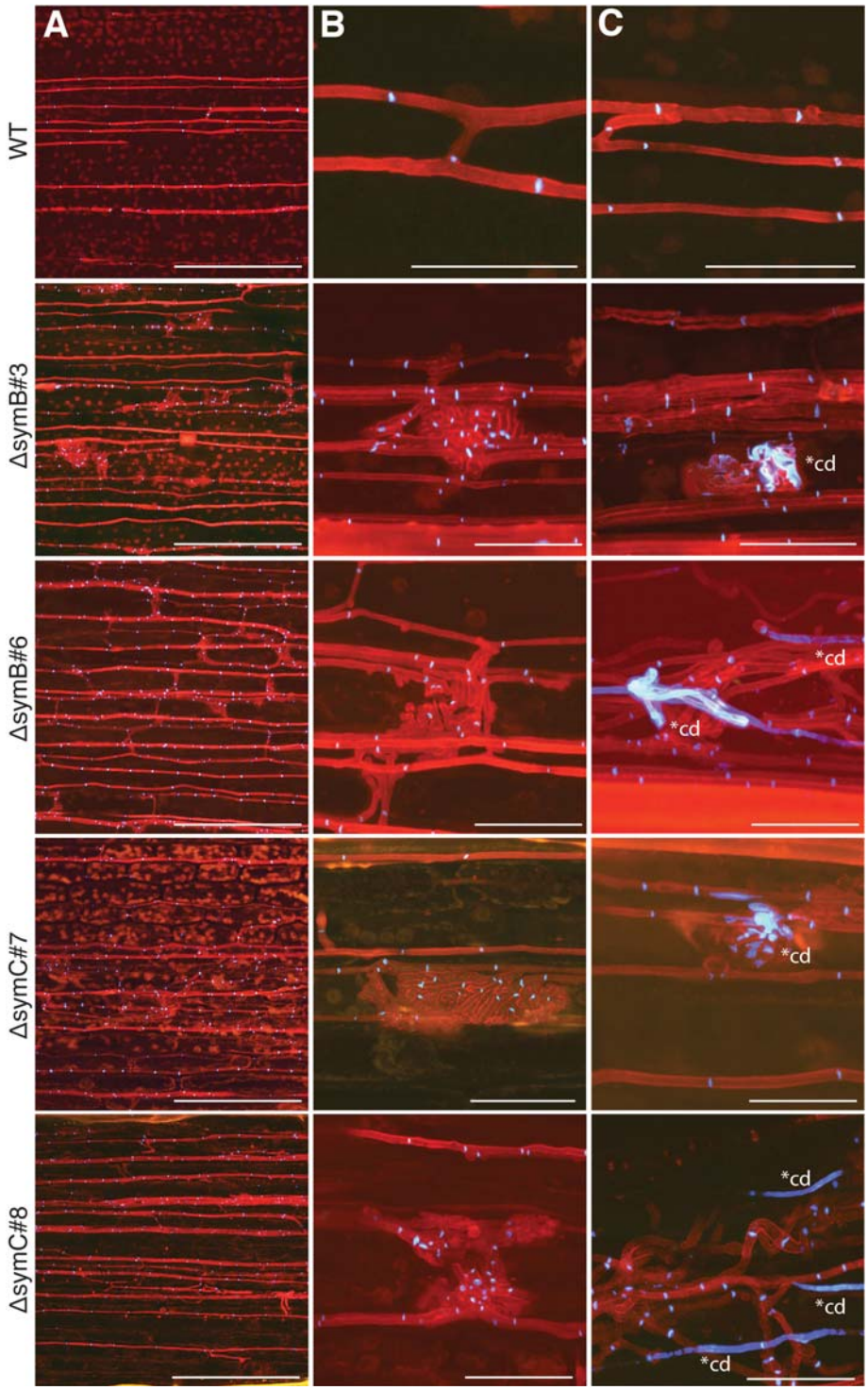

Fig. 5. *In planta* cellular phenotype of Δ*symB* and Δ*symC* mutants. Confocal depth series images of aniline blue (red pseudocolour) and WGA-AF488 (blue pseudocolour) stained *Lolium perenne* leaf sheaths infected with wild-type, Δ*symB* and Δ*symC* strains. Fluorescent images were generated by maximum-intensity projections of confocal *z*-stacks. **A,** CLSM *z*-stacks taken at 10-µm intervals of endophytic hyphae in leaves of *L. perenne* showing increased hyphal biomass of Δ*symB* and Δ*symC* mutants. Bar = 100 µm. Hyphal aggregates of Δ*symB* and Δ*symC* mutants with **B**, increased numbers of septa (blue pseudocolour) and **C**, increased patches of cell wall chitin (blue pseudocolour) compared to wild-type. Chitin depositions (cd) are indicated with a white asterisk. Bar = 25 µm.

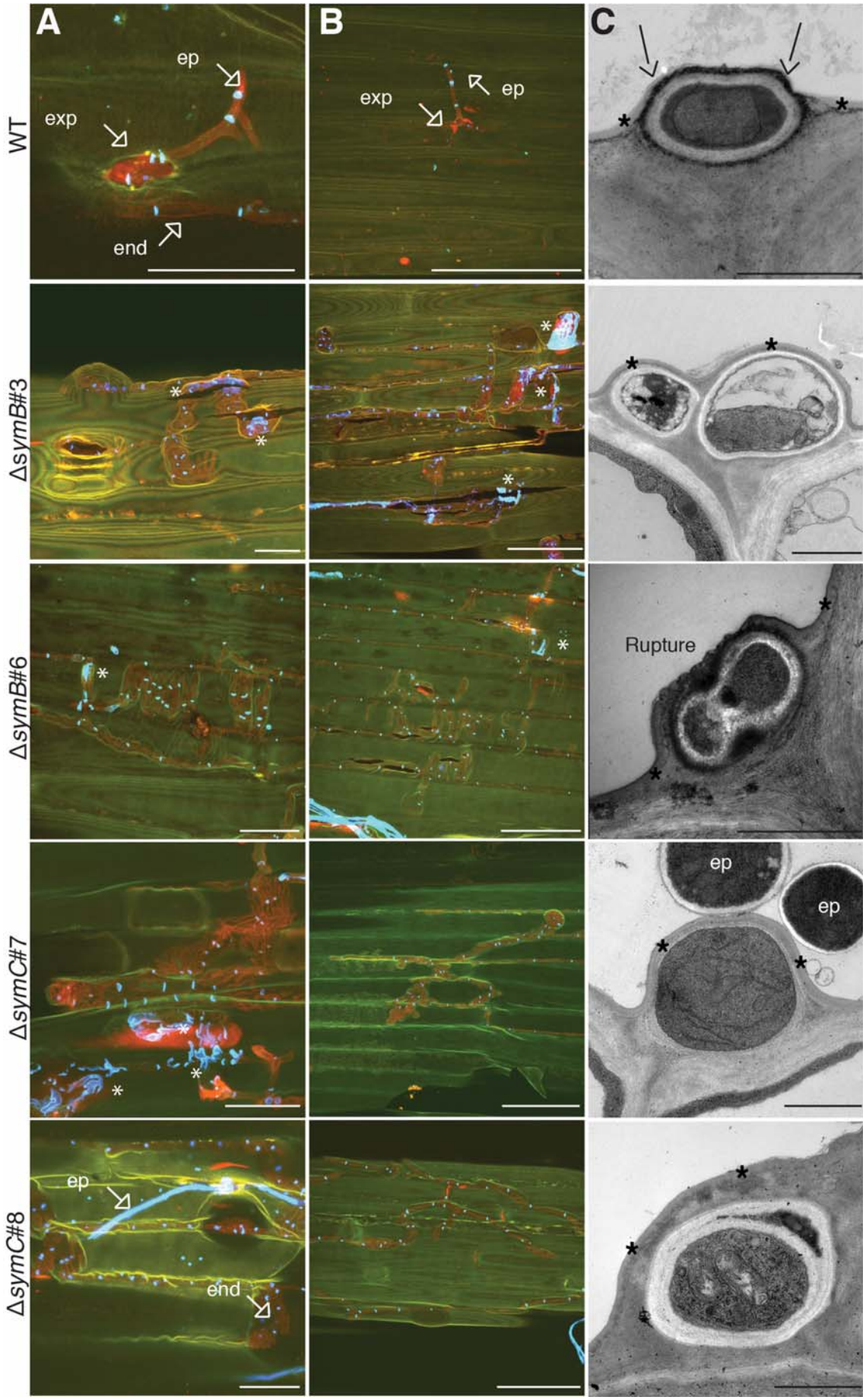
A
B
C
WT
ΔsymB#3
ΔsymB#6
ΔsymC#7
ΔsymC#8
ep
exp
end
Rupture

Fig. 6. Impaired development of expressoria in Δ*symB* and Δ*symC* mutants. A & B, Confocal depth series images of aniline blue (red pseudocolour) and WGA-AF488 (blue pseudocolour) stained *Lolium perenne* leaf sheaths infected with wild-type (WT), Δ*symB* and Δ*symC* strains. Fluorescent images were generated by maximum-intensity projections of compressed confocal *z*-stacks. In wild-type, endophytic (end) hyphae differentiate into expressoria (exp) which penetrate the cuticle (green pseudocolour) to give rise to an epiphyllous (ep) net on the surface of the blade. Δ*symB* and Δ*symC* strains failed to differentiate expressoria, instead forming highly reticulate sub-cuticular structures which had increased patches of cell wall chitin (*; blue pseudocolour) compared to wild-type. Bar = **A,** 25 µm and **B,** 50 µm. **C,** Transmission electron micrographs of pseudostem cross-sections showing degradation of the host cuticle layer in wild-type (WT) associations, as indicated by the arrows, and ultra-structure of sub-cuticular hyphae in Δ*symB* and Δ*symC* associations. The host cuticle is indicated by an asterisk. Bar = 1 µm.

MpkA and MpkB phosphorylation and localisation in Δ*symB* and Δ*symC* strains

To determine if deletion of either *symB* or *symC* impacts on signalling through the cell wall integrity (CWI) or pheromone response (PR) MAP kinase pathways we examined the phosphorylation status and localisation of MpkA and MpkB in *E. festucae*. MpkA and MpkB phosphorylation levels were assessed by Western analysis (**Fig. 7**), using protein extracts from *E. festucae* cultures grown in PD media alone (basal levels) and in PD media subjected to oxidative stress (plus H_2O_2) (Maddi *et al.*, 2012, Dettmann *et al.*, 2014). While, oxidative stress usually increased the level of phosphorylation of both MpkA and MpkB, no differences in intensity of signal were observed between wild-type and the Δ*symB* and Δ*symC* strains (**Figs. 7A & B**). As previously reported (Becker *et al.*, 2015), phosphorylation of MpkA is completely abolished in the CWI MAP kinase mutants, Δ*mkkA* and Δ*mpkA* (**Figs. 7A & B**).

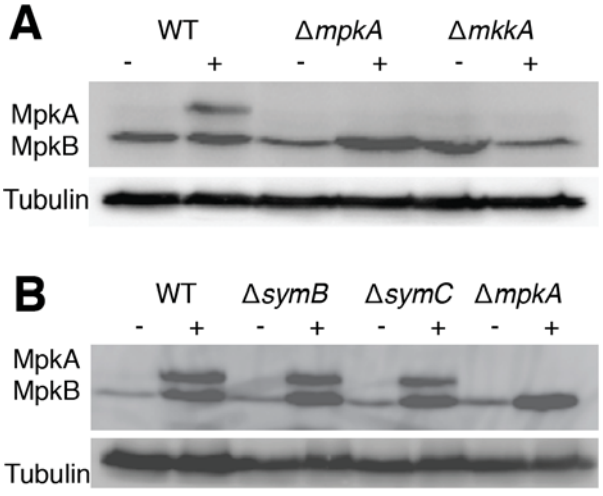

Fig. 7. Analysis of MpkA and MpkB phosphorylation in culture. Western blot analysis of MpkA phosphorylation in **A,** wild type, Δ*mpkA* and Δ*mkkA* mutants and **B,** WT, Δ*symB*#3, Δ*symC*#7 and Δ*mpkA* strains under non-stressed (-) and H_2O_2 stressed (+) conditions. Phosphorylated MpkA (47 kDa) and MpkB (41 kDa) were detected using anti-phospho p42/p44 MAPK antibodies. Tubulin (54 kDa) was used as a loading control and detected using an anti-α-tubulin antibody.

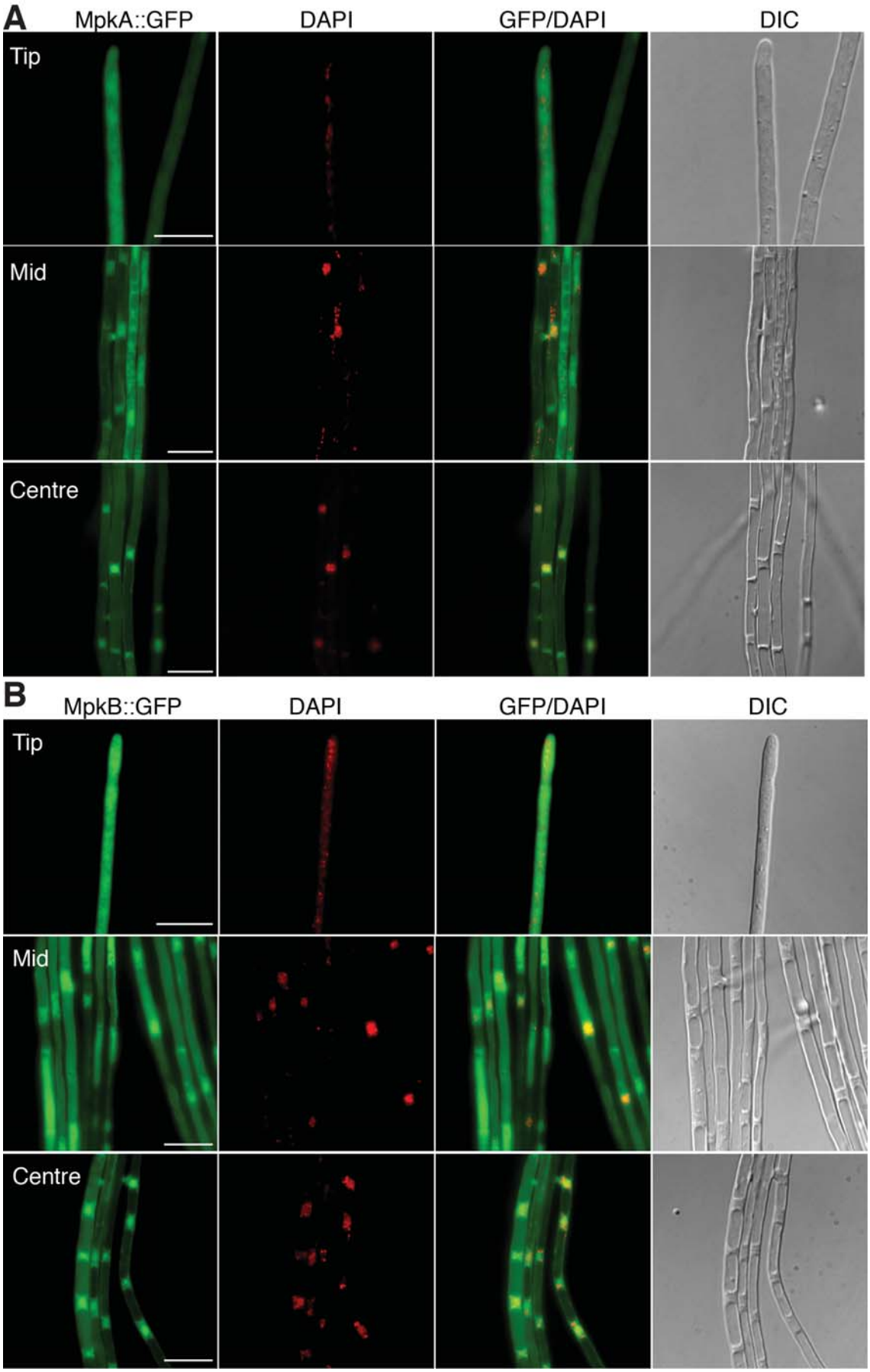
A
MpkA::GFP
DAPI
GFP/DAPI
DIC
Tip
Mid
Centre
B
MpkB::GFP
DAPI
GFP/DAPI
DIC
Tip
Mid
Centre

Fig. 8. Localisation of MpkA and MpkB in *E. festucae* cultures. Inverted fluorescent light microscopy and DIC microscopy of MpkA-eGFP and MpkB-eGFP cellular localisation in axenic cultures of *E. festucae*. **A**, Localisation of MpkA-eGFP in wild-type (PN2963) hyphae at the edge, mid-region and centre of a colony and corresponding GFP, DAPI and DIC images. **B,** Localisation of MpkB-eGFP in wild-type (PN3138) hyphae at the edge, mid-region and centre of a colony and corresponding GFP, DAPI and DIC images. Bar = 10 μm.

To determine whether MpkA or MpkB localisation was affected by deletion of *symB* or *symC*, we transformed MpkA-eGFP and MpkB-eGFP constructs into wild-type, Δ*symB* and Δ*symC* strains and analysed their subcellular localisation throughout the growing colony (**Fig. 8**). No noticeable differences in MpkA-eGFP or MpkB-eGFP localisation were observed between wild-type, and Δ*symB* and Δ*symC* mutants (**Figs. S10-S15**).

SymB and SymC cellular localisation

SymB is predicted to have a signal sequence and a C-terminal region for post-translational addition of a GPI-anchor, and SymC is predicted to have four transmembrane domains. Reporter constructs of the corresponding genes were generated to examine the cellular localisation of each protein in hyphae of *E. festucae* grown in axenic culture. As both the N- and C-termini of SymB are predicted to be post-translationally processed, eGFP was placed 10 amino acids upstream of the ω site for GPI addition (**Fig. S1**); a strategy successfully used in *S. macrospora* (Frey *et al.*, 2015). The mRFP tag was placed immediately before the SymC C-terminal stop condon. Constructs of *symB-eGFP* and *symC-mRFP1*, under the control of their native promoters (**Figs. S16 & S17C**), were transformed into Δ*symB* and Δ*symC* protoplasts, and transformants tested for cell-cell fusion. In both cases the fusion phenotype was restored indicating that the products of the *symB/C*-reporter gene fusions complemented the mutant phenotypes. Given fluorescence under the native promoter was very weak, over expression constructs were subsequently analysed (**Figs. 9 & 10**). SymB-eGFP was found to localise to the plasma membrane (**Fig. 9**), septa (**Figs. 9B & C**), tips of hyphal branches (**Figs. 9B & C**), apical tips (**Figs. 9A**) and at points of hyphal fusion (**Fig. 9D**). These results, together with the observation that SymB-eGFP co-localises with CFW (**Fig. S17A**), confirm that SymB is a membrane-associated protein.

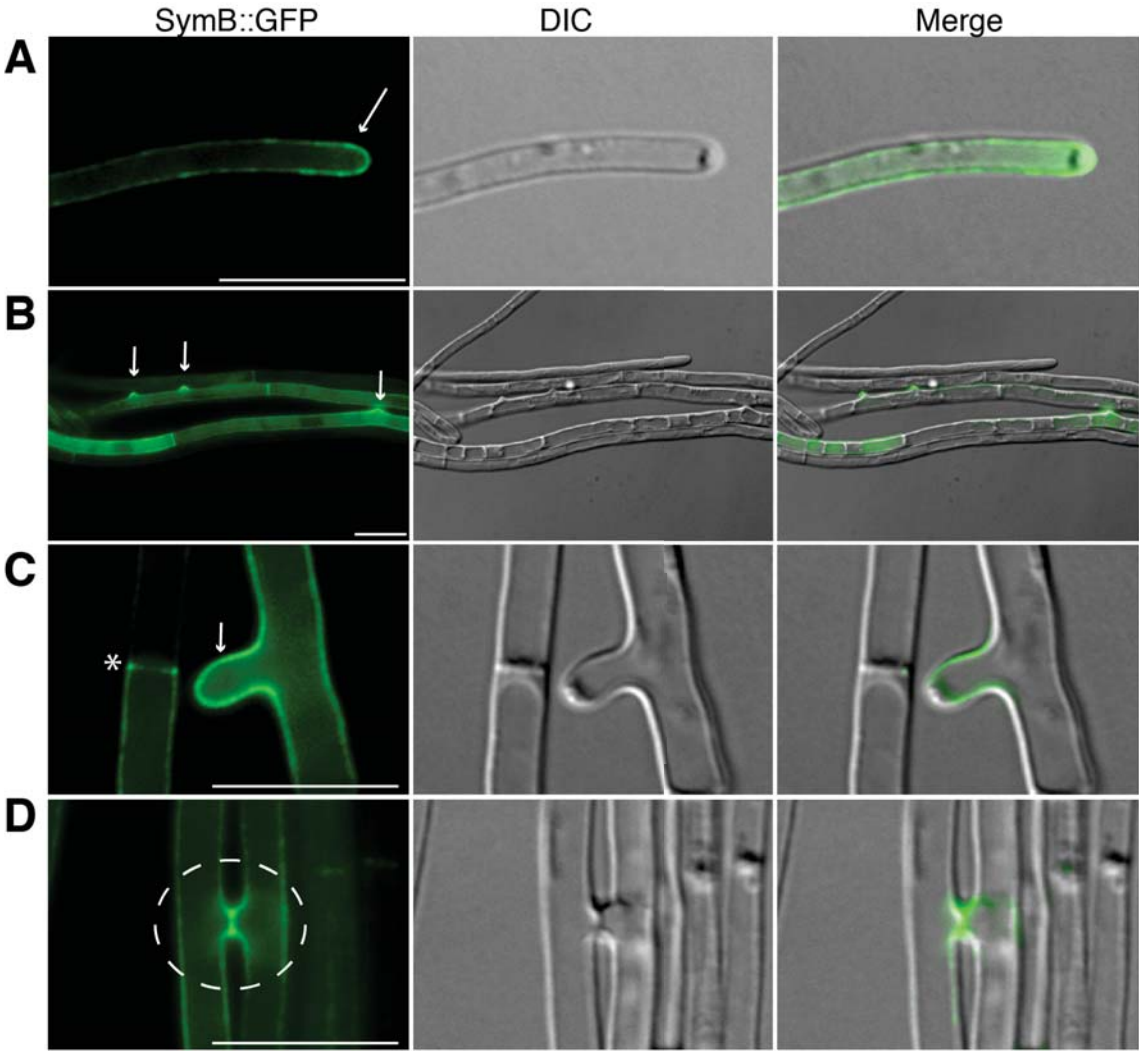

Fig. 9. Localisation of SymB-eGFP in *E. festucae* Δ*symB*. Inverted fluorescent light microscopy and DIC microscopy of SymB-eGFP (green pseudocolour) localisation in cultures of PN3131(Δ*symB*#3/pKG20) at **A,** hyphal tips, **B & C,** cell wall/branch points and septa (*) and **D,** cell-cell fusions. The P*tefA* promoter was used to express *symB-eGFP*. Bar = 10 µm.

Although SymC-mRFP1 appeared to be predominantly localised to vacuoles (**Fig. S16**), fluorescence was also observed at the cell periphery, septa, hyphal branch points, points of hyphal cell-cell fusion associated with septa, and in small, highly dynamic vesicles (**Fig. S16; Movie S1**). The accumulation of SymC-mRFP1 in vacuoles may be due to a highly efficient actin-dependent endocytosis pathway resulting in recycling of this protein from the cell periphery to vacuoles for degradation as previously reported for the membrane-associated mucin Msb2 in *Ustilago maydis* (Lanver *et al.*, 2010). To test this hypothesis we grew cells containing SymC-mRFP1 in the presence of latrunculin A (**Fig. 10**) and imaged by inverted light microscopy. Treatment with latrunculin A caused bulging of hyphal tips (**Fig 10A**) and enhanced the localisation of SymC-mRFP1 to the plasma membrane (**Figs. 10A & B & S17B**), small vesicles (**Fig. 10A**) and septa (**Figs. 10B & C**), demonstrating that the pattern of cellular localisation is very similar to that of SymB. When SymB-eGFP and SymC-mRFP1 were co-

expressed in a wild-type background they co-localised at the cell periphery, septa and in vacuole-like structures (**Fig. S17C**), suggesting they potentially function in the same cellular processes.

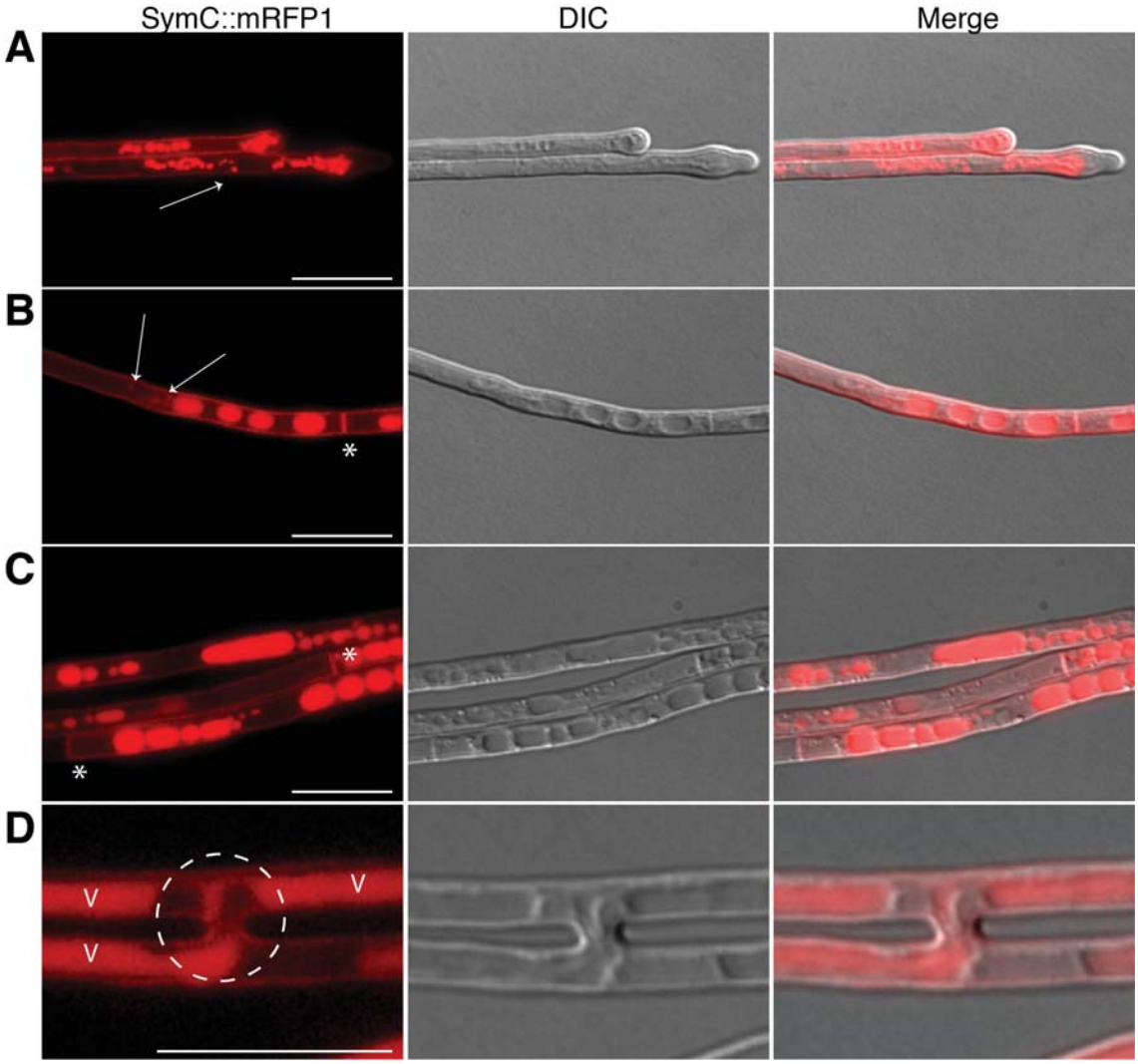

Fig. 10. Localisation of SymC-mRFP1 in *E. festucae* Δ*symC*. Inverted fluorescent light microscopy and DIC microscopy of SymC-mRFP1 (red pseudocolour) localisation in cultures of PN3132 (Δ*symC*#7/pKG21) treated with latrunculin A at **A,** hyphal tips, **B & C,** cell wall, vesicles (arrows), septa (*) and **D,** cell-cell fusions and vacuoles (v). The P*tefA* promoter was used to express *symC-mRFP1*. Bar = 10 µm.

DISCUSSION

In fungi, hyphal communication and cell-cell fusion is required for colony formation and nutrient transfer (Leeder *et al.,* 2013; Read *et al.,* 2009; Simonin *et al.,* 2010). Here we report that *symB* and *symC,* homologs of *P. anserina IDC2* and *IDC3* (Haedens *et al.,* 2005), are key components of the conserved signalling network that regulates cell-cell fusion in filamentous fungi. We have established for the first time that these two genes are down stream

of the transcription factor ProA within this conserved signalling network. Furthermore we have shown that SymB and SymC localise to the cell periphery and have a novel role in expressoria development.

From the published RNA seq data (Eaton *et al.,* 2015), this study identified that *symB* and *symC* expression is significantly down-regulated in *proA* mutants compared to wild-type. The alignment of *symB* and *symC* promoters from several closely related species identified highly conserved ProA binding sites as previously published (Tanaka *et al.,* 2013). ProA binding at these regions was confirmed by gel shift assays, indicating *symB* and *symC* are regulated by this transcription factor. Furthermore, this study showed that deletion of *symB* and *symC* abolishes cell-cell fusion in culture and results in a loss of mutualism *in planta*, similar to the *proA* deletion mutant (Tanaka *et al.,* 2013). Based on these phenotypes it is likely that ProA regulates *symB* and *symC* expression both in culture and *in planta*. The homologue of ProA in *S. macrospora*, PRO1, is a C6 Zinc finger transcription factor (Masloff *et al.,* 1999 & 2002) that is homologous to *N. crassa* ADV-1 (Colot *et al.,* 2006; Fu *et al.,* 2011), and both are essential for fruiting body development and cell-cell fusion. The homologue of *pro1* is required for female fertility and virulence in *Cryphonectria parasitica* (Sun *et al.,* 2009) and virulence in *Alternaria brassicicola* (Cho *et al.,* 2009). The similarities between mutant *pro1* phenotypes in other fungi suggests this transcription factor is part of a conserved signalling network which regulates cell-cell fusion, sexual development, virulence and mutualism in filamentous fungi. SymB and SymC homologues in *P. anserina* (IDC2 and IDC3; Haedens *et al.,* 2005), *N. crassa* (HAM-7; Maddi *et al.,* 2012) and *S. macrospora* show a high level of amino acid sequence conservation, presumably reflecting their evolutionary importance downstream of ProA within this conserved signalling network. Very few ProA regulated genes have been analysed in filamentous fungi and a large number of genes down-regulated in mutant *E. festucae proA* associations encode hypothetical proteins (Eaton *et al.,* 2015). Similar findings have been reported in the *S. macrospora pro1* mutant in culture (Nowrousian *et al.,* 2007). It would be interesting to determine whether, similar to *symB* and *symC,* additional ProA regulated genes can be identified.

This study showed that deletion of *E. festucae symB* and *symC* abolishes cell-cell fusion in culture, a phenotype conserved across *P. anserina IDC*^{2} and *IDC*^{3} (Haedens *et al.,* 2005*)* and *N. crassa* Δ*ham*-7 (Fu *et al.,* 2011*;* Maddi *et al.,* 2012) mutants. In *E. festucae*, *proA*, *noxA*, *noxR mpkA* and *mkkA* are required for vegetative cell-cell fusion (Tanaka *et al.,* 2013; Kayano *et al.,* 2013; Becker *et al.,* 2015). Homologues of these genes (ADV-1/PRO1, NOX-1, NOR-1, MEK-1 and MAK-1) are required for CAT and vegetative cell-cell fusion in *N. crassa* (Maddi *et al.,* 2012, Cano-Domınguez *et al.,* 2008; Lichius, 2010; Fu *et al.,* 2011; Read *et al.,* 2012; Lichius & Lord, 2012), vegetative cell-cell fusion in *S. macrospora* (Teichert *et al.,* 2014a &

2014b; Bernhards & Pöggler, 2011; Dirschnabel *et al.,* 2014) and cell-cell fusion (NOX1, NOXR, MPK1 and MKK1) in *P. anserina* (Kicka, & Silar, 2004; Malagnac *et al.,* 2004; Haedens *et al.,* 2005; Kicka et al. 2006; Jamet-Vierny et al. 2007; Lalucque *et al.,* 2012; Tong *et al.,* 2014), suggesting these proteins are part of the core signalling network which regulates cell-cell fusion. Several of these homologues are also required for fruiting body development, suggesting a relationship exists between cell-cell fusion and the development of sexual structures in filamentous fungi (Fu *et al.,* 2011; Read *et al.,* 2012; Lichius & Lord, 2014; Bernhards & Pöggler, 2011; Teichert *et al.,* 2014a; Haedens *et al.,* 2005; Tong *et al.,* 2014).

Unlike *S. macrospora*, *N. crassa* and *P. anserina,* which readily form fruiting bodies in culture (Lord & Read, 2011; Lichius *et al.,* 2012; Mai, 1976), the sexual cycle of *E. festucae* has only been reported to occur on the host plant (Bultman & Leuchtmann, 2008) and in culture *E. festucae* is only known to undergo asexual conidiation, which is extremely sparse and frequently associated with coil-like structures (Becker *et al.,* 2015). Here we show that deletion of *symB* and *symC* results in a hyper-conidiation phenotype in culture, similar to that previously reported for *proA, noxA*, *mkkA*, *mpkA* and *mobC* deletions (Tanaka *et al.,* 2013; Kayano *et al.,* 2013; Becker *et al.,* 2015; Green *et al.,* 2016). In contrast, *Cryphonectria parasitica pro1* (Sun *et al.,* 2009), *Magnaporthe oryzae nox-1* (Egan *et al.,* 2007) and *M. oryzae* and *Claviceps purpurea* CWI (Jeon et al. 2008; Mey et al. 2002) mutants show reduced conidiation. These findings indicate conidiation may be "regulated" differently in *E. festucae* compared to other fungi. In some fungi, conidiation can be induced by stress. For example alkaline pH in wild-type *E. festucae* (Lukito *et al.,* 2015), osmotic stress conditions in *A. flavus* (Duran *et al.,* 2010), mycelia wounding and nutrient depletion in *Trichoderma atroviride* induces conidiation (Hernández-Oñate *et al.,* 2012, Carreras-Villaseñor *et al.,* 2012). Whether Δ*symB* and Δ*symC* hyperconidiation phenotypes are directly related to gene deletions, or occur as a result of impaired cell-cell fusion nutrient transfer, hyphal starvation, hyphal stress or additional CWI defects, requires further research.

In culture, Δ*symB* and Δ*symC* mutants form intra-hyphal hyphae, which have been observed for Δ*mpkA* and Δ*mkkA* mutants (Becker *et al.,* 2015) and the STRIPAK complex mutant Δ*mobC* (Green *et al.,* 2016), but never within wild-type. Intra-hyphal hyphae formation involves the accumulation of newly synthesised cell wall components at the primary cell wall, which causes a secondary cell wall to form, which pushes through septal pores into adjacent hyphae. Intra-hyphal hyphae are known to form in other fungi (Kim & Hyun, 2007) in response to hyphal wounding, disrupted hyphal integrity, nutrient and water deprivation, altered cell wall composition and septation defects (Calonge, 1969; Buller, 1933; Bowman *et al.,* 2006; Takeshita *et al.,* 2006; Kim & Hyun; 2007). These structures allow hyphae to survive stressful conditions while encased within a protective layer, as they contain a separate cell wall,

cytoplasm, and organelles, and are capable of undergoing branching, anastomosis and even conidiophore production. Similar to hyperconidiation phenotypes, it is difficult to determine whether intra-hyphal hyphae formation is directly related to *symB* and *symC* gene deletions.

Within *L. perenne*, Δ*symB* and Δ*symC* strains exhibited prolific hyphal growth, a breakdown of the hyphal network, vascular bundle colonisation and a loss of mutualism. These phenotypes have previously characterised in Δ*proA*, Δ*noxA*, Δ*noxR*, Δ*bemA*, Δ*so*, Δ*mkkA*, Δ*mpkA*, and Δ*mobC* mutants (Tanaka *et al.,* 2006, 2008 & 2013; Takemoto *et al.,* 2008 & 2011; Kayano *et al.,* 2013; Charlton *et al.,* 2012; Becker *et al.,* 2015; Green *et al.,* 2016) and Δ*sidN* mutants which exhibit disrupted iron homeostasis (Johnson *et al.,* 2013). In Δ*proA* and Δ*noxA* associations, primary metabolism, peptide and sugar transport, and host cell wall degradation genes are significantly up-regulated and secondary metabolism genes are down-regulated, suggesting a starvation response occurs *in planta* (Eaton *et al.,* 2015). Transmission electron microscopy analysis showed Δ*symB* and Δ*symC* hyphae are more electron dense within the nutrient rich vascular bundles than hyphae in groups of three of more outside the vascular bundles, where multiple hyphae presumably compete for limited nutrients. Increased hyphal biomass and loss of the hyphal network may explain why Δ*symB* and Δ*symC* hyphae, as an attempt to seek out more nutrients, proliferate within the host vascular bundles. This location specific TEM staining pattern is similar to that reported for Δ*sidN* and Δ*mobC* mutants (Johnson *et al.,* 2013; Green *et al.,* 2016). In addition to disrupted host associations, Δ*symB* and Δ*symC* hyphae showed altered WGA-AF488 chitin staining *in planta*, similar to that previously reported in Δ*noxA*, Δ*proA*, Δ*mkkA*, Δ*mpkA* and Δ*mobC* associations (Eaton *et al.,* 2015; Becker *et al.,* 2015; Green *et al.,* 2016). Within *Saccharomyces cerevisiae* and *Aspergillus niger*, an increase in chitin synthesis has been reported in response to compromised hyphal growth and CWI defects (Popolo *et al.,* 1997; Ram *et al.,* 2004; Arias *et al.,* 2011). Altered chitin staining in Δ*symB* and Δ*symC* hyphae may indicate hyphal starvation or compromised hyphal integrity *in planta*.

Although *E. festucae* is considered to be an endophyte, it is also an epiphyte where endophytic hyphae emerge from within the leaf expansion zone to form an epiphyllous network on the surface of the host grass leaves. Here hyphae remain connected to the endophytic hyphal network and are thought to increase the resistance of the host to fungal pathogens through 'niche exclusion' (Christensen 1997; Moy *et al.,* 2000; Christensen & Voisey, 2007). It is only recently that the structure which allows hyphae to exit the host plant has been characterised in *E. festucae*. It resembles an inverted appressorium-like swelling, coined an "expressorium" (Becker *et al.,* 2016). This study showed that Δ*symB* and Δ*symC* strains form prolific sub-cuticular hyphae which have been observed in the Nox complex mutants Δ*noxA* and Δ*noxR* (Becker *et al.,* 2016), and the STRIPAK complex mutant Δ*mobC* (Green *et al.,* 2016), but never

within wild-type, suggesting *symB* and *symC* contribute to expressoria development. Homologues of *noxA* in *M. grisea* and *B. cinerea* (Egan *et al.,* 2007; Segmüller *et al.,* 2013) and *P. anserina* (Brun *et al.,* 2009) are required for host penetration and cellulose penetration respectively. In *Colletotrichum graminicola*, the STRIPAK complex gene, *str1*, is required for progressive colonisation following penetration (Wang *et al.,* 2016). Homologues of SymB and SymC have yet to be characterised within pathogenic fungi and it would be interesting to determine whether they are required for appressoria formation.

Here we show that SymB and SymC co-localise at the cell periphery, septa and hyphal fusion points and additionally SymC localises to small vesicle-like structures and hyphal vacuoles. The accumulation of SymC-mRFP1 in vacuoles, as reported for the membrane-associated mucin Msb2 in *Ustilago maydis* (Lanver *et al.,* 2010), may reflect a high level of SymC endocytosis. This co-localisation suggests SymB and SymC interact but we have yet to prove this experimentally. Whether SymB and SymC interact with each other or with additional cell signalling proteins, is of considerable interest. Similar localisations patterns have been observed for *N. crassa* LFD-1 and PRM-1, which facilitate membrane merging during cell-cell fusion (Fleiβner *et al.,* 2009b; Palma-Guerrero *et al.,* 2014), and HAM-6, HAM-7, HAM-8, which are required for cell-cell fusion (Fu *et al.,* 2011), associated with small vesicles and are proposed to be membrane-associated (Fu *et al.,* 2014). In *P. anserina*, fluorescently labelled NoxR shows increased signal at cell-cell fusion sites, similar to *E. festucae* SymB, and localises to small vesicles, similar to SymC (Lacaze *et al.,* 2014). In *P. anserina*, fluorescently labelled NoxD and Nox1 transition from the ER into the vesicle network where they co-localise with NoxR in aging hyphae (Lacaze *et al.,* 2014). Similar results have been reported in *B. cinerea* (Siegmund *et al.,* 2014). *E. festucae* NoxR and *B. cinerea* Bem1 are also associated with septa (Takemoto *et al.,* 2011; Giesbert *et al.,* 2014), similar to SymB and SymC. Given these findings, it would be interesting to determine whether SymB and SymC co-localise or interact with homologues of these proteins in *E. festucae.*

Here we report that Δ*symB* and Δ*symC* strains share similar phenotypes to Δ*mkkA* and Δ*mpkA* mutants (Becker *et al.,* 2015), suggesting *symB* and *symC* are associated with the CWI pathway. Plate stress tests, western analysis and localisation assays showed no differences between wild-type, Δ*symB* and Δ*symC* cultures and we were unable to link SymB and SymC to either the CWI or PR MAPK pathways. The homologue of SymB in *N. crassa*, HAM-7, has been shown to be required for wild-type MAK-1 (MpkA homologue) H_2O_2 stress induced phosphorylation (Maddi *et al.,* 2012), a difference which we could not detect in Δ*symB* or Δ*symC* mutants. Interestingly, *E. festucae* Δ*mkkA* and Δ*mpkA* strains are resistant to a multitude of stress media (Becker *et al.,* 2015) compared to corresponding mutants in other fungi. For example, deletion of the CWI components Bck1, Mkk2 and MpkA in *A. fumigatus* (Valiante *et*

al., 2008 & 2009), and the CWI protein kinase PkcA in *A. nidulans* (Teepe *et al.,* 2007), reduces fungal resistance to cell wall perturbing agents. Subtle differences in CWI signalling may therefore be harder to detect in *E. festucae* than in other fungi. In *S. cerevisiae*, five cell wall stress sensors, Wsc1-3, Mid2 and Mtl2, are involved in CWI MAPK signalling (Reviewed, Levin, 2011), and in a mutagenesis screen in *N. crassa,* 10 out of 65 mutants that had cell wall protein defects also showed altered CWI (Maddi *et al.,* 2012), suggesting a high level of redundancy among cell wall proteins. Although we did not detect differences in CWI signalling, SymB and SymC may be activated by a more specific stress mechanism than H_2O_2 stress or exhibit functional redundancy within the CWI MAPK cascade. Additionally, as we looked at only the CWI and PR MAPK pathways, SymB and SymC may function in an alternative pathway. Δ*symB* and Δ*symC* strains show similar phenotypes to *E. festucae* Δ*noxA* and Δ*noxR* mutants (Tanaka *et al.,* 2006 & 2008; Takemoto *et al.,* 2006 & 2011) and SymB and SymC show localisation patterns similar to *P. anserina* and *B. cinerea* NoxD and NoxA homologues (Lacaze *et al.,* 2014; Siegmund *et al.,* 2014). It would be interesting to determine whether SymB and SymC have a role in Nox complex signalling.

In conclusion, we have identified that the membrane-associated proteins SymB and SymC act downstream to the transcription factor ProA within the conserved signalling network required for cell-cell fusion in filamentous fungi. Additionally, were have shown that SymB and SymC are required for expressoria development and the maintenance of a mutualistic symbiotic interaction between *E. festucae* and *L. perenne*. Whether SymB and SymC interact or have a role in Nox complex, CWI or PR MAPK signalling, or contribute to an alternative signalling pathway is unclear.

MATERIALS AND METHODS

Strains and growth conditions.

Cultures of *S. cerevisiae* were grown in YPD media or on 2% YPD agar plates with or without uracil as previously described (Colot *et al.,* 2006). Cultures of *Escherichia coli* were grown overnight in LB (Luria-Bertani) broth or on 1.5% LB agar containing 100 μg/mL ampicillin as previously described (Miller, 1972). Cultures of *E. festucae* were grown on 2.4% (w/v) potato dextrose (PD), 1.5% water agar plates or in PD broth as previously described (Moon *et al.,* 1999, Moon *et al.,* 2000). When performing stress tests Congo Red (25 μg/mL) and Calcofluor White (Fluorescent Brightener 28; Sigma 25 μg/mL) were added to HEPES (50 mM, pH 6.5) buffered PDA. For pH tests Blankenship media was used as previously described (Blankenship *et al.,* 2001).

Plant growth and endophyte inoculation conditions.

Endophyte-free seedlings of perennial ryegrass (*Lolium perenne* cv. Samson) were inoculated with *E. festucae* as previously described (Latch & Christensen, 1985). Plants were grown in root trainers in an environmentally-controlled growth room at 22°C with a photoperiod of 16 h of light (~100 μE/m^2 per sec) and at 8 weeks post-inoculation tested for the presence of the endophyte by immunoblotting (Tanaka *et al.,* 2005).

DNA isolation, PCR and sequencing.

Plasmid DNA from *S. cerevisiae* cultures was extracted as previously described (Colot *et al.,* 2006). Plasmid DNA from *E. coli* cultures was extracted using the High Pure Plasmid Isolation Kit (Roche) according to the manufacturer's instructions. Fungal genomic DNA used for Southern digests was extracted from freeze-dried mycelium as previously described (Byrd *et al.,* 1990). Standard PCR amplification was performed with *Taq* DNA polymerase (Roche) as per the manufacturer's instructions in a 50 μL volume. Where proofreading activity was required Phusion® High-Fidelity DNA Polymerase (Thermo Scientific) was used as per the manufacturer's instructions in a 50 μL volume. Sequencing reactions were performed using the dideoxynucleotide chain termination method with the Big-Dye™ Terminator Version 3.1 Ready Reaction Cycle Sequencing Kit (Applied BioSystems) and separated using an ABI3730 genetic analyser (Applied BioSystems). Sequence data was then assembled and analysed using the MacVector sequence assembly software, Version 12.0.5.

Preparation of deletion, complementation and localisation constructs.

Lists of all plasmids and the primer sequences used to prepare constructs can be found in **Tables S1 and S2.**

The *symB* and *symC* replacement constructs were prepared by yeast recombinational cloning (Gietz & Woods, 2002). The *symB* replacement construct (pKG1) was made by recombining *Xho*I and *Eco*RI restriction enzyme linearized pRS426 vector with 1.1-kb 5' and 3' (primer pairs KG1/2 and KG3/4) *symB* flanks, amplified from *E. festucae* genomic Fl1 DNA, and a 1.4-kb hygromycin resistance cassette (primers hphF and hphR), amplified from pSF15.15 plasmid DNA. The *symC* replacement construct (pKG2) was made by recombining *Xho*I and *Eco*RI restriction enzyme linearized pRS426 vector with 2.1-kb 5' and 1-kb 3' (primer pairs KG5/6 and KG7/8) *symC* flanks, amplified from *E. festucae* genomic Fl1 DNA, with a 1.7-kb geneticin resistance cassette (primers genF and genR), amplified from pII99 plasmid DNA. The *in vitro* recombined DNA mixtures were transformed into electrocompetent *E. coli* DH5α cells and ampicillin resistant transformants screened using Clonechecker™ for plasmids with restriction enzyme digest patterns predicted from *in silico* construction of pKG1 and pKG2. The

order of the fragments within these clones was verified by DNA sequencing. The *symB* and *symC* replacement fragments contained within pKG1 and pKG2 were excised by *Hind*III/*Eco*RI and *Kpn*I/*Eco*RV digestion, gel purified and transformed into *E. festucae* protoplasts, as described below, using Hyg^R and Gen^R selection.

The *symB* complementation construct (pKG5) was prepared by TOPO™ cloning as per the manufacture's instructions (Invitrogen) using a PCR amplified 3.9-kb fragment containing the *symB* gene (primers KG49_3 and KG50_2) amplified from cosmid #33H4 DNA. The pKG5 *symB* insert was excised, using an *Eco*RI digest (Roche), and ligated into *Eco*RI linearized pII99 vector, excised from pYR33, to create pKG7. The *symC* complementation construct (pKG6) was prepared by TOPO™ cloning as per the manufacture's instructions (Invitrogen), using a PCR amplified 4.1-kb fragment containing the *symC* gene (primers KG51_2 and KG 52) amplified from cosmid #51D9 DNA. The *in vitro* recombined DNA mixtures were transformed into chemically competent *E. coli* DH5α cells and screened for correct inserts as described above. pKG7 and pKG6 plasmids were co-transformed with pII99 and pSF15.15 into *E. festucae* Δ*symB* and Δ*symC* protoplasts as described below using geneticin and hygromycin selections respectively.

The *symB*-eGFP native promoter expression construct (pKG13) was prepared by Gibson Assembly (Gibson *et al.,* 2009) using PCR amplified 4.7-kb and 3.1-kb fragments (primers KG71_3/81_3 and KG49_4/80_2), amplified from pKG5 plasmid DNA, and a 768-bp 3xGlycine-Alanine-eGFP fragment, amplified from pPN94 plasmid DNA (primers gfpF2 and gfpR5). The 3xGA-eGFP fragment was inserted immediately after amino acid 194, upstream of the predicted *symB* GPI anchor ω site, to avoid post-translational cleavage of eGFP. The *symC*-mRFP1 native promoter expression construct (pKG12) was prepared by Gibson Assembly (Gibson *et al.,* 2009) using PCR amplified 4.4-kb and 3.7-kb fragments (primers KG76/74 and KG51_2/ 79), amplified from pKG6 plasmid DNA, and a 693-bp 3xGA-mRFP1 fragment (primers mrfpF2 and R2), amplified from pCA56 plasmid DNA. The 3xGA-mRFP1 fragment was inserted before the *symC* stop codon.

The *symB*-GFP over expression construct (pKG20) was prepared via Gibson Assembly (Gibson *et al.,* 2009) by recombining a 1.7-kb *symB*-3xGA-eGFP-*symB* fragment (primers KG92 and 93), amplified from pKG13 plasmid DNA, with a 5.2-kb fragment (primers ptefF and ptefR), amplified from pPN94 plasmid DNA. The *symC*-mRFP1 over expression construct (pKG21) was prepared via Gibson Assembly (Gibson *et al.,* 2009) by recombining a 1.8-kb *symC*-3xGA-mRFP1 fragment (primers KG94 and 95), amplified from pKG12 plasmid DNA, with a 5.2-kb fragment (primers ptefF and R), amplified from pPN94 plasmid DNA. The *in vitro* recombined DNA mixtures were transformed into chemically competent *E. coli* DH5α cells and screened for the correct inserts as described above. Plasmids pKG13/20 and pKG12/21 were co-transformed with pII99 and pSF15.15 into *E. festucae* Δ*symB* and Δ*symC* protoplasts as

described below using Gen^R and Hyg^R selection.

Plasmid pCE81 (MpkA-eGFP) was co-transformed with pII99 and pSF15.15 into *E. festucae* Δ*symB* and Δ*symC* protoplasts as described below using Gen^R and Hyg^R selection.

Plasmid pMpkB-eGFP was prepared by cloning the *E. festucae mpkB* cDNA, amplified from an Fl1 cDNA library using primers IF140-EfMpkB-F and IF140-EfMpkB-F, into *Bam*HI-cut pNPP140 (pPN94 containing 3GA-GFP) (Niones & Takemoto, 2015).

Fungal transformations.

E. festucae protoplasts were prepared as previously described by (Young *et al.,* 2005). Protoplasts were transformed with 2-3 μg of linear restriction enzyme-excised or circular plasmid DNA as previously described (Itoh *et al.,* 1994). Transformants were selected on RG media containing either hygromycin (150 μg/mL) or geneticin (200 μg/mL) and nuclear purified by three rounds of sub-culturing on the selection medium.

DNA hybridization.

E. festucae genomic digests, separated by agarose gel electrophoresis, were transferred to positively charged nylon membranes (Roche)(Southern, 1975) and fixed by UV light cross-linking in a Cex-800 UV light cross-linker (Ultra-Lum) at 254 nm for 2 min. Filters were probed with [α-^{32}P]-dCTP (3000 Ci mmol^{-1}, Amersham BioSciences)-labelled probes. DNA probes were labelled by primed synthesis with Klenow fragment using a High-Prime kit (Roche). Hybridizations were performed according to the manufacturer's instructions.

Western blot analysis.

E. festucae cultures were grown for 4 days in 50 ml of PD and 1.5 g aliquots weighed into fresh duplicate 50 mL PD flasks and incubated with shaking (200 rpm) overnight. Samples were treated with or without H_20_2 stress (32 mM) for 30 minutes and then washed, flash frozen in liquid nitrogen and freeze-dried overnight. Protein was then extracted from ground mycelia samples in 1 mL of Lysis Buffer [50 mM Tris-HCl pH 8, 100 mM NaCl, 10 mM EDTA, 1μl/mL IGEPAL CA-630 (Sigma-Aldrich), 0.5 mM PMSF, 2 mM DTT, and 10 μl/mL Phosphatase Inhibitor (Sigma-P5726)] and centrifuged at 14,000 rpm for 15 min at 4°C. Protein samples (50 μg) were separated by SDS-PAGE [10% (w/v) (Bio-Rad)] and transferred to PVDF membranes (Roche). The phosphorylation of MpkA and MpkB was detected using anti-phospho-p44/42 MAPK (Erk1/2) antibody (Number 9102; Cell Signalling Technology). To check sample loading, the membrane was reprobed with 12G10 anti-α-tubulin (Developmental Studies Hybridoma Bank, University of Iowa). Primary antibodies were detected using HPR-conjugated secondary antibodies and ECL Prime Western Blotting Detection Reagent (GE Healthcare Amersham).

Microscopy.

Cultures to be analysed by microscopy were inoculated at the edge of a thin layer of water agar (1.5%), layered on top of a glass microscope slide, and grown for 5 days. Square blocks were then extracted and placed onto new slides, covered with a cover slip, and analysed using an Olympus IX71 inverted fluorescence microscope using filters set for capturing DIC, CFW/DAPI, GFP or mRFP1. For quantifying hyphal fusions, 10 fields of view were examined at 400× magnification from three independent colonies. For quantifying conidiation, three PD agar plates, each containing 5 colonies were grown at 22°C for 7 days. Conidia were harvested by scrubbing colonies with 2 mL of sterile water, followed by filtration through glass wool-packed tips. Suspensions of 200, 300 and 500 µL were then spread onto PD agar plates for imaging and quantification. For analysing SymC::mRFP1 localisation Latrunculin A (Sigma-Aldrich, dissolved in DMSO) was applied at a final concentration of 10 µM. When staining nuclei DAPI (dissolved in water) was applied at a final concentration of (10 µM).

Growth and morphology of hyphae *in planta* was determined by staining leaves with aniline blue diammonium salt (Sigma) and Wheat Germ Agglutinin conjugated-AlexaFluor®488 (WGA-AF488; Molecular Probes/Invitrogen) as follows. Infected pseudostem tissue was sequentially incubated at 4°C in 95% (v/v) ethanol overnight, then treated with 10% (w/v) potassium hydroxide for three hours. The tissue was washed three times in PBS (pH 7.4) and incubated in staining solution (0.02% (w/v) aniline blue, 10 ng/mL WGA-AF488 (w/v), and 0.02% (v/v) Tween®-20 (Invitrogen) in PBS [pH 7.4]) for five min, followed by a 30-min vacuum infiltration step. Images were captured by CLSM using a Leica SP5 DM6000B confocal microscope (488 nm argon and 561 nm DPSS laser, 40× or 60× oil immersion objectives, NA=1.3)(Leica Microsystems). For TEM, pseudostem sections were fixed in 3% (v/v) glutaraldehyde and 2% (v/v) formaldehyde in 0.1 M phosphate buffer, pH 7.2 for 1 h as previously described (Spiers & Hopcroft, 1993). A Philips CM10 TEM was used to examine the fixed samples and the images were acquired using a SIS Morada digital camera.

Electrophoretic Mobility Shift Assay (EMSA).

EMSA was carried out to detect the ProA protein binding to the *symB* and *symC* promoters as previously described (Tanaka *et al.,* 2013). A series of DNA fragments were amplified by PCR using the primers listed in Table S2. The purified protein (0.5 µg) was incubated with 20 ng of DNA fragment at room temperature for 20 min in the binding buffer provided by the EMSA kit (Thermo Fisher Scientific). The protein-DNA complexes were resolved on 6% (w/v) nondenaturing polyacrylamide gels (Thermo Fisher Scientific) and stained with SYBR green dye.

Bioinformatic analyses.

E. festucae genes were identified by tBLASTn analysis of the *E. festucae* Fl1 (E894) genome (http://csbio-l.csr.uky.edu/ef894-2011) with protein sequences obtained from either NCBI GenBank database (http://www.ncbi.nlm.nih.gov/) or the Broad Institute (http://www.broad.mit.edu). Identity and similarity scores were calculated after ClustalW pairwise alignments of sequences (Thompson *et al.,* 1994), using MacVector Version 12.0.5. The *E. festucae* genome sequence data (Schardl *et al.,* 2013), as curated by C.L. Schardl at the University of Kentucky, is available at http://csbio-l.csr.uky.edu/ef894-2011/.

SignalP (v. 4.1) (Petersen *et al.,* 2011, Nielsen *et al.,* 1997) was used for signal peptide detection and TMHMM (v. 2.0c) (Krogh *et al.,* 2001, Sonnhammer *et al.,* 1998) was used for detection of transmembrane domains. Domain analysis was also performed using InterProScan (v. 5) (Quevillon *et al.,* 2005, Zdobnov & Apweiler, 2001), InterProScan lookup service (v. 43.1) and phobius (v. 1.01) (Kall *et al.,* 2004), plus all software given by default with InterProScan (BlastProDom, FprintScan, HMMPIR, HMMPfam, HMMSmart, HMMTigr, ProfileScan, HAMAP, PatternScan, SuperFamily, Gene3D). The "big-PI Fungal Predictor" (Eisenhaber *et al.,* 2004) was used to check for GPI-lipid anchor modification sites.

ACKNOWLEDGEMENTS

Kimberly Green was supported by a Massey University PhD and DAAD short-term research scholarship and Barry Scott by an Alexander von Humboldt Research Award. The authors thank Doug Hopcroft, Jianyu Chen, Jordan Taylor and Matthew Savoian (Manawatu Microscopy and Imaging Centre, Massey University), Arvina Ram, Anne Dettman and Yvonne Heilig for technical assistance. We thank Lynda Ciuffetti (Oregon State University) for provision of plasmids pCT74 and pCA56. We thank Chris Schardl for provision of Clavicipitaceae genome sequences, made available through funding from the U.S. National Science Foundation (grant no. EF-0523661), the U.S. Department of Agriculture National Research initiative (grant no. 2005-35319-16141), and the National Institutes of Health (grant no. 2 P20 RR-16481).

LITERATURE CITED

Aldabbous, M. S., Roca, M. G., Stout, A., Huang, I. C., Read, N. D. and Free, S. J. (2010) The *ham-5*, *rcm-1* and *rco-1* genes regulate hyphal fusion in *Neurospora crassa*. *Microbiology,* **156,** 2621-2629.

Arias, P., Díez-Muñiz, S., García, R., Nombela, C., Rodríguez-Peña, J. M., & Arroyo, J. (2011) Genome-wide survey of yeast mutations leading to activation of the yeast cell integrity MAPK pathway:

Novel insights into diverse MAPK outcomes. *BMC Genomics,* **12(390),** doi:10.1186/1471-2164-12-390.

Becker, M., Becker, Y., Green, K. and Scott, B. (2016) The endophytic symbiont *Epichloë festucae* establishes an epiphyllous net on the surface of *Lolium perenne* leaves by development of an expressorium, an appressorium-like leaf exit structure. *New Phytol.,* DOI:10.1111/nph.13931.

Becker, Y., Eaton, C. J., Brasell, E., May, K. J., Becker, M., Hassing, B., *et al.* (2015) The fungal cell wall integrity MAPK cascade is crucial for hyphal network formation and maintenance of restrictive growth of *Epichloë festucae* in symbiosis with *Lolium perenne*. *Mol. Plant-Microbe Interact,* **28,** 69-85.

Bernhards, Y. and Pöggeler, S. (2011) The phocein homologue SmMOB3 is essential for vegetative cell fusion and sexual development in the filamentous ascomycete *Sordaria macrospora*. *Curr. Genet.,* **57,** 133-149.

Blankenship, J. D., Spiering, M. J., Wilkinson, H. H., Fannin, F. F., Bush, L. P. and Schardl, C. L. (2001) Production of loline alkaloids by the grass endophyte, *Neotyphodium uncinatum*, in defined media. *Phytochemistry,* **58,** 395-401.

Bloemendal, S., Bernhards, Y., Bartho, K., Dettmann, A., Voigt, O., Teichert, I., *et al.* (2012) A homologue of the human STRIPAK complex controls sexual development in fungi. *Mol. Microbiol.,* **84,** 310-323.

Bloemendal, S., Lord, K. M., Rech, C., Hoff, B., Engh, I., Read, N. D., *et al.* (2010) A mutant defective in sexual development produces aseptate ascogonia. *Eukaryot. Cell,* **9,** 1856-1866.

Buller, A. H. R. (1933) The translocation of protoplasm through the septate myceliumof certain pyrenomycetes, discomycetes, and hymenomycetes. *Researches on fungi*, **5,** 75-167 Longmans, Greena nd Co., New York.

Bultman, T. L., & Leuchtmann, A. (2008) Biology of the *Epichloë–Botanophila* interaction: An intriguing association between fungi and insects. *Fungal Biology Reviews,* **22(3-4),** 131-138.

Brun, S., Malagnac, F., Bidard, F., Lalucque, H., & Silar, P. (2009) Functions and regulation of the Nox family in the filamentous fungus *Podospora anserina:* a new role in cellulose degradation. *Molecular Microbiology,* **74(2),** 480-496.

Bowman, S. M., Piwowar, A., Dabbous, M. e. A., Vierula, J., & Free, S. J. (2006) Mutational analysis of the glycosylphosphatidylinositol (GPI) anchor pathway demonstrates that GPI-anchored proteins are required for cell wall biogenesis and normal hyphal growth in *Neurospora crassa*. *Eukaryotic Cell,* **5(3),** 587-600.

Byrd, A. D., Schardl, C. L., Songlin, P. J., Mogen, K. L. and Siegel, M. R. (1990) The β-tubulin gene of *Epichloë typhina* from perennial ryegrass (*Lolium perenne*). *Curr. Genet.,* **18,** 347-354.

Calonge, F. D. (1969). Ultrastructure of the haustoria or intracellular hyphae in four different fungi. *Archiv für Mikrobiologie,* **67(3),** 209-226.

Cano-Domınguez, N., Alvarez-Delfin, K., Hansberg, W., & Aguirre, J. (2008) NADPH oxidases NOX-1 and NOX-2 require the regulatory subunit NOR-1 to control cell differentiation and growth in *Neurospora crassa*. *Eukaryotic Cell,* **7,** 1352-1361.

Carreras-Villasenor, N., Sanchez-Arreguın, J. A., & Herrera-Estrella, A. H. (2012). *Trichoderma*: sensing the environment for survival and dispersal. *Microbiology,* **158(Pt-1),** 3-16.

Charlton, N. D., Shoji, J. Y., Ghimire, S. R., Nakashima, J. and Craven, K. D. (2012) Deletion of the fungal gene *soft* disrupts mutualistic symbiosis between the grass endophyte *Epichloë festucae* and the host plant. *Eukaryot. Cell,* **11,** 1463-1471.

Cho, Y., Kim, K.H., La Rota, M., Scott, D., Santopietro, G., Callihan, M., *et al*. (2009) Identification of novel virulence factors associated with signal transduction pathways in *Alternaria brassicicola*. *Mol Microbiol* **72,** 1316–1333.

Christensen, M. J., Ball, O. J.-P., Bennett, R. J. and Schardl, C. L. (1997) Fungal and host genotype effects on compatibility and vascular colonisation by *Epichloë festucae*. *Mycol. Res.,* **101,** 493-501.

Christensen, M. J., Bennett, R. J. & Schmid, J. (2002) Growth of *Epichloë*/*Neotyphodium* and p-endophytes in leaves of *Lolium* and *Festuca* grasses. *Mycol. Res.,* **106,** 93-106.

Christensen, M. J., & Voissey, C. R. (2007) The biology of the endophyte/grass partnership. In Popay AJ, Thom ER, eds. *Proceedings of the 6th International Symposium on Fungal Endophytes of Grasses. Grasslands Research and Practice Series* **No. 13.**Christchurch, New Zealand: New Zealand Grassland Association, 123–133.

Christensen, M. J., Bennett, R. J., Ansari, H. A., Koga, H., Johnson, R. D., Bryan, G. T., *et al.* (2008) *Epichloë* endophytes grow by intercalary hyphal extension in elongating grass leaves. *Fungal Genet. Biol.,* **45,** 84-93.

Colot, H. V., Park, G., Turner, G. E., Ringelberg, C., Crew, C. M., Litvinkova, L., *et al.* (2006) A high-throughput gene knockout procedure for *Neurospora* reveals functions for multiple transcription factors. *Proc. Natl. Acad. Sci. USA,* **103,** 10352-10357.

Dettmann, A., Heilig, Y., Ludwig, S., Schmitt, K., Illgen, J., Fleißner, A., *et al.* (2013) HAM-2 and HAM-3 are central for the assembly of the *Neurospora* STRIPAK complex at the nuclear envelope and regulate nuclear accumulation of the MAP kinase MAK-1 in a MAK-2-dependent manner. *Mol. Microbiol.,* **90,** 796-812.

Dettmann, A., Heilig, Y., Valerius, O., Ludwig, S. and Seiler, S. (2014) Fungal Communication Requires the MAK-2 Pathway Elements STE-20 and RAS-2, the NRC-1 Adapter STE-50 and the MAP Kinase Scaffold HAM-5. *PLoS Genet,* **10,** e1004762.

Dirschnabel, D. E., Nowrousian, M., Cano-Domínguez, N., Aguirre, J., Teichert, I., & Kück, U. (2014). New insights into the roles of NADPH oxidases in sexual development and ascospore germination in *Sordaria macrospora*. *Genetics,* **196,** 729–744.

Duran, R., Cary, J. W., & Calvo, A. M. (2010). Role of the osmotic stress regulatory pathway in morphogenesis and secondary metabolism in filamentous fungi. *Toxins,* **2,** 367-381.

Eaton, C. J., Cox, M. P., Ambrose, B., Becker, M., Hesse, U., Schardl, C. L., *et al.* (2010) Disruption of signaling in a fungal-grass symbiosis leads to pathogenesis. *Plant Physiol.,* **153,** 1780-1794.

Eaton, C. J., Dupont, P.-Y., Solomon, P. S., Clayton, W., Scott, B. and Cox, M. P. (2015) A core gene set describes the molecular basis of mutualism and antagonism in *Epichloë* species. *Mol. Plant-Microbe Interact,* **28,** 218-231.

Eaton, C. J., Jourdain, I., Foster, S. J., Hyams, J. S. and Scott, B. (2008) Functional analysis of a fungal endophyte stress-activated MAP kinase. *Curr. Genet.,* **53,** 163-174.

Egan, M. J., Wang, Z.-Y., Jones, M. A., Smirnoff, N., & Talbot, N. J. (2007). Generation of reactive oxygen species by fungal NADPH oxidases is required for rice blast disease. *PNAS,* **104(28),** 11772-11777.

Eisenhaber, B., Schneider, G., Wildpaner, M. and Eisenhaber, F. (2004) A sensitive predictor for potential GPI lipid modification sites in fungal protein sequences and its application to genome-wide studies for *Aspergillus nidulans*, *Candida albicans*, *Neurospora crassa*, *Saccharomyces cerevisiae* and *Schizosaccharomyces pombe*. *J. Mol. Biol.,* **337,** 243-253.

Fleiβner, A. and Glass, N. L. (2007) SO, a protein involved in hyphal fusion in *Neurospora crassa*, localises to septal plugs. *Eukaryot. Cell,* **6,** 84-94.

Fleiβner, A., Leeder, A. C., Roca, M. G., Read, N. D. and Glass, N. L. (2009a) Oscillatory recruitment of signaling proteins to cell tips promotes coordinated behavior during cell fusion. *Proc. Natl. Acad. Sci. USA,* **106,** 19387-19392.

Fleiβner, A., Diamond, S., & Glass, N. L. (2009b). The Saccharomyces cerevisiae PRM1 homolog in *Neurospora crassa* is involved in vegetative and sexual cell fusion events but also has postfertilization functions. *Genetics, 181*(2), 497-510.

Fleiβner, A., Simonin, A. R. and Glass, N. L. (2008) Cell fusion in the filamentous fungus, *Neurospora crassa*. *Methods Mol. Biol.,* **475,** 21-38.

Frey, S., Lahmann, Y., Hartmann, T., Seiler, S. and Pöggeler, S. (2015) Deletion of Smgpi1 encoding a GPI-anchored protein suppresses sterility of the STRIPAK mutant Δ*Smmob3* in the filamentous ascomycete *Sordaria macrospora*. *Mol. Microbiol.,* **97,** 676-697.

Fu, C., Ao, J., Dettmann, A., Seiler, S. and Free, S. J. (2014) Characterization of the *Neurospora crassa* Cell Fusion Proteins, HAM-6, HAM-7, HAM-8, HAM-9, HAM-10, AMPH-1 and WHI-2. *PLoS One,* **9,** e107773.

Fu, C., Iyer, P., Herkal, A., Abdullah, J., Stout, A. and Free, S. J. (2011) Identification and characterization of genes required for cell-to-cell fusion in *Neurospora crassa*. *Eukaryot. Cell,* **10,** 1100-1109.

Gibson, D. G., Young, L., Chuang, R. Y., Venter, J. C., Hutchison, C. A., III and Smith, H. O. (2009) Enzymatic assembly of DNA molecules up to several hundred kilobases. *Nat Methods,* **6,** 343-345.

Giesbert, S., Siegmund, U., Schumacher, J., Kokkelink, L., & Tudzynski, P. (2014) Functional analysis of BcBem1 and its interaction partners in *Botrytis cinerea*: impact on differentiation and virulence. *PLoS ONE,* **9(5),** e95172.

Gietz, R. D. and Woods, R. A. (2002) Transformation of yeast by lithium acetate/single-stranded carrier DNA/polyethylene glycol method. *Meth. Enzymol.,* **350,** 87-96.

Green, K. A., Becker, Y., Fitzsimons, H. L. and Scott, B. (2016) An *Epichloë festucae* homolog of MOB3, a component of the STRIPAK complex, is required for establishment of a mutualistic symbiotic interaction with *Lolium perenne*. *Mol. Plant Path.* 10.1111/mpp.12443

Haedens, V., Malagnac, F. and Silar, P. (2005) Genetic control of an epigenetic cell degeneration syndrome in *Podospora anserina*. *Fungal Genet. Biol.,* **42,** 564-577.

Hernández-Oñate, M. A., Esquivel-Naranjo, E. U., Mendoza-Mendoza, A., Stewart, A., & Herrera-Estrella, A. H. (2012). An injury-response mechanism conserved across kingdoms determines entry of the fungus *Trichoderma atroviride* into development. *PNAS,* **109(37),** 14918–14923.

Itoh, Y., Johnson, R. and Scott, B. (1994) Integrative transformation of the mycotoxin-producing fungus, *Penicillium paxilli*. *Curr. Genet.,* **25,** 508-513.

Jamet-Vierny, C., Debuchy, R., Prigent, M. and Silar, P. (2007) *IDC1*, a pezizomycotina-specific gene that belongs to the PaMpk1 MAP kinase transduction cascade of the filamentous fungus *Podospora anserina*. *Fungal Genet. Biol.,* **44,** 1219-1230.

Jeon, J., Goh, J., Yoo, S., Ch, M.-H., Choi, J., Rho, H.-S., *et al.,* (2008). A putative MAP kinase kinase kinase, MCK1, is required for cell wall integrity and pathogenicity of the rice blast fungus, *Magnaporthe oryzae*. *MPMI,* **21(5),** 525-534.

Johnson, L. J., Koulman, A., Christensen, M., Lane, G. A., Fraser, K., Forester, N., *et al.* (2013). An extracellular siderophore is required to maintain the mutualistic interaction of Epichloe¨ festucae with Lolium perenne. *Plos Pathogens, **9,*** e1003332.

Jonkers, W., Leeder, A. C., Ansong, C., Wang, Y., Yang, F., Starr, T. L., *et al.* (2014) HAM-5 Functions As a MAP Kinase Scaffold during Cell Fusion in Neurospora crassa. *PLoS Genet,* **10,** e1004783.

Kall, L., Krogh, A. and Sonnhammer, E. L. (2004) A combined transmembrane topology and signal peptide prediction method. *J. Mol. Biol.,* **338,** 1027-1036.

Kayano, Y., Tanaka, A., Akano, F., Scott, B. and Takemoto, D. (2013) Differential roles of NADPH oxidases and associated regulators in polarized growth, conidiation and hyphal fusion in the symbiotic fungus *Epichloë festucae*. *Fungal Genet. Biol.,* **56,** 87-97.

Kicka, S., Bonnet, C., Sobering, A. K., Ganesan, L. P. and Silar, P. (2006) A mitotically inheritable unit containing a MAP kinase module. *Proc. Natl. Acad. Sci. USA,* **103,** 13445-13450.

Kicka, S. and Silar, P. (2004) PaASK1, a mitogen-activated protein kinase kinase kinase that controls cell degeneration and cell differentiation in *Podospora anserina*. *Genetics,* **166,** 1241-1252.

Kim, K. W., & Hyun, J.-W. (2007). Nonhost-associated proliferation of intrahyphal hyphae of citrus scab fungus *Elsinoe fawcettii:* Refining the perception of cell-within-a-cell organization. *Micron,* **38(6),** 565-571.

Krogh, A., Larsson, B., von Heijne, G. and Sonnhammer, E. L. (2001) Predicting transmembrane protein topology with a hidden Markov model: application to complete genomes. *J. Mol. Biol.,* **305,** 567-580.

Kück, U., Beier, A. M. and Teichert, I. (2016) The composition and function of the striatin-interacting phosphatases and kinases (STRIPAK) complex in fungi. *Fungal Genet. Biol.,* **90,** 31-38.

Kück, U., Pöggeler, S., Nowrousian, M., Nolting, N. and Engh, I. (2009) *Sordaria macrospora*, a model system for fungal development. In: *The Mycota.* (Anke, T., ed.). Heidelberg, New York, Tokyo: Springer, pp. 17-39.

Lacaze, I., Lalucque, H., Siegmund, U., Silar, P. and Brun, S. (2015) Identification of NoxD/Pro41 as the homologue of the p22phox NADPH oxidase subunit in fungi. *Mol. Microbiol.,* **95,** 1006-1024.

Lalucque, H., Malagnac, F., Brun, S., Kicka, S. and Silar, P. (2012) A non-Mendelian MAPK-generated hereditary unit controlled by a second MAPK pathway in *Podospora anserina*. *Genetics,* **191,** 419-433.

Lanver, D., Mendoza-Mendoza, A., Brachmann, A. and Kahmann, R. (2010) Sho1 and Msb2-related proteins regulate appressorium development in the smut fungus *Ustilago maydis*. *Plant Cell,* **22,** 2085-2101.

Latch, G. C. M. and Christensen, M. J. (1985) Artificial infection of grasses with endophytes. *Ann. Appl. Biol.,* **107,** 17-24.

Leeder, A. C., Jonkers, W., Li, J., & Glass, N. L. (2013). Early colony establishment in *Neurospora crassa* requires a MAP kinase regulatory network. *Genetics,* **195,** 883-898.

Leuchtmann, A., Schardl, C. L. and Siegel, M. R. (1994) Sexual compatibility and taxonomy of a new species of *Epichloë* symbiotic with fine fescue grasses. *Mycologia,* **86,** 802-812.

Levin, D. E. (2011) Regulation of Cell Wall Biogenesis in Saccharomyces cerevisiae: The Cell Wall Integrity Signaling Pathway. *Genetics,* **189,** 1145-1175.

Lichius, A., (2010) Cell fusion in *Neurospora crassa*. Ph.D thesis, University of Edinburgh, Edinburgh, UK.

Lichius, A., Lord, K. M., Jeffree, C. E., Oborny, R., Boonyarungsrit, P., & Read, N. D. (2012). Importance of MAP kinases during protoperithecial morphogenesis in *Neurospora crassa*. *PLoS ONE,* **7(8),** e42565.

Lichius, A., & Lord, K. M. (2014) Chemoattractive Mechanisms in Filamentous Fungi. *The Open Mycology Journal,* **8,** 28-57.

Lord, K. M., & Read, N. D. (2011) Perithecium morphogenesis in *Sordaria macrospora*. *Fungal Genetics and Biology,* , **48,** 388-399.

Lukito, Y., Chujo, T., & Scot, B. (2015). Molecular and cellular analysis of the pH response transcription factor PacC in the fungal symbiont Epichloë festucae. *Fungal Genetics and Biology,* **85,** 25–37.

Maddi, A., Dettman, A., Fu, C., Seiler, S. and Free, S. J. (2012) WSC-1 and HAM-7 are MAK-1 MAP kinase pathway sensors required for cell wall integrity and hyphal fusion in Neurospora crassa. *PLoS One,* **7,** e42374.

Malagnac, F., Lalucque, H., Lepère, G. and Silar, P. (2004) Two NADPH oxidase isoforms are required for sexual reproduction and ascospore germination in the filamentous fungus *Podospora anserina*. *Fungal Genet. Biol.,* **41,** 982-997.

Mai, S. H. (1976). Morphological studies in *Podospora anserina*. *American Journal of Botany,* **63,** 821-825.

Masloff, S., Pöggeler, S. and Kück, U. (1999) The pro1(+) gene from *Sordaria macrospora* encodes a C6 zinc finger transcription factor required for fruiting body development. *Genetics,* **152,** 191-199.

Masloff, S., Jacobsen, S., Poggeler, S., & Kuck, U. (2002) Functional analysis of the C6 zinc finger gene pro1 involved in fungal sexual development. *Fungal Genetics and Biology,* **36,** 107-116.

Mey, G., Held, K., Scheffer, J., Tenberge, K. B., & Tudzynski, P. (2002). CPMK2, an SLT2-homologous mitogen-activated protein (MAP) kinase, is essential for pathogenesis of *Claviceps purpurea* on

rye: evidence for a second conserved pathogenesis-related MAP kinase cascade in phytopathogenic fungi. *Molecular Microbiology,* **42(2),** 305-318.

Miller, J. H. (1972) *Experiments in Molecular Genetics.* New York: Cold Spring Harbor Laboratory Press.

Moon, C. D., Scott, B., Schardl, C. L. and Christensen, M. J. (2000) The evolutionary origins of *Epichloë* endophytes from annual ryegrasses. *Mycologia,* **92,** 1103-1118.

Moon, C. D., Tapper, B. A. and Scott, B. (1999) Identification of *Epichloë* endophytes *in planta* by a microsatellite-based PCR fingerprinting assay with automated analysis. *Appl. Environ. Microbiol.,* **65,** 1268-1279.

Moy M, Belanger F, Duncan R, Freehof A, Leary C, Meyer W, Sullivan R, White JF Jr. (2000) Identification of epiphyllous mycelial nets on leaves of grasses infected by clavicipitaceous endophytes. *Symbiosis,* **28,** 291–302.

Nielsen, H., Engelbrecht, J., Brunak, S. and von Heijne, G. (1997) Identification of prokaryotic and eukaryotic signal peptides and prediction of their cleavage sites. *Protein Eng,* **10,** 1-6.

Niones, J. T. and Takemoto, D. (2015) VibA, a homologue of a transcription factor for fungal heterokaryon incompatibility, Is involved in antifungal compound production in the plant-symbiotic fungus Epichloe festucae. *Eukaryot. Cell,* **14,** 13-24.

Nordzieke, S., Zobel, T., Fränzel, B., Wolters, D. A., Kück, U. and Teichert, I. (2015) A fungal sarcolemmal membrane-associated protein (SLMAP) homolog plays a fundamental role in development and localises to the nuclear envelope, endoplasmic reticulum, and mitochondria. *Eukaryot. Cell,* **14,** 345-358.

Nowrousian, M., Frank, S., Koers, S., Strauch, P., Weitner, T., Ringelberg, C., *et al.* (2007) The novel ER membrane protein PRO41 is essential for sexual development in the filamentous fungus *Sordaria macrospora*. *Mol. Microbiol.,* **64,** 923-937.

Palma-Guerrero, J., Leeder, A. C., Welch, J., & Glass, N. L. (2014) Identification and characterization of LFD1, a novel protein involved in membrane merger during cell fusion in *Neurospora crassa. Mol Microbiol,* **92(1),** 164-182.

Park, G., Pan, S. and Borkovich, K. A. (2008) Mitogen-activated protein kinase cascade required for regulation of development and secondary metabolism in *Neurospora crassa*. *Eukaryot. Cell,* **7,** 2113-2122.

Petersen, T. N., Brunak, S., von Heijne, G. and Nielsen, H. (2011) SignalP 4.0: discriminating signal peptides from transmembrane regions. *Nat Methods,* **8,** 785-786.

Pöggeler, S. and Kück, U. (2004) A WD40 repeat protein regulates fungal cell differentiation and can be replaced functionally by the mammalian homologue striatin. *Eukaryot. Cell,* **3,** 232-240.

Popolo, L., Gilardelli, D., Bonfante, P., & Vai, M. (1997) Increase in chitin as an essential response to defects in assembly of cell wall polymers in the *ggp1*delta mutant of *Saccharomyces cerevisiae. J Bacteriol,* **179(2),** 463-469.

Quevillon, E., Silventoinen, V., Pillai, S., Harte, N., Mulder, N., Apweiler, R., *et al.* (2005) InterProScan: protein domains identifier. *Nucleic Acids Res.,* **33,** W116-120.

Ram, A. F. J., Arentshorst, M., Damveld, R. A., van Kuyk, P. A., Klis, F. M., & van den Hondel, C. A. M. J. J. (2004) The cell wall stress response in *Aspergillus niger* involves increased expression of the glutamine : fructose-6-phosphate amidotransferase-encoding gene (*gfaA*) and increased deposition of chitin in the cell wall. *Microbiology,* **150(10),** 3315–3326.

Read, N. D., Lichius, A., Shoji, J.-Y., & Goryachev, A. B. (2009). Self-signalling and self fusion in filamentous fungi. *Current Opinion in Microbiology,* **12,** 608-615.

Read, N. D., Goryachev, A. B., & Lichius, A. (2012). The mechanistic basis of self-fusion between conidial anastomosis tubes during fungal colony initiation. *Fungal Biology Reviews, **26,*** I-II.

Schardl, C. L. (2001) *Epichloë festucae* and related mutualistic symbionts of grasses. *Fungal Genet. Biol.,* **33,** 69-82.

Schardl, C. L., Young, C. A., Hesse, U., Amyotte, S. G., Andreeva, K., Calie, P. J., *et al.* (2013) Plant-symbiotic fungi as chemical engineers: multi-genome analysis of the Clavicipitaceae reveals dynamics of alkaloid loci. *PLoS Genetics,* **9,** e1003323.

Scott, B., Becker, Y., Becker, M. and Cartwright, G. (2012) Morphogenesis, growth and development of the grass symbiont *Epichloë festucae*. In: *Morphogenesis and Pathogenicity in Fungi.* (Martin, J. P. and Di Pietro, A., eds.). Heidelberg: Springer-Verlag, pp. 243-264.

Segmueller, N., Kokkelink, L., Giesbert, S., Odinius, D., van Kan, J., & Tudzynski, P. (2008) NADPH Oxidases are involved in differentiation and pathogenicity in Botrytis cinerea. *Molecular Plant-Microbe Interactions,* **21(6),** 808-819. Siegmund, U., Marschall, R. and Tudzynski, P. (2015) BcNoxD, a putative ER protein, is a new component of the NADPH oxidase complex in *Botrytis cinerea*. *Mol. Microbiol.,* **95,** 988-1005.

Siegmund, U., Marschall, R. & Tudzynski, P. (2015) BcNoxD, a putative ER protein, is a new component of the NADPH oxidase complex in *Botrytis cinerea*. *Mol. Microbiol.,* **95,** 988–1005.

Silar, P., Haedens, V., Rossignol, M. and Lalucque, H. (1999) Propagation of a novel cytoplasmic, infectious and deleterious determinant is controlled by translational accuracy in *Podospora anserina*. *Genetics,* **151,** 87-95.

Simonin, A. R., Rasmussen, C. G., Yang, M. and Glass, N. L. (2010) Genes encoding a striatin-like protein (*ham-3*) and a forkhead associated protein (*ham-4*) are required for hyphal fusion in *Neurospora crassa*. *Fungal Genet. Biol.,* **47,** 855-868.

Sonnhammer, E. L., von Heijne, G. and Krogh, A. (1998) A hidden Markov model for predicting transmembrane helices in protein sequences. . In: *Proceedings of the International Conference on Intelligent Systems for Molecular Biology; ISMB. International Conference on Intelligent Systems for Molecular Biology* pp. 175-182.

Southern, E. M. (1975) Detection of specific sequences among DNA fragments separated by gel electrophoresis. *J. Mol. Biol.,* **98,** 503-517.

Spiers, A. G. and Hopcroft, D. H. (1993) Black canker and leaf spot of Salix in New Zealand caused by *Glomerella miyabeana* (*Colletotrichum gloeosporioides*). *Eur. J. Forest Pathol.,* **23,** 92-102.

Sun, Q., Choi, G.H., and Nuss, D.L. (2009) Hypovirusresponsive transcription factor gene *pro1* of the chestnut blight fungus *Cryphonectria parasitica* is required for female fertility, asexual spore development, and stable maintenance of hypovirus infection. *Eukaryot Cell* **8,** 262–270.

Takemoto, D., Kamakura, S., Saikia, S., Becker, Y., Wrenn R. *et al.*, (2011) Polarity proteins Bem1 and Cdc24 are components of the filamentous fungal NADPH oxidase complex. *Proc. Natl. Acad. Sci. USA* **108,** 2861–2866.

Takemoto, D., Tanaka, A. and Scott, B. (2006) A p67(Phox)-like regulator is recruited to control hyphal branching in a fungal-grass mutualistic symbiosis. *Plant Cell,* **18,** 2807-2821.

Takeshita, N., Yamashita, S., Ohta, A., & Horiuchi, H. (2006) *Aspergillus nidulans* class V and VI chitin synthases CsmA and CsmB, each with a myosin motor-like domain, perform compensatory functions that are essential for hyphal tip growth. *Molecular Microbiology,* **59(5),** 1380-1394.

Tan, Y. Y., Spiering, M. J., Scott, V., Lane, G. A., Christensen, M. J. and Schmid, J. (2001) In planta regulation of extension of an endophytic fungus and maintenance of high metabolic rates in its mycelium in the absence of apical extension. *Appl. Environ. Microbiol.,* **67,** 5377-5383.

Tanaka, A., Cartwright, G. M., Saikia, S., Kayano, Y., Takemoto, D., Kato, M., *et al.* (2013) ProA, a transcriptional regulator of fungal fruiting body development, regulates leaf hyphal network development in the *Epichloë festucae-Lolium perenne* symbiosis. *Mol. Microbiol.,* **90,** 551-568.

Tanaka, A., Christensen, M. J., Takemoto, D., Park, P. and Scott, B. (2006) Reactive oxygen species play a role in regulating a fungus-perennial ryegrass mutualistic association. *Plant Cell,* **18,** 1052-1066.

Tanaka, A., Takemoto, D., Hyon, G. S., Park, P. and Scott, B. (2008) NoxA activation by the small GTPase RacA is required to maintain a mutualistic symbiotic association between *Epichloë festucae* and perennial ryegrass. *Mol. Microbiol.,* **68,** 1165-1178.

Tanaka, A., Tapper, B. A., Popay, A., Parker, E. J. and Scott, B. (2005) A symbiosis expressed non-ribosomal peptide synthetase from a mutualistic fungal endophyte of perennial ryegrass confers protection to the symbiotum from insect herbivory. *Mol. Microbiol.,* **57,** 1036-1050.

Teepe, A. G., Loprete, D. M., He, Z., Hoggard, T. A., & Hill, T. W. (2007) The protein kinase C orthologue PkcA plays a role in cell wall integrity and polarized growth in *Aspergillus nidulans*. *Fungal Genet. Biol.,* **44(6),** 554-562.

Teichert, I., Nowrousian, M., Pöggeler, S. and Kück, U. (2014a) The filamentous fungus *Sordaria macrospora* as a genetic model to study fruiting body development. *Adv Genet,* **87,** 199-244.

Teichert, I., Steffens, E. K., Schnass, N., Franzel, B., Krisp, C., Wolters, D. A., *et al.* (2014b) PRO40 is a scaffold protein of the cell wall integrity pathway, linking the MAP kinase module to the upstream activator protein kinase C. *PLoS Genet,* **10,** e1004582.

Thompson, J. D., Higgins, D. G. and Gibson, T. J. (1994) CLUSTAL W: improving the sensitivity of progressive multiple sequence alignment through sequence weighting, position-specific gap penalties and weight matrix choice. *Nucleic Acids Res.,* **22,** 4673-4680.

Tong, L. C., Silar, P. and Lalucque, H. (2014) Genetic control of anastomosis in *Podospora anserina*. *Fungal Genet. Biol.,* **70,** 94-103.

Valiante, V., Heinekam, T., Jain, R., Hartl, A., & Brakhage, A. A. (2008) The mitogen-activated protein kinase MpkA of *Aspergillus fumigatus* regulates cell wall signaling and oxidative stress response. *Fungal Genet. Biol.,* **45(5),** 618-627.

Valiante, V., Jain, R., Heinekamp, T., & Brakhage, A. A. (2009) The MpkA MAP kinase module regulates cell wall integrity signaling and pyomelanin formation in *Aspergillus fumigatus*. *Fungal Genet. Biol.,* **49(12),** 909-918.

Wang, C.-L., Shim, W. B. & Shaw, B. D. (2016) The *Colletotrichum graminicola* striatin ortholog Str1 is necessary for anastomosis and is a virulence factor. *Mol Plant Pathol,* DOI: 10.1111/mpp.12339.

Young, C. A., Bryant, M. K., Christensen, M. J., Tapper, B. A., Bryan, G. T. and Scott, B. (2005) Molecular cloning and genetic analysis of a symbiosis-expressed gene cluster for lolitrem biosynthesis from a mutualistic endophyte of perennial ryegrass. *Mol. Gen. Genomics,* **274,** 13-29.

Zdobnov, E. M. and Apweiler, R. (2001) InterProScan--an integration platform for the signature-recognition methods in InterPro. *Bioinformatics,* **17,** 847-848.

Supporting Information

Supplementary Table 1: Biological Material

Biological material	Relevant characteristics	Reference
Yeast strains		
S. cerevisiae		
PN2806 (FY834)	*MATa his3Δ200 ura3-52 leu2Δ1 lys2Δ202 trp1Δ63*	Winston *et al.*, 1995
Fungal strains		
Epichloë festucae		
PN2278 (WT)	Fl1	Young *et al.*, 2005
PN2988 (Δ*mpkA* #10.8)	Fl1/Δ*mpkA*::P*trpC-hph*; Hyg^R	Becker *et al.*, 2015
PN2892 (Δ*mkkA* #4.2)	Fl1/Δ*mkkA*::P*trpC-hph*; Hyg^R	Becker *et al.*, 2015
PN2958 (Δ*symB*#3)	Fl1/Δ*symB*::P*trpC-hph*; Hyg^R	This study
PN2955 (Δ*symB*#6)	Fl1/Δ*symB*::P*trpC-hph*; Hyg^R	This study
PN2957 (Δ*symC*#7)	Fl1/Δ*symC*::P*trpC-gen*; Gen^R	This study
PN2956 (Δ*symC*#8)	Fl1/Δ*symC*::P*trpC-gen*; Gen^R	This study
PN2832 (Fl1::*m*RFP1)	Fl1/pCA56; Gen^R	Becker *et al.*, 2015
PN2833 (Fl1::*e*GFP)	Fl1/pCT74; Hyg^R	Becker *et al.*, 2015
PN3016 (Δ*symB*#3::*m*RFP1 #1)	Δ*symB*#3/pII99, pCA56; Gen^R, Hyg^R	This study
PN3017 (Δ*symB*#3::*e*GFP #1)	Δ*symB*#3/pII99, pCT74; Gen^R, Hyg^R	This study
PN3019 (Δ*symB*#6::*m*RFP1 #10)	Δ*symB*#6/pII99, pCA56; Gen^R, Hyg^R	This study
PN3018 (Δ*symB*#6::*e*GFP #4)	Δ*symB*#6/pII99, pCT74; Gen^R, Hyg^R	This study
PN3015 (Δ*symC*#7::*m*RFP1 #3)	Δ*symC*#7/pSF15.15, pCA56; Hyg^R, Gen^R	This study
PN3014 (Δ*symC*#7::*e*GFP #3)	Δ*symC*#7/pSF15.15, pCT74; Hyg^R, Gen^R	This study
PN3012 (Δ*symC*#8::*m*RFP1 #18)	Δ*symC#8*/pSF15.15, pCA56; Hyg^R, Gen^R	This study
PN3013 (Δ*symC*#8::*e*GFP #13)	Δ*symC*#8/pSF15.15, pCT74; Hyg^R, Gen^R	This study
PN3050 (Δ*symB*#3/*symB* #5)	Δ*symB*#3/P*symB-symB-TsymB* (pKG7); Gen^R, Hyg^R	This study
PN3051 (Δ*symB*#6/*symB* #1)	Δ*symB*#6/P*symB-symB-TsymB* (pKG7); Gen^R, Hyg^R	This study
PN3052 (Δ*symC*#7/*symC* #22)	Δ*symC*#7/P*symC-symC*-T*symC* (pKG6), pSF15.15; Gen^R, Hyg^R	This study
PN3053 (Δ*symC*#8/*symC* #23)	Δ*symC*#8/P*symC-symC*-T*symC* (pKG6), pSF15.15; Gen^R, Hyg^R	This study
PN2963 (Fl1/MpkA-*e*GFP)	Fl1/pCE81; Hyg^R	Becker *et al.*, 2015
PN3105 (Δ*symB*#3/MpkA-*e*GFP #17)	Δ*symB*#3/pII99, pCE81; Gen^R, Hyg^R	This study

PN3106 (Δ*symB*#6/MpkA-*e*GFP #12)	Δ*symB*#6/pII99, pCE81; Gen^R, Hyg^R	This study
PN3107 (Δ*symC*#7/MpkA-*e*GFP #8)	Δ*symC*#7/pSF15.15, pCE81; Gen^R, Hyg^R	This study
PN3108 (Δ*symC*#8/MpkA-*e*GFP #7)	Δ*symC*#8/pSF15.15, pCE81; Gen^R, Hyg^R	This study
PN3138 (Fl1/MpkB-*e*GFP)	Fl1/pMpkB-*e*GFP; Hyg^R	This study
PN3140 (Δ*symB*#3/MpkB-*e*GFP #2)	Δ*symB*#3/pMpkB-*e*GFP & pII99; Gen^R, Hyg^R	This study
PN3141 (Δ*symC*#7/MpkB-*e*GFP #1)	Δ*symC*#7/pMpkB-*e*GFP; Gen^R, Hyg^R	This study
PN3103 (Δ*symB*#3/pKG13 #39)	Δ*symB*#3/P*symB-symB-3GA-GFP-symB-TsymB* (pKG13); Gen^R, Hyg^R	This study
PN3104 (Δ*symB*#6/pKG13 #37)	Δ*symB*#6/P*symB-symB-3GA-GFP-symB-TsymB* (pKG13); Gen^R, Hyg^R	This study
PN3128 (Δ*symC*#7/pKG12 #3)	Δ*symC*#7/P*symC-symC::mRFP-TsymC* (pKG12), pSF15.15; Gen^R, Hyg^R	This study
PN3129 (Δ*symC*#8/pKG12 #12)	Δ*symC*#8/P*symC-symC::mRFP-TsymC* (pKG12), pSF15.15; Gen^R, Hyg^R	This study
PN3130 (Fl1/pKG12 & pKG13 #17)	Fl1/P*symC-symC*-3GA-mRFP1-T*symB* (pKG12), P*symB-symB-3GA-GFP-symB-TsymB* (pKG13), pSF15.15; Hyg^R	This study
PN3131 (Δ*symB*#3/pKG20 #3)	Δ*symB*#3/P*tef-symB-3GA-GFP-symB* (pKG20), pII99; Gen^R, Hyg^R	This study
PN3132 (Δ*symC*#7/pKG21 #1)	Δ*symC*#7/P*tef-symC::mRFP* (pKG21); Gen^R, Hyg^R	This study
Bacterial strains		
E.coli		
PN1687	Source of pII99; Amp^R Gen^R	Namiki *et al.*, 2001
PN1862	Source of pSF15.15; Amp^R Hyg^R	S. Foster
PN413	Source of pRS426; Amp^R	Christianson *et al.*, 1992
PN4175	Source of pCT74; Amp^R	Lorang *et al.*, 2001
PN4178	Source of pCA56; Amp^R	Andrie *et al.*, 2005
PN4205	Source of pCE81; Amp^R Hyg^R	C. Eaton
PN4236	Source of pYR33; Amp^R Gen^R	Becker *et al.*, 2015
PN4279	Source of pMpkB-*e*GFP; Amp^R Hyg^R	D. Takemoto
PN1994	Source of pPN94; Amp^R Hyg^R	Takemoto et al 2006
PN4249	Source of pKG1; Amp^R	This study
PN4250	Source of pKG2; Amp^R	This study
PN4264	Source of pKG5; Amp^R	This study
PN4265	Source of pKG6; Amp^R	This study
PN4266	Source of pKG7; Amp^R	This study
PN4272	Source of pKG12; Amp^R	This study
PN4273	Source of pKG13; Amp^R	This study
PN4284	Source of pKG20; Amp^R	This study
PN4285	Source of pKG21; Amp^R	This study
Plasmids		
pII99	P*trpC-nptII*-T*trpC*; Amp^R/Gen^R	Namiki *et al.*, 2001
pSF15.15	P*trpC*-hph-T*trpC*; Amp^R/Hyg^R	S. Foster
pRS426	ori(f1)-lacZ-T7 promoter-MCS (KpnI-SacI)-T3 promoter-lacI-ori(pMB1)-ampR-ori (2 micron), URA3, Amp^R	Winston et al, 1995
pCR4-Topo®	Amp^R	Roche
pCT74	P*toxA*::e*GFP*; Amp^R/Hyg^R	Lorang *et al.*, 2001
pCA56	P*toxA*::*mRFP1*; Amp^R/Hyg^R	Andrie *et al.*, 2005
pCE81	pRS426 containing P*gpd*::*mpkA*::*eGFP-TrpC;* Amp^R/ Ura^+	C. Eaton
pYR33	pII99 containing 5'- and 3'- *mkkA* PCR product; Amp^R/Gen^R	Becker *et al.*, 2015

pMpkB-eGFP	pPN94 containing P*tef::MpkB::3GA::eGFP::*T*trpC*; Amp^R/Hyg^R	D. Takemoto
pPN94	P*tef:: eGFP*; Amp^R/Hyg^R	Takemoto et al 2006
pKG1	pRS426 containing 5'*symB*-P*trpC-hph*-3'*symB*; Amp^R /Hyg^R	This study
pKG2	pRS426 containing 5'*symC*-P*trpC-gen*-3'*symC*; Amp^R /Gen^R	This study
pKG5	pCR4-Topo® containing 3.9kb P*symB::symB::TsymB* complementation construct	This study
pKG6	pCR4-Topo® containing 4.1kb P*symC::symC::TsymC* complementation construct	This study
pKG7	pII99 vector from YB33 containing 3.9kb *symB* complementation construct *EcoRI* ligated out of pKG5	This study
pKG12	pCR4-Topo® containing P*symC::SymC-3GA-mRFP1-TsymC*; Amp^R	This study
pKG13	pCR4-Topo® containing P*symB::SymB-3GA-eGFP-SymB-TsymB*; Amp^R	This study
pKG20	P*tef::SymB-3GA-GFP-SymB*; Amp^R/Hyg^R	This study
pKG21	P*tef::SymC-3GA-mFP1*; Amp^R/Hyg^R	This study

Supplementary Table 2: Primers used in this study.

Primer	Sequence	Purpose
NptF	GATATTGAAGGAGCACTTTTTG	Geneticin fragment
NptR	CTACCCATCTTAGTAGGAATG	Geneticin fragment
hph-F	AGCTTGGAACTGATATTGAAGG	Hygromycin fragment
hph-R	CTATTCCTTTGCCCTCGGACG	Hygromycin fragment
gfpF2	GTACACCATTGCCACCAAGGGTGCTGGTGCTGGTGCT	GFP fragment
gfpR5	GCGTCGGTGCCAGAGTTCTTGTACAGCTCGTCCATGC	GFP fragment
mRFPF2	CAGCACCAAAGCTCGCGAGGTGCTGGTGCTGGTGCTGCCTCCT CCGAGGACG	mRFP1 fragment
mRFPR2	CCGAAGCGTGACAACGGCCTAGGCGCCGGTGGAGTG	mRFP1 fragment
ptefF	ACTTAACGTTACTGAAATCATC	pPN94 backbone
ptefR	CTAGAGGTTTGACGGTGATG	pPN94 backbone
KG1	GTAACGCCAGGGTTTTCCCAGTCACGACGAAAGCTTCTACAGG GTAAGCG	*symB* KO 5' fragment
KG2	ATGCTCCTTCAATATCAGTTCCAAGCTATAGAGAGGGTCTTGA TGAGACCA	*symB* KO 5' fragment
KG3	CCAGCACTCGTCCGAGGGCAAAGGAATAGGTGGATAATGAGC TAGCTTCAGG	*symB* KO 3' fragment
KG4	GCGGATAACAATTTCACACAGGAAACAGCCAGTCGCTAGAATT CGTCGTC	*symB* KO 3' fragment
KG5	GTAACGCCAGGGTTTTCCCAGTCACGACTCGTGTCACGGTACC GTATCTC	*symC* KO 5' fragment
KG6	CCAAGCCCAAAAAGTGCTCCTTCAATATCCCGTTTAAGGACCA TGGCC	*symC* KO 5' fragment
KG7	GAAAATCATTCCTACTAAGATGGGTAGGCTCGCGATAGGCCGT TGT	*symC* KO 3' fragment
KG8	GCGGATAACAATTTCACACAGGAAACAGCGCGACACGGATAT CTTGCAGC	*symC* KO 3' fragment
KG9	GCTCGTGGTGGTGGATGA	*symB* LF screening primer
KG10	ACTAGCTCCAGCCAAGCC	*symB* LF screening primer
KG11	GCTGTGTAGAAGTACTCGCC	*symB* RF screening primer
KG12	TGTGCTGCAATCTCTCCG	*symB* RF screening primer
KG13	GCGGAACTGGTCTCATCAAG	*symB* KO screening primer
KG14	TGGGTCCTGAAGCTAGCTC	*symB* KO screening primer

KG15-2	TTTCGCTCATCAGGAGTCC	*symC* LF screening primer
KG16-2	CAAACGCACCAAGTTATCG	*symC* LF screening primer
KG17-2	GCACTGTTTCTTCCTTGAAC	*symC* RF screening primer
KG18-2	ATGTCACTCACTGCTGGACC	*symC* RF screening primer
KG19-2	CGTCGACCCAATTGGCTG	*symC* KO screening primer
KG20-2	TCCACATCTCTCCTGCATC	*symC* KO screening primer
KG23	GAAGCTCACCTTGTTCACATCG	*symC* screening primer
KG24	TGTCGCAGAGGAAGCTGTC	*symC* screening primer
KG41	GGATTCTCGGGAACGGCT	*symB* KO Southern analysis primer
KG42	GAATGATGACGGCGTGGC	*symB* KO Southern analysis primer
KG43	GGCTAGGGTCTGTATCCAAT	*symC* KO Southern analysis primer
KG44	TAACAGTGGGCTTGCGAG	*symC* KO Southern analysis primer
KG49_3	GCTTGAGGATCCATCATCATC	*symB* complementation fragment
KG49_4	GCTACTAAATGCGGTCCCTTGC	SymB localisation construct
KG50_2	GCTCCATCCTGTCTAGAAAC	*symB* complementation fragment
KG51_2	CACTTCAGCATAGACTTGGC	*symC* complementation fragment
KG52	TCTCACTGGATCCTTCACAC	*symC* complementation fragment
KG71_3	GCAAGGGACCGCATTTAGTAGC	SymB localisation fragment
KG74	GCCAAGTCTATGCTGAAGTG	SymC localisation fragment
KG76	CACTCCACCGGCGCCTAGGCCGTTGTCACGCTTCGG	SymC localisation fragment
KG79	AGCACCAGCACCAGCACCTCGCGAGCTTTGGTGCTG	SymC localisation fragment
KG80_2	CTTGGTGGCAATGGTGTACATGTCTGCGAAGCCCA	SymB localisation fragment
KG81_3	GAGCTGTACAAGAACTCTGGCACCGACGC	SymB localisation fragment
KG92	CATCACCGTCAAACCTCTAGATGTTCCTCGCCATCATTGC	SymB::GFP construct
KG93	GATGATTTCAGTAACGTTAAGTCTACAACGCGGTCAACACG	SymB::GFP construct
KG94	CATCACCGTCAAACCTCTAGATGAAGCTCACCTTGTTCAC	SymB::mRFP1 construct
KG95	GATGATTTCAGTAACGTTAAGTCTAGGCGCCGGTGGAGTGGC	SymB::mRFP1 construct
KG99	CTTGGGCTTTTCGATCTGGGCCGGTGCTGGTGCTGGTGCTGCC	SymC C-terminal fragment
P*symB*.f1	TGCCTCGCCTTTCTTTCTG	*symB* F1 fragment
P*symB*.r1	CGGAGTATGTATGCTTGGG	*symB* F1 fragment
P*symB*.f2	ACATTGACCCTTCCCGCTTG	*symB* F2 fragment
P*symB*.r2	CTTGATGAGACCAGTTCCG	*symB* F2 fragment
P*symB*.f5	TCGCCCGGGCGCTTAACTTG	*symB* R1 fragment
P*symB*.r4	GTGTGTCATTGGTCGAGCTG	*symB* R1 fragment
P*symB*.f5-2	GGCGCTTAACTTGGTCCCCTG	*symB* R2 fragment
P*symB*.r4	GTGTGTCATTGGTCGAGCTG	*symB* R2 fragment
P*symB*.f1	TGCCTCGCCTTTCTTTCTG	*symB* R3 fragment
P*symB*.r10	GGGGACCAAGTTAAGCGCCCGGGCGAGCAG	*symB* R3 fragment
P*symB*.f1	TGCCTCGCCTTTCTTTCTG	*symB* R4 fragment
P*symB*.r11	AAGTTAAGCGCCCGGGCGAGCAG	*symB* R4 fragment
P*symB*.f1	TGCCTCGCCTTTCTTTCTG	*symB* R5 fragment
P*symB*.r11m1	TTTTTAAGCGCCCGGGCGAGCAG	*symB* R5 fragment
P*symB*.f1	TGCCTCGCCTTTCTTTCTG	*symB* R6 fragment
P*symB*.r8	TGGTTGGCTGGCAGGGGACC	*symB* R6 fragment
P*symB*.f1	TGCCTCGCCTTTCTTTCTG	*symB* R7 fragment
P*symB*.r7	CGAGCAGGGTGTAGTGGGGC	*symB* R7 fragment
P*symC*.f1	TCCGTACCGCCGGAGCAATC	*symC* F1 fragment
P*symC*.r1	AAAGCCATGAGATGCCGC	*symC* F1 fragment
P*symC*.f2	CCCGTCGACCCAATTGGCTG	*symC* F2 fragment
P*symC*.r2	GAGCCCGTTTAAGGACCATG	*symC* F2 fragment

P*symC*.f3	TGCAGGCGCTTAAGCATCCC	*symC* R1 fragment
P*symC*.r2	GAGCCCGTTTAAGGACCATG	*symC* R1 fragment
P*symC*.f3-2	GGCGCTTAAGCATCCC	*symC* R2 fragment
P*symC*.r2	GAGCCCGTTTAAGGACCATG	*symC* R2 fragment

Supplementary Table 3: Analysis of plant survival rates.

	Planted	Survived (S)	Infected (I)	% S	% I
Experiment 1					
WT	48	16	13	0.33	0.81
Δ*symB*#3	56	6	3	0.11	0.50
Δ*symB*#6	44	2	0	0.05	0.00
Δ*symC*#7	36	11	4	0.31	0.36
Δ*symC*#8	48	10	4	0.21	0.40
Experiment 2					
WT	56	33	21	0.59	0.64
Δ*symB*#3	56	15	3	0.24	0.20
Δ*symB*#6	56	14	4	0.25	0.29
Δ*symC*#7	56	13	4	0.23	0.31
Δ*symC*#8	56	17	2	0.30	0.12

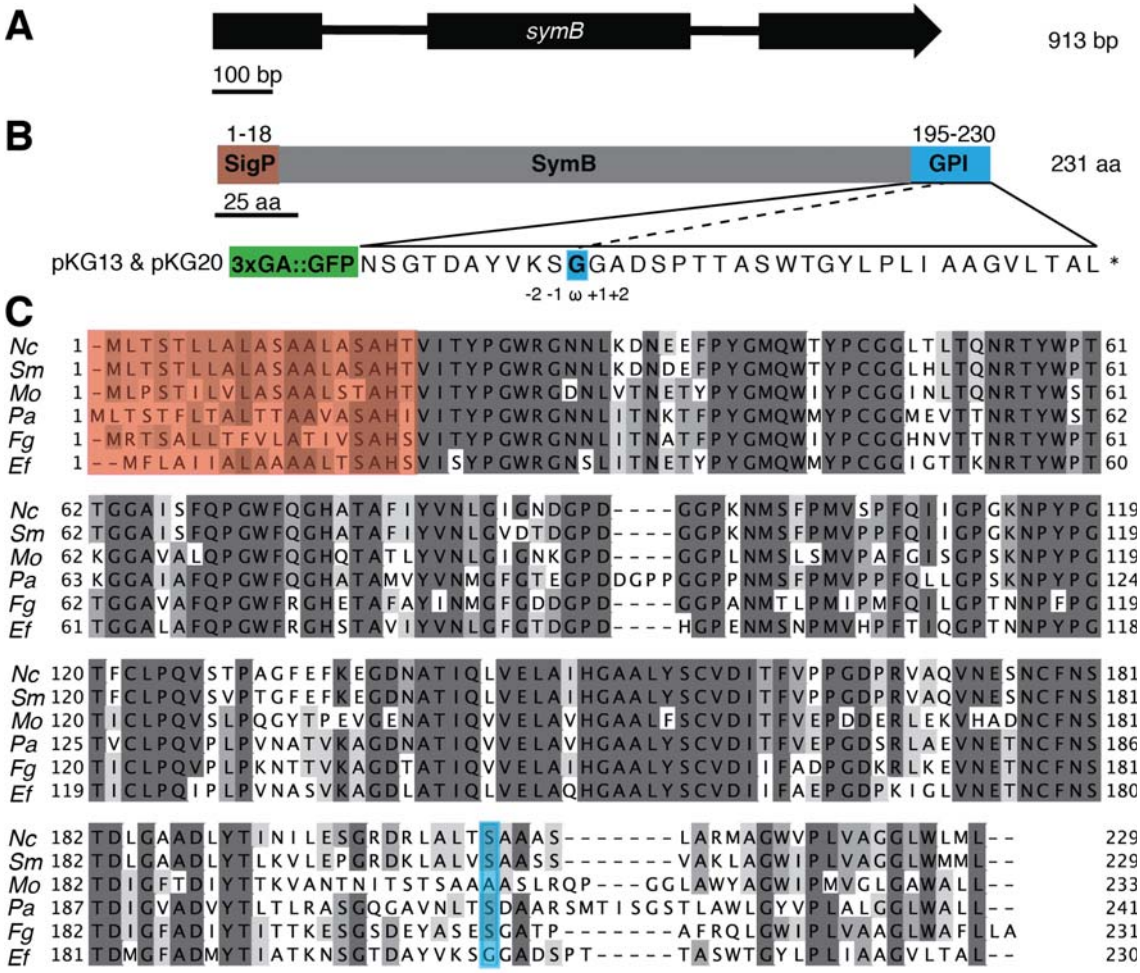

Fig. S1. *Epichloë festucae symB* gene structure, encoded protein domain structure and amino acid sequence alignment. A, Gene structure of *E. festucae symB* containing three exons of 136, 329 and 228 bp, and two introns of 133 and 116 bp. Bar = 100 bp. **B,** Protein

domain structure of *E. festucae* SymB showing the predicted signal peptide (Sig P, red) and GPI anchor (GPI, blue), the amino acid sequence of the latter showing the predicted ω site for transamidase cleavage and attachment of GPI, and the site of insertion of a 3xGA linker-eGFP for SymB localisation. **C,** Multiple sequence alignment (ClustalW) of SymB Ef, *Epichloë festucae* EfM3.029010; *Fg*, *Fusarium graminearum* FGSG_02810.3 (XM_382986.1); *Nc*, *Neurospora crassa* (HAM-7) NCU00881 (XM_959704.2); *Pa*, *Podospora anserina* (IDC2) Pa_1_16080 (XM_001907012.1); *Mo*, *Magnaporthe oryzae* MGG_10586.6 (XM_003721313.1); *Sm*, *Sordaria macrospora* SMAC_01568 (XM_003352686.1) protein homologues.

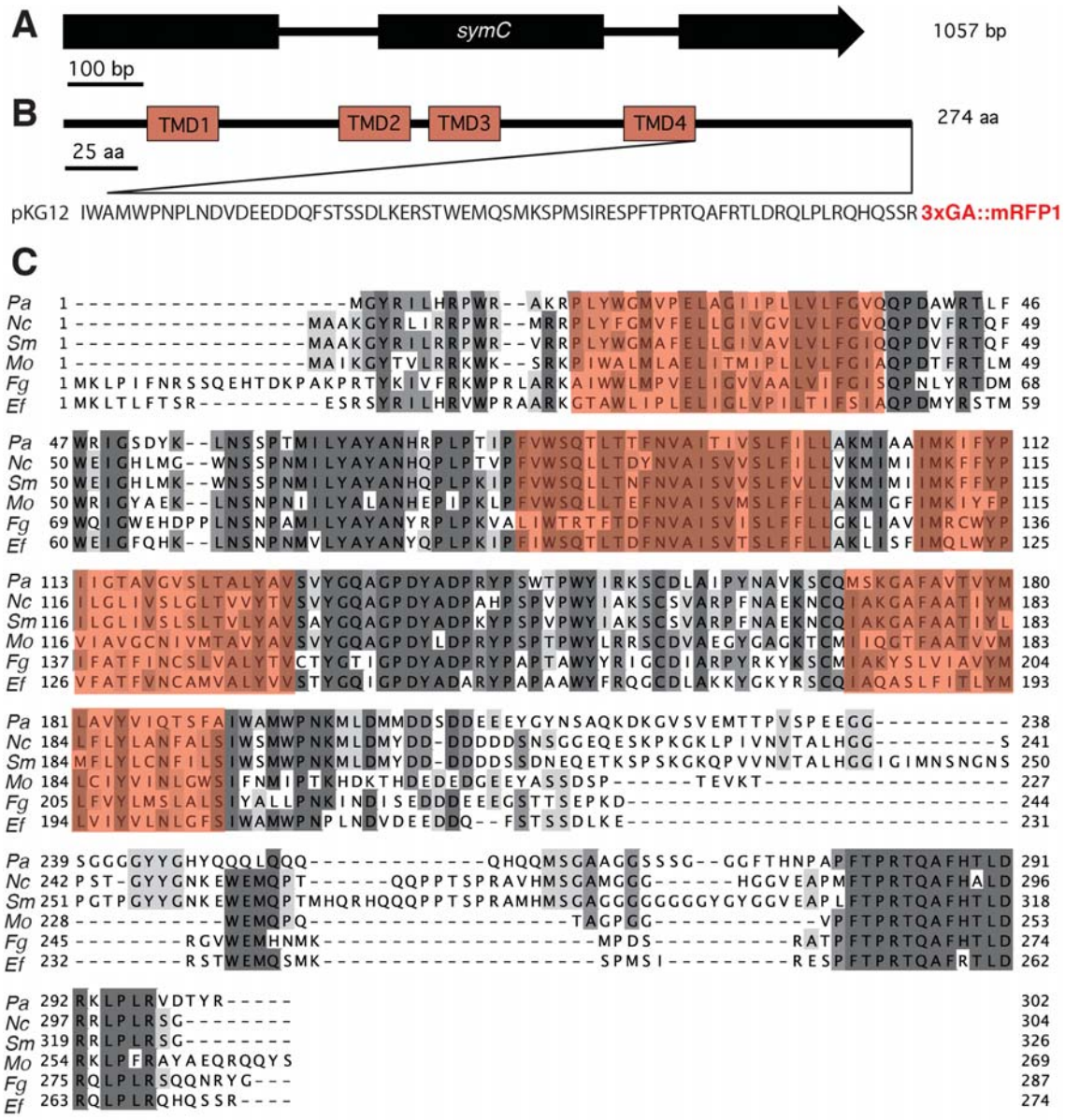

Fig. S2. *Epichloë festucae symC* gene structure, encoded protein domain structure, and amino acid sequence alignment. A, Gene structure of *E. festucae symC* containing three exons of 284, 297 and 244 bp, and two introns 132 and 100 bp. **B,** Protein domain structure of *E. festucae* SymC showing four transmembrane domains (TMD) as predicted by TMHMM software (Krogh *et al.,* 2001, Sonnhammer *et al.,* 1998) and the site of insertion of a 3xGA linker-mFP1 for SymC localisation.

Regions between TMD1 and TMD2, and between TMD3 and TMD4, are predicted as being extracellular domains with N-terminus, region between TMD2 and TMD3, and C-terminus, being cytosolic domains. **C,** Multiple sequence alignment of SymC Ef, *Epichloë festucae* EfM3.029020; Fg, *Fusarium graminearum* FGSG_00855 (XM_381031.1); Nc, *Neurospora crassa* NCU00938.5 (XM_959671.2); Pa, *Podospora anserina* (IDC3) Pa_1_1990 (XM_001912357.1); Mo, *Magnaporthe oryzae* MGG_01229.6 (XM_003714083); Sm, *Sordaria macrospora* SMAC_00214 (XM_003351624.1) protein homologues.

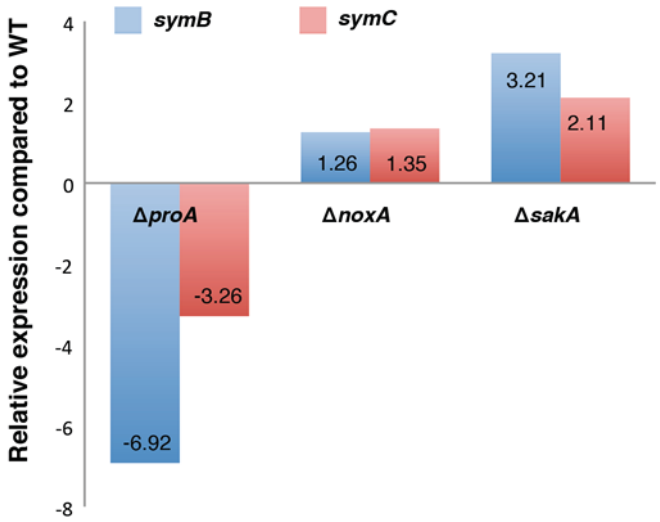

Fig. S3. Fold change of *symB* and *symC* expression *in planta* for Δ*proA*, Δ*noxA* and Δ*sakA* associations compared to wild-type. Data was extracted from Eaton *et al.*, (2015).

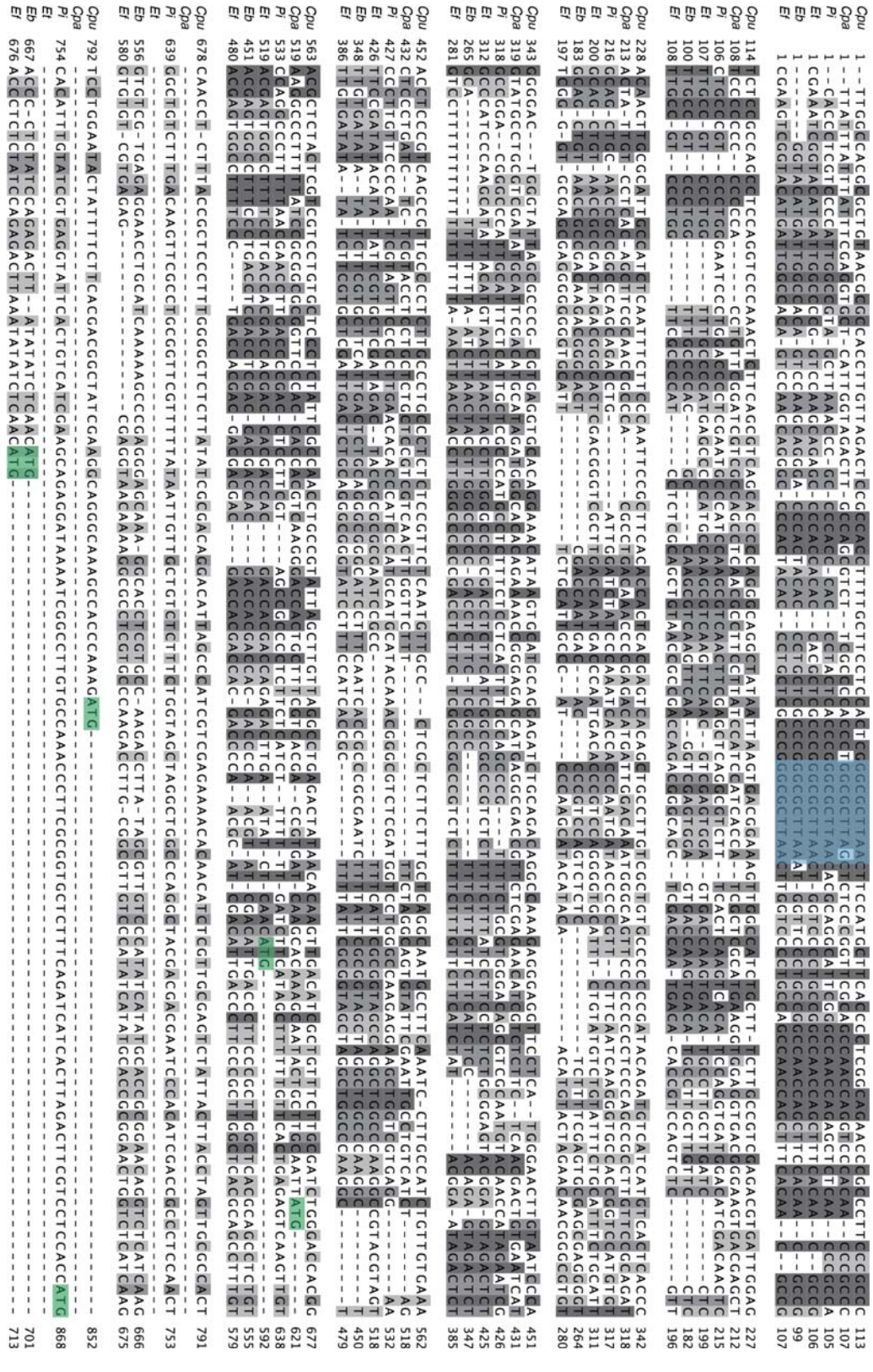

Fig. S4. Identification of ProA binding site in *symB* promoter. Multiple sequence alignment of *symB* promoter region and homologous sequences from other Clavicipitaceae species including *Claviceps purpurea* (Cpu), *C. paspali* (Cpa), *Periglandula ipomoeae* (Pi), *E. typhina* (Et), *E. bromicola* (Eb) and *E. festucae* (Ef). The conserved predicted ProA binding site is shaded in blue and ATG start sites in green.

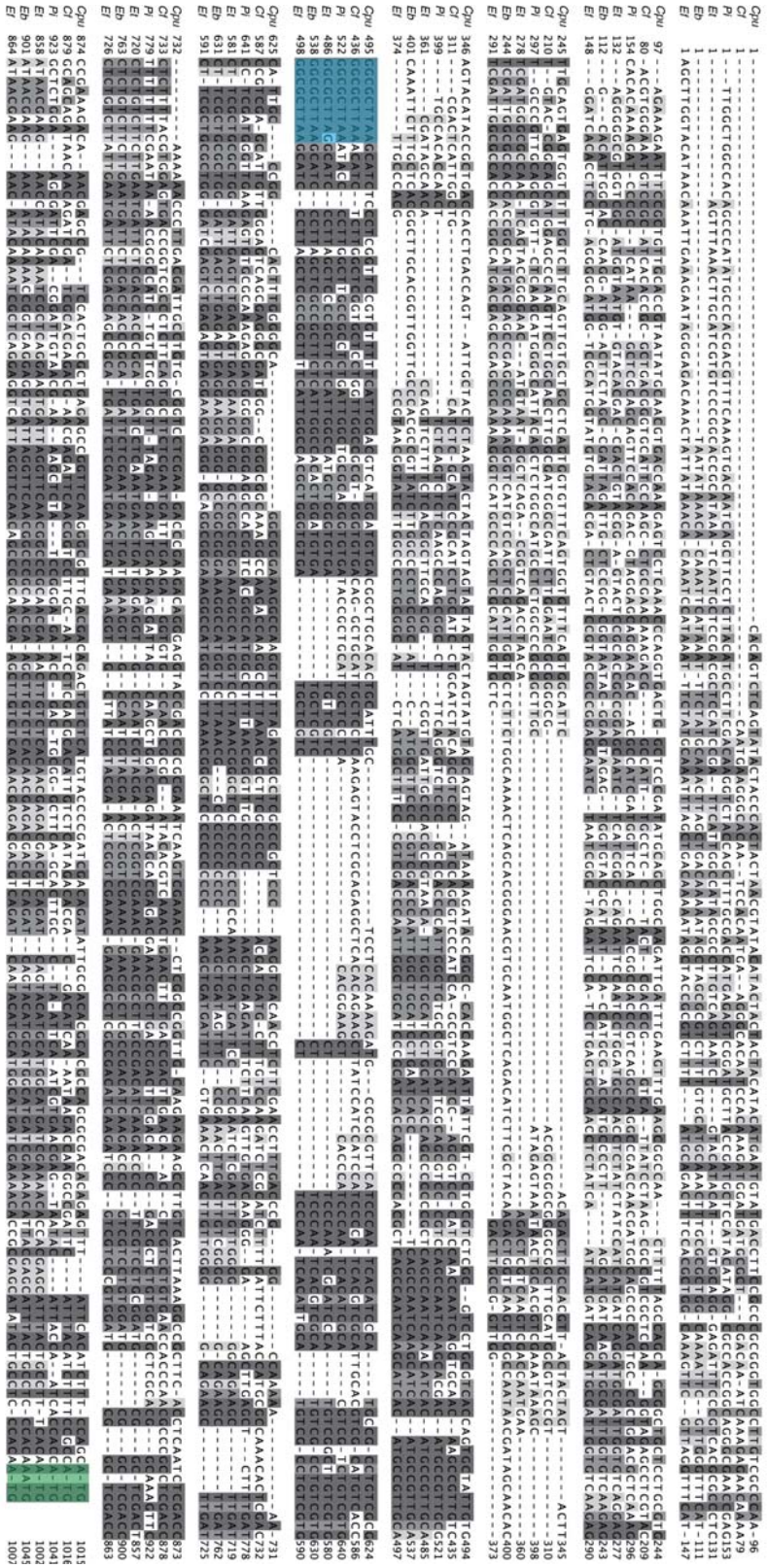

Fig. S5. Identification of ProA binding site in *symC* promoter. Multiple sequence alignment of *symC* promoter region and homologous sequences from other Clavicipitaceae species including *Claviceps purpurea* (Cpu), *C. fusiformis* (Cf), *Periglandula ipomoeae* (Pi), *E. typhina* (Et), *E. bromicola* (Eb) and *E. festucae* (Ef). The conserved predicted ProA binding site is shaded in blue and ATG start sites in green.

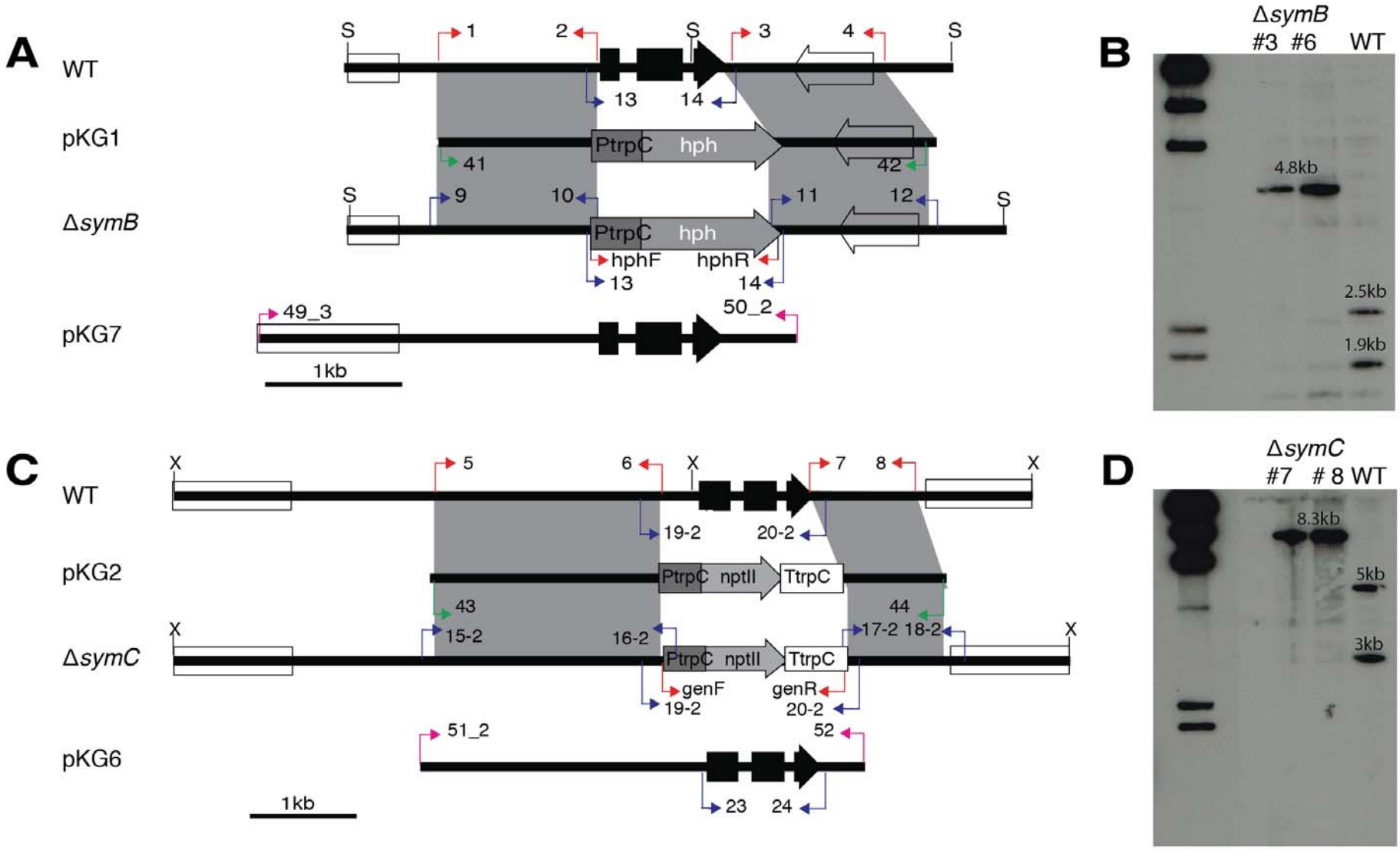
A
WT
pKG1
ΔsymB
pKG7
S
1
2
S
3
4
S
13
14
PtrpC
hph
41
42
9
10
11
12
hphF
hphR
49_3
50_2
1kb
B
ΔsymB
#3 #6 WT
4.8kb
2.5kb
1.9kb
C
WT
pKG2
ΔsymC
pKG6
X
5
6
7
8
19-2
20-2
PtrpC
nptII
TtrpC
43
44
15-2
16-2
17-2 18-2
genF
genR
51_2
52
23
24
1kb
D
ΔsymC
#7 # 8 WT
8.3kb
5kb
3kb

Fig. S6. *symB* and *symC* deletion and complementation construct design, screening primers and Southern analysis. A & C, Physical maps of the wild type (WT) *symB* and *symC* loci, Δ*symB* and Δ*symC* mutant loci, linear inserts of *symB* and *symC* replacement, pKG1 and pKG2, and complementation, pKG7 and pKG6, constructs. Regions of recombination are indicated by grey shading. Primer pairs used to amplify genomic 5' and 3' flanking regions and resistance cassettes for yeast recombinational-cloning are shown in red, PCR knock-out and complementation screening in blue, generation of [^{32}P] labeled probes for Southerns in green, and primers used to amplify complementation constructs for TOPO cloning in pink. *Sal*I (S) and *Xho*I (X) restriction enzyme sites used for Southern analysis and the predicted fragment sizes are as shown. Bar = 1kb. Autoradiographs of **B,** *Sal*I and **D,** *Xho*I genomic digests (1.5 µg) of Δ*symB* and Δ*symC* transformants (#) probed with [^{32}P]-labelled inserts of pKG1 and pKG2, respectively.

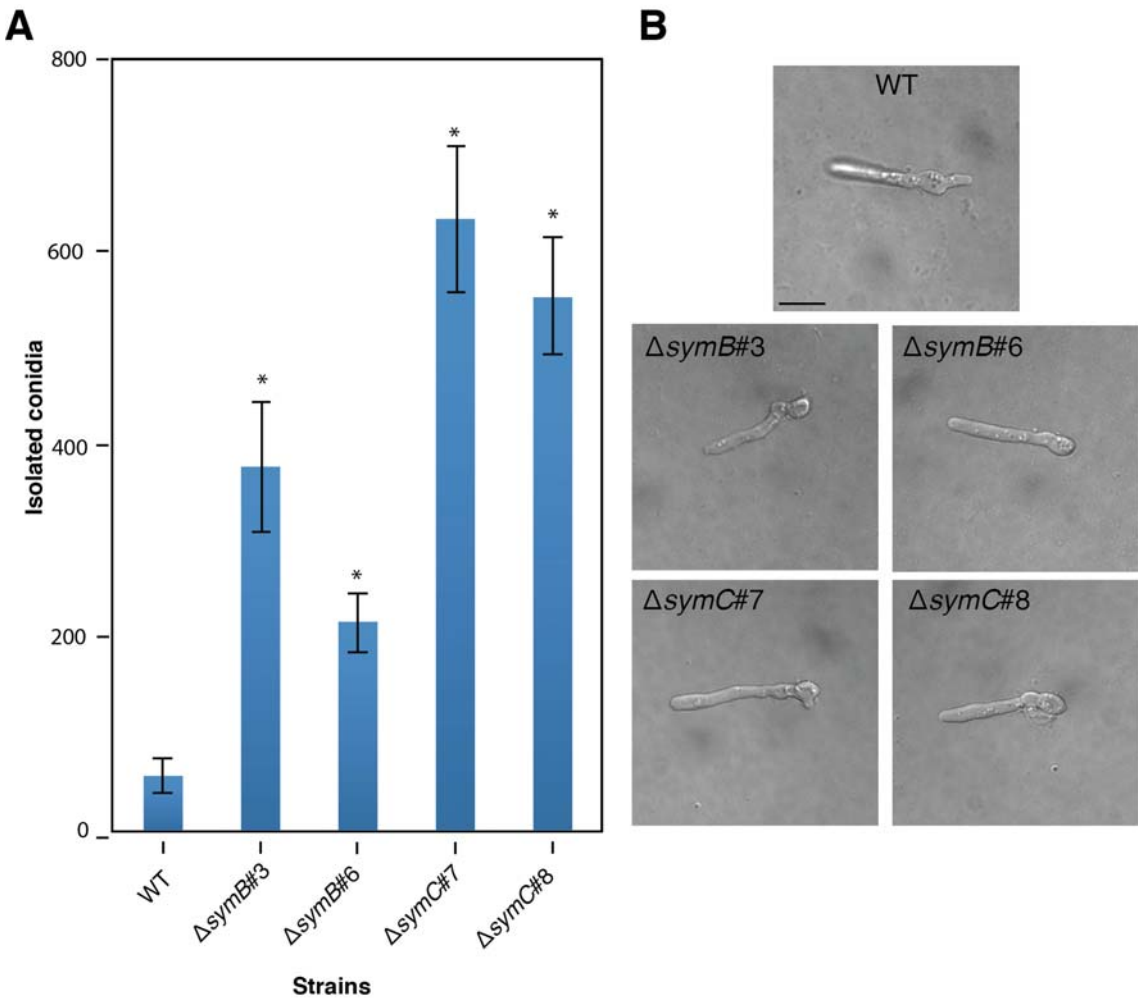

Fig. S7. Quantification and morphology of conidia recovered from Δ*symB*, Δ*symC* and wild-type cultures. A, Number of conidia isolated from 200 µL conidia suspensions pooled from 15 cultures. Bars represent ± standard error across three independent tests. An asterisk indicates significant differences from wild-type (WT) as determined by Welch's *t* test. **B,** Conidia germination morphology on PD agar after 24 h. Bar = 10 µM.

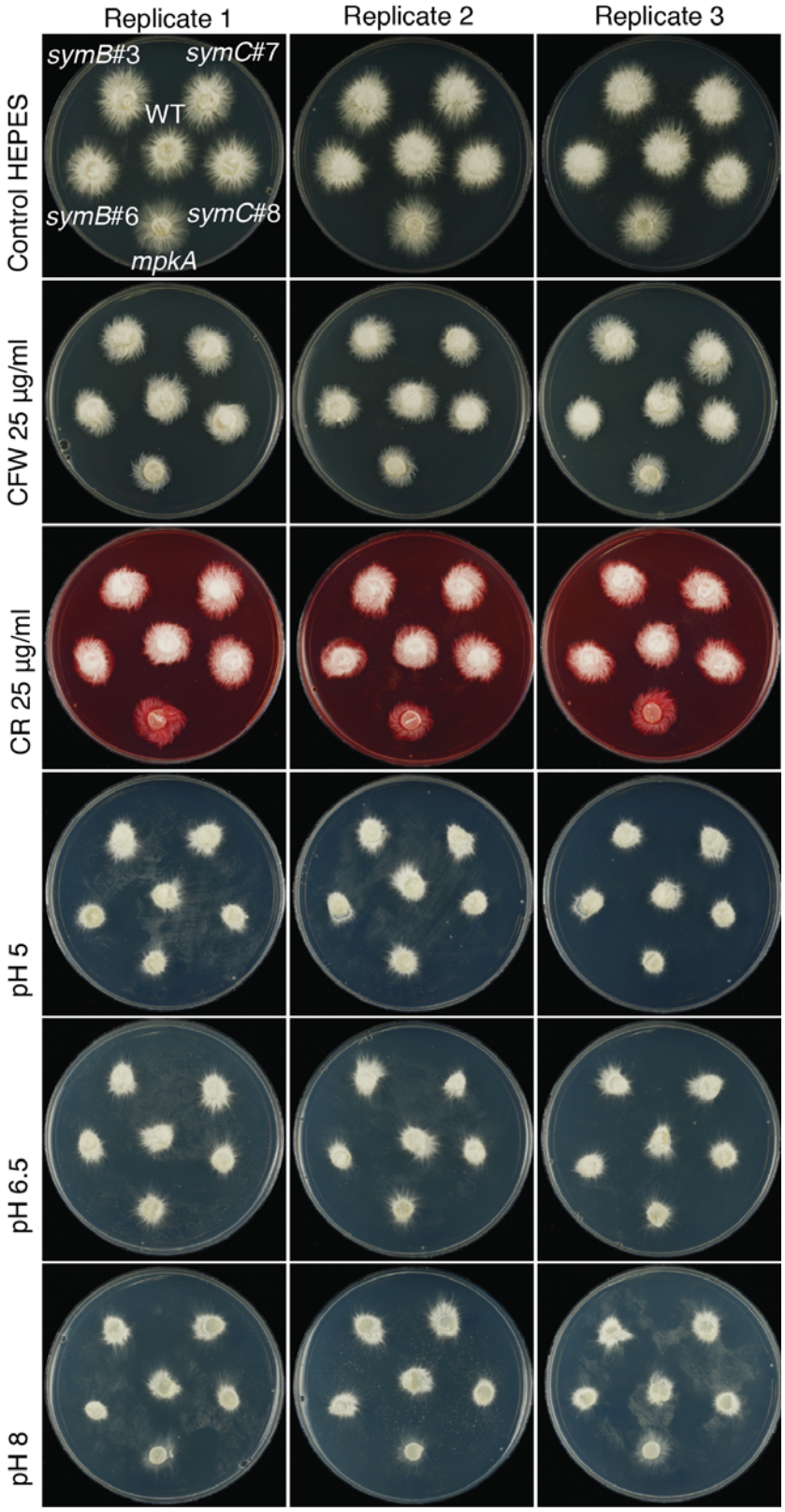

Fig. S8. Effect of cell wall stress agents and pH on growth of *E. festucae* wild-type (WT), Δ*mpkA*, Δ*symB* and Δ*symC* strains. Cultures were grown on 2.4% PDA buffered media (50 mM HEPES, pH 6.5) with and without Calcofluor White (CWF, 25 µg/ml), on Congo red (CR, 25 µg/ml), and buffered at pH 5, 6.5 and 8 in Blankenship media.

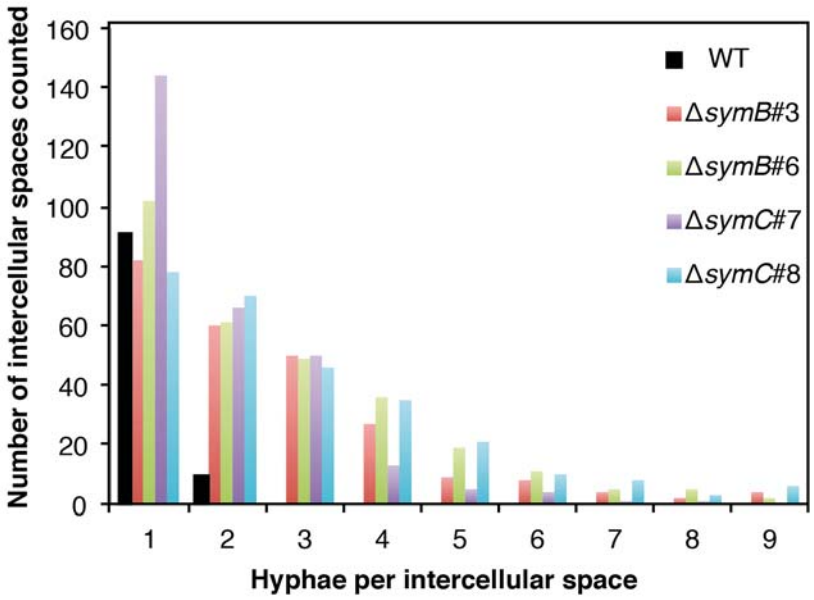

Fig. S9. Quantification of wild-type (WT), Δ*symB* and Δ*symC* hyphae colonising the intercellular spaces of host cells.

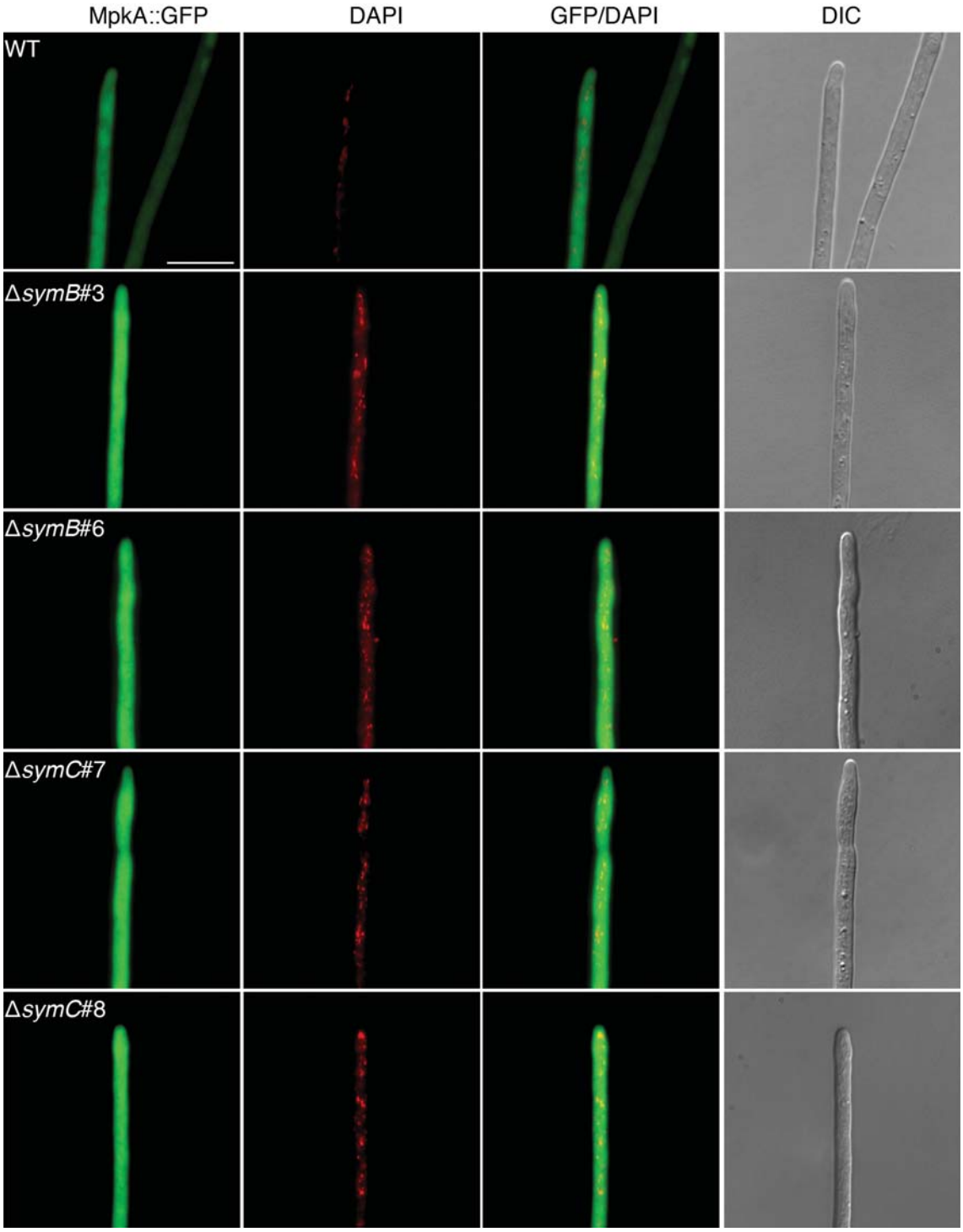

Fig. S10. Localisation of MpkA-eGFP in *E. festucae* wild-type, Δ*symB* and Δ*symC* hyphal tips. Inverted light microscopy of MpkA-eGFP cellular localisation in axenic cultures of *E. festucae* PN2963 (Fl1/pCE81), PN3105 (Δ*symB*#3/pCE81), PN3106 (Δ*symB*#6/pCE81), PN3107 (Δ*symC*#7/pCE81), PN3108 (Δ*symC*#8/pCE81), and corresponding DAPI and DIC images. Bar = 10 μm.

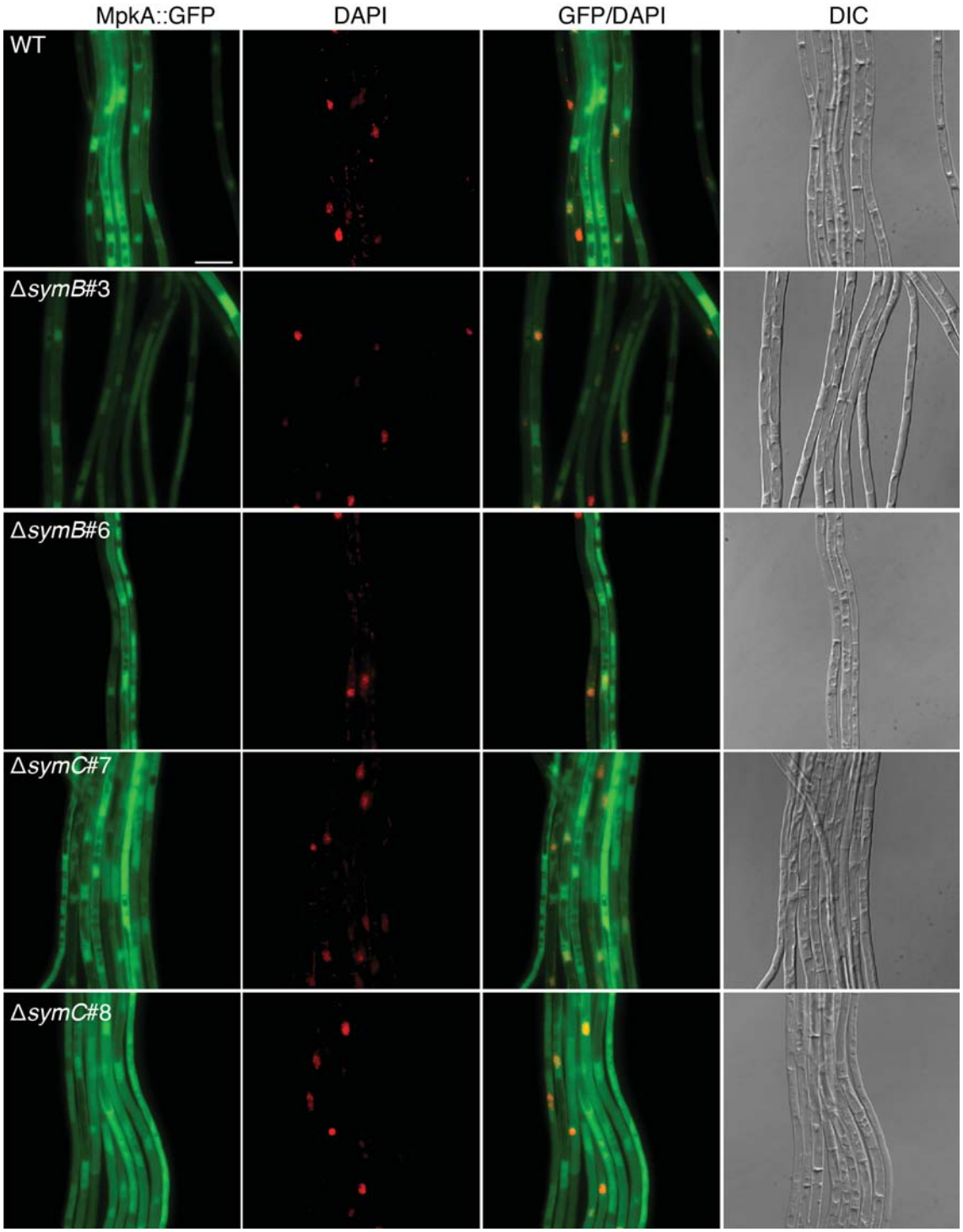

Fig. S11. Localisation of MpkA-eGFP in *E. festucae* wild-type, Δ*symB* and Δ*symC* hyphae from a mid-section of the colony. Inverted light microscopy of MpkA-eGFP cellular localisation in axenic cultures of *E. festucae* PN2963 (Fl1/pCE81), PN3105 (Δ*symB*#3/pCE81), PN3106 (Δ*symB*#6/pCE81), PN3107 (Δ*symC*#7/pCE81), PN3108 (Δ*symC*#8/pCE81), and corresponding DAPI and DIC images. Bar = 10 μm.

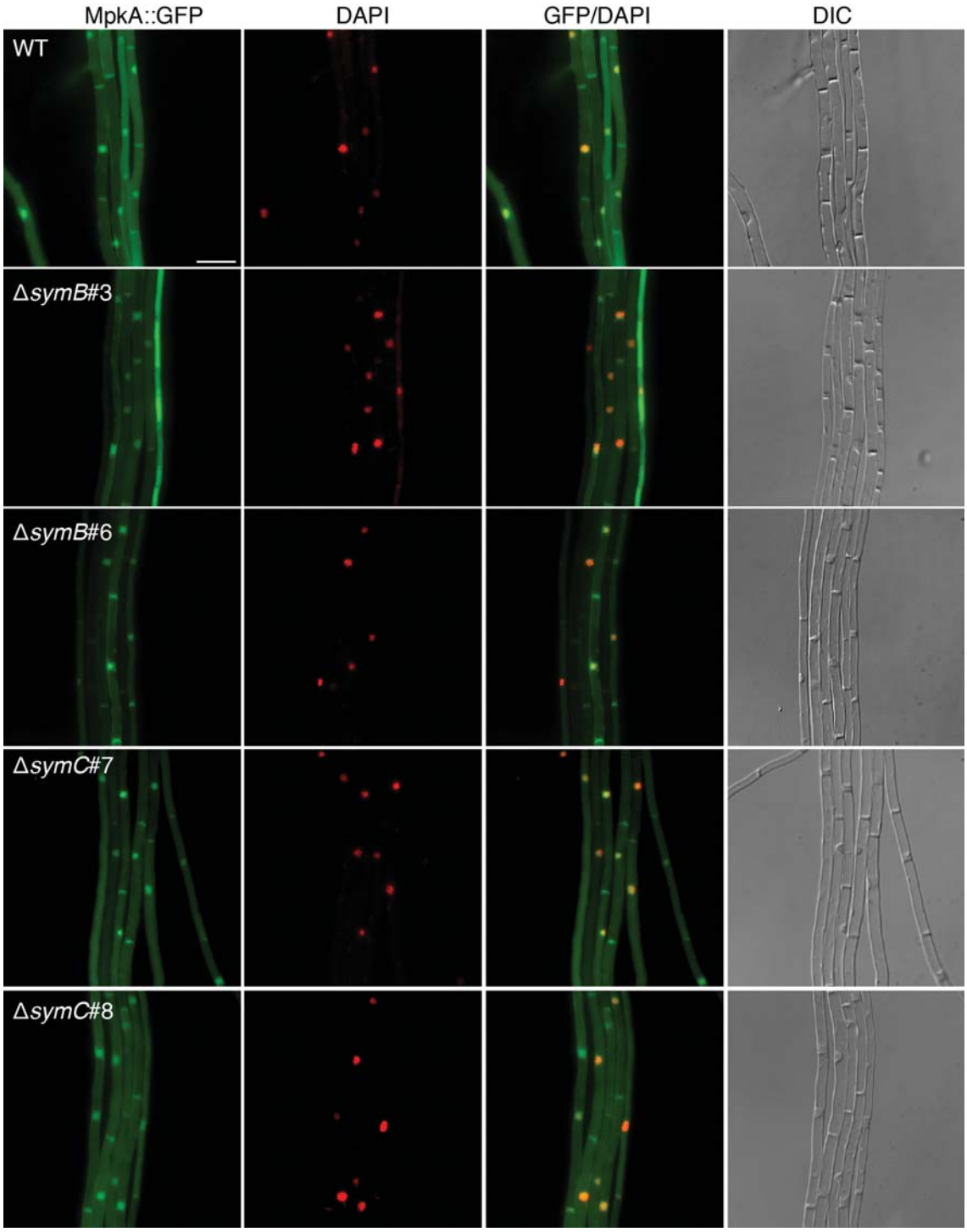

Fig. S12. Localisation of MpkA-eGFP in *E. festucae* wild-type, Δ*symB* and Δ*symC* hyphae from centre of the colony. Inverted light microscopy of MpkA-eGFP cellular localisation in axenic cultures of *E. festucae* PN2963 (Fl1/pCE81), PN3105 (Δ*symB*#3/ pCE81), PN3106 (Δ*symB*#6/pCE81), PN3107 (Δ*symC*#7/pCE81), PN3108 (Δ*symC*#8/ pCE81), and corresponding DAPI and DIC images. Bar = 10 μm.

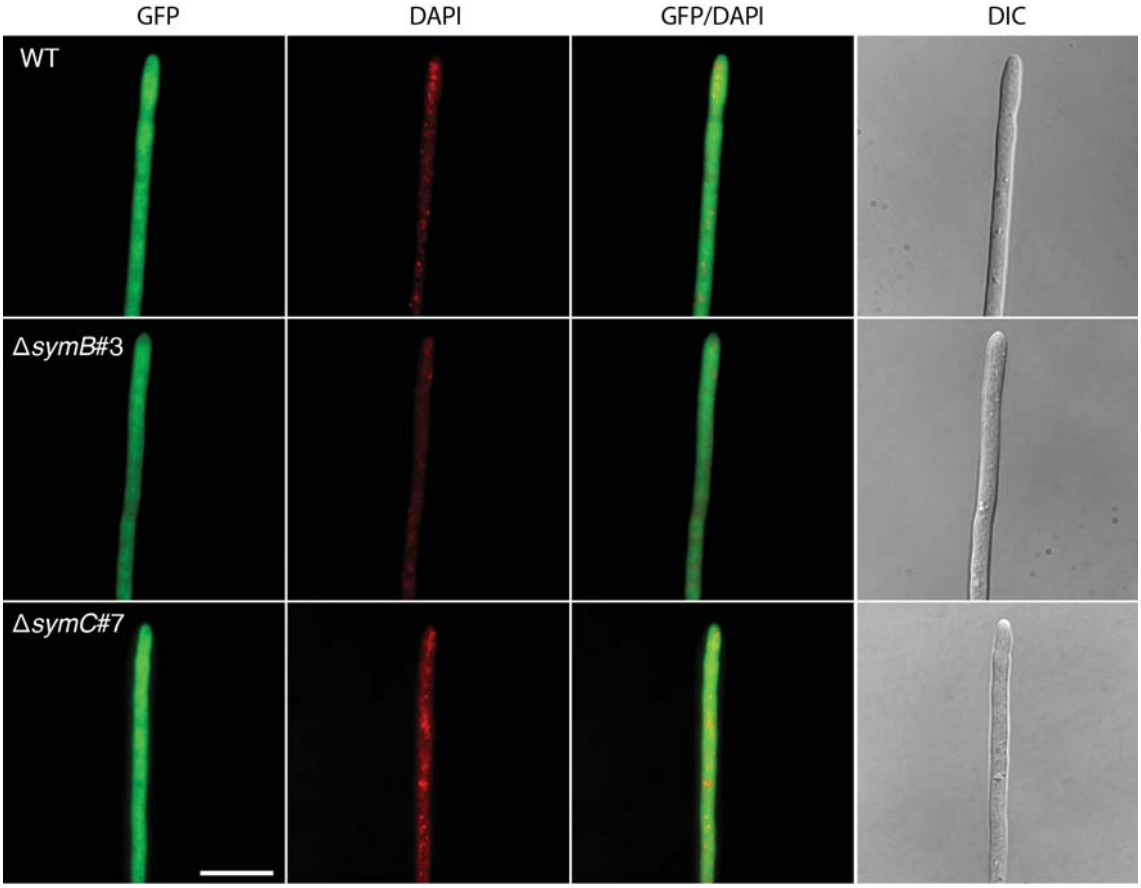

Fig. S13. Localisation of MpkB-eGFP in *E. festucae* wild-type, Δ*symB* and Δ*symC* hyphal tips. Inverted light microscopy of MpkB-eGFP cellular localisation in axenic cultures of *E. festucae* PN3138 (Fl1/pMpkB-*e*GFP), PN3140 (Δ*symB*#3/pMpkB-*e*GFP) and PN3141 (Δ*symC*#7/pMpkB-*e*GFP) with corresponding DAPI and DIC images. Bar = 10 μm.

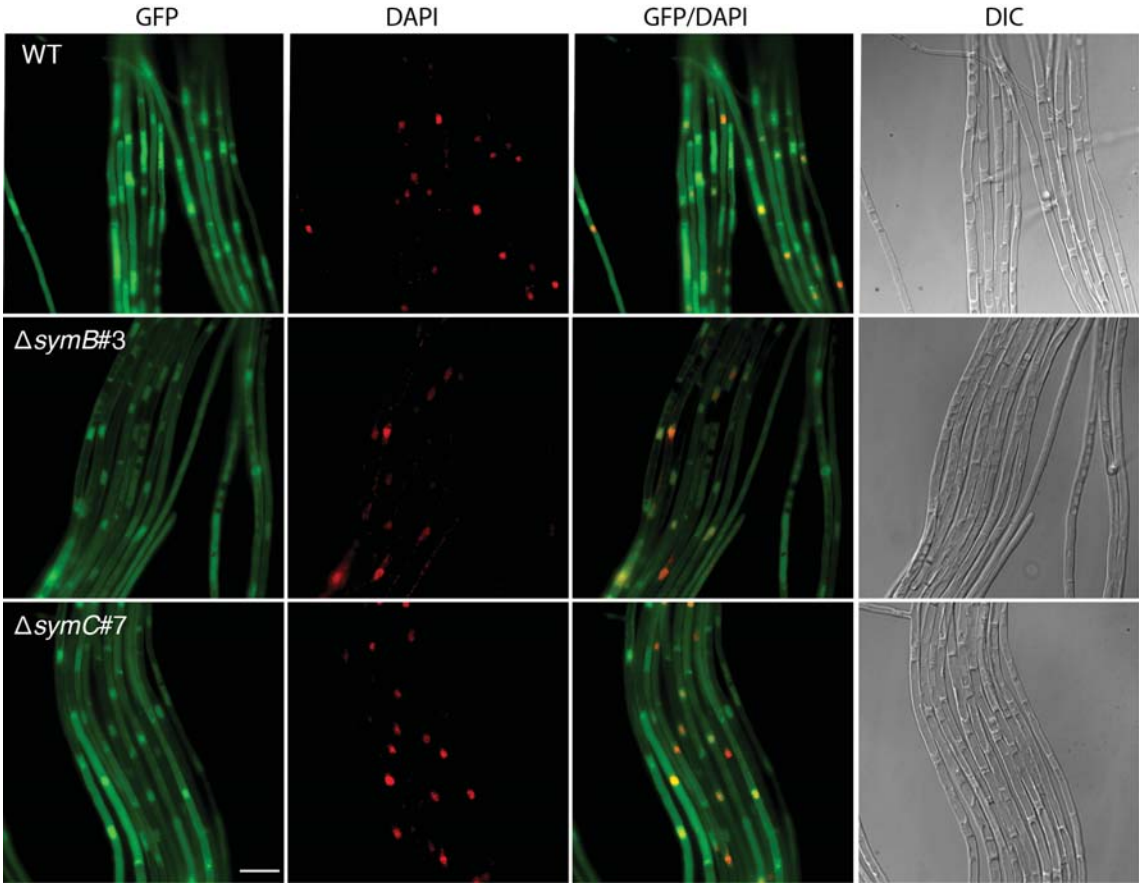

Fig. S14. Localisation of MpkB-eGFP in *E. festucae* wild-type, Δ*symB* and Δ*symC* hyphae from a mid-section of the colony. Inverted light microscopy of MpkB-eGFP cellular localisation in axenic cultures of *E. festucae* PN3138 (Fl1/pMpkB-*e*GFP), PN3140 (Δ*symB*#3/pMpkB-*e*GFP) and PN3141 (Δ*symC*#7/pMpkB-*e*GFP) with corresponding DAPI and DIC images. Bar = 10 µm.

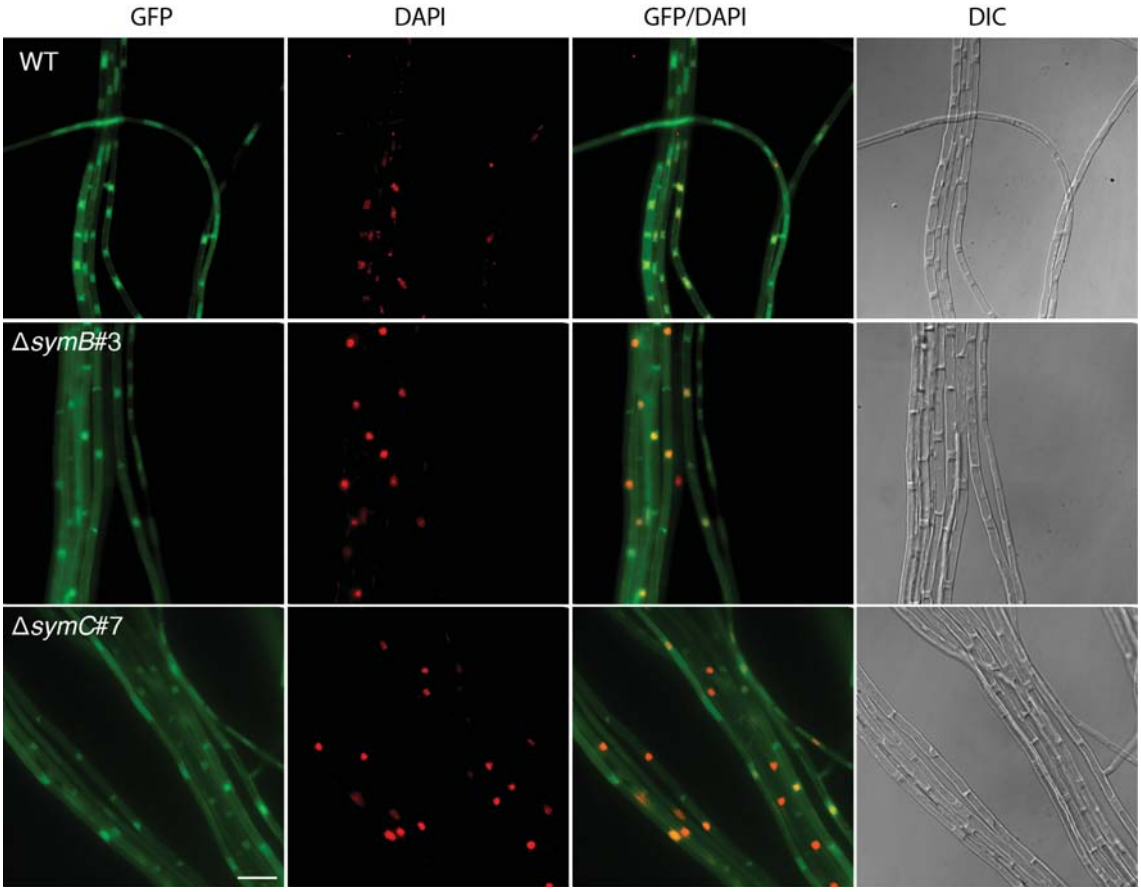

Fig. S15. Localisation of MpkB-eGFP in *E. festucae* wild-type, Δ*symB* and Δ*symC* hyphae from centre of the colony. Inverted light microscopy of MpkB-eGFP cellular localisation in axenic cultures of *E. festucae* PN3138 (Fl1/pMpkB-*e*GFP), PN3140 (Δ*symB*#3/pMpkB-*e*GFP) and PN3141 (Δ*symC*#7/pMpkB-*e*GFP) with corresponding DAPI and DIC images. Bar = 10 µm.

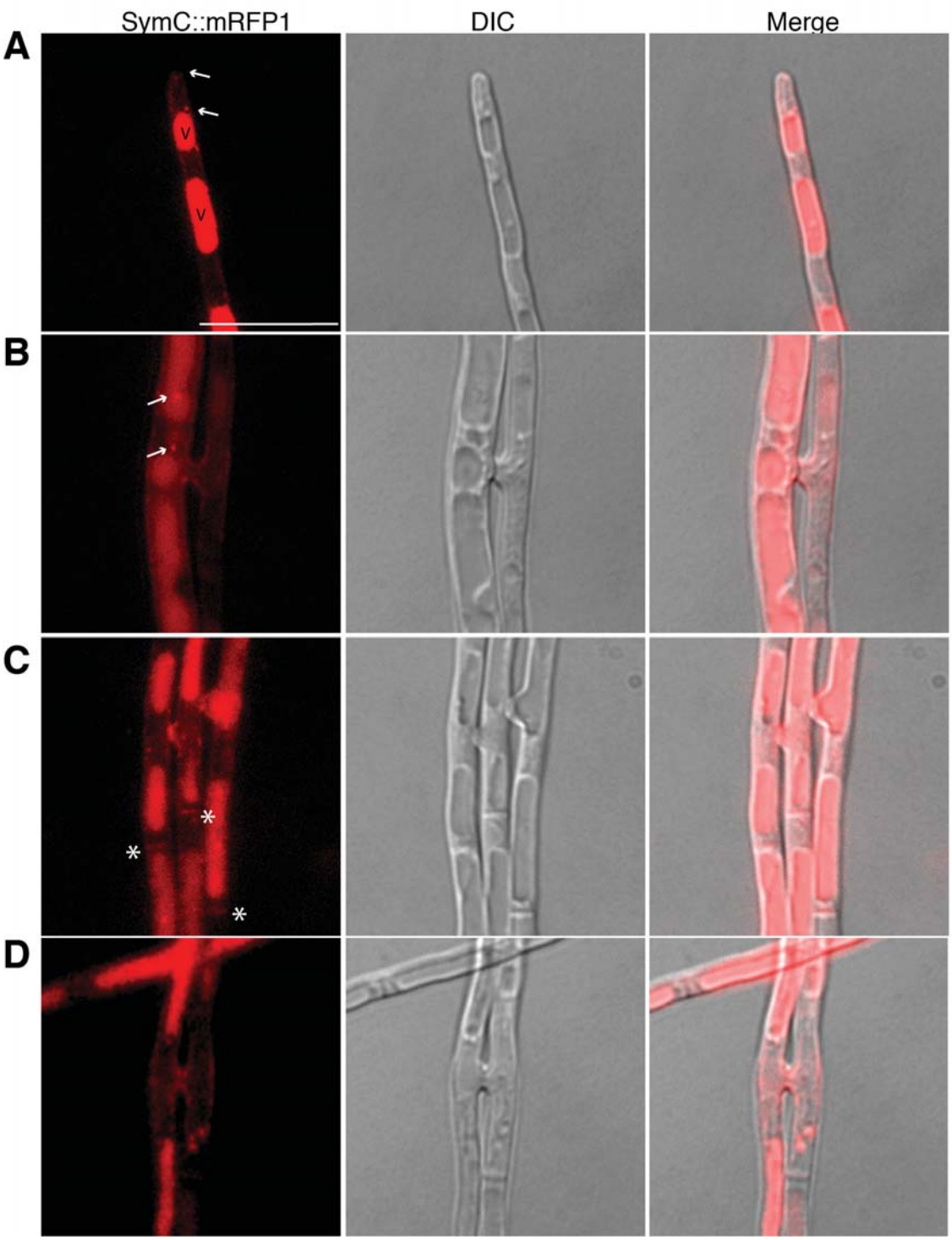

Fig. S16. Localisation of SymC-mRFP1 in *E. festucae* Δ*symC*. Inverted light and DIC microscopy of SymC-mRFP1 (red pseudocolour) localisation in **A,** vacuoles (v) and small vesicles (arrows) of hyphal tips and **B-D,** in small vesicles, at septa (*) and points of cell-cell fusions in PN3128(Δ*symC*#7/pKG12). The native P*symC* promoter was used to express *symC-mRFP1*. Bar = 10 µm.

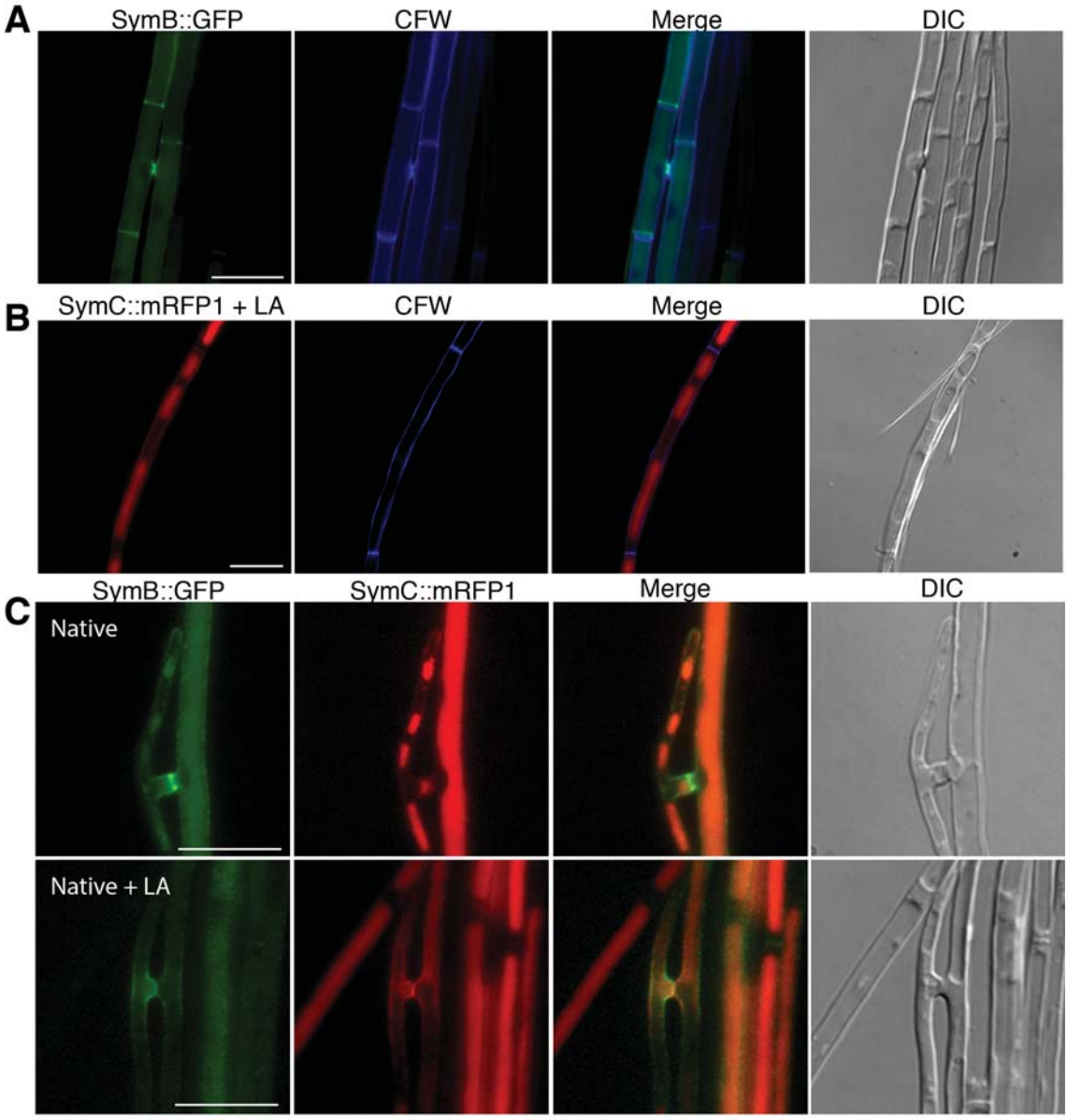

Fig. S17. Localisation of SymB-eGFP and SymC-mRFP1 in *E. festucae* Δ*symB* and Δ*symC*. Inverted light microscopy of **A**, SymB-eGFP (green pseudocolour) co-localisation with the cell wall marker Calcofluor white in PN3131 (Δ*symB*#3/pKG20). The native P*tefA* promoter was used to express *symB-eGFP*. Bar = 10 µm. **B**, SymC-mRFP1 (red pseudocolour) co-localisation with Calcofluor white in PN3132 (Δ*symC*#7/pKG21) treated with latrunculin A. The P*tefA* P*symC* promoter was used to express *symC-mRFP1*. Bar = 10 µm. **C**, SymB-eGFP (green pseudocolour) and SymC-mRFP1 (red pseudocolour) co-localisation in native PN3130 (Fl1/pKG13 & pKG12) expression cultures incubated with and without latrunculin A (LA). Bar = 10 µm.

Movie S1.

Supplementary References

Andrie, R. M., Martinez, J. P. and Ciuffetti, L. M. (2005) Development of ToxA and ToxB promoter-driven fluorescent protein expression vectors for use in filamentous ascomycetes. *Mycologia,* **97,** 1152-1161.

Becker, Y., Eaton, C. J., Brasell, E., May, K. J., Becker, M., Hassing, B., *et al.* (2015) The fungal cell wall integrity MAPK cascade is crucial for hyphal network formation and maintenance of restrictive growth of *Epichloë festucae* in symbiosis with *Lolium perenne*. *Mol. Plant-Microbe Interact,* **28,** 69-85.

Christianson, T. W., Sikorski, R. S., Dante, M., Shero, J. H. and Hieter, P. (1992) Multifunctional yeast high-copy-number shuttle vectors. *Gene,* **110,** 119-122.

Eaton, C. J., Dupont, P.-Y., Solomon, P. S., Clayton, W., Scott, B. and Cox, M. P. (2015) A core gene set describes the molecular basis of mutualism and antagonism in *Epichloë* species. *Mol. Plant-Microbe Interact,* **28,** 218-231.

Krogh, A., Larsson, B., von Heijne, G. and Sonnhammer, E. L. (2001) Predicting transmembrane protein topology with a hidden Markov model: application to complete genomes. *J. Mol. Biol.,* **305,** 567-580.

Lorang, J. M., Tuori, R. P., Martinez, J. P., Sawyer, T. L., Redman, R. S., Rollins, J. A., *et al.* (2001) Green fluorescent protein is lighting up fungal biology. *Appl. Environ. Microbiol.,* **67,** 1987-1994.

Namiki, F., Matsunaga, M., Okuda, M., Inoue, I., Nishi, K., Fujita, Y., *et al.* (2001) Mutation of an arginine biosynthesis gene causes reduced pathogenicity in *Fusarium oxysporum* f. sp. *melonis*. *Mol. Plant-Microbe Interact.,* **14,** 580-584.

Sonnhammer, E. L., von Heijne, G. and Krogh, A. (1998) A hidden Markov model for predicting transmembrane helices in protein sequences. . In: *Proceedings of the International Conference on Intelligent Systems for Molecular Biology; ISMB. International Conference on Intelligent Systems for Molecular Biology* pp. 175-182.

Winston, F., Dollard, C. and Ricupero-Hovasse, S. L. (1995) Construction of a set of convenient *Saccharomyces cerevisiae* strains that are isogenic to S288C. *Yeast,* **11,** 53-55.

Young, C. A., Bryant, M. K., Christensen, M. J., Tapper, B. A., Bryan, G. T. and Scott, B. (2005) Molecular cloning and genetic analysis of a symbiosis-expressed gene cluster for lolitrem biosynthesis from a mutualistic endophyte of perennial ryegrass. *Mol. Gen. Genomics,* **274,** 13-29.

4 SymC C-terminal Analysis

4.1 Introduction

Previous analysis of SymC::mRFP1 localisation (Chapter 3) showed that SymC is a four transmembrane domain protein that localises to the cell periphery, septa and small vesicles. Furthermore, phenotypic analysis of Δ*symC* mutants showed that disruption of *symC* results in similar phenotypes to Δ*mpkA* and Δ*idcA* mutants (Becker *et al.*, 2015; Eaton *et al.*, 2013), suggesting SymC acts in either the CWI or PR pathway. However, as shown in Chapter 3, MpkA and MpkB phosphorylation and localisation in Δ*symC* strains is similar to WT, indicating that SymC cannot be linked to the CWI or PR pathway from these experiments alone. The following chapter is focused on determining whether the C-terminus of SymC is essential for cell-cell fusion and identifying proteins that interact with this region.

4.2 Materials and Methods

4.2.1 Strains and primers

Table 4.1: Primers used in this study.

Primer	Sequence 5'- 3'	Purpose
mRFPR2	CCGAAGCGTGACAACGGCCTAGGCGCCGGTGGAGTG	mRFP cloning fragments
KG19_2	CGTCGACCCAATTGGCTG	Sequencing
KG20_2	TCCACATCTCTCCTGCATC	Sequencing
KG23	GAAGCTCACCTTGTTCACATCG	Sequencing
KG51	GAACTGCAGCCTGAGTGC	Sequencing
KG51_2	CACTTCAGCATAGACTTGGC	pKG6 & C-terminal
KG52	TCTCACTGGATCCTTCACAC	pKG6 fragment
KG72	GGTCGATCGCTCCTTGAGG	pKG9 fragment
KG73	CCTCAAGGAGCGATCGACCTAGGCCGTTGTCACGCTTC	pKG9 fragment
KG72	GGTCGATCGCTCCTTGAGG	Sequencing
KG74	GCCAAGTCTATGCTGAAGTG	C-terminal fragments
KG76	CACTCCACCGGCGCCTAGGCCGTTGTCACGCTTCGG	pKG19 fragment
KG77	GGCCCAGATCGAAAAGC	C-terminal fragments
KG78	GCTTTTCGATCTGGGCCTAGGCCGTTGTCACGCTTC	pKG10 fragment
KG82	GCTTTTCGATCTGGGCCTGGGAGATGCAGAGC	pKG11 &19 fragments
KG99	CTTGGGCTTTTCGATCTGGGCCGGTGCTGGTGCTGGTGCTGCC	pKG23 fragment
KG104	GCATATGGCCATGGAGGCCGAATTCTGGGCCATGTGGCCAAACCC	pKG24 fragment
KG105	TGCTAGTTATGCGGCCGCTGCAGGCTATCGCGAGCTTTGGTGC	pKG24 fragment
KG106	ATGGCCATGGAGGCCAGTGAATTCACGAGCGTGAGTGCAGTTCAAGC	pKG25 fragment
KG107	GATTCATCTGCAGCTCGAGCTCGATTAGTACAACACCTCTACAGCG	pKG25 fragment
KG108	ATGGCCATGGAGGCCAGTGAATTCCCGGCCTACAACTCCATCTTCAAC	pKG26 fragment
KG109	GATTCATCTGCAGCTCGAGCTCGATTACAACGCCTTGCCCATGAAC	pKG26 fragment
KG110	ATGGCCATGGAGGCCAGTGAATTCAAAAATCTCCTTCAGCTTGCC	pKG27 fragment
KG111	GATTCATCTGCAGCTCGAGCTCGACTAGAAGTAACGAATCACAGC	pKG27 fragment
KG112	ATGGCCATGGAGGCCAGTGAATTCCCCCAGAACGTTGGCATCAAGGCC	pKG28 fragment
KG113	GATTCATCTGCAGCTCGAGCTCGATTACGCCTGGACCTTGTACTCGC	pKG28 fragment
pGBKT7_F	CATCATGGAGGAGCAGAAGC	Sequencing
pGADT7_F	CGCCATGGAGTACCCATACG	Sequencing
pGADT7_R	CAGTATCTACGATTCATCTGC	Sequencing

Table 4.2: Strains used in this study.

Biological material	Relevant characteristics	Reference
Yeast strains		
S. cerevisiae		
AH109	*MATa; trp1-901; leu2-3,112; ura3-52; his3-200; ade2-101; gal4Δ; gal80Δ; LYS2::GAL1UAS GAL1TATA HIS3; GAL2 UASGAL2TATA -ADE2; URA3::MEL1UAS -MEL1 TATA-lacZ; MEL1*	James *et al*., 1996
Y187	*MATα, ura3-52, his3-200, ade2-101, trp1-901, leu2-3, 112, gal4Δ, met–, gal80Δ, URA3 : : GAL1UAS-GAL1TATA-lacZ*	Harper *et al*., 1993
Y187 + *N. crassa* cDNA library	Y187; *N. crassa* cDNA library	Braunschweig, Germany
AH109/pGBKT7& pGADT7	AH109; pGBKT7 & pGADT7	This study
AH109/pGBKT7-p53 & pGADT7-T	AH109; pGBKT7-p53 & pGADT7-T	This study
AH109/pKG14 & pGADT7-laminin C	AH109; pKG14 & pGADT7-laminin C	This study
AH109/pKG14 & RanBPM	AH109; pKG14 & RanBPM	This study
AH109/pKG14 & pGADT7-RHO-1 DN	AH109; pKG14 & pGADT7-RHO-1 DN	This study
AH109/pKG14 & pGADT7-RHO-1 DA	AH109; pKG14 & pGADT7-RHO-1 DA	This study
AH109/pKG14 & pGADT7-PKC-1	AH109; pKG14 & pGADT7-PKC-1	This study
AH109/pKG14 & pGADT7-MIK-1 N-term	AH109; pKG14 & pGADT7-MIK-1 N-term	This study
AH109/pKG14 & pGADT7-MIK-1 C-term	AH109; pKG14 & pGADT7-MIK-1 C-term	This study
AH109/pKG14 & pGADT7-MEK-1	AH109; pKG14 & pGADT7-MEK-1	This study
AH109/pKG14 & pGADT7-MEK-1 N-term	AH109; pKG14 & pGADT7-MEK-1 N-term	This study
AH109/pKG14 & pGADT7-MEK-1 C-term	AH109; pKG14 & pGADT7-MEK-1 C-term	This study
AH109/pKG14 & pGADT7-MAK-1	AH109; pKG14 & pGADT7-MAK-1	This study
AH109/pKG14 & pGADT7-BEM-1	AH109; pKG14 & pGADT7-BEM-1	This study
AH109/pKG14 & pGADT7-NOR-1	AH109; pKG14 & pGADT7-NOR-1	This study
AH109/pKG24 & pGBADT7	AH109; pKG24 & pGBADT7	This study
AH109/pKG25 & pGADT7	AH109; pKG25 & pGADT7	This study
AH109/pKG26 & pGADT7	AH109; pKG26 & pGADT7	This study
AH109/pKG27 & pGADT7	AH109; pKG27 & pGADT7	This study
AH109/pKG28 & pGADT7	AH109; pKG28 & pGADT7	This study
AH109/pKG24 & pKG25	AH109; pKG24 & pKG25	This study
AH109/pKG24 & pKG26	AH109; pKG24 & pKG26	This study
AH109/pKG24 & pKG27	AH109; pKG24 & pKG27	This study
AH109/pKG24 & pKG28	AH109; pKG24 & pKG28	This study
Fungal strains		
Epichloë festucae		
PN2278 (Fl1)	Wild-type isolated from *Festuca trachyphylla*	Young *et al*., 2005
PN2957 (Δ*symC*#7)	Fl1/Δ*symC*::P*trpC-gen*; Gen^R	This study
PN2956 (Δ*symC*#8)	Fl1/Δ*symC*::P*trpC-gen*; Gen^R	This study
PN3073 (Δ*symC*#7/pKG9 #3)	Δ*symC*#7/ P*symC-symC* half C-terminal deletion-T*symC* (pKG9), pSF15.15; Gen^R, Hyg^R	This study
PN3074 (Δ*symC*#7/pKG9 #14)	Δ*symC*#7/ P*symC-symC* half C-terminal deletion-T*symC* (pKG9), pSF15.15; Gen^R, Hyg^R	This study
PN3075 (Δ*symC*#8/pKG9 #2)	Δ*symC*#8/ P*symC-symC* half C-terminal deletion-T*symC* (pKG9), pSF15.15; Gen^R, Hyg^R	This study

PN3076 (Δ*symC*#8/pKG9 #4)	Δ*symC*#8/ P*symC-symC* half C-terminal deletion-T*symC* (pKG9), pSF15.15; Gen^R, Hyg^R	This study
PN3133 (Δ*symC*#7/pKG10 #3)	Δ*symC*#7/ P*symC-symC* full C-terminal deletion-T*symC* (pKG10), pSF15.15; Gen^R, Hyg^R	This study
PN3132 (Δ*symC*#8/pKG10 #4)	Δ*symC*#8/ P*symC-symC* full C-terminal deletion-T*symC* (pKG10), pSF15.15; Gen^R, Hyg^R	This study
PN3142 (Δ*symC*#7/pKG11 #2)	Δ*symC*#7/ P*symC-symC* truncated C-terminal deletion-T*symC* (pKG10), pSF15.15; Gen^R, Hyg^R	This study
PN3143 (Δ*symC*#8/pKG11 #2)	Δ*symC*#7/ P*symC-symC* truncated C-terminal deletion-T*symC* (pKG10), pSF15.15; Gen^R, Hyg^R	This study
PN3144 (Δ*symC*#7/pKG19 &pSF15.15)	Δ*symC*#7/ P*symC-symC* truncated C-terminal deletion-*mRFP*-T*symC* (pKG19), pSF15.15; Gen^R, Hyg^R	This study
PN3145 (Δ*symC*#7/pKG23 & pSF15.15)	Δ*symC*#7/ P*symC-symC* full C-terminal deletion-*mRFP*-T*symC* (pKG23), pSF15.15; Gen^R, Hyg^R	This study

Bacterial strains

E.coli

PN1687	Source of pII99; Amp^R	Namiki *et al*. 2001
PN1862	Source of pSF15.15; Amp^R	S. Foster
PN4265	Source of pKG6; Amp^R	This study
PN4269	Source of pKG9; Amp^R	This study
PN4270	Source of pKG10; Amp^R	This study
PN4271	Source of pKG11; Amp^R	This study
PN4272	Source of pKG12; Amp^R	This study
PN4283	Source of pKG19; Amp^R	This study
PN4286	Source of pKG23; Amp^R	This study
PN4287	Source of pKG24; Kan^R	This study
PN4288	Source of pKG25; Amp^R	This study
PN4289	Source of pKG26; Amp^R	This study
PN4290	Source of pKG27; Amp^R	This study
PN4290	Source of pKG28; Amp^R	This study

Plasmids

pII99	P*trpC-nptII*-T*trpC*; Amp^R, Gen^R	Namiki *et al*. (2001)
pSF15.15	P*trpC-hph*-T*trpC*; Amp^R, Hyg^R	S. Foster
pKG6	pCR4-Topo®; P*symC::symC::*T*symC* complementation construct; Amp^R	This study
pKG9	pCR4-Topo®; P*symC::symC* half C-terminal deletion*::*T*symC*; Amp^R	This study
pKG10	pCR4-Topo®; P*symC::symC* full C-terminal deletion:: T*symC*; Amp^R	This study
pKG11	pCR4-Topo®; P*symC::symC* truncated C-terminal deletion::T*symC*; Amp^R	This study
pKG12	pCR4-Topo®; P*symC::symC::3GA::mRFP::*T*symC* complementation construct; Amp^R	This study
pKG14	pGBKT7; *NCU00938* C-terminal region; Kan^R	This study
pKG19	pCR4-Topo®; P*symC::symC* truncated C-terminal deletion::*3GA::mRFP::*T*symC*; Amp^R	This study
pKG23	pCR4-Topo®; P*symC::symC* full C-terminal deletion*::3GA::mRFP::*T*symC*; Amp^R	This study
pKG24	pGBKT7; *symC* C-terminal cDNA, Kan^R	This study

pKG25	pGADT7; *gpiA* cDNA, Amp^R	This study
pKG26	pGADT7; *arp3* cDNA, Amp^R	This study
pKG27	pGADT7; *uthA* cDNA, Amp^R	This study
pKG28	pGADT7; *ergM* cDNA, Amp^R	This study
pGBKT7	pGBKT7 backbone; *TRP1, GAL4-BD,* Kan^R	Clontech,
pGADT7	pGADT7 backbone; *LEU2, GAL4-AD,* Amp^R	Clontech,
pGBKT-p53	pGBKT7; murine $p53_{aa72-390}$ cDNA, Kan^R	Clontech,
pGBKT-laminin C	pGBKT7; human laminin C cDNA, Kan^R	Clontech,
pGADT7-T	pGADT7; SV40 large T-$atigen_{aa86-708}$ cDNA, Amp^R	Clontech,
pGAD-RanBPM	pGADT7; RanBPM cDNA, Amp^R	Clontech,
pGADT7-RHO-1 DN	pGADT7; *rho-1* DN cDNA, Amp^R	Germany
pGADT7-RHO-1 DA	pGADT7; *rho-1* DA cDNA, Amp^R	Germany
pGADT7-PKC-1	pGADT7; *pck-1* cDNA, Amp^R	Germany
pGADT7-MIK-1 N-term	pGADT7; *mik-1* 13kb N-term cDNA, Amp^R	Germany
pGADT7-MIK-1 C-term	pGADT7; *mik-1* 13kb C-term cDNA, Amp^R	Germany
pGADT7-MEK-1	pGADT7; *mek-1* cDNA, Amp^R	Germany
pGADT7- MEK-1 N-term	pGADT7; *mek-1* N-term cDNA, Amp^R	Germany
pGADT7- MEK-1 C-term	pGADT7; *mek-1* C-term cDNA, Amp^R	Germany
pGADT7-MAK-1	pGADT7; *mak-1* cDNA, Amp^R	Germany
pGADT7-BEM-1	pGADT7; *bem-1* cDNA, Amp^R	Germany
pGADT7-NOR-1	pGADT7; *nor-1* cDNA, Amp^R	Germany

4.2.2 Sterile conditions

Media was prepared with Barnstead NANO pure water (Thermo Scientific) and sterilized by autoclaving at 121°C for 20 minutes. All experiments involving the culturing of yeast, bacteria or fungal cells and the pouring of culture plates were performed under a UV sterilized laminar flow hood.

4.2.3 *Saccharomyces cerevisiae* growth conditions and media

Yeast strains were cultured for 3-4 days at 30°C under darkness on Yeast Extract Peptone Dextrose (YPD), YPD + Adenine (YPDA), Synthetic Drop out (SD) plates or in 50 mL liquid cultures shaken at 200 rpm overnight (O/N). For short-term storage strains were kept on plates at 4°C and for long-term storage strains were kept at -80°C in 30% (v/v) glycerol.

4.2.3.1 YPD and YPDA medium

The YPD medium (pH 5.8) contained 4 g of Yeast Extract and 8 g of Mycological Peptone (Difco) per 380 mL. An additional 40 mg of adenine hemisulfate was added for YPDA medium and 8 g of agar when making plates. After autoclaving 20 mL of a 40% (w/v) glucose solution was added to bring the final volume to 400 mL.

4.2.3.2 SD medium

The SD medium (pH 5.8) contained 72.9 g D-Sorbitol, 2.68 g Yeast Nitrogen Base without amino acids (BD Bioscience), 0.26 g drop out (DO) supplement, being either Ura-, Leu-/Trp- or Leu-/Trp-/His-/Ade- (BD Bioscience Clontech), and 8 g agar per 380 mL. After autoclaving, 20 mL of a 40% (w/v) glucose solution was added to a final volume to 400 mL.

4.2.4 *Escherichia coli* growth conditions and media

E. coli strains were cultured overnight at 37°C either in 5 mL Luria-Bertani (LB) liquid medium at 200 rpm or on LB plates. For short-term storage strains were kept on plates at 4°C and for long-term storage strains were kept at -80°C under 50% (v/v) glycerol storage.

4.2.4.1 Luria-Bertani (LB) medium

LB medium (pH 7-7.5) contained 85 mM NaCl, 1% (w/v) Bacto Tryptone and 0.5% (w/v) Difco Yeast Extract with 15 g/L of agar added when making plates. To obtain selection media either ampicillin (Amp) 100 μg/mL or kanamycin (Kan) 50 μg/mL was added.

4.2.4.2 SOC medium

The SOC medium contained 2% (w/v) Tryptone, 0.5% (w/v) Yeast Extract, 10 mM NaCl, 2.5 mM KCl, 10 mM $MgCl_2$, 10 mM $MgSO_4.7H_2O$ and 20 mM glucose.

4.2.4.3 SOB medium

The SOB medium (pH 7) contained 20 g/L Tryptone, 5 g/L Yeast Extract, 0.5 g/L NaCl, 10 mL of a 250 mM KCl solution and 5 mL of 2 M $MgCl_2$.

4.2.5 *Epichloë festucae* growth conditions and media

Epichloë strains were cultured at 22°C for 5-7 days on Potato dextrose (PD) or 1.5% (w/v) water agar plates and for 10-14 days on Regeneration (RG) plates. Liquid cultures were grown for 3-4 days in 50 mL of PD broth with shaking at 200 rpm. For short-term storage strains were kept on plates at 4°C and long-term storage strains were kept at 4°C on PD slants under mineral oil or at -80°C under 30% (w/v) glycerol storage.

4.2.5.1 Potato dextrose (PD) medium

PD liquid media contained 2.4% (w/v) PD with 1.5% (w/v) agar added to obtain solid PD plates. Selection media contained either 150 μg/mL of hygromycin (Hph) or 200 μg/mL of geneticin (Gen) which was added after autoclaving.

4.2.5.2 Regeneration medium (RG)

The RG medium (pH 6.5) contained 2.4% (w/v) PD and 0.8 M Sucrose with either 1.5% or 0.8% (w/v) agar added to obtain base media and overlays respectively. Hygromycin or geneticin was included in the overlay media to obtain final concentrations (RG plate + RG overlay) of 150 μg/mL or 200 μg/mL respectively.

4.2.5.3 Water agar

Water agar plates contained 3% and 1.5% (w/v) agar. When performing fusion tests a glass slide was positioned on 20 mL of pre-set 3% agar and overlaid with an additional 5-10 mL of 1.5% agar. Strains were sub-cultured onto the edges of the microscope slides and after 5-7 days mycelia blocks, growing across the agar slide, were extracted for microscopy.

4.2.6 DNA and RNA isolation and quantification

4.2.6.1 Plasmid isolation

E. coli cultures were grown O/N in 5 mL of LB-selection broth. Plasmid DNA was extracted using a High Pure Plasmid Isolation Kit (Roche) according to the manufacturer's instructions.

4.2.6.2 *Epichloë festucae* crude DNA extractions

Crude DNA extractions were performed by freeze drying mycelia from 5-7 day old colonies grown on PD plates. Mycelia was ground in liquid nitrogen and resuspended in 150 μL of Lysis buffer (100 mM Tris (pH 8), 100 mM Na_2 EDTA (pH 8) and 1% (w/v) SDS) and samples incubated for 30 mins at 70°C. 5 M potassium acetate (150 μL) was added and samples incubated on ice for 20 mins. Following centrifugation (13,000 x *g*, 10 mins), the supernatant was transferred into a fresh tube and DNA precipitated by the addition of 300 μL of isopropanol and an incubation step at -20°C for 20 mins. DNA was pelleted (13,000 x *g*, 15 mins), washed with 70% (v/v) ethanol, pelleted again, air-dried and resuspended in 20 μL of sterile Milli-Q water.

4.2.6.3 *Epichloë festucae* RNA extraction and cDNA synthesis

Fresh *E. festucae* mycelium grown in liquid PD was freeze dried overnight, ground in liquid nitrogen and resuspended in 1 mL TRIzol (Invitrogen). RNA was then extracted as per the manufacture's instructions. RNA (1 μg) was heat denatured and reverse transcribed into cDNA using SuperScriptTM II reverse transcriptase (Invitrogen) according to the manufacturer's instructions.

4.2.7 DNA manipulation

4.2.7.1 *Taq* and *Q5* Polymerase PCR amplification

Taq (Roche) PCR reactions were set up in 0.2 mL PCR tubes using 41 µL Mill-Q water, 5 µL 10 x Buffer, 1 µL dNTPs (1.25 mM), 1 µL (10 pmol/µL) forward primer, 1 µL (10 pmol/µL) reverse primer, 1 µL template and 2 units of polymerase. *Taq* PCR parameters were as follows, an initial denaturation step at 95ºC for 2 min followed by successive denaturation (95ºC for 30 seconds), annealing (50-60ºC for 30 seconds) and extension (72ºC 1 min/kb) steps repeated for 36 cycles and a final 72ºC elongation step for 4 min.

Q5 polymerase PCR reactions were set up in 0.2 mL PCR tubes using Mill-Q water to 50 µL, 10 µL 5x Buffer, 1 µL dNTPs (1.25 mM), 2.5 µL (10 pmol/µL) forward primer, 2.5 µL (10 pmol/µL) reverse primer, 1 µL template DNA with 0.5 µL of *Q5* polymerase. PCR parameters were as follows, an initial denaturation step at 98ºC for 30 seconds followed by successive denaturation (98ºC for 10 seconds), annealing (50-60ºC for 30 seconds), and extension (72ºC 30s min/kb), steps repeated for 36 cycles and a final 72ºC elongation step for 5 min.

4.2.7.2 Gel purification of PCR products

PCR and restriction enzyme products were purified using the Wizard® SV Gel and PCR Clean-Up System (Promega) as per the manufacturer's instructions.

4.2.7.3 Restriction Enzyme digests

All digests were performed at 37ºC for 1-2 hours for standard digests or overnight for later purification using 3 units of restriction enzyme, 10 µL of buffer, 100 ng - 1.5 µg DNA and Milli-Q water to a final volume of 100 µL.

4.2.8 Cloning

4.2.8.1 Gibson Assembly

Purified DNA fragments (100-150 ng) were assembled in 10 µL of Gibson Assembly master mix containing water (3.67 µL), Isothermal buffer (5% PEG 8000, 100 mM Tris-HCl (pH 7.5), 10 mM $MgCl_2$, 10 mM DTT, 1 mM NAD & 0.2 mM dNTPs), *T5* exonuclease (0.08 µL), *Phusion* Polymerase (0.25 µL) and *Taq* ligase (2 µL) to a final volume of 20 µL. Samples were incubated for 1 hour at 50°C.

4.2.8.2 Preparation and transformation of chemical competent *E. coli* cells

A single *E. coli* colony was inoculated into 1.5 mL SOB media and grown overnight at 200 rpm. Inoculated media was transferred into 200 mL of SOB and incubated at 22°C and 200 rpm until the mid-log phase (A_{600} 0.4-0.8). Cells were centrifuged (10 min, 5000 x *g*), the supernatant removed and cells resuspended in 67 mL of ice-cold transformation buffer on ice for 10 min (pH 7, PIPES 1.5 g/500 mL, $CaCl_2 2H_20$ 1.1 g/500 mL and KCl 9.3 g/500 mL). Cells were centrifuged again (10 min, 5000 x *g*), the supernatant removed and cells resuspended in 16 mL of transformation buffer. DMSO (1.2 mL) was added, cells flash frozen in liquid nitrogen and stored at -80 ºC in 100 µL aliquots. When transforming *E. coli*, 1-2 µl of DNA was added and cells incubated on ice for 20 mins. Cells were heat-shocked, at 42ºC for 60 seconds, and chilled on ice for a further 2 minutes. SOC medium (300 µL) was added and cells incubated for 1 hour at 37ºC before being spread on selection plates and grown overnight at 37ºC.

4.2.8.3 Invitrogen Clone Checker™ system

Candidate *E. coli* transformants were transferred into 0.2 mL PCR tubes containing 8 µL of Clone Checker™ Green-Solution (0.1 M NaCl, 10 mM Tris-HCL (pH 8.0), 1 mM EDTA (pH 8.0) and 0.5% Triton X-100) and incubated at 100 ºC for 30 seconds. 1 unit of restriction enzyme and 1 µL of buffer was added and samples digests at 37 ºC for 30 minutes. Digests were screened for fragments of the correct size, as visualized on 0.8% (w/v) agarose gels by staining with ethidium bromide.

4.2.8.4 Sequencing

Sequencing reactions were performed using the Massy Genome Sequencing facilities located at Massey University Palmerston North using 1 µL of primer (3.2 pmol/µL), 400-600 ng DNA template in a final volume of 30 µL.

4.2.9 Generation of C-terminal deletion and expression and Yeast-2-hybrid constructs

4.2.9.1 *E. festucae* SymC C-terminal deletion and expression constructs

SymCΔ235-274 C-terminal construct

The SymCΔ235-274 deletion construct (pKG9, **Supplementary Figure 7.16**) was made by Gibson Assembly by recombining 3.6 kb (primers KG51_2 and 72) and 4.4 kb (primers KG73 and 74) fragments amplified from pKG6 plasmid DNA using *Q5* Polymerase.

SymCΔ208-274 C-terminal construct

The SymCΔ208-274 deletion construct (pKG10, **Supplementary Figure 7.17**) was made by Gibson Assembly by recombining 3.5 kb (primers KG51_2 and 77) and 4.4 kb (primers KG78 and 74) fragments amplified from pKG6 plasmid DNA using *Q5* Polymerase.

SymCΔ208-235 C-terminal construct

The SymCΔ208-235 deletion construct (pKG11, **Supplementary Figure 7.18**) was made by Gibson Assembly by recombining 3.5 kb (primers KG51_2 and 77) and 4.4 kb (primers KG82 and 74) fragments amplified from pKG6 plasmid DNA using *Q5* Polymerase.

SymCΔ208-235 C-terminal construct tagged with mRFP1

The SymCΔ208-235 mRFP1 tagged construct (pKG19, **Supplementary Figure 7.22**) was made by Gibson Assembly by recombining 3.5 kb (primers KG51_2 and 77) and 5.2 kb (primers KG82 and 74) fragments amplified from pKG12 plasmid DNA using *Q5* Polymerase.

SymCΔ208-274 C-terminal construct tagged with mRFP1

The SymCΔ208-274 mRFP1 tagged construct (pKG23, **Supplementary Figure 7.25**) was made via Gibson Assembly by recombining 3.5 kb (primers KG51_2 and 77) and 5 kb (primers KG99 and 74) fragments amplified from pKG12 plasmid DNA using *Q5* Polymerase.

4.2.9.2 *N. crassa* Yeast-2-hybrid constructs

NCU00938 C-terminal tail

The *symC N. crassa* homologue C-terminal yeast-2-hybrid construct (pKG14, **Supplementary Figure 7.21**) was made by Gibson Assembly by recombining an *EcoR*1 and *Nde*I linearized pGBKT7 vector with a 366 bp *NCU00938* gene fragment (primers KG83 and 83) amplified from *N. crassa* genomic DNA using *Q5* polymerase.

4.2.9.3 *E. festucae* Yeast-2-hybrid constructs

SymC C-terminal tail

To construct the *E. festucae* Sym*C* C-terminal (amino acids 206-274) Yeast-2-hybrid construct (pKG24, **Supplementary Figure 7.28**) *EcoR*I and *Pst*I linearized pGBKT7 vector was recombined, via Gibson Assembly, with a 259 bp *symC* fragment amplified from Fl1 *E. festucae* cDNA using *Q5* polymerase and the primer pair KG104 and 105.

GpiA

To construct the *E. festucae* GpiA homologue yeast-2-hybrid construct (pKG25,

Supplementary Figure 7.29) *EcoR*I and *Xho*I linearized pGADT7 vector was recombined, via Gibson Assembly, with a 705 bp full length GpiA fragment amplified from *E. festucae* Fl1 cDNA using *Q5* polymerase and the primer pair KG106 and 107.

ARP3

To construct the *E. festucae* Arp2/3 complex sub-unit 3 yeast-2-hybrid construct (pKG26, **Supplementary Figure 7.30**) *EcoR*I and *Xho*I linearized pGADT7 vector was recombined, via Gibson Assembly, with a 624 bp full length ARP2/3 fragment amplified from *E. festucae* Fl1 cDNA using *Q5* polymerase and the primer pair KG108 and 109.

UthA

To construct the *E. festucae* UthA homologue yeast-2-hybrid construct (pKG27, **Supplementary Figure 7.31**) *EcoR*I and *Xho*I linearized pGADT7 vector was recombined, via Gibson Assembly, with a 1347 bp full length UthA fragment amplified from *E. festucae* Fl1 cDNA using *Q5* polymerase and the primer pair KG110 and 111.

ErgM

To construct the *E. festucae* ErgM homologue yeast-2-hybrid construct (pKG28, **Supplementary Figure 7.32**) *EcoR*I and *Xho*I linearized pGADT7 vector was recombined, via Gibson Assembly, with a 1356 bp full length ErgM fragment amplified from *E. festucae* Fl1 cDNA using Q5 polymerase and the primer pair KG112 and 113.

4.2.10 Fungal transformations

4.2.10.1 *E. festucae* protoplast preparation

Fresh mycelium (1 cm^2) was inoculated into flasks containing 50 mL PD medium and incubated at 22 °C for 4 days at 150 rpm. The mycelium was filtered through nappy liners (Silk brand), washed with Milli-Q water 3x and rinsed in OM buffer (1.2 M $MgSO_4$,10 mM Na_2HPO_4, adjusted to pH 5.8 with 100 mM $NaH_2PO_4.2H_2O$) before being weighed into a new flask. For every 1 g of mycelia 10 mL of filter sterilized Glucanex (10 mg/mL) was added and samples incubated overnight at 22°C at 80-100 rpm. Protoplasts were filtered through nappy liners into a 200 mL Schott bottle and 5 mL aliquots transferred into new 15 mL Falcon tubes and overlaid with 2 mL of ST buffer (0.1 M Tris-HCl (pH 8), 0.6 M Sorbitol). Following centrifugation (4300 rpm, 15 min at 4°C) protoplasts were transferred from the interface into new 15 mL tubes and washed three times with 5 mL of STC buffer (0.05 M Tris-HCl (pH 8), 1 M Sorbitol, 50 mM $CaCl_2$) with the resulting supernatant discarded following centrifugation

(4300 rpm for 5 minutes). The final protoplast pellet was resuspended in 200-500 µL of STC buffer and, using a haemocytometer counting chamber to estimate the number of protoplasts, diluted in STC to a final concentration of 1.25 x 10^8 protoplasts/mL and stored in 80 µL protoplast/ 20 µL 40% (w/v) PEG (40% PEG 4000, 0.05 M Tris-HCL (pH 8), 50 mM $CaCl_2$, 1 M Sorbitol) aliquots at -80°C.

4.2.10.2 *E. festucae* transformations and screening

Following the addition of 2 µL of spermidine, 5 µL of heparin and 3-5 µg of target DNA, protoplasts were incubated on ice for 30 mins. A 40% (w/v) PEG (40% PEG 4000, 0.05 M Tris-HCL (pH.8), 50 mM $CaCl_2$, 1 M Sorbitol) solution (900 µL) was then added and samples incubated for a further 20 mins on ice. Aliquots (100 µL) were then dispensed onto RG agar plates, overlaid with 3.5 mL of RG overlay agar (0.8% w/v agar) and incubated overnight at 22°C. An additional 5 mL of overlay RG agar + selection marker was overlaid and transformants left to grow for 11-14 days. Transformants were nuclear purified on selection media, via three rounds of subculturing, and screened by PCR or for mRFP1 fluorescence.

4.2.10.3 *S. cerevisiae* single yeast-2-hybrid transformations

Yeast transformations and Yeast-2-hybrid screening was carried out using the method outlined by Gietz RD & Woods RA (2002). A single freshly-grown AH109 colony was inoculated into 5 mL of YPD and grown overnight at 30°C at 200 rpm to an OD_{600} of 0.3-0.5. 2.5x 10^8 cells were added to 50 mL YPDA and grown for a further 4-5 h to a final concentration of around 2 x 10^7 cells/mL. Following centrifugation (5 min; 4300 x *g*), pelleted cells were washed with 20 mL sterile H_2O, pelleted again and resuspended in 1 mL of sterile H_2O. Samples (100 µL) were then transferred into new tubes, centrifuged (30 sec; 13,000 x *g*) and the supernatant removed. The transformation mix, 330 µL, (240 µL 50% PEG 3500, 36 µL 1 M LiAc and 10 µL of denatured Salmon Sperm Carrier DNA (10 mg/mL Clontech) and 1.2 µg of each BD and AD yeast-2-hybrid plasmid was added and samples incubated at 42°C for 30 min. Following centrifugation (15 seconds; 4,000 x *g*) the supernatant was removed, cells resuspended in 700 µL of H_2O and 200 µL aliquots plated onto Leu-/Trp- and Leu-/Trp-/Ade-/His- SD plates and plates incubated at 30°C for 3-4 days. Single colonies were transferred into 5 mL of YPD and grown overnight at 30°C at 200 rpm to a similar OD_{600} absorbance. Cells were washed with 2% (w/v) glucose, centrifuged (5 min; 4300 x *g*), resuspended in 5 mL 2% (w/v) glucose and left to grow for a further 5 hours. Serial dilutions of 10^1 to 10^3 were plated onto Leu-/Trp- and Leu-/Trp-/Ade-/His- SD plates and incubated at 30°C for 3-4 days.

4.2.10.4 *S. cerevisiae* library yeast-2-hybrid transformation

The following experimental method was performed by Ulrike Brandt (Braunschweig University). pKG14 was transformed into AH109 as per the Clontech yeast-2-hybrid manual. The resulting yeast strain was cultured in 200 mL of 2x YPD media to a final volume of 4.8 x 10^{10} cells. Cells were pelleted by centrifugation, the resulting supernatant removed and cells resuspended in 1.8 mL of water and 1.8 mL of a previously prepared *N. crassa* cDNA library contained in the yeast strain Y187 (stored at Braunschweig University). Yeast suspensions (100 µL) were spotted onto 38 YPD plates and left to mate overnight. Suspensions were scraped off YPD plates, suspended in 30 mL of water and 150 µL suspensions plated onto SD Leu-/Trp-/His-/Ade- media and cultured for 2 days. Resulting colonies were replica plated using sterile velvet cloths onto SD Leu-/Trp- β-Gal plates and incubated for a further 2 days. A total of 665 blue colonies were PCR screened using the Clontech primers designed to amplify across the pGADT7 cloning cassette. A total of 47 PCR products between 700-1500 bp were selected for sequencing and the yeast-2-hybrid interaction partners identified using BLASTn searches against the *N. crassa* database (http://www.broadinstitute.org/annotation/genome/neurospora/Blast.html).

4.2.11 Microscopy

Cultures to be analysed by microscopy were inoculated onto a thin layer of 1.5% (w/v) water agar layered on top of a glass slide placed on a base layer of 3% (w/v) water agar. Square blocks were cut from the agar and analysed via an Olympus IX71 inverted fluorescence microscope using the filter settings set for capturing mRFP1 fluorescence and DIC images. DIC and mRFP1 images were overlaid with ImageJ software.

4.2.12 Bioinformatics

4.2.12.1 Sequence acquisition

Gene and protein sequences were acquired from the NCBI database found at http://www.ncbi.nlm.nih.gov using a tBLASTn search and the *Neurospora crassa* NCU homologues as a query sequence. *Epichloë festucae* Fl1 homologues were acquired from the University of Kentucky Genome Project at http://www.endophyte.uky.edu using the blast search tools provided.

4.2.12.2 Protein alignment and domain predictions

Signal peptides were predicted using the SignalP 4.1 server located at http://www.cbs.dtu.dk/services/SignalP/ and transmembrane domains predicted using the TMHMM server 2.0 located at http://www.cbs.dtu.dk/services/TMHMM/. All other domains

were predicted using the Prosite and InterProScan tools located at http://prosite.expasy.org and http://www.ebi.ac.uk/Tools/pfa/iprscan/. Protein alignments were constructed using MacVector™ 12.6.0 ClustalW software.

4.3 Results

4.3.1 *E. festucae* SymC C-terminal domain deletion analysis

SymC is predicted to be a four transmembrane domain (TMD) protein, which is highly conserved across other fungi. The C-terminal end of SymC is predicted to be cytoplasmic, suggesting this domain may potentially transmit external signals to initiate cell-cell fusions via an interaction with other membrane bound or membrane-associated proteins (**Figure 4.1A**). To determine whether the C-terminal domain of SymC is required for function, various SymC C-terminal deletion constructs were co-transformed with pSF15.15 (Hph^R) into Δ*symC*#7 and #8 protoplasts, and resulting transformants screened for restoration of cell-cell fusion (**Figure 4.1 B-D**). pKG9 (**Supplementary Figure 7.16**), which contained a deletion of amino acid residues 235-274, restored cell-cell fusion in 19/22 transformants indicating these residues are not essential for cell-cell fusion. In contrast, 29/29 transformants containing pKG10 (**Supplementary Figure 7.17**), containing a deletion of residues 208-274, were fusion negative, suggesting the entire C-terminus is essential. To further analyse the involvement of these residues in regulating cell-cell fusions a truncated construct, with amino acid residues 208-234 deleted (pKG11, **Supplementary Figure 7.18**), was transformed into Δ*symC*#7 protoplasts and 24/24 of the transformants were restored for cell-cell fusion (**Figure 4.1 B-C**). There are two explanations for these apparent contradictory results.

1) Each C-terminal half exhibits redundancy and the functional region spans the entire C-terminus

Or

2) The proximity of the pKG10 deletion to the fourth transmembrane domain of SymC disrupts functional localisation.

To address this, mRFP1 tagged deletion constructs pKG19 (residues 208-234 deleted, **Supplementary Figure 7.22**) and pKG23 (residues 208-274 deleted, **Supplementary Figure 7.25**) were transformed into Δ*symC*#7 protoplasts and found to restore cell-cell fusion (**Figure 4.1 B & D**). These results support explanation two, in that the SymC C-terminus is not essential for fusion.

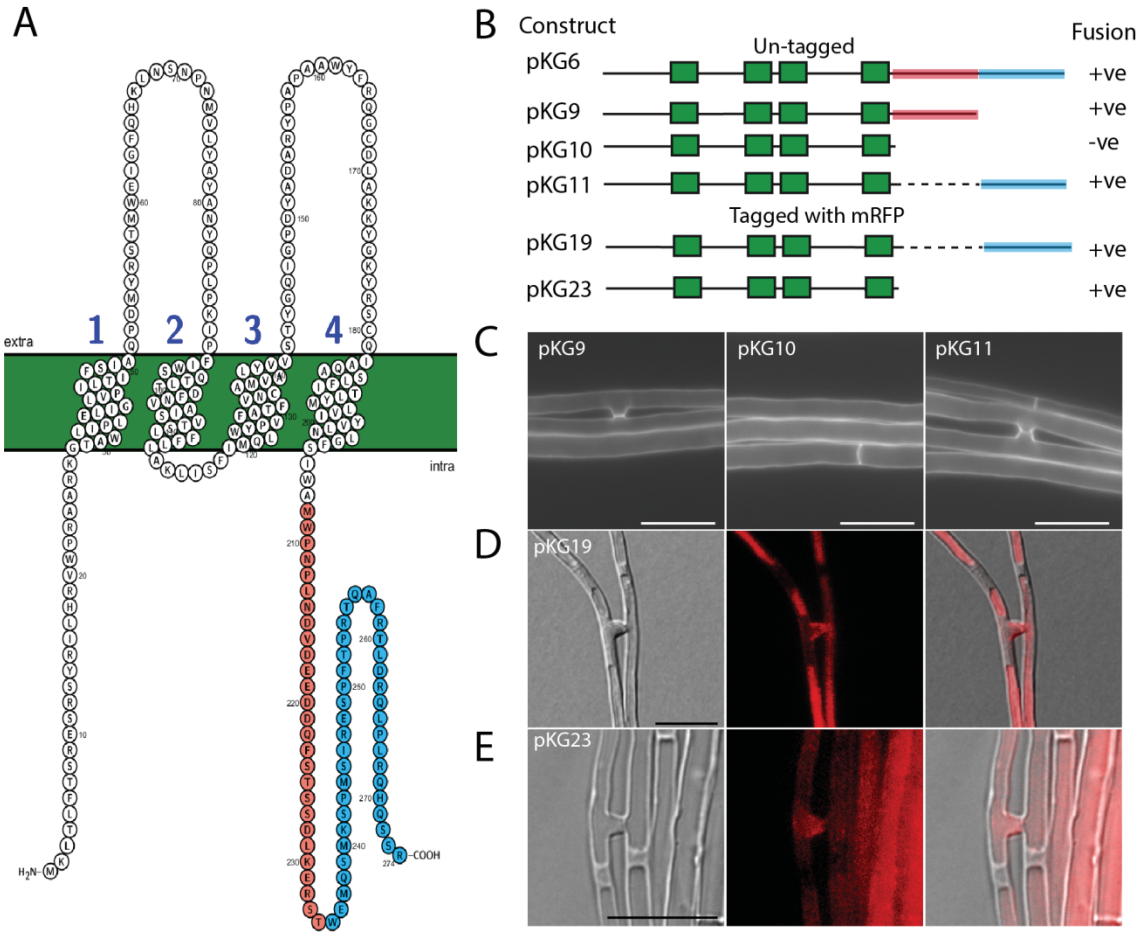

Figure 4.1 *E. festucae* SymC C-terminal domain deletion analysis. A, Predicted SymC membrane topology. Transmembrane domains and deleted amino acids in relation to Section B, are as indicated. **B,** C-terminal deletion constructs transformed into Δ*symC* protoplasts with the resulting cell-cell fusion phenotypes as indicated. **C,** Hyphae of transformants containing pKG9, 10 and 11 constructs stained with Calcofluor white. Bar = 10 μm. **D-E,** Hyphae containing pKG19 and pKG23 mRFP1 tagged constructs. DIC, mRFP1 and merged DIC/mRFP1 images are as shown. Bar = 10 μm.

4.3.2 *Neurospora crassa* Yeast-2-hybrid screening.

Mutant *E. festucae* Δ*symC* strains exhibit pleiotropic defects. Although the SymC C-terminus is not essential for cell-cell fusion this does not discount the possibility that it is involved in regulating other developmental pathways aside from fusion, or that it is a non-essential scaffold region for other communication proteins. To identify potential C-terminal interacting proteins, a yeast-2-hybrid library screen was performed using the SymC *N. crassa* homologue (NCU00938) C-terminal domain as bait against a *N. crassa* yeast-2-hybrid library (pKG14, **Supplementary Figure 7.21**). Additionally, the C-terminus was screened against available *N. crassa* CWI components PKC-1, MIK-1, MEK-1 or MAK-1 and NOX complex components RHO-1, NOR-1 and BEM-1 (**Supplementary Figures 7.33-43**).

When screened against the CWI MAP kinase pathway and Nox complex proteins no interactions were detected, indicating that the C-terminal region of SymC does not signal directly into these pathways via the components tested (**Figure 4.2**). When screened against the *N. crassa* yeast-2-hybrid library nineteen candidates were identified (**Table 4.3**). Thirteen of these, NCU06300, NCU02325, NCU08535, NCU02380, NCU03857, NCU01515 NCU06843, NCU06892, NCU08389, NCU01221, NCU01793, NCU09999 & NCU16635, shaded grey in the table, were not conserved in *E. festucae* or were unlikely to be relevant based on their predicted function, particularly those predicted to be ribosomal or RNA proteins. Six of these, NCU09375, NCU02668, NCU03922, NCU09572, NCU09722 & NCU06509, shaded white in the table, were of potential interest, as they were either membrane-associated, differentially regulated in the *E. festucae* Δ*noxA,* Δ*proA* or Δ*sakA in planta* RNA-seq data set (obtained from Eaton *et al.*, 2015) or were linked to cell-cell fusion, cell wall remodelling or virulence in other organisms (see discussion for more detail). Homologues of four of these in *E. festucae* were sequentially identified via tBLASTn searches and aligned using multiple amino acid sequence alignments.

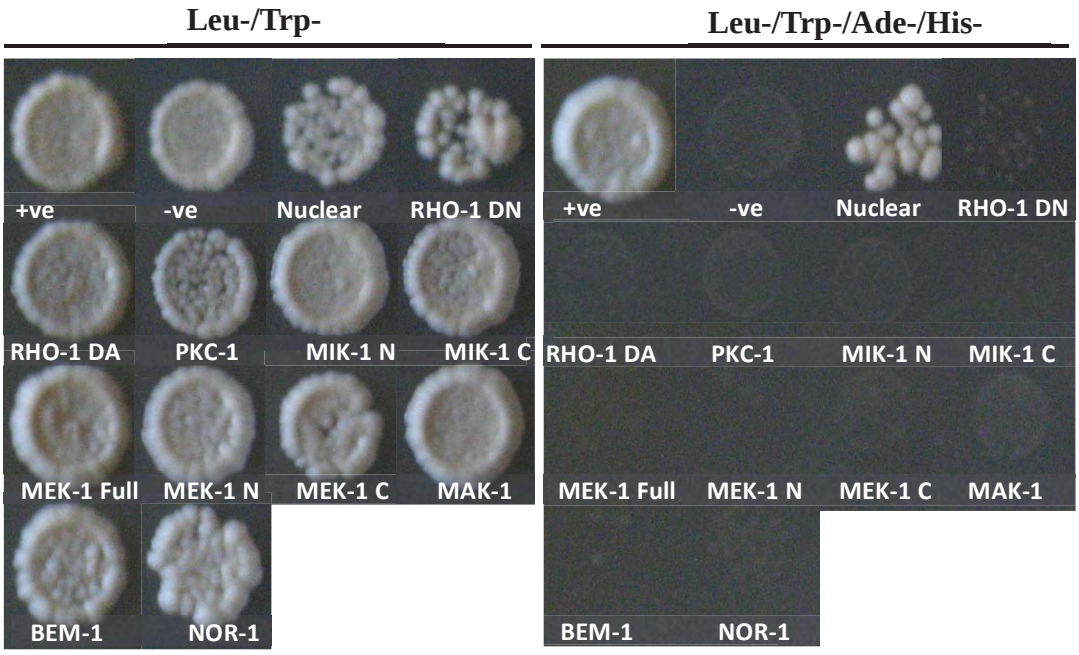

Figure 4.2 *Neurospora crassa* Yeast-2-hybrid analysis. Interaction test using the *Neurospora crassa* SymC C-terminal domain as bait against components of the Cell Wall Integrity MAP kinase and Nox complex pathways. Positive (+ve) pGADT7-T/pGBKT-p53, negative (-ve) pGADT7-T/pGBKT-laminin and nuclear pGAD-RanBPM/pKG14 (SymC C-terminal domain) controls are also shown.

Table 4.3 Yeast-2-hybrid candidates that interact with the *NCU00938* C-terminus

Hits	*NCU #*	*Nc* fusion	*Ef* M3#	Predicted function/homologue	Δ*noxA*	Δ*proA*	Δ*sakA*
1	09375	Yes	3.04621	GPI1 (*Sordaria*)	1.15	1.97	2.39
1	02668	?	3.02343	UTH1 (Septation protein)	1.08	1.49	1.36
1	03922	?	3.03927	ERG-13 (Mevalonate/ ergosterol synthesis)	-1.33	1.18	1.03
1	09572	Reduced in Het	3.02863	ARP2/3 Complex (Actin assembly)	-1.28	1.38	1.51
1	09722	?	3.0026	Hypothetical (Acidic rich C-terminus)	-2.7	1.99	2.27
2	06509	?	3.0072	Hypothetical membrane protein	-1.09	1.22	1.05
1	02325	-	3.02013	Gua 3 GMP synthase	-1.35	1.16	1.01
1	08535	-	3.0454	Acetyl-CoA carboxylase	-1.14	-1.48	1.61
6	02380	-	3.05802	Threonyl t-RNA Synthetase	-1.39	1.05	1.74
1	03857	-	3.16103	Tricarboxylic acid-5	1.13	1.30	1.20
8	06300	-	3.03103	Guanylate Kinase	1.03	1.33	1.06
17	01515	-	3.04386	DNA-directed RNA polymerase II polypeptide	-1.45	1.01	1.57
1	06843	-	3.05757	60S ribosomal protein L3	-1.16	1	1.14
3	06892	-	3.00254	40S rib Prot.	-1.65	1.92	1.74
2	08389	-	3.06486	60S ribosomal protein L20	-1.69	2.02	1.01
1	01221	-	3.01359	60S ribosomal protein L16	-1.27	1.40	1.09
5	01793	-	3.17276	RNA bind Domain Prot	NA	NA	NA
6	09999	-	NA	Hypothetical not conserved	NA	NA	NA
4	16635	-	NA	Not found in *E.festucae*	NA	NA	NA

The *Sordaria macrospora* homologue of NCU09375, GPI1, has been recently characterised as a cysteine-rich, GPI anchored protein which localises to the cell wall and interacts with the STRIPAK complex component MOB3 to suppress fruiting body development (Frey *et al*., 2015a). The *E. festucae* homologue of GPI1, GpiA, encodes a 219 amino acid (aa) protein containing a signal peptide and GPI anchor (**Figure 4.3**). GpiA shares 43% identity with *N. crassa* NCU09375 and 42% identify with *S. macrospora* GPI1 with all cysteine residues conserved. The *E. festucae gpiA* gene (721 bp gene with two 212 & 448 bp exons and one 61 bp intron) is up-regulated *in planta* during Δ*sakA* associations compared to WT.

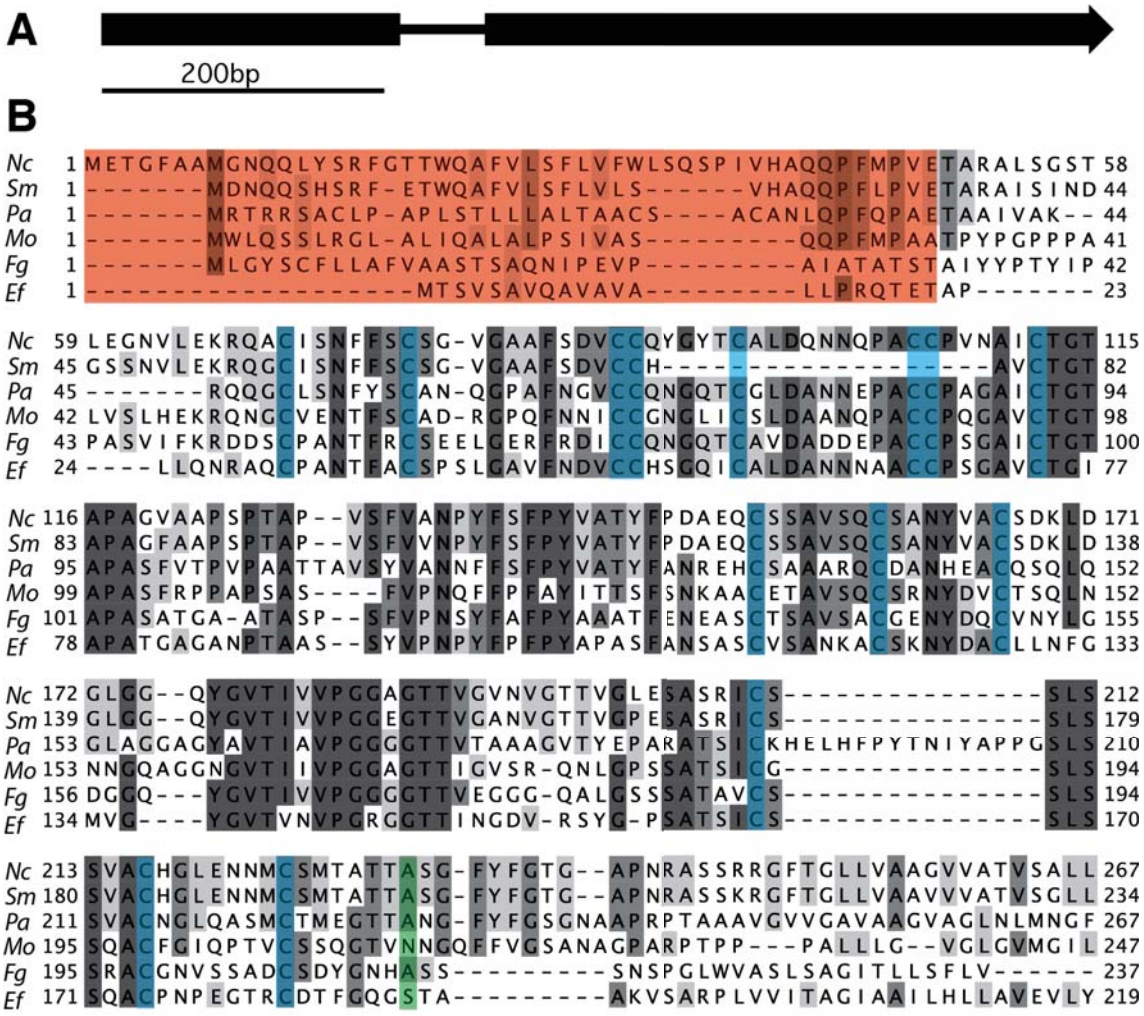

Figure 4.3 ***Epichloë festucae gpiA*** **gene structure and amino acid alignment. A,** Gene structure containing two exons and one intron of 212, 448 and 61 bp respectively. Bar = 200 bp. **B,** ClustalW alignment of amino acid sequences. Gene ID's with associated GenBank protein accession are as shown. *Ef*, *Epichloë festucae* GpiA EfM3.046210; *Fg*, *Fusarium graminearum* FGSG_01368 (XM_011318862); *Nc*, *Neurospora crassa* NCU09375 (XM_958653); *Pa*, *Podospora anserina* Pa_1_14100 (XM_001905079); *Mo*, *Magnaporthe oryzae* MGG_16429 (XM_003710475.1) and *Sm*, *Sordaria macrospora* SMAC_12074/GPI1 (XM_003350887). Predicted signal peptide (orange), conserved cysteine residues (blue) and GPI anchor site (green) are as shown.

The *E. festucae* homologue of NCU02668 (UTH1), UthA, encodes a 439 aa protein with a predicted 21 aa N-terminal signal peptide and C-terminal SUN homology domain (**Figure 4.4**). When aligned UthA shares 60% identity with *N. crassa* NCU02668. The *E. festucae uthA* gene (1405 bp gene with two exons, 1305 & 45 bp, and one intron, 55 bp) was not differentially expressed in the RNA-seq data.

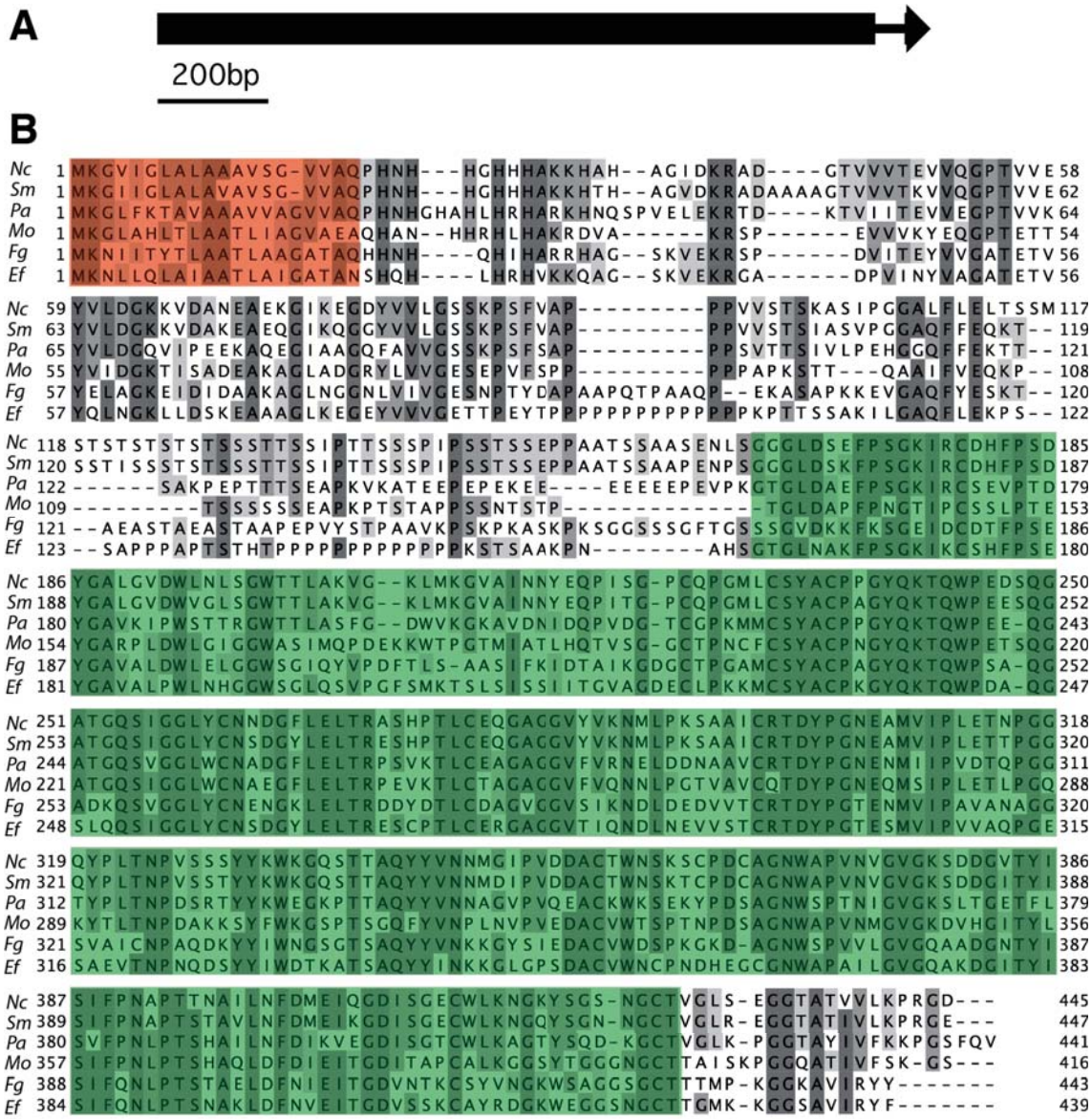

Figure 4.4 *Epichloë festucae uthA* gene structure and amino acid alignment. A, Gene structure containing two exons and one intron of 1305, 45 and 55 bp respectively. Bar = 200 bp. **B,** ClustalW alignment of amino acid sequences. Gene ID's with associated GenBank protein accession are as shown. *Ef*, *Epichloë festucae* UthA EfM3.023430; *Fg*, *Fusarium graminearum* FGSG_01351 (XM_011318840); *Nc*, *Neurospora crassa* NCU02668 (XM_011394696); *Pa*, *Podospora anserina* Pa_1_16850 (XM_001907097); *Mo*, *Magnaporthe oryzae* MGG_00505 (XM_003718506) and *Sm*, *Sordaria macrospora* SMAC_04326 (XM_003350974). Predicted signal peptide (red) and SUN domain (green) are as shown.

The *E. festucae* homologue of NCU03922 (ERG-13), ErgM, encodes a 455 aa protein, containing a HMG-CoA synthase domain which condenses Acetyl-CoA and acetoacetyl-CoA to form HMG-CoA. When aligned ErgM shares 89% identity to *N. crassa* ERG-13 (**Figure 4.5**). The *E. festucae ergM* gene (1758 bp gene containing four exons 60, 103, 1067 & 138 bp and three introns 138, 1208, 110 bp) was not differentially expressed in mutant symbiotic

interactions.

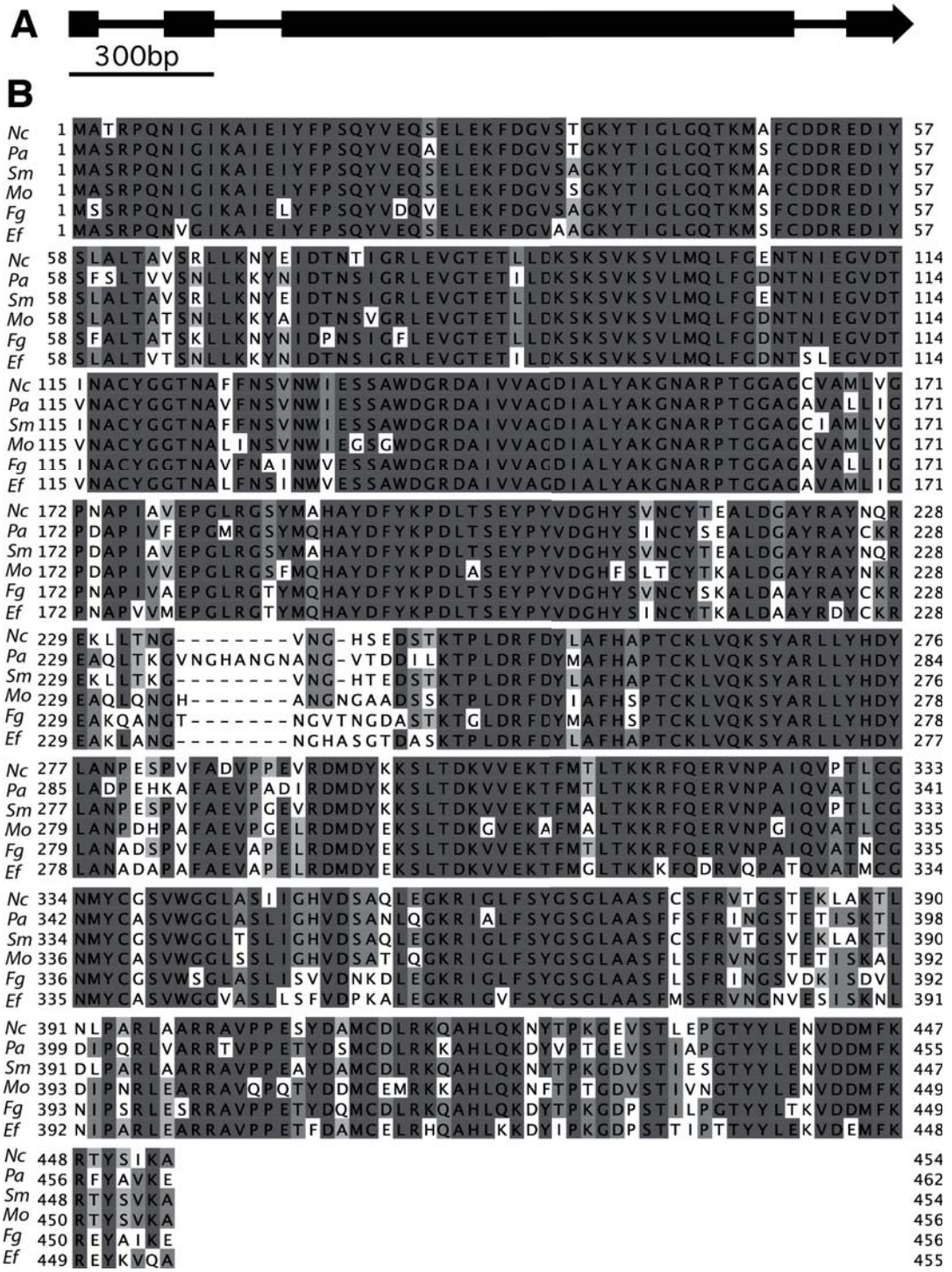

Figure 4.5 ***Epichloë festucae ergM*** **gene structure and amino acid alignment. A,** Gene structure containing four exons and three introns of 60, 103, 1067 and 138 and 55138, 1208, 110 bp respectively. Bar = 300 bp. **B,** ClustalW alignment of amino acid sequences. Gene ID's with associated GenBank protein accession are as shown. *Ef*, *Epichloë festucae* ErgM EfM3.039270; *Fg*, *Fusarium graminearum* FGSG_09266 (XM_011330200); *Nc*, *Neurospora crassa* NCU03922/ERG-13 (XM_952468); *Pa*, *Podospora anserina* Pa_4_8290 (XM_001905964); *Mo*, *Magnaporthe oryzae*

MGG_01026 (XM_003717869) and *Sm*, *Sordaria macrospora* SMAC_06340 (XM_003345891). Predicted HMG-COA synthase domain (grey) is as shown.

The *E. festucae* homologue of NCU09572 encodes a 192aa protein, which shares 87% identity with *N. crassa* NCU09572 and contains a predicted ARP2/3 domain involved in actin assembly (**Figure 4.6**). The *E. festucae arp3* gene (884 bp gene, three exons 6, 396 & 177 bp and two introns 150 & 155 bp) was not differentially expressed in the mutant symbiotic RNA-seq data.

Figure 4.6 *Epichloë festucae arp3* gene structure and amino acid alignment. A, Gene structure containing three exons and two introns of 6, 396 and 177 and 150 and 155 bp respectively. Bar = 200 bp. **B,** ClustalW alignment of amino acid sequences. Gene ID's with associated GenBank protein accession are as shown. *Ef*, *Epichloë festucae* Arp3 EfM3.028630; *Fg*, *Fusarium graminearum* FGSG_11977 (XM_011319120); *Nc*, *Neurospora crassa* NCU09572 (XM_954590); *Pa*, *Podospora anserina* Pa_5_2810 (XM_001904003); *Mo*, *Magnaporthe oryzae* MGG_00307 (XM_003718735) and *Sm*, *Sordaria macrospora* SMAC_05714 (XM_003348571). Predicted ARP2/3 domain (grey) is as shown.

NCU09722 and NCU06509 encode hypothetical *N. crassa* proteins. NCU09722 is significantly down regulated (-2.7) in Δ*noxA* & up-regulated in Δ*sakA* (+2.27) *E. festucae* associations *in planta* (**Table 4.3**). NCU06509 is a hypothetical membrane protein.

4.3.3 *E. festucae* yeast-2-hybrid screening.

To determine whether the predicted *N. crassa* candidates also interact in *E. festucae*, homologues of GPI1 (GpiA), UTH1 (UthA), ERG-13 (Erg-M) and Arp3 were cloned into the yeast-2-hybrid pGADT7 vector and screened against the C-terminal region of SymC, which was cloned into the yeast-2-hybrid vector pGBKT7 (**Supplementary Figures 7.26-32**). All candidates showed positive interactions and did not undergo self-activation, confirming an interaction with the C-terminal tail of SymC in *E. festucae* (**Figure 4.7**). Collectively these results show that the C-terminus of SymC is not essential for cell-cell fusion and that it interacts with GpiA, UthA, ErgM and Arp3.

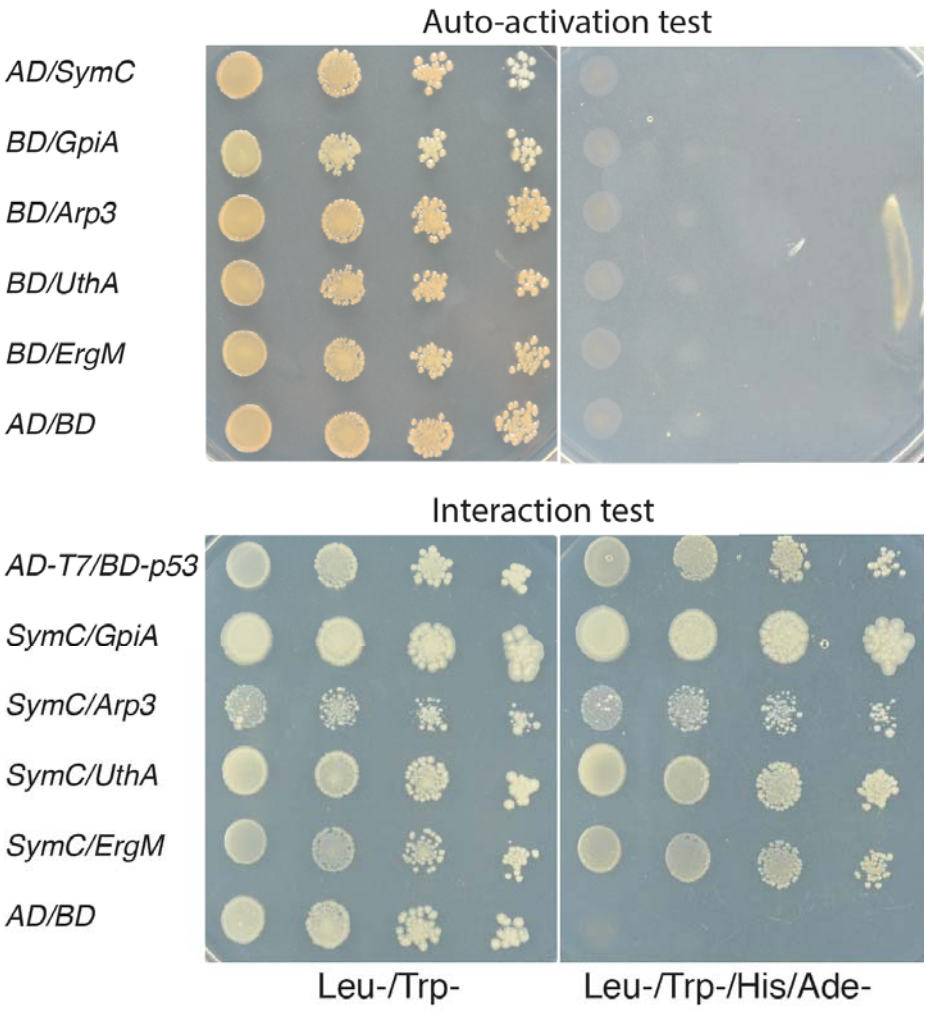

Figure 4.7 Yeast-2-hybrid interaction test using the *E. festucae* SymC C-terminal domain as bait against GpiA, UthA, ErgM and Arp3 homologues. Positive (+ve) pGADT7-T/pGBKT-p53 and negative (-ve) pGADT7/pGBKT7 controls are shown. Undiluted and diluted (10^{-2}, 10^{-3} and 10^{-4}) cultures were spotted onto plates.

4.4 Discussion

4.4.1 The C-terminal region of SymC is not required for cell-cell fusion

SymC is essential for cell-cell fusion and domain analysis of SymC showed that the un-tagged SymCΔ208-274 C-terminal deletion construct, which contains only three residues following TMD4, does not restore cell-cell fusion in Δ*symC* strains, while in comparison the mRFP1-tagged SymCΔ208-274 construct does. These results indicate that several residues either beyond or in close proximity to SymC TMD4 are required for either correct protein localisation or stability, and that overall the C-terminus is not required for cell-cell fusion. Similar findings with respect to the C-terminal domain have been observed in the *Saccharomyces cerevisiae* transmembrane protein Pma1. Deletions of more than nine amino acids after the Pma1 TMD10 resulted in altered protein localisation, indicating that proximal C-terminal residues contribute to Pma1 structure rather than function (Mason *et al.*, 2014). Given the C-terminus of SymC is not required for cell-cell fusion, it would be interesting to further determine whether the N-terminal amino acid residues of SymC and those located between TMD2-3 and TMD3-4 are required for cell-cell fusion and signalling, as these regions were not included in the initial deletion analysis and their function is unknown. Interestingly, homologues of SymC contain two highly conserved cysteine residues located between TMD3 and TMD4. Cysteine residues are often involved in the formation of disulphide bonds and can contribute to protein structure and stability (reviewed, Trivedi, *et al.,* 2009). The presence of disulphide bonds can protect proteins against damage and irreversible inactivation or stabilise protein-protein interactions (reviewed, Poole & Nelson, 2008). They can also be required for correct protein activity by altering the accessibility of residues required for signal activation or repression (reviewed, Trachootham *et al*., 2008). Additionally, as cysteine residues contain thiol groups that can undergo oxidation, cysteines can be important for transducing redox signals (reviewed, Barford *et al.*, 2004). In *P. anserina*, deletion of the two conserved cysteine residues in IDC3 (SymC homologue) results in a loss of IDC3 function, suggesting these cysteines are either important for disulphide bond formation and protein structure, or potentially respond to redox changes and are required for signal transduction (unpublished results, Silar *et al.*,). Given their conserved nature and functional importance in *P. anserina*, the further analysis of SymC cysteine residues is of considerable interest as they may be important for signalling via a currently-undetermined mechanism.

Deletion of *symC* results in pleiotropic phenotypes indicating SymC may be required for multiple developmental pathways. Although the C-terminus of SymC is not essential for cell-cell fusion, it has yet to be determined whether this domain functions as a repression domain, is required for other signalling pathway aside from cell-cell fusion, or acts as a non-

essential scaffolding region. Results from the SymC C-terminal *N. crassa* yeast-2-hybrid library screen identified several proteins NCU09375 (GPI1), NCU02668 (UTH1p), NCU03922 (ERG-13), NCU09572 (ARP2/3), NCU09722 & NCU06509 that may be of considerable further interest as they interact with the C-terminus of SymC.

4.4.2 Identification of proteins that interact with the SymC C-terminus

4.4.2.1 NCU09375 (GpiA): *Sordaria macrospora* GPI1 homologue

The homologue of NCU09375 GPI1 has recently been characterised in *Sordaria macrospora* as a cysteine-rich, GPI anchored protein, which localises to mitochondria and the cell wall/plasma membrane and interacts with the STRIPAK complex component MOB, to suppress fruiting body development (Frey *et al.*, 2015a, **Figure 4.8**). Interestingly, MOB3 does not localise to the cell periphery but can be found within the cytoplasm and mitochondria. The exact nature of MOB3-GPI1 interactions has yet to be determined, however the current hypotheses are that either 1) posttranslational modified portions of MOB3 and GPI1 interact within the cytoplasm or mitochondria and transduce signals required for fruiting body development via the STRIPAK complex or 2) GPI1 interacts with an unidentified plasma membrane or cell wall protein to suppress signals required for fruiting body development. In *E. festucae*, SymC and GpiA show conserved positive yeast-2-hybrid interactions and similar to *S. macrospora* GPI1, SymC localises to the cell periphery, suggesting SymC may be potentially repressed by GPI1 at the cell membrane. However given the nature of yeast-2-hybrid screens, where false positives are often observed, and the lack of further supporting evidence, this hypothesis remains to be tested further. Interestingly, SymC-GpiA interactions may explain why the C-terminus of SymC is dispensable for cell-cell fusion as it would be involved in signal repression rather than signal activation. Additionally, it may explain why Δ*symC* strains show similar phenotypes to the CWI mutants but unaltered MpkA phosphorylation and localisation, as SymC-GpiA-MobC interactions may indirectly affect the CWI pathway via the STRIPAK complex rather than through SymC directly. Furthermore, a SymC-GpiA interaction may explain why *E. festucae* Δ*mobC* mutants fuse, albeit at a reduced frequency, as SymC mediated cell-cell fusion may be independent of MobC, but MobC may be required for downstream positive signal modulations. Given the putative SymC-GpiA interactions and SymC's punctate localisation, it would be interesting to further determine whether SymC localises to mitochondria or co-localises with GpiA, and whether SymC-GpiA-MobC interactions are involved in regulating cell-cell fusions and symbiosis in *E. festucae*.

Figure 4.8 Model summarising the proposed *Sm*GPI1 and *Sm*MOB3 interactions in WT and mutant *S. macrospora* strains. Image taken directly from Frey *et al.*, (2015a). Arrows indicate signal intensity.

4.4.2.2 NCU02668 (UthA): Septation protein Sun4 homologue

Septal pores allow cytoplasmic proteins, nuclei, vesicles and mitochondria to be transported between hyphal compartments divided by a septum (reviewed, Markham, 1994). Organelles known as Woronin bodies regulate and restrict the flow of material through septal pores and localise to septal pores in response to hyphal stress or injury to maintain colony integrity and prevent cytoplasmic leakage (reviewed, Markham & Collinge, 1987). In *N. crassa*, when hyphae of genetically different *het* loci undergo cell-cell fusion septal pores become plugged due to heterokaryotic incompatibility, which often results in localised hyphal death or severe growth inhibition (Glass & Kaneko, 2003). In *N. crassa, B. cinera, M. grisea* and *E. festucae*, several proteins that localise to septa or are associated with septal development, are required for cell-cell fusion, symbiosis and virulence, suggesting common regulatory proteins exist with these developmental pathways. In *M. grisea*, the tetraspanin Pls1 (Clergeot *et al.*, 2007) and the Nox complex protein Nox1 (Egan *et al.*, 2007) are required for pathogenicity. In *N. crassa*, NOX-1, SO and HAM-2 are required for cell-cell fusion (reviewed, Read *et al.,* 2012) and NOX-1, SO and PLS-1 proteins localise to septa (Fleißner *et al.*, 2005 & 2007; Hernández-Galván *et al.*, 2015). In *S. macrospora*, the homologue of HAM-2, PRO22, is required for correct septation (Bloemendal *et al.,* 2010). In *B. cinerea*, Bem1 is required for virulence and cell-cell fusion, localises to septa and interacts with the formin Sep1, essential for virulence and septum formation (Giesbert *et al.*, 2014). In *E. festucae*, SymB, SymC and NoxR localise to septa and SymB, SymC, NoxR, NoxA and So are required for cell-cell fusion and mutualistic associations (Takemoto *et al.*, 2011, Charlton *et al.*, 2012).

The C-terminus of SymC and UthA *E. festucae* and *N. crassa* homologues show positive yeast-2-hybrid interactions and are highly conserved across fungi, suggesting they perform similar functions. In *N. crassa*, *uth1* is up regulated during heterokaryotic incompatibility (Hutchison *et al.*, 2009). In *Aspergillius nidulans*, *sun1,* which contains a SUN domain similar to UTH1, is involved in septation and Δ*sun1* strains form intra-hyphal hyphae and show an increase in the number of Woronin bodies around the septal pore (Gastebois *et al.*, 2013). In *Ustilaginoidea virens*, SUN2, which contains an SUN domain similar to UTH1, is required for virulence (Yu *et al.,* 2015). Given SymC interacts with UthA, localises to septa and that similar proteins to UthA are associated with septation and virulence in other fungi, UthA could be an interesting protein to analyse further in *E. festucae*, as it may have a role regulating septal pore closure following cell-cell fusion and/or symbiosis.

4.4.2.3 NCU03922 (ErgM): Erg-13 homologue

N. crassa NCU03922 (ERG-13) is predicted to encode a HMG-CoA synthase which catalyses the second reaction in the mevalonate-dependent isoprenoid biosynthesis pathway where Acetyl-CoA condenses with acetoacetyl-CoA to form 3-hydroxy-3-methylglutaryl-CoA (HMG-CoA) which is converted into mevalonate. Mevalonate is then required for either ergosterol or siderophore biosynthesis. In *Neurospora*, Δ*erg-13* mutants exhibit hyphal branching defects (Seiler & Plamann, 2003), Δ*erg-2* mutants a loss of cell-cell fusion and Δ*erg10a/b* mutants arrested plasma membrane fusion (unpublished results Fleißner *et al.,*), suggesting that the ergosterol composition strongly influences the assembly of cell-cell communication complexes at the plasma membrane and affects cell-cell fusion. Evidence for this has also been shown in *S. cerevisiae*, where *erg2*, *3*, and *6* mutations inhibit membrane fusion and recruitment of the pheromone response pathway scaffold Ste5 (essential for cell-cell fusion) to the membrane (Jin *et al.*, 2008). In addition to cell-cell fusion, ergosterol and siderophore synthesis have also been implicated in virulence and symbiosis. In *Magnaporthe oryzae*, HMG-CoA synthase (*erg13*) and HMG-CoA reductase (*hmg1*) genes are up-regulated during appresorium formation (Oh *et al.*, 2008) and the deletion of the *F. graminearum* ergosterol synthesis genes, *hmg1, erg-3, erg-5* and *erg-4* (Seong *et al.*, 2006; Liu *et al.*, 2013; Yun *et al.*, 2014), and *A. fumigatus* siderophore biosynthesis genes, *sidA, I, H, F* and *D,* attenuates virulence (Hissen *et al.*, 2005; Yasmin *et al.*, 2011; Leal *et al.*, 2013). In contrast, in *E. festucae* the siderophore synthesis gene *sidN* is required for beneficial symbiotic associations as their deletion results in a switch from mutualism to pathogenicity (Johnson *et al.*, 2007 & 2013). Irrespective of whether the yeast-2-hybrid SymC-ErgM interactions are biologically relevant it would be interesting to study components of the ergosterol synthesis pathway further, as this pathway has yet to be characterised within *Epichloë* endophytes and based on its characterisation in other fungi, likely contributes to cell-cell fusion and pathogenesis.

4.4.2.4 NCU09572 (Arp3): APR2/3 complex subunit 3

The homologue of NCU09572 shows a positive yeast-2-hybrid interaction with the C-terminus of *E. festucae* SymC and is predicted to be part of the ARP2/3 Complex, specifically the ARP2/3 complex subunit 3 involved in actin assembly. Deletions to this complex are reported as being ascospore-lethal in *N. crassa* meaning that many homokaryon mutant ARP2/3 complex phenotypes cannot be studied. However, the ability to generate heterokaryons, where nuclei contain both WT and mutant alleles, has suggested that the ARP2/3 Complex mediates cell fusion events as NCU09572 heterokaryons exhibit significantly lowered CAT fusions compared to WT (Roca *et al.*, 2010). Actin assembly is crucial for multiple developmental pathways and it has be shown that prior to CAT fusion events in *N. crassa*, actin filaments are recruited at the homing hyphal tip during CAT fusion and dissipate when CAT fusion is completed (Berepiki *et al.*, 2010). Regardless of the proposed SymC-Apr3 yeast-2-hybrid interaction a loss of cell-cell fusion and expressoria formation may be related to delocalised actin filaments, and it would be interesting to determine if actin localisation is disrupted in Δ*symC* strains.

In conclusion, the C-terminus of SymC not essential for cell-cell fusion and yeast-2-hybrid analysis showed that this region interacts with GpiA, UthA, ErgM and Arp3.

5 Conclusions and Future Work

5.1 Conclusions

Several key findings have emerged from this research (**Figure 5.1**). 1). The homologue of the STRIPAK complex component MOB3, MobC, is required for *E. festucae – L. perenne* symbiosis. 2). SymB and SymC act down-stream of the transcription factor ProA. 3). SymB and SymC are membrane-associated proteins, suggesting they are part of a receptor complex at the cell periphery. 4). A putative SymC-GpiA interaction was identified which may link SymC to STRIPAK complex signalling. Overall, this study highlights that SymB, SymC and MobC are important for mutualistic *E. festucae – L. perenne* interactions, and are part of a conserved signalling network in filamentous fungi, which regulates cell-cell fusion. The final conclusions and key research findings are summarised below.

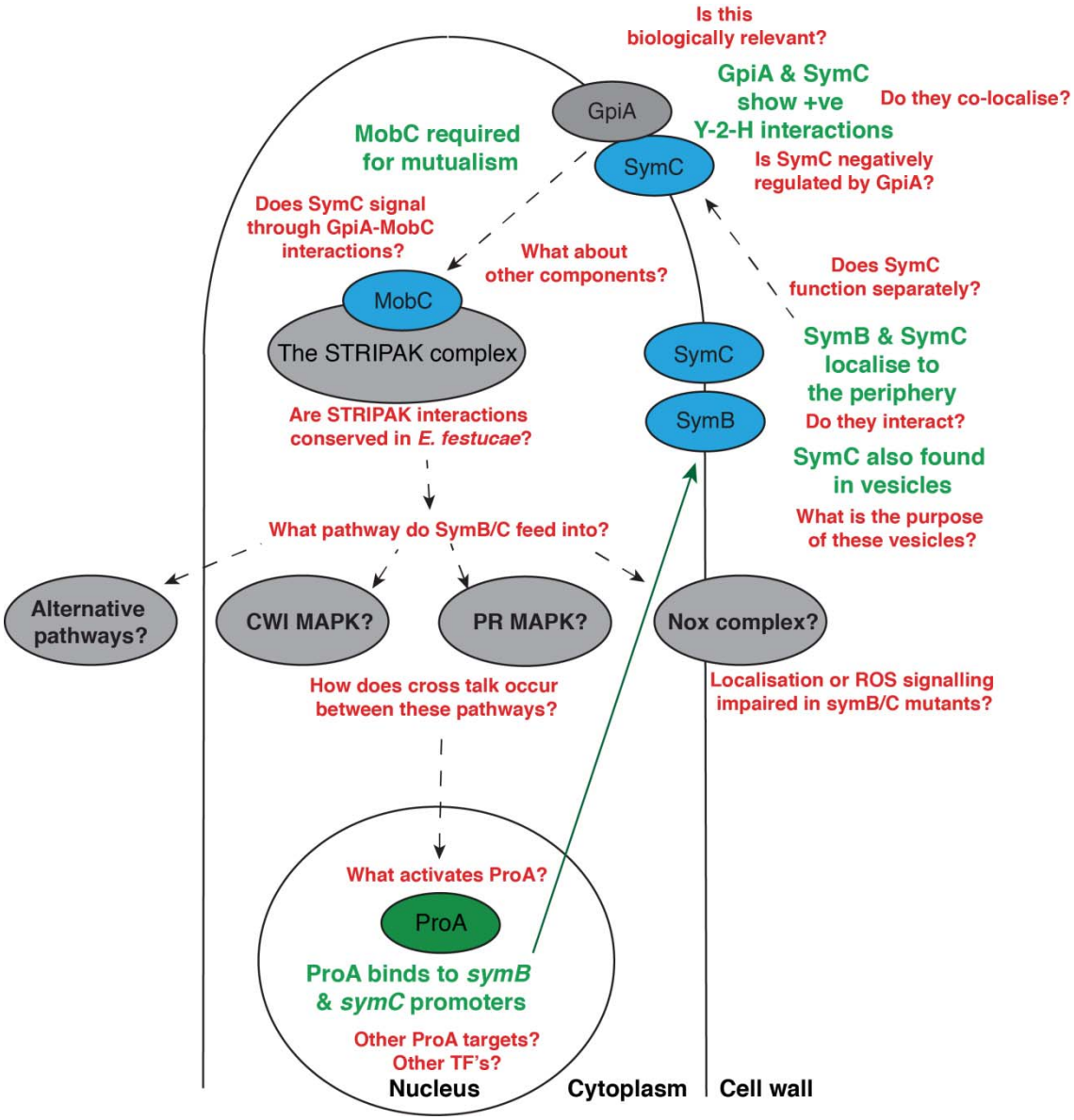

Figure 5.1 Summary of key findings. Key findings have been shown in green and future questions in red.

1. MobC is essential for mutualistic associations and has an accessory role in regulating expressoria formation in planta and cell-cell fusion in culture. STRIPAK complex homologues, including *mobC,* were identified in *E. festucae*. Targeted deletion of *mobC* results in reduced cell-cell fusion, hyper-conidiation and intra-hyphal hyphae formation in culture. Deletion of *mob3* in *S. macrospora* (Bernhards & Pöggler, 2011) and *N. crassa* (Maerz *et al*., 2009; Fu *et al*., 2011) abolishes cell-cell fusion, whereas *E. festucae* Δ*mobC* strains still fuse. These findings highlight that MobC has evolved different regulatory constraints in *E. festucae*, presumably due to different life cycle selection pressures. *In planta,* deletion of *mobC* results in disrupted host associations, prolific hyphal growth, vascular bundle colonisation, sub-cuticular hyphal growth, and reduced expressoria formation. These finding are the first report of the STRIPAK complex component MobC being required for mutualistic associations and expressorium development.

2. SymB and SymC are required for cell-cell fusion, mutualistic associations, expressoria formation and are regulated by the transcription factor ProA. Homologues of SymB and SymC are conserved in filamentous fungi. In Δ*proA* associations, *symB* and *symC* expression is significantly down-regulated (Eaton *et al.,* 2015). Analysis of the *symB* and *symC* promoters identified highly conserved ProA binding sites (Tanaka *et al.,* 2013). ProA binding at these regions was confirmed by gel shift assays. This is the first report that places *symB* and *symC* downstream of ProA. In culture, deletion of *symB* and *symC* abolishes cell-cell fusion and results in hyper-conidiation and intra-hyphal hyphae phenotypes, which is consistent with *IDC2* and *IDC3* in *P. anserina* (Haedens *et al.,* 2005) and *ham-7* in *N. crassa* (Fu *et al.,* 2011; Maddi *et al.,* 2012) being required for cell-cell fusion. *In planta,* deletion of *symB* and *symC* results in a stunted host phenotype, prolific hyphal growth, vascular bundle colonisation, altered cell wall morphology and disrupted expressorium formation. This study is the first to show that SymB and SymC are required for mutualistic associations and expressorium development.

3. SymB and SymC co-localise, suggesting they interact to form a receptor complex at the cell periphery. SymB-GFP and SymC-mRFP1 co-localise at the cell-periphery and septa. Additionally SymC-mRFP1 localises to small vesicles. Although HAM-7 localisation has been reported in *N. crassa* (Fu *et al.,* 2014), this is the first report that shows SymB localisation at the cell periphery and septa, and SymC localisation at the cell periphery, septa and small vesicles, in filamentous fungi. Deletion of *symB* and *symC* has no effect on MpkA and MpkB phosphorylation, or MpkA-GFP and MpkB-GFP localisation and a link between the CWI and PR MAPK pathways was not detected. Yeast-2-hybrid analysis did not detect protein interactions between the C-terminus of SymC, and components of the CWI MAPK pathway or the Nox complex. Whether SymB and SymC interact, and what pathways SymB and SymC feed into, remains to be determined.

4. The C-terminus of SymC interacts with GpiA but it is not essential for cell-cell fusion. Analysis of several deletion constructs showed that the C-terminal region of SymC is not essential for cell-cell fusion. Yeast-2-hybrid analysis showed that the C-terminal region of SymC interacts with GpiA, the homologue of the *S. macrospora* STRIPAK complex associated protein GPI1 (Frey *et al.,* 2015a). This is the first report to show that SymC may be negatively regulated by GpiA and linked to STRIPAK complex signalling.

5.2 Future work

Although the main research aims of this thesis have been addressed, these findings raise several new questions that may be of particular interest to pursue further.

5.2.1 Identification of upstream ProA signalling and further ProA targets

Signals that regulate ProA activity are unknown and a large number of genes down-regulated in Δ*proA* associations encode unknown proteins (Eaton *et al.,* 2015). These genes are of considerable interest as they may be regulated by the transcription factor ProA and encode novel signalling components that contribute to cell-cell fusion and mutualism. As shown for *symB* and *symC* promoters, determining whether the promoters of these genes contain predictive ProA binding sites is something to look at in future. Additionally, as it is not known which pathway acts upstream to ProA, proteins that interact with ProA and mutants that show altered *proA* expression are of importance, as their identification may help place ProA downstream of a signalling cascade. Whether *proA* is differentially expressed in Δ*noxA,* Δ*mpkA*, Δ*idcA,* Δ*mpkB* mutants, and whether ProA functions downstream to Nox complex, CWI or PR MAPK signalling, or an alternative signalling pathway, is an important research question.

5.2.2 The involvement of SymB and SymC in a signalling pathway

In culture and *in planta* Δ*symB* and Δ*symC* strains show similar phenotypes to the Nox complex (reviewed by Scott, 2015), CWI (Becker *et al.,* 2015) and the PR scaffold MAP kinase (Eaton *et al.,* 2013) mutants, but no clear link to either of these pathways has been established. ROS production was not analysed in Δ*symB* and Δ*symC* strains, and whether this is impaired, and whether SymB and SymC are involved in regulating Nox complex signalling, remains to be determined. RNA-seq analysis of individual Δ*symB*, Δ*symC*, Δ*mpkA*, Δ*idcA* and Δ*mpkB* mutants would provide further information as to which pathways SymB and SymC feed into, particularly if the Nox complex, CWI or PR MAP kinase genes are differentially expressed in Δ*symB* and Δ*symC* cultures, or if similar genes are differentially expressed in Δ*symB*, Δ*symC*, Δ*mpkA*, Δ*idcA* and Δ*mpkB* mutants. When combined with the existing data sets for Δ*noxA*, Δ*proA* and Δ*sakA* mutants (Eaton *et al.,* 2015), this analysis would provide new information on

two very important MAPK pathways, required for cell-cell fusion and symbiosis, where RNA-seq data is not available. This will be of considerable interest to future studies involving the characterisation of novel genes.

SymB and SymC co-localise at the cell periphery and determining if they interact and form a receptor complex is of considerable importance. When testing for SymB-SymC interactions, yeast-2-hybrid experiments may be limited, as this technique does not work well for membrane-associated proteins (McAlister-Henn *et al.,* 1999). Co-immunoprecipitation experiments may also be limited, as the SymC-mRFP1 signal is weak at the cell periphery and the majority of the protein is within vacuoles. This suggests that a high level of SymC-mRFP1 degradation occurs and that obtaining enough full length SymC protein to show an interaction between SymC and SymB may be difficult. Another approach could be to use Tandem affinity purification (TAP) coupled with mass spectrometry, a method that successfully identified proteins which interacted with the membrane-associated STRIPAK complex protein PRO22 (Bloemendal *et al*., 2012). However this approach could still be problematic for SymC interactions, given the observed degradation of SymC-mRFP1, and if SymB or SymC interactions are weak they may not be detected at low levels. SymC shows positive yeast-2-hybrid interactions with GpiA, the homologue of the *S. macrospora* STRIPAK complex associated repressor protein GPI1 (Frey *et al.,* 2015a). SymC-GpiA interactions could be something to pursue further as they would explain why the C-terminus of SymC is not essential for cell-cell fusion and potentially link SymC to STRIPAK complex signalling.

5.2.3 Further characterisation of the STRIPAK complex

The core STRIPAK complex components are essential for cell-cell fusion in *N. crassa* and *S. macrospora* (reviewed Kück *et al.,* 2016) whereas in *E. festucae*, MobC is only partially required. The signals required for STRIPAK complex activation, recruitment of STRIPAK signalling proteins and how the STRIPAK complex transduces signals from and between the PR and CWI pathway, are not fully understood. The further generation and analysis of STRIPAK complex deletion strains would provide insight as to whether *E. festucae pro11* and *pro22* homologues are essential for cell-cell fusion, while MobC and additional STRIPAK proteins collectively modulate signal progressions.

5.2.4 Expressoria formation in *E. festucae*

The recent study on Δ*noxA*, Δ*noxB*, Δ*noxA/B* and Δ*noxR* mutants (Becker *et al*., 2016), and the combined analysis of Δ*symB*, Δ*symC* and Δ*mobC* mutants, has shown that cell-cell fusion defects are often linked with altered *E. festucae* expressorium formation. Given the novelty of this structure, the further characterisation of genes involved in appressoria

development and how they relate to *E. festucae* expressoria development is an exciting research area, and further research is required to determine how expressoria form *in planta*. Similar to work performed in *Magnaporthe oryzae* on appressoria development (Dagdas *et al*., 2012; Ryder *et al*., 2013), it would be interesting to determine how actin filaments assemble during *E. festucae* expressoria pore formation, via the introduction of a Life-Act fluorescent reporter, and whether or not actin assembly is disrupted in Δ*symB* and Δ*symC* strains. Determining where NoxA, NoxR, SymB and SymC localise and which proteins are recruited during expressoria pore formation, and whether Δ*idcA*, Δ*proA*, Δ*mpkA* and Δ*mkkA* mutants form expressoria, would provide further insight as to which signalling pathways are required for expressoria formation.

5.2.5 The ergosterol synthesis pathway in *E. festucae*

The ergosterol synthesis pathway has been implicated in cell-cell fusion, pathogenicity, and recruitment of signalling components to the membrane (unpublished results Fleißner *et al.*,; Jin *et al.*, 2008; Seong *et al.*, 2006; Liu *et al.*, 2013; Yun *et al.*, 2014). Given its role in other organisms, it would be interesting to determine whether components of the ergosterol pathway are required for cell-cell fusion and mutualistic *E. festucae* associations via targeted gene deletions.

5.2.6 Cell-cell fusion: a culture phenotype for symbiosis mutant screening

Mutagenesis screening for symbiosis mutants has previously been performed in *E. festucae*. This method can take upwards of two months before inoculated hosts are ready to be analysed. A number of mutants initially identified this way, specifically *noxA*, *proA* and *mkkA*, are defective in cell-cell fusion (Tanaka *et al.,* 2006 & 2013; Becker *et al.,* 2015). Interestingly, a mutant defective in cell-cell fusion that retains asymptomatic associations has never been characterised in *E. festucae,* suggesting cell-cell fusion and symbiosis phenotypes are interconnected. Cell-cell fusion phenotypes may therefore help predict whether a mutant will display disrupted symbiosis, prior to its inoculation into plants, and facilitate accelerated mutagenesis screening. Given the complexity of cell signalling cascades, it is likely that several components required for cell-cell fusion have not been identified in filamentous fungi. Further *E. festucae* mutagenesis screening may help identify new components required for cell-cell fusion as well as novel symbiosis genes.

6 References

The references contained in this section include only those that appear in chapters 1, 4 and 5. Those related to the MobC (chapter 3) and SymB and SymC (chapter 4) manuscripts have been included within the references lists associated with these sections.

Aldabbous, M. S., Roca, M. G., Stout, A., Huang, I. C., Read, N. D. & Free, S. J. (2010) The *ham-5*, *rcm-1* and *rco-1* genes regulate hyphal fusion in *Neurospora crassa*. *Microbiology,* **156,** 2621-2629.

Anderson, J. P., Gleason, C. A., Foley, R. C., Thrall, P. H., Burdon, J. B., & Singh, K. B. (2010) Plants versus pathogens: an evolutionary arms race. *Funct Plant Biol,* **37(6),** 499-512.

Aguirre, J., Ríos-Momberg, M., Hewitt, D., & Hansberg, W. (2005) Reactive oxygen species and development in microbial eukaryotes. *Trends Microbiol* **13,** 111–118.

Baillat, G., Moqrich, A., Castets, F., Baude, A., Bailly, Y., Benmerah, A., & Monneron, A. (2001) Molecular cloning and characterization of phocein, a protein found from the Golgi complex to dendritic spines. *Mol Biol Cell,* **12,** 663-673.

Barford, D. (2004). The role of cysteine residues as redox-sensitive regulatory switches. *Current Opinion in Structural Biology,* **14(6),** 679–686.

Becker, M., Becker, Y., Green, K. & Scott, B. (2016) The endophytic symbiont *Epichloë festucae* establishes an epiphyllous net on the surface of *Lolium perenne* leaves by development of an expressorium, an appressorium-like leaf exit structure. *New Phytol.,* **211,** 240-254.

Becker, Y., Eaton, C. J., Brasell, E., May, K. J., Becker, M., Hassing, B., *et al.* (2015) The fungal cell wall integrity MAPK cascade is crucial for hyphal network formation and maintenance of restrictive growth of *Epichloë festucae* in symbiosis with *Lolium perenne*. *Mol. Plant-Microbe Interact,* **28,** 69-85.

Berepiki, A., Lichius, A., Shoji, J.-Y., Tilsner, J., & Read, N. D. (2010) F-Actin Dynamics in *Neurospora crassa*. *Eukaryotic Cell*, ***9*(4),** 547-557.

Bernhards, Y. & Pöggeler, S. (2011) The phocein homologue SmMOB3 is essential for vegetative cell fusion and sexual development in the filamentous ascomycete *Sordaria macrospora*. *Curr. Genet.,* **57,** 133-149.

Bloemendal, S., Lord, K. M., Rech, C., Hoff, B., Engh, I., Read, N. D., *et al.* (2010) A mutant defective in sexual development produces aseptate ascogonia. *Eukaryot. Cell,* **9,** 1856-1866.

Bloemendal, S., Bernhards, Y., Bartho, K., Dettmann, A., Voigt, O., Teichert, I., *et al.* (2012) A homologue of the human STRIPAK complex controls sexual development in fungi. *Mol. Microbiol.,* **84,** 310-323.

Boyce, K. J., Hynes, M. J., Andrianopoulos, A. (2003) Control of morphogenesis and actin localization by the *Penicillium marneffei* RAC homolog. *J Cell Sci* **116,** 1249–1260.

Breitenbach, M., Weber, M., Rinnerthaler, M., Karl, T. & Breitenbach-Koller, L., (2015) Oxidative stress in fungi: Its function in signal transduction, interaction with plant hosts, and lignocellulose degradation. *Biomolecules,* **5,** 318-342.

Brun, S., Malagnac, F., Bidard, F., Lalucque, H., & Silar, P. (2009) Functions and regulation of the Nox family in the filamentous fungus *Podospora anserina*: a new role in cellulose degradation. *Molecular Microbiology*, **74(2),** 480-496.

Cano-Domınguez, N., Alvarez-Delfin, K., Hansberg, W., & Aguirre, J. (2008) NADPH oxidases NOX-1 and NOX-2 require the regulatory subunit NOR-1 to control cell differentiation and growth in *Neurospora crassa. Eukaryotic Cell, **7,*** 1352-1361.

Charlton, N. D., Shoji, J. Y., Ghimire, S. R., Nakashima, J. & Craven, K. D. (2012) Deletion of the fungal gene *soft* disrupts mutualistic symbiosis between the grass endophyte *Epichloë festucae* and the host plant. *Eukaryot. Cell*, **11(12),** 1463-1471.

Chen, C., & Dickman, M. B. (2004). Dominant active Rac and dominant negative Rac revert the dominant active Ras phenotype in *Colletotrichum trifolii* by distinct signalling pathways. *Mol. Microbiol.* **51,** 1493–1507

Chen, J., Zheng, W., Zheng, S., Zhang, D., Sang, W., Chen, X., *et al.* (2008) Rac1 is required for pathogenicity and Chm1-dependent conidiogenesis in rice fungal pathogen *Magnaporthe grisea*. *Plos Pathogens*, **4(11),** doi: e1000202.

Chisholm, S. T., Coaker, G., Day, B., & Staskawicz, B. J. (2006) Host-microbe interactions: shaping the evolution of the plant immune response. *Cell, **124,*** 803-814.

Christensen, M. J., Ball, O. J.-P., Bennett, R. J. and Schardl, C. L. (1997) Fungal and host genotype effects on compatibility and vascular colonisation by *Epichloë festucae*. *Mycol. Res.*, **101,** 493-501.

Christensen, M. J., Bennett, R. J. & Schmid, J. (2002) Growth of *Epichloë*/*Neotyphodium* and p-endophytes in leaves of *Lolium* and *Festuca* grasses. *Mycol. Res.*, **106,** 93-106.

Christensen, M. J., Bennett, R. J., Ansari, H. A., Koga, H., Johnson, R. D., Bryan, G. T., *et al.* (2008) *Epichloë* endophytes grow by intercalary hyphal extension in elongating grass leaves. *Fungal Genet. Biol.*, **45,** 84-93.

Chujo, T., & Scott, B. (2014) Histone H3K9 and H3K27 methylation regulates fungal alkaloid biosynthesis in a fungal endophyte–plant symbiosis. *Molecular Microbiology*, **90(2),** 413–434.

Clay, K. & Schardl, C. (2002) Evolutionary origins and ecological consequences of endophyte symbiosis with grasses. *Amer. Naturalist*, **160,** S99-S127.

Clergeot, P. H., Gourgues, M., Cots, J., Laurans, F., Latorse, M.-P., Pepin, R., *et al.* (2007) PLS1, a gene encoding a tetraspanin-like protein, is required for penetration of rice leaf by the fungal pathogen *Magnaporthe grisea*. *PNAS*, **98(2),** 6963-6968.

Colot, H. V., Park, G., Turner, G. E., Ringelberg, C., Crew, C. M., Litvinkova, L., *et al.* (2006) A high-throughput gene knockout procedure for *Neurospora* reveals functions for multiple transcription factors. *Proc. Natl. Acad. Sci. USA*, **103,** 10352-10357.

Coppin, E., Debuchy, R., S. Arnaise, & Picard, M. (1997) Mating types and sexual development in filamentous ascomycetes. *Microbiology and Molecular Biology Reviews*, **61,** 411-428.

Dagdas, Y. F., Yoshino, K., Dagdas, G., Ryder, L. S., Bielska, E., Steinberg, G., & Talbot, N. J. (2012) Septin-mediated plant cell invasion by the rice blast fungus, *Magnaporthe oryzae*. *Science*, **336,** 1590-1595.

Dettmann, A., Illgen, J., Marz, S., Schurg, T., Fleißner, A., & Seiler, S. (2012) The NDR Kinase Scaffold HYM1/MO25 is essential for MAK2 MAP Kinase signaling in *Neurospora crassa*. *Plos Genetics,* **8(9),** e1002950.

Dettmann, A., Heilig, Y., Ludwig, S., Schmitt, K., Illgen, J., Fleißner, A., *et al.* (2013) HAM-2 and HAM-3 are central for the assembly of the *Neurospora* STRIPAK complex at the nuclear envelope and regulate nuclear accumulation of the MAP kinase MAK-1 in a MAK-2-dependent manner. *Mol. Microbiol.,* **90,** 796-812.

Dettmann, A., Heilig, Y., Valerius, O., Ludwig, S. & Seiler, S. (2014) Fungal Communication Requires the MAK-2 Pathway Elements STE-20 and RAS-2, the NRC-1 Adapter STE-50 and the MAP Kinase Scaffold HAM-5. *PLoS Genet*, **10,** e1004762.

Dirschnabel, D.E., Nowrousian, M., Cano-Domínguez, N., Aguirre, J., Teichert, I., & Kück, U. (2014) New insights into the roles of NADPH oxidases in sexual development and ascospore germination in *Sordaria macrospora*. *Genetics,* **196,** 729–744.

Dupont, P.-Y., Eaton, C. J., Wargent, J. J., Fechtner, S., Solomon, P., Schmid, J., *et al.* (2015) Fungal endophyte infection of ryegrass reprograms host metabolism and alters development. *New Phytologist,* **208,** 1227–1240.

Eaton, C. J., Cox, M. P., Ambrose, B., Becker, M., Hesse, U., Schardl, C. L., *et al.* (2010) Disruption of signaling in a fungal-grass symbiosis leads to pathogenesis. *Plant Physiol.,* **153,** 1780-1794.

Eaton, C., Mitic, M., & Scott, B. (2012). Signalling in the *Epichloe festucae*: Perennial ryegrass mutualistic symbiotic interaction. *Signaling and Communication in Plants, 11*.

Eaton, C. J., Staerkel, C., & Scott, B. (2013) Role of the cell fusion gene *idcA* in fungal mutualism. *27th Fungal Genetics Conference*.

Eaton, C. J., Dupont, P.-Y., Solomon, P. S., Clayton, W., Scott, B. & Cox, M. P. (2015) A core gene set describes the molecular basis of mutualism and antagonism in *Epichloë* species. *Mol. Plant-Microbe Interact,* **28,** 218-231.

Egan, M. J., Wang, Z.-Y., Jones, M. A., Smirnoff, N., & Talbot, N. J. (2007) Generation of reactive oxygen species by fungal NADPH oxidases is required for rice blast disease. *PNAS,* **104(28),** 11772-11777.

Engh, I., Wurtz, C., Witzel-Schlomp, K., Zhang, H. Y., Hoff, B., Minou Nowrousian, *et al.* (2007) The WW domain protein PRO40 is required for fungal fertility and associates with Woronin Bodies. . *Eukaryotic Cell,* **6(5)**, 831-843.

Engh, I., Nowrousian, M. & Kück, U. (2010) *Sordaria macrospora*, a model organism to study fungal cellular development. *Eur J Cell Biol,* **89,** 864-872.

Fleißner, A., Sarkar, S., Jacobson, D. J., Roca, M. G., Read, N. D., & Glass, N. L. (2005) The so locus is required for vegetative cell fusion and postfertilization events in *Neurospora crassa*. *Eukaryot. Cell, 5,* 920-930.

Fleißner, A. &Glass, N. L. (2007) SO, a protein involved in hyphal fusion in *Neurospora crassa*, localizes to septal plugs. *Eukaryot. Cell,* **6,** 84-94.

Fleißner, A., Leeder, A. C., Roca, M. G., Read, N. D. & Glass, N. L. (2009) Oscillatory recruitment of signaling proteins to cell tips promotes coordinated behavior during cell fusion. *Proc. Natl. Acad. Sci. USA,* **106,** 19387-19392.

Fleißner, A. (2015). *Cell-cell communication and fusion in Neurospora crassa.* Paper presented at the 28th Fungal Genetics Conference, Asilomar, Pacific Grove, CA.

Frey, S., Lahmann, Y., Hartmann, T., Seiler, S. & Pöggeler, S. (2015a) Deletion of Smgpi1 encoding a GPI-anchored protein suppresses sterility of the STRIPAK mutant Δ*Smmob3* in the filamentous ascomycete *Sordaria macrospora*. *Mol. Microbiol.,* **97,** 676-697.

Frey, S., Reschka, E. J. & Pöggeler, S. (2015b) Germinal center kinases SmKIN3 and SmKIN24 are associated with the *Sordaria macrospora* Striatin-Interacting Phosphatase and Kinase (STRIPAK) complex. *PLoS One,* **10,** e0139163.

Fu, C., Iyer, P., Herkal, A., Abdullah, J., Stout, A. & Free, S. J. (2011) Identification and characterization of genes required for cell-to-cell fusion in *Neurospora crassa*. *Eukaryot. Cell,* **10,** 1100-1109.

Fu, C., Ao, J., Dettmann, A., Seiler, S. & Free, S. J. (2014) Characterization of the *Neurospora crassa* Cell Fusion Proteins, HAM-6, HAM-7, HAM-8, HAM-9, HAM-10, AMPH-1 and WHI-2. *PLoS One,* **9,** e107773.

Gastebois, A., Aimanianda, V., Bachellier-Bassi, S., Nesseir, A., Firon, A., Beauvais, A., *et al.* (2013) SUN-proteins belong to a novel family of b-(1,3)-glucan modifying enzymes involved in fungal morphogenesis. *Journal of Biological Chemistry,* **288(19),** 13387-13396.

Gentile, A., Rossi, M. S., Cabral, D., Craven, K. D., & Schardl, C. L. (2005). Origin, divergence, and phylogeny of *Epichloë* endophytes of native Argentine grasses. *Molecular Phylogenetics and Evolution*, ***35*(1)**, 196–208.

Gibson, D. G., Young, L., Chuang, R. Y., Venter, J. C., Hutchison, C. A., III & Smith, H. O. (2009) Enzymatic assembly of DNA molecules up to several hundred kilobases. *Nat Methods,* **6,** 343-345.

Giesbert, S., Siegmund, U., Schumacher, J., Kokkelink, L., & Tudzynski, P. (2014) Functional analysis of BcBem1 and its interaction partners in *Botrytis cinerea*: impact on differentiation and virulence. *PLoS ONE,* **9(5),** e95172.

Gietz, R. D. &Woods, R. A. (2002) Transformation of yeast by lithium acetate/single-stranded carrier DNA/polyethylene glycol method. *Meth. Enzymol.,* **350,** 87-96.

Glass, N. L., & Kaneko, I. (2003) Fatal attraction: Nonself recognition and heterokaryon incompatibility in filamentous fungi. *Eukaryotic Cell,* **2(1),** 1-8.

Goryachev, A. B., Lichius, A., Wright, G. D., & Read, N. D. (2012) Excitable behavior can explain the ‘‘ping-pong’’ mode of communication between cells using the same chemoattractant. *Bioessays,* **34,** 259–266.

Haedens, V., Malagnac, F. & Silar, P. (2005) Genetic control of an epigenetic cell degeneration syndrome in *Podospora anserina*. *Fungal Genet. Biol.,* **42,** 564-577.

Hamel, L.-P., Nicole, M.-C., Duplessis, S., & Ellis, B. E. (2012) Mitogen-Activated Protein Kinase signaling in plant-interacting fungi: Distinct messages from conserved messengers. *The Plant Cell*, **24,** 1327-1351.

Herrmann, A., Tillmann, B. A. M., Schuermann, J., Boelker, M., & Tudzynski, P. (2014) Small-GTPase-associated signaling by the guanine nucleotide exchange factors CpDock180 and CpCdc24, the GTPase effector CpSte20, and the scaffold protein CpBem1 in C*laviceps purpurea. Eukaryotic Cell,* **13(4),** 470-482.

Hernández-Galván, M., Cano-Domínguez, N., Robledo-Briones, A., Castro-Longoria, E., Lichius, A., & Aguirre, J. (2015). *The tetraspanin PLS-1 is required for NOX-1 and NOX-2 functions in cell fusion, cell growth and differentiation in the fungus Neurospora crassa.* Presented at the 28th Fungal Genetics Conference, Asilomar, Pacific Grove, CA.

Hissen, A. H. T., Wan, A. N. C., Warwa, M. L., Pinto, L. J., & Moore, M. M. (2005). The *Aspergillus fumigatus* siderophore biosynthetic gene *sidA*, encoding L-ornithine N5-oxygenase, is required for virulence. *Infection and Immunity,* **73(9),** 5493-5503.

Hock, B., Bahn, M., Walk, R.-A., & Nitschke, U. (1978). The control of fruiting body formation in the ascomycete *Sordaria macrospora* by regulation of hyphal development. *Planta,* **141(1),** 93-103.

Hutchison, E., Brown, S., Tian, C., & Glass, N. L. (2009) Transcriptional profiling and functional analysis of heterokaryon incompatibility in *Neurospora crassa* reveals that reactive oxygen species, but not metacaspases, are associated with programmed cell death. *Microbiology,* **155(Pt 1-2),** 3957-3970.

Jamet-Vierny, C., Debuchy, R., Prigent, M. & Silar, P. (2007) *IDC1*, a pezizomycotina-specific gene that belongs to the PaMpk1 MAP kinase transduction cascade of the filamentous fungus *Podospora anserina*. *Fungal Genet. Biol.,* **44,** 1219-1230.

Jin, H., McCaffery, J. M., & Grote, E. (2008) Ergosterol promotes pheromone signaling and plasma membrane fusion in mating yeast. *The Journal of Cell Biology*, **180(4),** 813-826.

Johnson, L. J., Steringa, M., Koulman, A., Christensen, M., Johnson, R. D., Voisey, C. R., . *et al.* (2007) *Biosynthesis of an extracellular siderophore is essential for maintenance of mutualistic endophyte-grass symbioses*. Paper presented at the New Zealand Grassland Association: Endophyte Symposium, NZ.

Johnson, L. J., Koulman, A., Christensen, M., Lane, G. A., Fraser, K., Forester, N., *et al.* (2013) An extracellular siderophore is required to maintain the mutualistic interaction of *Epichloë festucae* with *Lolium perenne*. *PLoS Pathog,* **9,** e1003332.

Jonkers, W., Leeder, A. C., Ansong, C., Wang, Y., Yang, F., Starr, T. L., *et al.* (2014) HAM-5 Functions As a MAP Kinase Scaffold during Cell Fusion in Neurospora crassa. *PLoS Genet,* **10,** e1004783.

Kayano, Y., Tanaka, A., Akano, F., Scott, B. & Takemoto, D. (2013) Differential roles of NADPH oxidases and associated regulators in polarized growth, conidiation and hyphal fusion in the symbiotic fungus *Epichloë festucae*. *Fungal Genet. Biol.,* **56,** 87-97.

Kicka, S. & Silar, P. (2004) PaASK1, a mitogen-activated protein kinase kinase kinase that controls cell degeneration and cell differentiation in *Podospora anserina*. *Genetics,* **166,** 1241-1252.

Kicka, S., Bonnet, C., Sobering, A. K., Ganesan, L. P. & Silar, P. (2006) A mitotically inheritable unit containing a MAP kinase module. *Proc. Natl. Acad. Sci. USA,* **103,** 13445-13450.

Kim, H., & Borkovich, K. A. (2004). A pheromone receptor gene, pre-1, is essential for mating type-specific directional growth and fusion of trichogynes and female fertility in *Neurospora crassa*. *Mol Microbiol, 52*(6), 1781-1798.

Kogel, K.-H., Franken, P., & Huckelhoven, R. (2006) Endophyte or parasite – what decides? *Current Opinion in Plant Biology, **9,*** 358-363.

Kokkelink L, Minz A, Al-Masri M, Giesbert S, Barakat R, *et al.* (2011) The small GTPase BcCdc42 affects nuclear division, germination and virulence of the gray mold fungus *Botrytis cinerea*. Fungal Genet Biol **48,** 1012–1019.

Kück, U., Pöggeler, S., Nowrousian, M., Nolting, N., Engh, I., (2009) *Sordaria macrospora*, a model system for fungal development. In: Anke, T., Weber, D. (Eds.), *The Mycota XV, Physiology and Genetics.* Springer, Berlin/Heidelberg, pp. 17–39.

Kück, U., Beier, A. M. & Teichert, I. (2016) The composition and function of the striatin-interacting phosphatases and kinases (STRIPAK) complex in fungi. *Fungal Genet. Biol.,* **90,** 31-38.

Kuldau, G., & Bacon, C. (2008). Clavicipitaceous endophytes: Their ability to enhance resistance of grasses to multiple stresses. *Biological Control,* **46(1),** 57–71.

Lacaze, I., Lalucque, H., Siegmund, U., Silar, P. & Brun, S. (2014) Identification of NoxD/Pro41 as the homologue of the p22phox NADPH oxidase subunit in fungi. *Mol. Microbiol.,* **95,** 1006-1024.

Lalucque, H., Malagnac, F., Brun, S., Kicka, S. & Silar, P. (2012) A non-Mendelian MAPK-generated hereditary unit controlled by a second MAPK pathway in *Podospora anserina*. *Genetics,* **191,** 419-433.

Lalucque, H., & Silar, P. (2003) NADPH oxidase: an enzyme for multicellularity? *Trends Microbiol,* **11**, 9–12.

Lambou, K., Malagnac, F., Barbisan, C., Tharreau, D., Lebrun, M.-H., & Silar, P. (2008) The crucial role of the Pls1 Tetraspanin during ascospore germination in *Podospora anserina* provides an example of the convergent evolution of morphogenetic processes in fungal plant pathogens and saprobes. *Eukaryotic Cell, **7*****(10),*** 1809–1818.

Lara-Ortiz, T., Riveros-Rosas, H., & Aguirre, J. (2003) Reactive oxygen species generated by microbial NADPH oxidase NoxA regulate sexual development in *Aspergillus nidulans*. *Molecular Microbiology,* **50(4),** 1241-1255.

Leeder, A. C., Jonkers, W., Li, J., & Glass, N. L. (2013) Early colony establishment in Neurospora crassa requires a MAP kinase regulatory network. *Genetics,* **195(5),** 883-898.

Leal, S. M. J., Roy, S., Vareechon, C., Carrion, S., Clark, H., Lopez-Berges, M., *et al.* (2013) Targeting iron acquisition blocks infection with the fungal pathogens *Aspergillus fumigatus* and *Fusarium oxysporum*. *Plos Pathogens,* **9(7),** e1003436.

Li, D., Bobrowicz, P., Wilkinson, H. H., & Ebbole, D. J. (2005) A mitogen-activated protein kinase pathway essential for mating and contributing to vegetative growth in *Neurospora crassa*. *Genetics* **170,** 1091–1104.

Lichius, A., (2010). Cell fusion in *Neurospora crassa*. Ph.D thesis, University of Edinburgh, Edinburgh, UK.

Lichius, A., Lord, K. M., Jeffree, C. E., Oborny, R., Boonyarungsrit, P., & Read, N. D. (2012). Importance of MAP Kinases during protoperithecial morphogenesis in *Neurospora crassa*. *PLoS ONE, **7(8),*** e42565.

Lichius, A., & Lord, K. M. (2014) Chemoattractive mechanisms in filamentous fungi. *The Open Mycology Journal,* **8,** 28-57.

Liu, X., Jiang, J., Yin, Y., & Ma, Z. (2013) Involvement of FgERG4 in ergosterol biosynthesis, vegetative differentiation and virulence in *Fusarium graminearum*. *Mol Plant Pathol,* **14(1),** 71-83.

Lord, K. M., & Read, N. D. (2011) Perithecium morphogenesis in *Sordaria macrospora*. *Fungal Genetics and Biology*, **48,** 388-399.

Lukito, Y., Chujo, T., & Scot, B. (2015) Molecular and cellular analysis of the pH response transcription factor PacC in the fungal symbiont *Epichloë festucae*. *Fungal Genetics and Biology,* **85,** 25–37.

Maddi, A., Dettman, A., Fu, C., Seiler, S. & Free, S. J. (2012) WSC-1 and HAM-7 are MAK-1 MAP kinase pathway sensors required for cell wall integrity and hyphal fusion in Neurospora crassa. *PLoS One,* **7,** e42374.

Maerz, S., Dettmann, A., Ziv, C., Liu, Y., Valerius, O., Yarden, O., *et al.* (2009) Two NDR kinase-MOB complexes function as distinct modules during septum formation and tip extension in *Neurospora crassa*. *Mol. Microbiol.,* **74,** 707-723.

Malagnac, F., Lalucque, H., Lepère, G. & Silar, P. (2004) Two NADPH oxidase isoforms are required for sexual reproduction and ascospore germination in the filamentous fungus *Podospora anserina*. *Fungal Genet. Biol.,* **41,** 982-997.

Markham, P. (1994) Occlusions of septal pores in filamentous fungi. Mycol. Res, **98(10),** 1089-1106.

Markham, P., & Collinge, A. J. (1987) Woronin bodies of filamentous fungi. *FEMS Microbiology Reviews,* **46,** 1-11.

Masloff, S., Pöggeler, S. & Kück, U. (1999) The pro1(+) gene from *Sordaria macrospora* encodes a C6 zinc finger transcription factor required for fruiting body development. *Genetics,* **152,** 191-199.

Masloff, S., Jacobsen, S., Poggeler, S., & Kück, U. (2002) Functional analysis of the C6 zinc finger gene pro1 involved in fungal sexual development. *Fungal Genetics and Biology*, **36,** 107-116.

Mason, A. B., Allen, K. E., & Slayman, C. W. (2014) C-terminal truncations of the *Saccharomyces cerevisiae* PMA1 H+-ATPase have major impacts on protein conformation, trafficking, quality control, and function. *Eukaryot Cell, **13*(1),** 43-52.

Mahlet, M., Leveleki, L., Hlubek, A., Sandrock, B., Bölker, M. (2006) Rac1 and Cdc42 regulate hyphal growth and cytokinesis in the dimorphic fungus *Ustilago maydis. Mol Microbiol,* **59,** 567–578.

Mayrhofer, S., Weber, J. M., & Pöggeler, S. (2006) Pheromones and pheromone receptors are required for proper sexual development in the homothallic Ascomycete *Sordaria macrospora*. *Genetics*, **172,** 1521–1533.

McAlister-Henn, L., Gibson, N., & Panisko, E. (1999) Applications of the Yeast Two-Hybrid System. *Methods,* **19,** 330-337.

Moy M, Belanger F, Duncan R, Freehof A, Leary C, Meyer W, *et al,*. (2000). Identification of epiphyllous mycelial nets on leaves of grasses infected by clavicipitaceous endophytes. *Symbiosis* **28**, 291–302.

Nordzieke, S., Zobel, T., Fränzel, B., Wolters, D. A., Kück, U. & Teichert, I. (2015) A fungal sarcolemmal membrane-associated protein (SLMAP) homolog plays a fundamental role in development and localizes to the nuclear envelope, endoplasmic reticulum, and mitochondria. *Eukaryot. Cell*, **14,** 345-358.

Nowrousian, M., Frank, S., Koers, S., Strauch, P., Weitner, T., Ringelberg, C., *et al.* (2007) The novel ER membrane protein PRO41 is essential for sexual development in the filamentous fungus *Sordaria macrospora*. *Mol. Microbiol.*, **64,** 923-937.

Oh, Y., Donofrio, N., Pan, H., Coughlan, S., Brown, D. E., Meng, S., *et al.* (2008) Transcriptome analysis reveals new insight into appressorium formation and function in the rice blast fungus *Magnaporthe oryzae*. *Genome Biology,* **9(5),** Article R85.

Ozaki, Y., Tanaka, A., kameoka, S., Okamura, A., Kayano, Y., Saikia, S., ***et al.,*** (2015) Identification and characterization of a nuclear protein, NsiA, essential for hyphal fusion and symbiotic infection of endophytic fungus *Epichloë festucae*. *28th Fungal Genetics Conference*.

Pandey, A., Roca, M. G., Read, N. D., & Glass, N. L. (2004) Role of a Mitogen-Activated Protein Kinase pathway during conidial germination and hyphal fusion in *Neurospora crassa*. *Eukaryot. Cell, **3*****(2),*** 348-358.

Poole, L. B., & Nelson, K. J. (2008) Discovering mechanisms of signaling-mediated cysteine oxidation. *Current Opinion in Chemical Biology*, **12(1),** 18-24.

Pöggeler, S. & Kück, U. (2004) A WD40 repeat protein regulates fungal cell differentiation and can be replaced functionally by the mammalian homologue striatin. *Eukaryot. Cell,* **3,** 232-240.

Read, N. D., Lichius, A., Shoji, J., & Goryachev, A. B. (2009) Self-signalling and self fusion in filamentous fungi. . *Current Opinion in Microbiology*, **12,** 608-615.

Read, N. D., Goryachev, A. B. & Lichius, A. (2012) The mechanistic basis of self-fusion between conidial anastomosis tubes during fungal colony initiation. *Fungal Biology Reviews,* **26,** 1-11.

Rispail, N., D. M. Soanes, C. Ant, R. Czajkowski, A. Grunler *et al.*, (2009) Comparative genomics of MAP kinase and calcium-calcineurin signalling components in plant and human pathogenic fungi. *Fungal Genet. Biol*, **46,** 287–298.

Roca, M. G., Arlt, J., Jeffree, C. E. & Read, N. D. (2005) Cell biology of conidial anastomosis tubes in *Neurospora crassa*. *Eukaryot. Cell,* **4,** 911-919.

Roca, M. G., Kuo, H.-C., Lichius, A., Freitag, M., & Read, N. D. (2010) Nuclear dynamics, mitosis, and the cytoskeleton during the early stages of colony initiation in *Neurospora crassa. Eukaryot Cell,* **9(8),** 1171-1183.

Roca, M. G., Weichert, M., Siegmund, U., Tudzynski, P., & Fleißner, A. (2012) Germling fusion via conidial anastomosis tubes in the grey mould *Botrytis cinerea* requires NADPH oxidase activity. *Fungal Biology*, **116,** 379-387.

Rolke Y, Tudzynski P. (2008) The small GTPase Rac and the p21-activated kinase Cla4 in *Claviceps purpurea*: interaction and impact on polarity, development and pathogenicity. *Mol Microbiol* **68,** 405–423.

Ryder, L. S., Dagdas, Y. F., Mentlak, T. A., Kershaw, M. J., Thornton, C. R., Schuster, M., *et al.* (2013) NADPH oxidases regulate septin-mediated cytoskeletal remodeling during plant infection by the rice blast fungus. *Proceedings of the National Academy of Sciences of the United States of America*, **110(8),** 3179-3184.

Schardl, C. L. (1996) *Epichloë* species: fungal symbionts of grasses. *Annu. Rev. Phytopathol.,* **34,** 109-130.

Schardl, C. L., & Clay, K. (1997) Evolution of mutualistic endophytes from plant pathogens (Vol. 5B). Heidelberg: Springer Berlin Heidelberg.

Schardl, C. L. (2001) *Epichloë festucae* and related mutualistic symbionts of grasses. *Fungal Genet. Biol.,* **33,** 69-82.

Schardl, C. L. (Ed.). (2002) *Symbiotic parasites and mutualistic pathogens*: Springer Science.

Schardl, C. L., Grossman, R. B, Nagabhyru, P, Faulkner, J. R., Mallik, U. P. (2007) Loline alkaloids: Currencies of mutualism. *Phytochemistry*, **68(7)**, 980-96.

Schardl, C. L., Young, C. A., Pan, J., Florea, S., Takach, J. E., Panaccione, D. G., *et al.* (2013a). Currencies of mutualisms: Sources of alkaloid genes in vertically transmitted Epichloae. *Toxins*, **5(6),** 1064–1088.

Schardl, C. L., Young, C. A., Hesse, U., Amyotte, S. G., Andreeva, K., Calie, P. J., *et al.* (2013b) Plant-symbiotic fungi as chemical engineers: Multigenome analysis of the Clavicipitaceae reveals dynamics of alkaloid loci. *Plos Genetics*, **9(2),** e1003323.

Schürg, T., Brandt, U., Adis, C. & Fleißner A. (2012) The Saccharomyces cerevisiae BEM1 homologue in *Neurospora crassa* promotes co-ordinated cell behaviour resulting in cell fusion. *Mol Microbiol*. **86(2),** 349-66.

Scott, B., & Eaton, C. (2008) Role of reactive oxygen species in fungal cellular differentiations. *Current Opinion in Microbiology*, **11,** 488-493.

Scott, B., Becker, Y., Becker, M. & Cartwright, G. (2012) Morphogenesis, growth and development of the grass symbiont *Epichloë festucae*. In: *Morphogenesis and Pathogenicity in Fungi.* (Martin, J. P. and Di Pietro, A., eds.). Heidelberg: Springer-Verlag, pp. 243-264.

Scott, B. (2015) Conservation of fungal and animal nicotinamide adenine dinucleotide phosphate oxidase complexes. *Molecular Microbiology,* **95(6),** 910-913.

Schürg, T., Brandt, U., Adis, C., & Fleißner, A. (2012) The Saccharomyces cerevisiae BEM1 homologue in Neurospora crassa promotes co-ordinated cell behaviour resulting in cell fusion. *Molecular Microbiology*, **86(2),** 349-366.

Segmüller, N., Kokkelink, L., Giesbert, S., Odinius, D., van Kan, J., & Tudzynski, P. (2008). NADPH Oxidases are involved in differentiation and pathogenicity in Botrytis cinerea. *Molecular Plant-Microbe Interactions, 21*(6), 808-819. doi: 10.1094/mpmi-21-6-0808

Seiler, S., & Plamann, M. (2003) The genetic basis of cellular morphogenesis in the filamentous fungus *Neurospora crassa*. *Mol Biol Cell,* **14(11),** 4352-4364.

Seiler, S., Vogt, N., Ziv, C., Gorovits, R., & Yarden, O. (2006) The STE20/germinal center kinase POD6 interacts with the NDR Kinase COT1 and is involved in polar tip extension in *Neurospora crassa*. *Molecular Biology of the Cell,* **17,** 4080-4092.

Seong, K., Li, L., Hou, Z., Tracy, M., Kistler, H. C., & Xu, J. R. (2006) Cryptic promoter activity in the coding region of the HMG-CoA reductase gene in *Fusarium graminearum*. *Fungal Genetics and Biology*, **43(1),** 34-41.

Shoji, J.-y., Charlton, N. D., Yi, M., Young, C. A., & Craven, K. D. (2015). Vegetative hyphal fusion and subsequent nuclear behavior in *Epichloë* grass endophytes. *Plos One, **10*(4)**, e0121875.

Siegmund, U., Heller, J., van Kan, J. A. L., & Tudzynski, P. (2013) The NADPH Oxidase Complexes in *Botrytis cinerea*: Evidence for a close association with the ER and the Tetraspanin Pls1. *Plos One,* **8(2).** doi: e55879.

Siegmund, U., Marschall, R. & Tudzynski, P. (2014) BcNoxD, a putative ER protein, is a new component of the NADPH oxidase complex in *Botrytis cinerea*. *Mol. Microbiol.,* **95,** 988-1005.

Silar, P., Haedens, V., Rossignol, M. & Lalucque, H. (1999) Propagation of a novel cytoplasmic, infectious and deleterious determinant is controlled by translational accuracy in *Podospora anserina*. *Genetics,* **151,** 87-95.

Silar, P., Lalucque, H., & Vierny, C. (2001) Cell degeneration in the model system *Podospora anserina. Biogerontology*, **2,** 1–17.

Silar, P., Lalucque, H., Malagnac, F., Grognet, P., & Tong, L. C. H. (2015) *Two new redox signaling proteins from Podospora anserina.* Paper presented at the 28th Fungal Genetics Conference, Asilomar, Pacific Grove CA.

Simonin, A. R., Rasmussen, C. G., Yang, M. & Glass, N. L. (2010) Genes encoding a striatin-like protein (*ham-3*) and a forkhead associated protein (*ham-4*) are required for hyphal fusion in *Neurospora crassa*. *Fungal Genet. Biol.,* **47,** 855-868.

Tan, Y. Y., Spiering, M. J., Scott, V., Lane, G. A., Christensen, M. J. & Schmid, J. (2001) In planta regulation of extension of an endophytic fungus and maintenance of high metabolic rates in its mycelium in the absence of apical extension. *Appl. Environ. Microbiol.,* **67,** 5377-5383.

Takemoto, D., Tanaka, A. & Scott, B. (2006) A $p67^{Phox}$-like regulator is recruited to control hyphal branching in a fungal-grass mutualistic symbiosis. *Plant Cell,* **18,** 2807-2821.

Takemoto, D., Tanaka, A., & Scott, B. (2007) NADPH oxidases in fungi: Diverse roles of reactive oxygen species in fungal cellular differentiation. *Fungal Genetics and Biology*, **44(11),** 1065-1076.

Takemoto, D., Kamakura, S., Saikia, S., Becker, Y., Wrenn, R., Tanaka, A., *et al.* (2011) Polarity proteins Bem1 and Cdc24 are components of the filamentous fungal NADPH oxidase complex. *Proc. Natl. Acad. Sci. USA,* **108,** 2861-2866.

Takemoto, D., & Kayano, Y. (2015) Two closely related Rho GTPases, Cdc42 and RacA, have opposite roles for the ROS production and symbiotic infection of endophytic fungus *Epichloë festucae*. *28th Fungal Genetics Conference*, **67**.

Tanaka, A., Christensen, M. J., Takemoto, D., Park, P. & Scott, B. (2006) Reactive oxygen species play a role in regulating a fungus-perennial ryegrass mutualistic association. *Plant Cell*, **18,** 1052-1066.

Tanaka, A., Takemoto, D., Hyon, G. S., Park, P. & Scott, B. (2008) NoxA activation by the small GTPase RacA is required to maintain a mutualistic symbiotic association between *Epichloë festucae* and perennial ryegrass. *Mol. Microbiol.*, **68,** 1165-1178.

Tanaka, A., Cartwright, G. M., Saikia, S., Kayano, Y., Takemoto, D., Kato, M., *et al.* (2013) ProA, a transcriptional regulator of fungal fruiting body development, regulates leaf hyphal network development in the *Epichloë festucae-Lolium perenne* symbiosis. *Mol. Microbiol.*, **90,** 551-568.

Teichert, I., Steffens, E. K., Schnass, N., Franzel, B., Krisp, C., Wolters, D. A., *et al.* (2014) PRO40 is a scaffold protein of the cell wall integrity pathway, linking the MAP kinase module to the upstream activator protein kinase C. *PLoS Genet*, **10,** e1004582.

Tong, L. C., Silar, P. & Lalucque, H. (2014) Genetic control of anastomosis in *Podospora anserina*. *Fungal Genet. Biol.*, **70,** 94-103.

Trachootham, D., Lu, W., Ogasawara, M. A., Valle, N. R.-D., & Huang, P. (2008) Redox regulation of cell survival. *Antioxid Redox Signal*, **10(8),** 1343-1374.

Trivedi, M. V., Laurence, J. S., & Siahaan, T. J. (2009) The role of thiols and disulfides in protein chemical and physical stability. *Curr Protein Pept Sci*, **10(6),** 614-625.

Wang, C.-L., Shim, W. B. & Shaw, B. D. (2010) *Aspergillus nidulans* striatin (StrA) mediates sexual development and localizes to the endoplasmic reticulum. *Fungal Genet. Biol.*, **47,** 789-799.

Wang, C.-L., Shim, W. B. & Shaw, B. D. (2016) The *Colletotrichum graminicola* striatin ortholog Str1 is necessary for anastomosis and is a virulence factor. *Mol Plant Pathol*, DOI: 10.1111/mpp.12339.

Weinzierl, G., Leveleki, L., Hassel, A., Kost, G., Wanner, G., &Bolker, M. (2002) Regulation of cell separation in the dimorphic fungus *Ustilago maydis*. *Mol. Microbiol.* **45,** 219–231.

Yamamura, Y. & Shim, W. B. (2008) The coiled-coil protein-binding motif in *Fusarium verticillioides* Fsr1 is essential for maize stalk rot virulence. *Microbiology*, **154,** 1637-1645.

Yan, K., Yanling, J., Kunran, Z., Hui, W., Huimin, M., & Zhiwei, W. (2011). A new *Epichloë* species with interspecific hybrid origins from Poa pratensis ssp. pratensis in Liyang, China. *Mycologia* **(103),** 1341–1350.

Yasmin, S., Alcazar-Fuoli, L., Gründlinger, M., Puempel, T., Cairns, T., Blatzer, M., *et al.* (2011) Mevalonate governs interdependency of ergosterol and siderophore biosyntheses in the fungal pathogen *Aspergillus fumigatus*. *PNAS*, **109(8),** E497–E504.

Yu, M., Yu, J., Hu, J., Huang, L., Wang, Y., Yin, X., *et al.* (2015) Identification of pathogenicity-related genes in the rice pathogen *Ustilaginoidea virens* through random insertional mutagenesis. *Fungal Genet. Biol.*, **76,** 10-19.

Yun, Y., Yin, D., Dawood, D. H., Liu, X., Chen, Y., & Maa, Z. (2014) Functional characterization of *Fg*ERG3 and *Fg*ERG5 associated with ergosterol biosynthesis, vegetative differentiation and virulence of *Fusarium graminearum*. *Fungal Genet. Biol.*, **68,** 60-70.

7 Appendicies

Figure 7.1 pRS426 vector

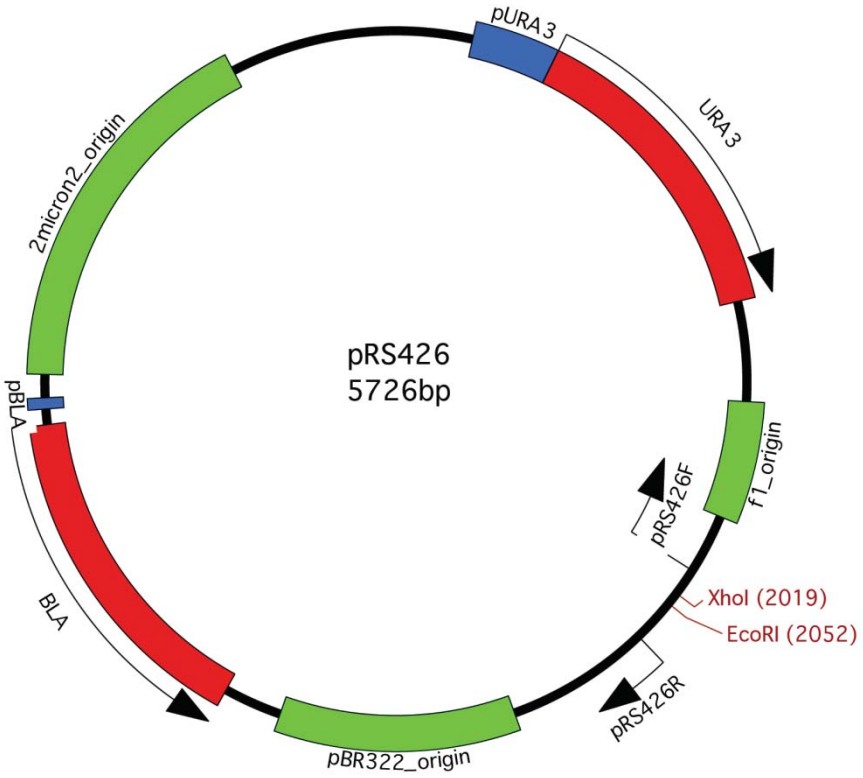

Figure 7.2 pSF15.15 vector

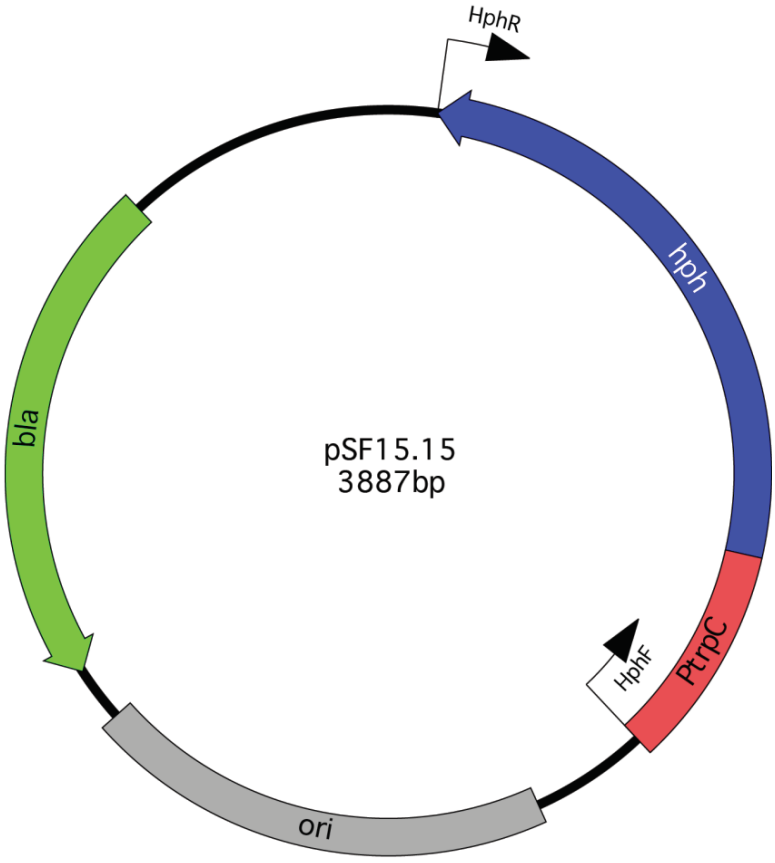

Figure 7.3 pII99 vector

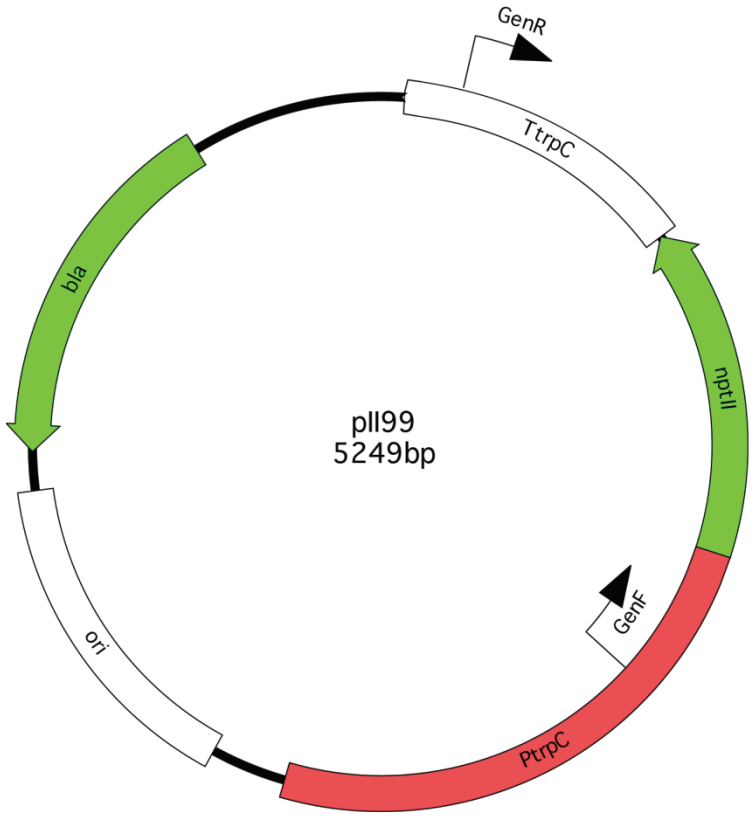

Figure 7.4 pCR4-Topo®

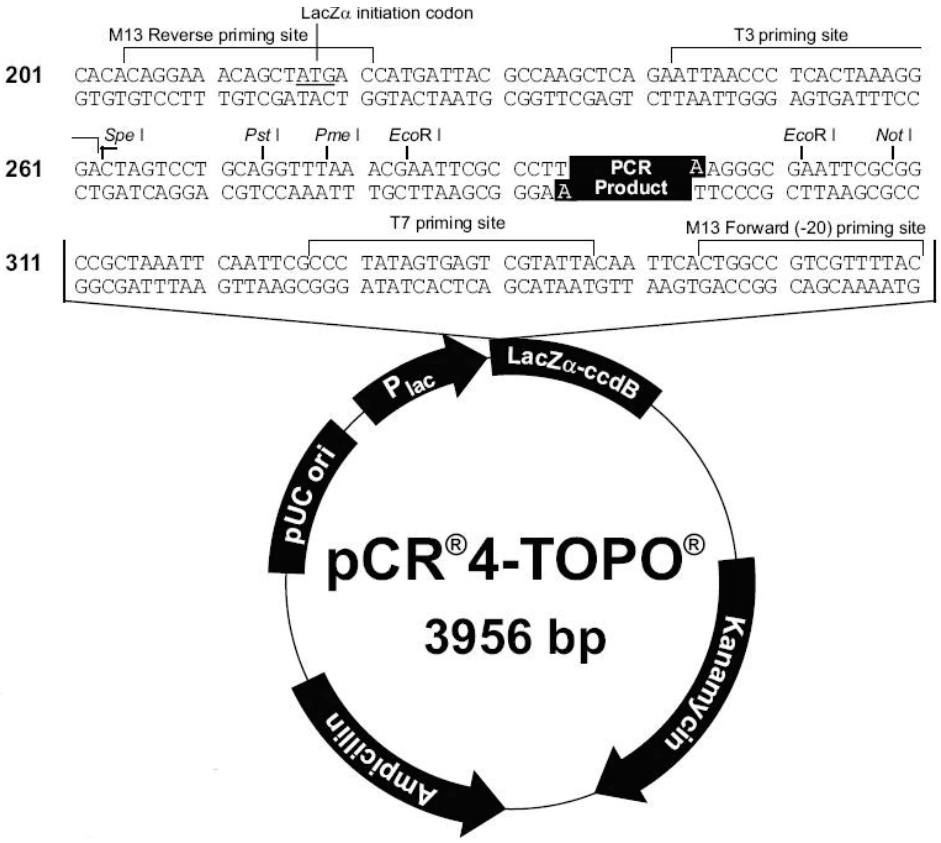

Figure 7.5 pYR33 vector

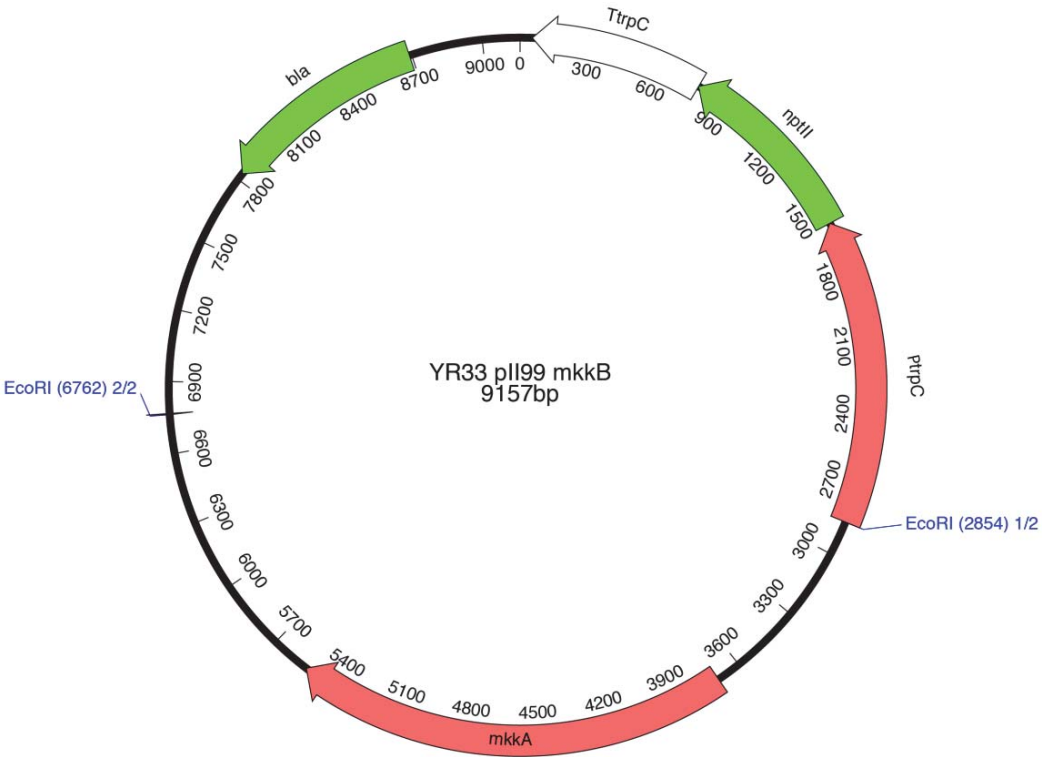

Figure 7.6 pPN94 vector

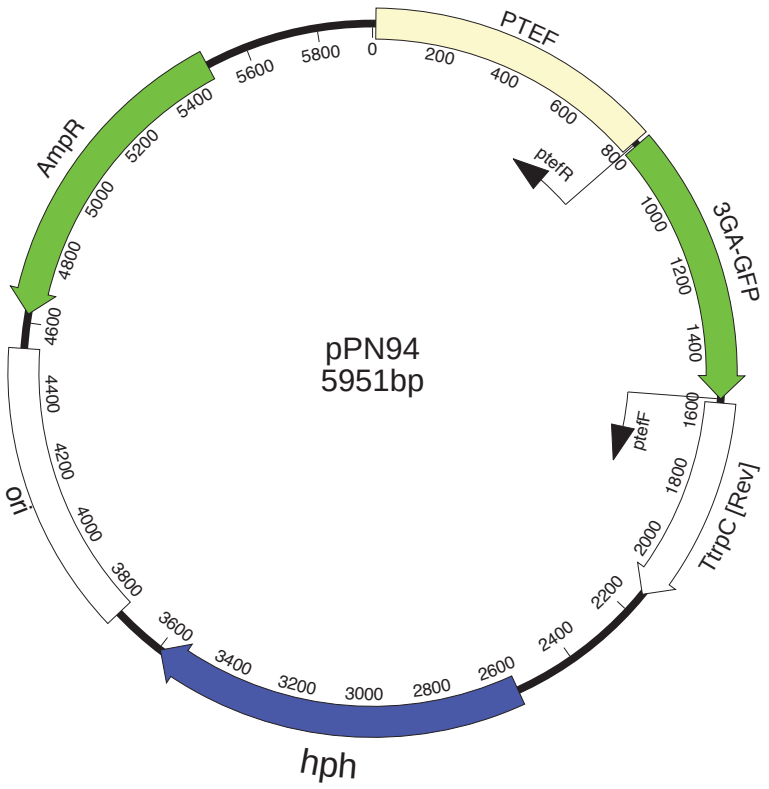

Figure 7.7 pCE81

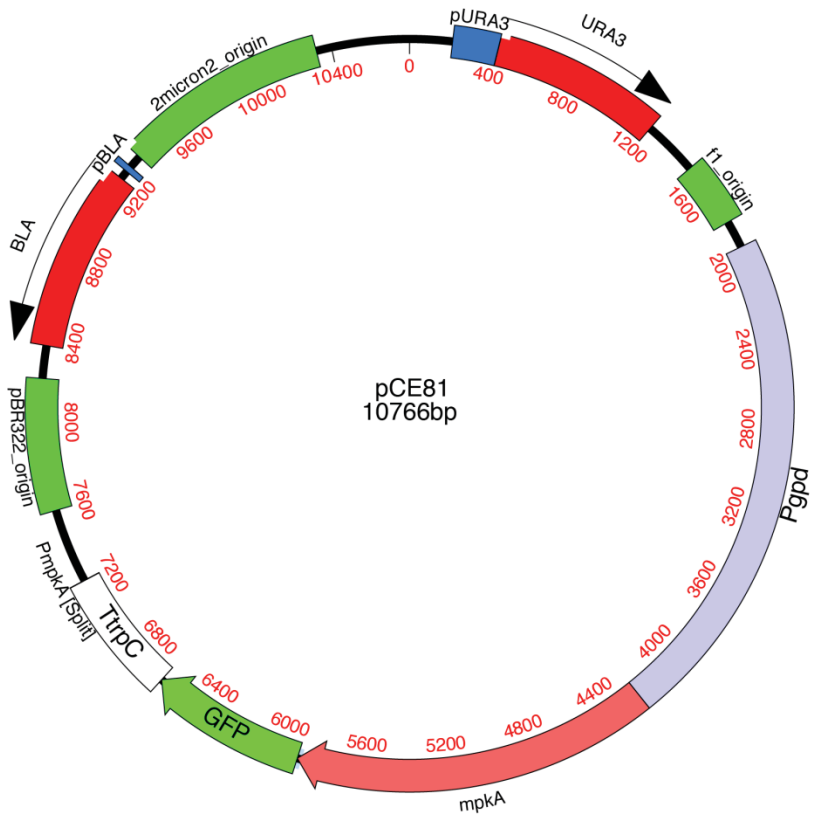

Figure 7.8 pMpkB-eGFP

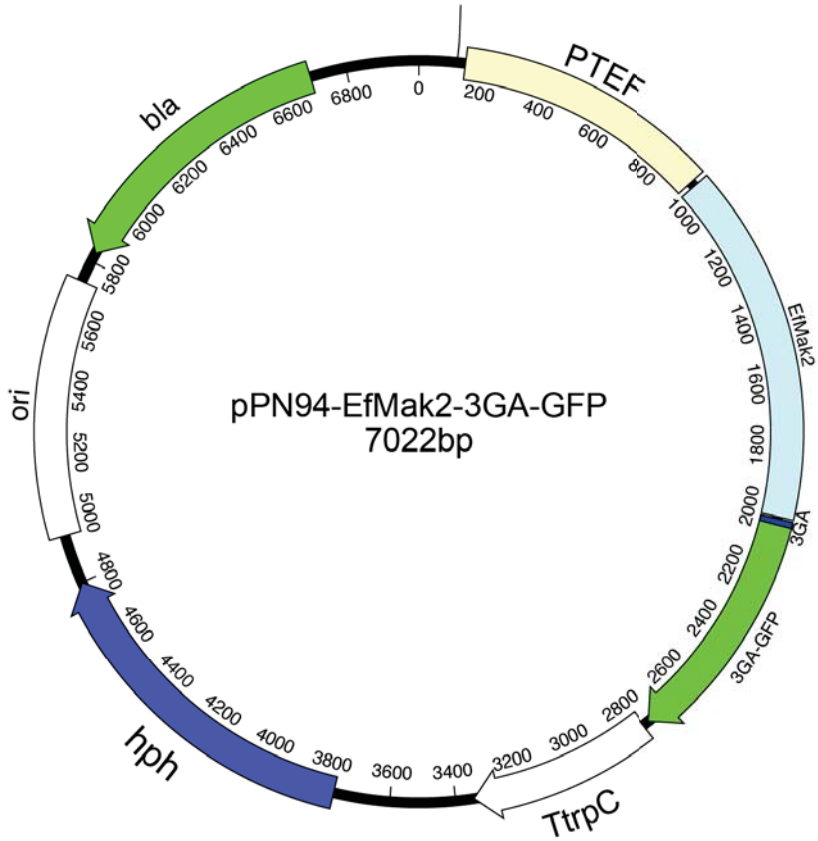

Figure 7.9 pKG1 containing the *E. festucae symB* deletion construct

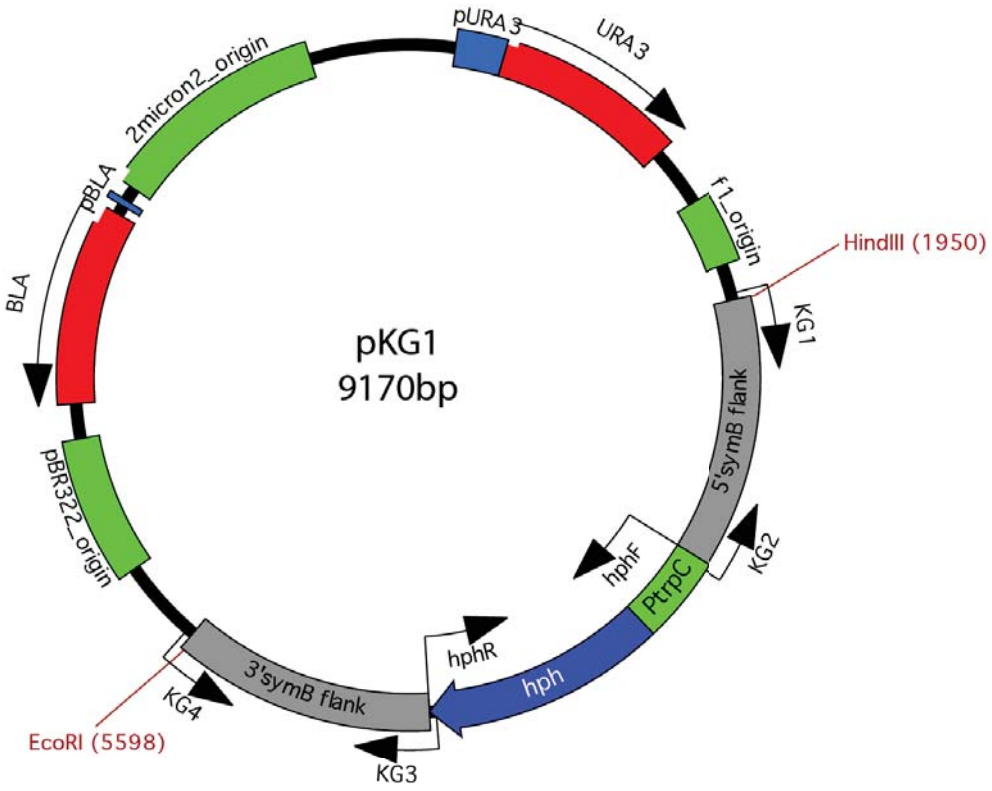

Figure 7.10 pKG2 containing the *E. festucae symC* deletion construct

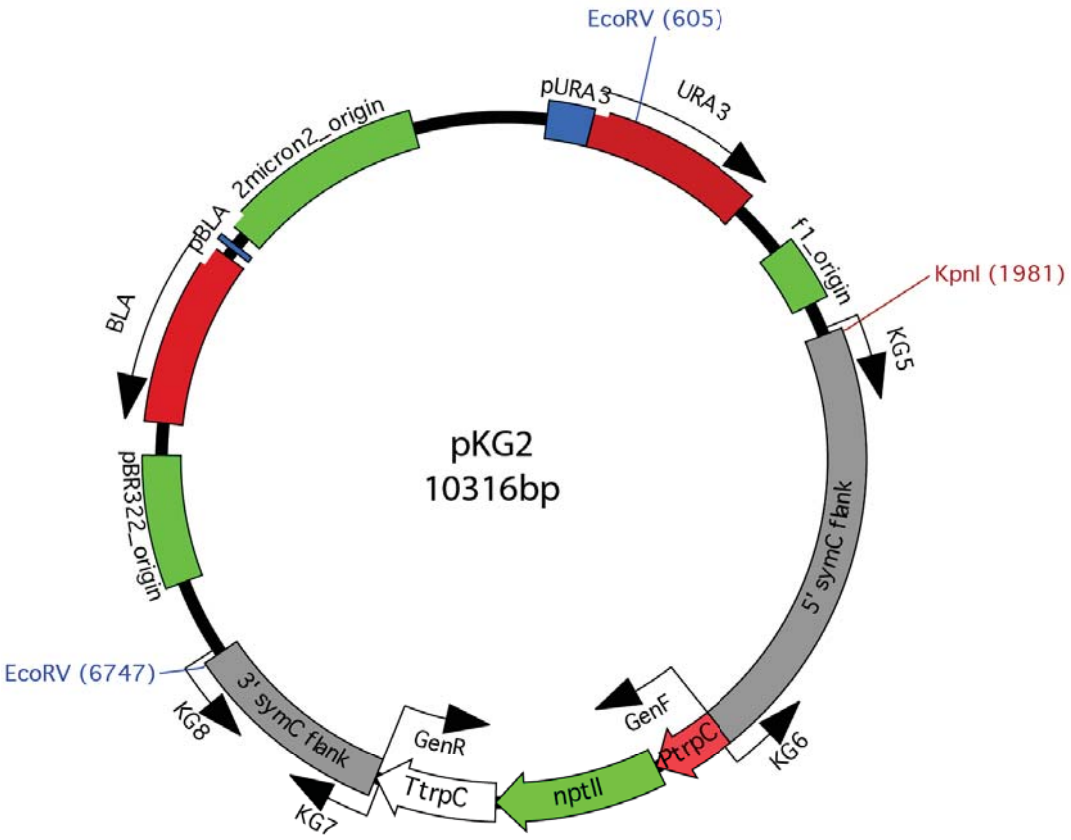

Figure 7.11 pKG4 containing the *E. festucae mobC* deletion construct

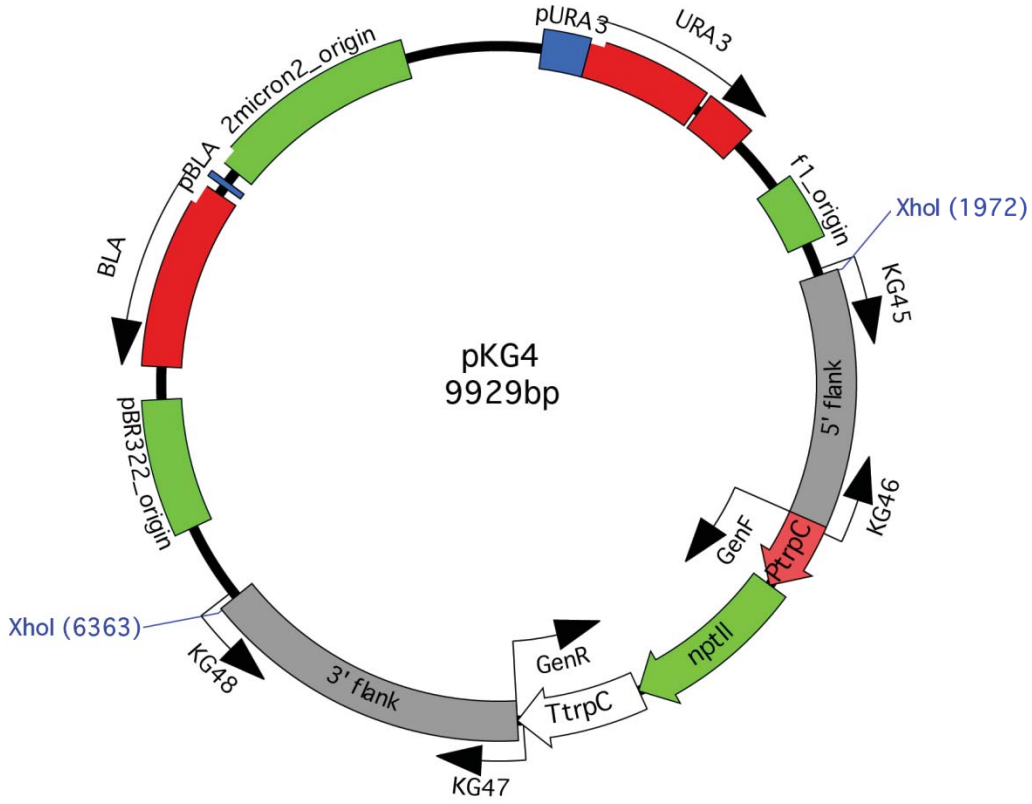

Figure 7.12 pKG5 containing the first *E. festucae symB* complementation construct

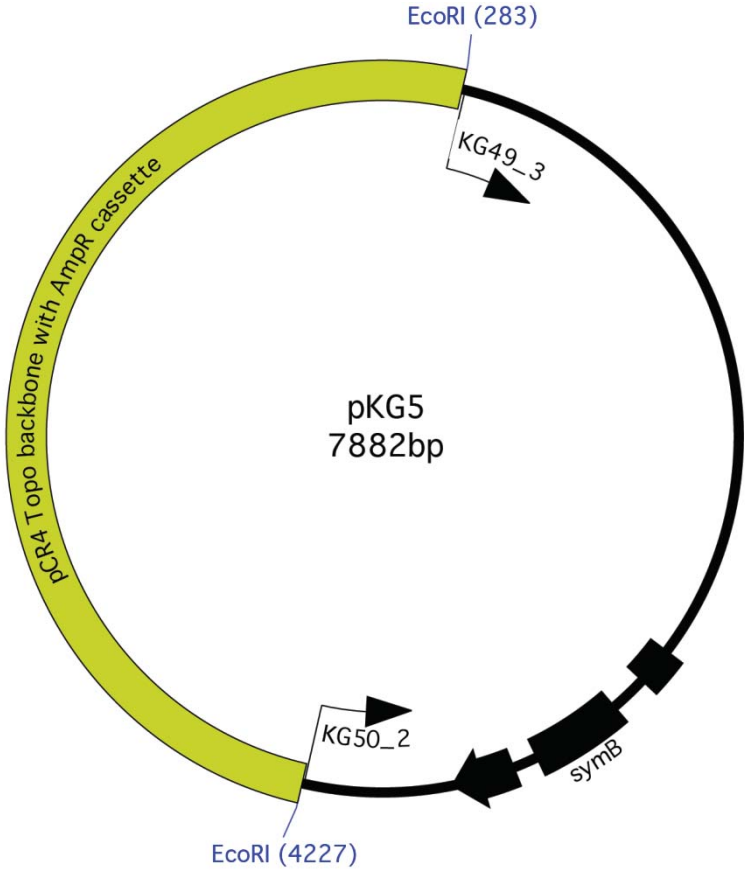

Figure 7.13 pKG6 containing the *E. festucae symC* complementation construct

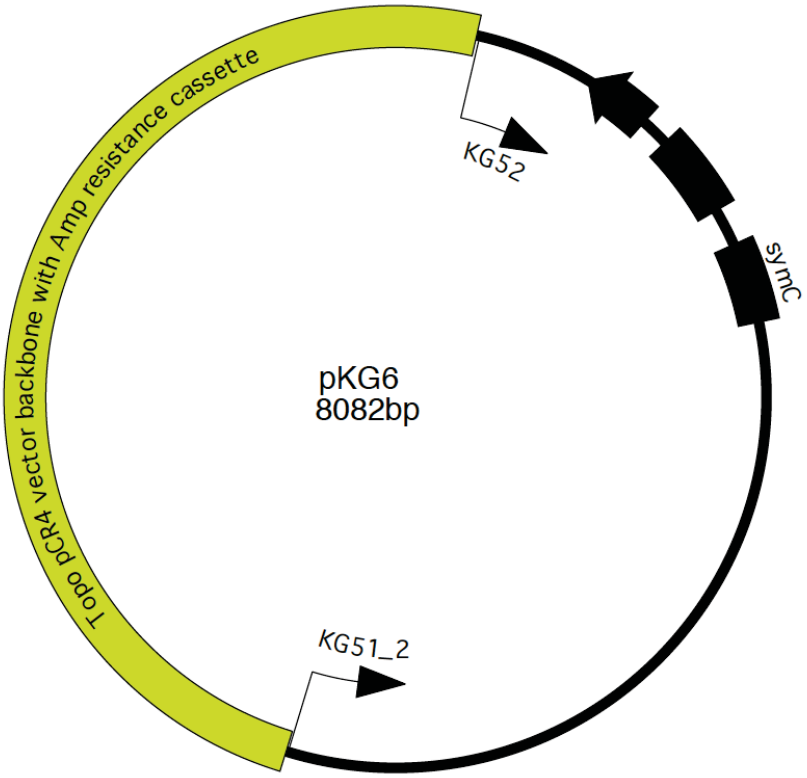

Figure 7.14 pKG7 containing the final *E. festucae symB* complementation construct

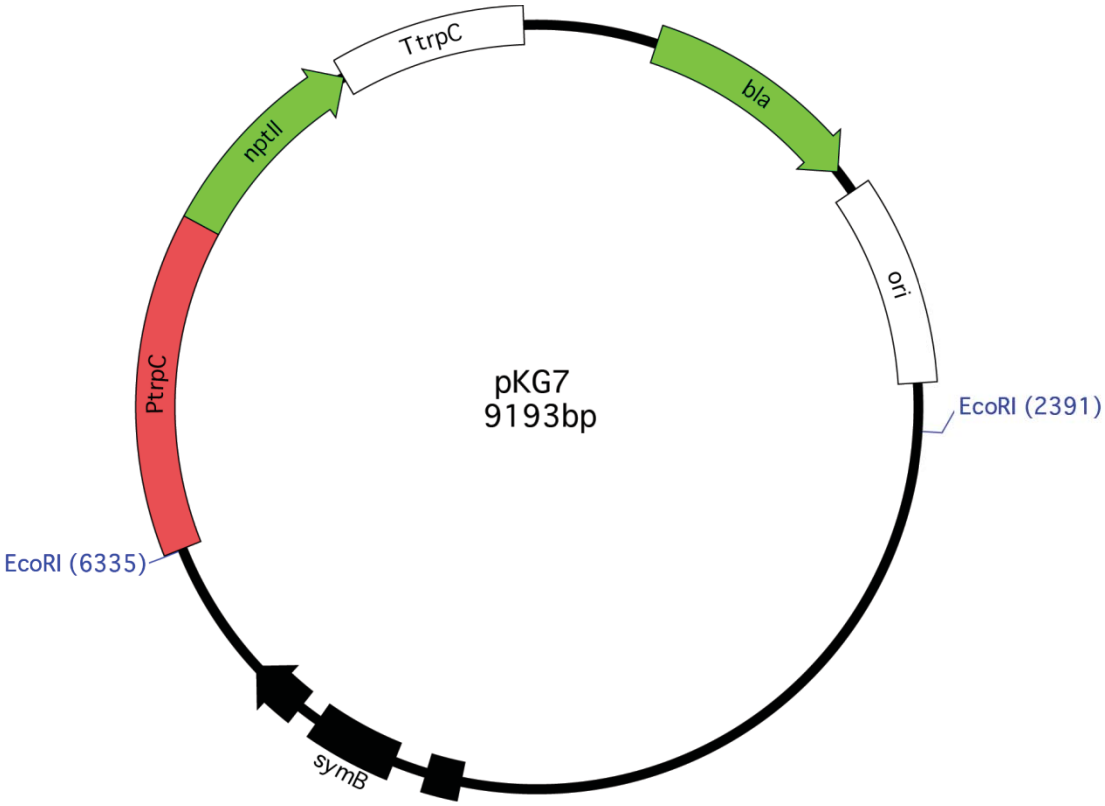

Figure 7.15 pKG8 containing the *E. festucae mobC* complementation construct

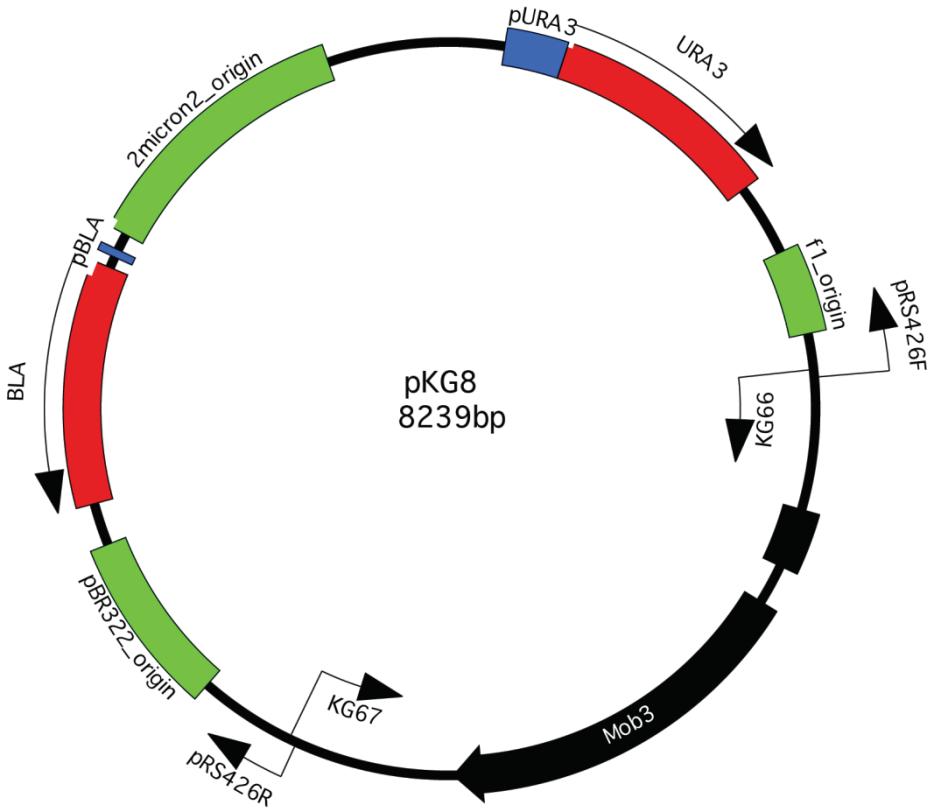

Figure 7.16 pKG9 containing the *E. festucae* half SymC C-terminal deletion construct

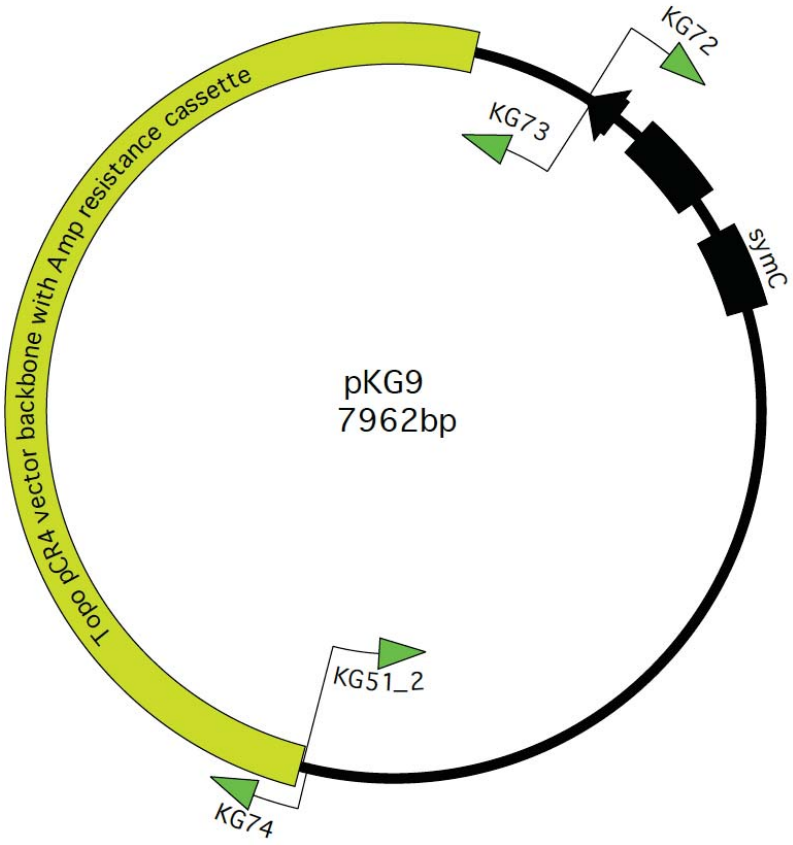

Figure 7.17 pKG10 containing the *E. festucae* full SymC C-terminal deletion construct

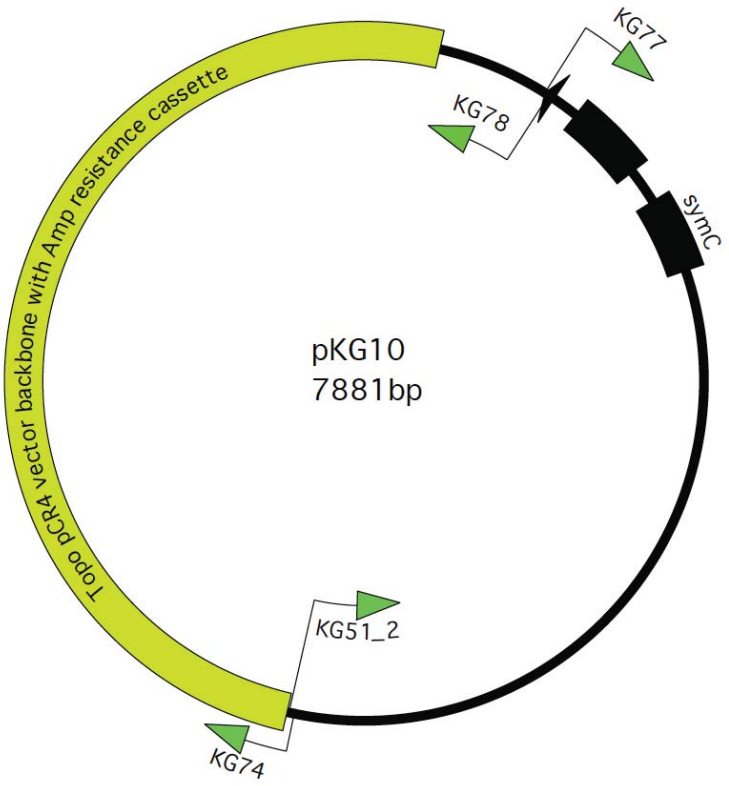

Figure 7.18 pKG11 containing the *E. festucae* truncated SymC C-terminal deletion construct

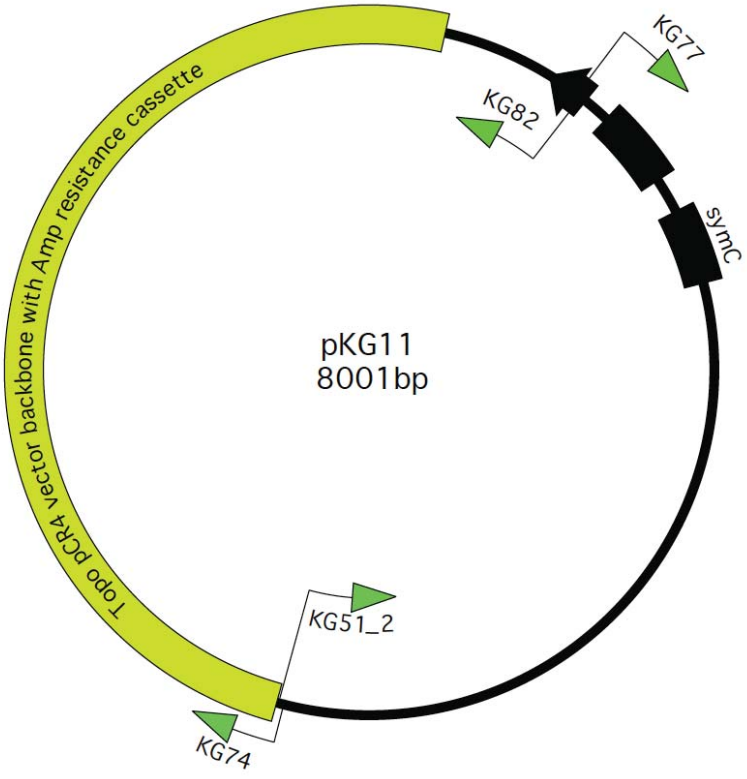

Figure 7.19 pKG12 containing the native *E. festucae symC::3GA::mRFP* construct

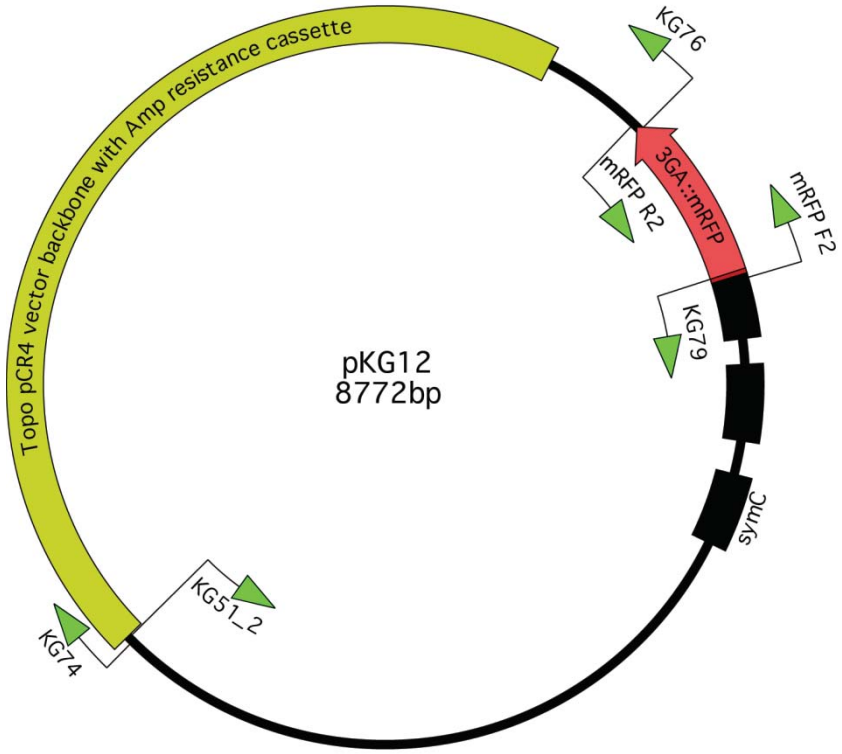

Figure 7.20 pKG13 containing the native *E. festucae symB::3GA::GFP* construct

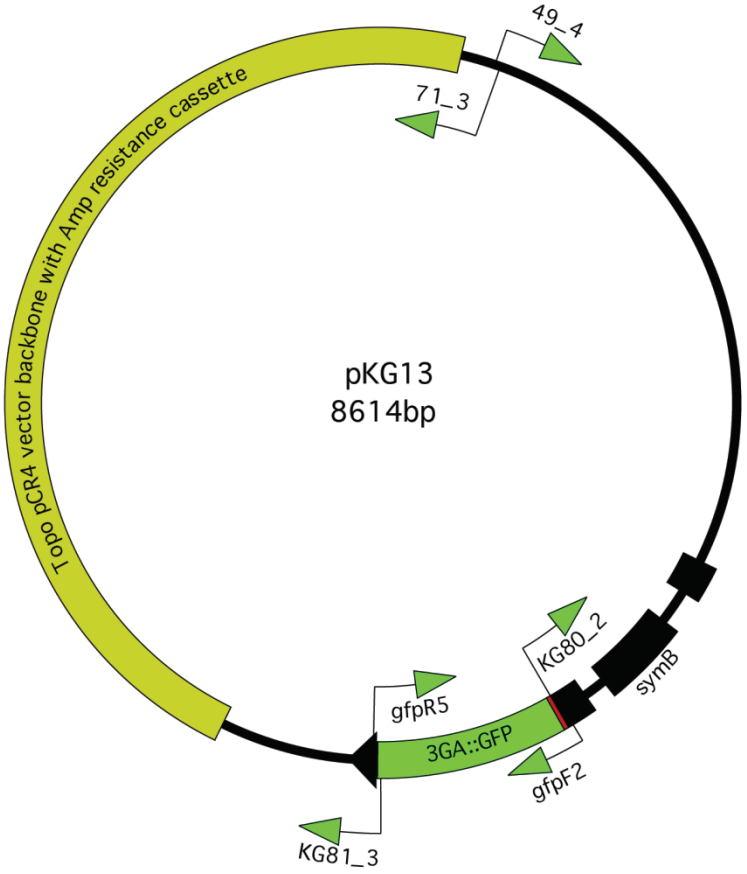

Figure 7.21 pKG14, pGBKT7 Yeast-2-hybrid vector fused to *NCU00939* C-terminus

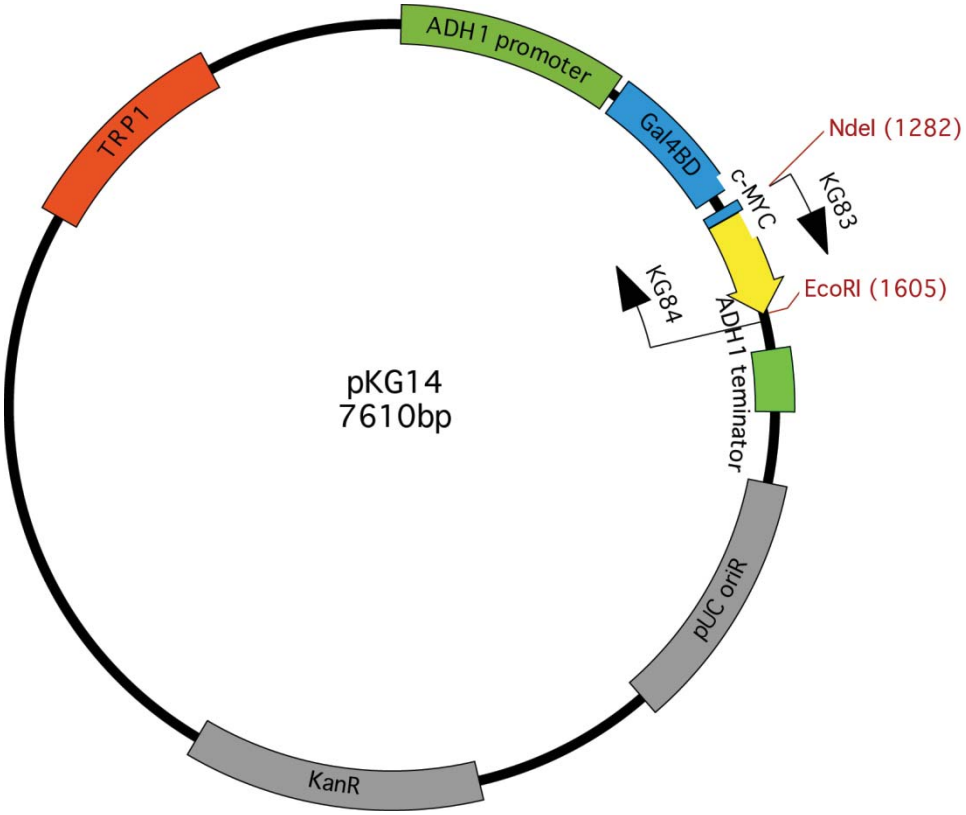

Figure 7.22 pKG19 containing the *E. festucae* truncated SymC C-terminal deletion construct fused to mRFP

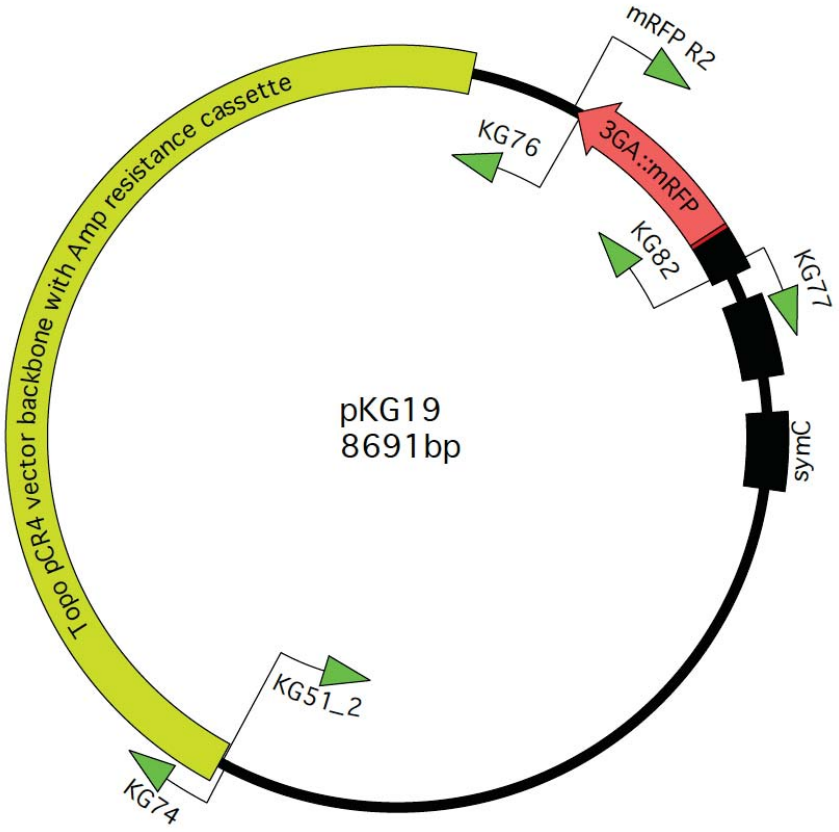

Figure 7.23 pKG20 containing the over expression *E. festucae symB::3GA::GFP* construct

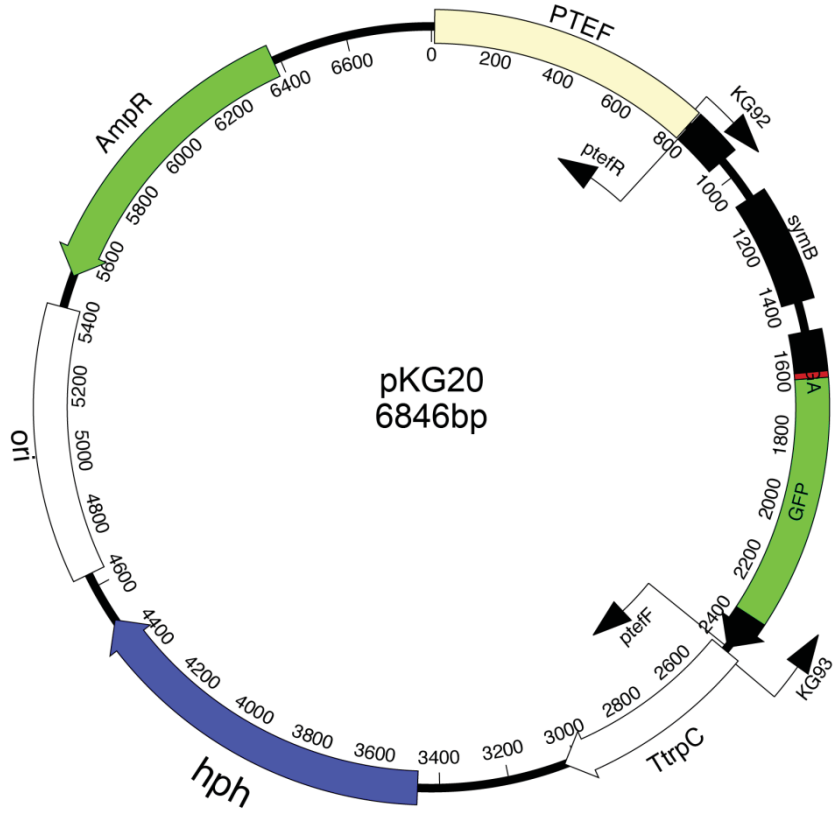

Figure 7.24 pKG21 containing the over expression *E. festucae symC::3GA::mRFP* construct

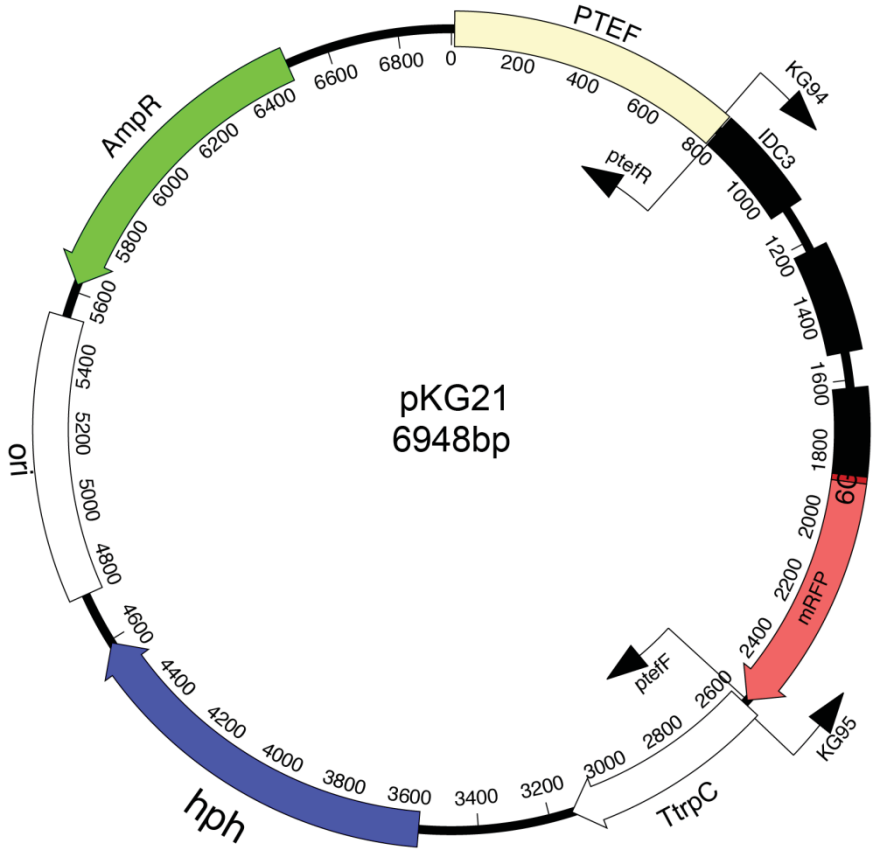

Figure 7.25 pKG23 containing the *E. festucae* full length SymC C-terminal deletion construct fused to mRFP

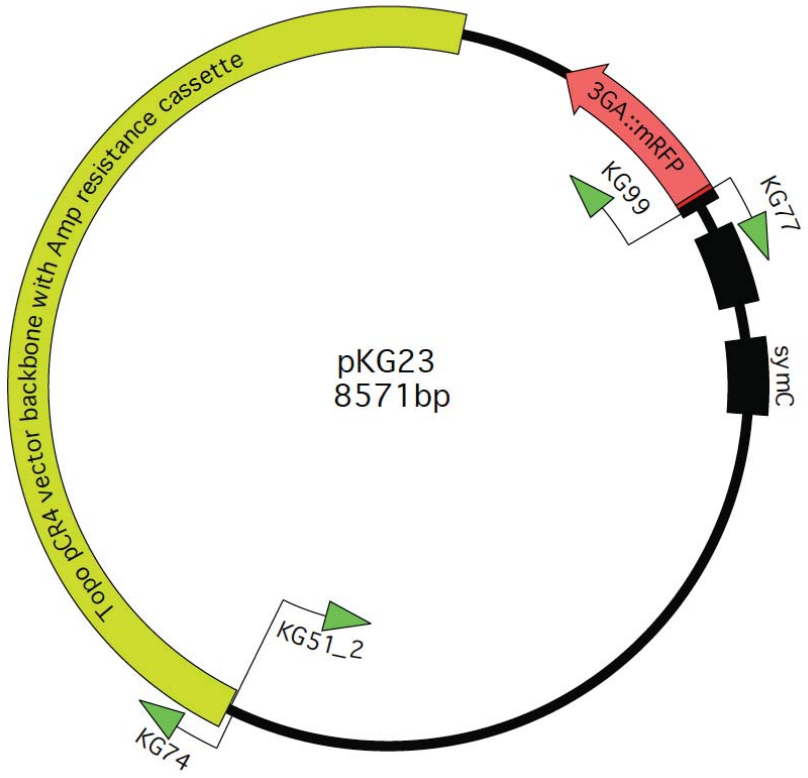

Figure 7.26 pGADT7 Yeast-2-hybrid vector

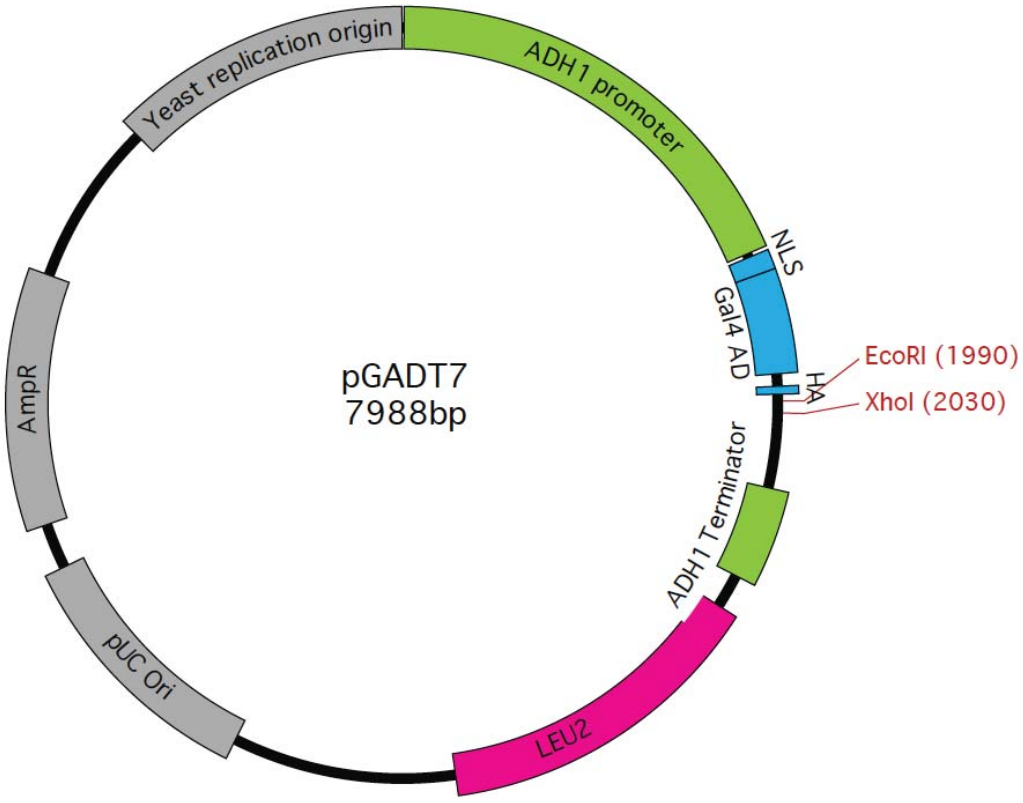

Figure 7.27 pGBKT7 Yeast-2-hybrid vector

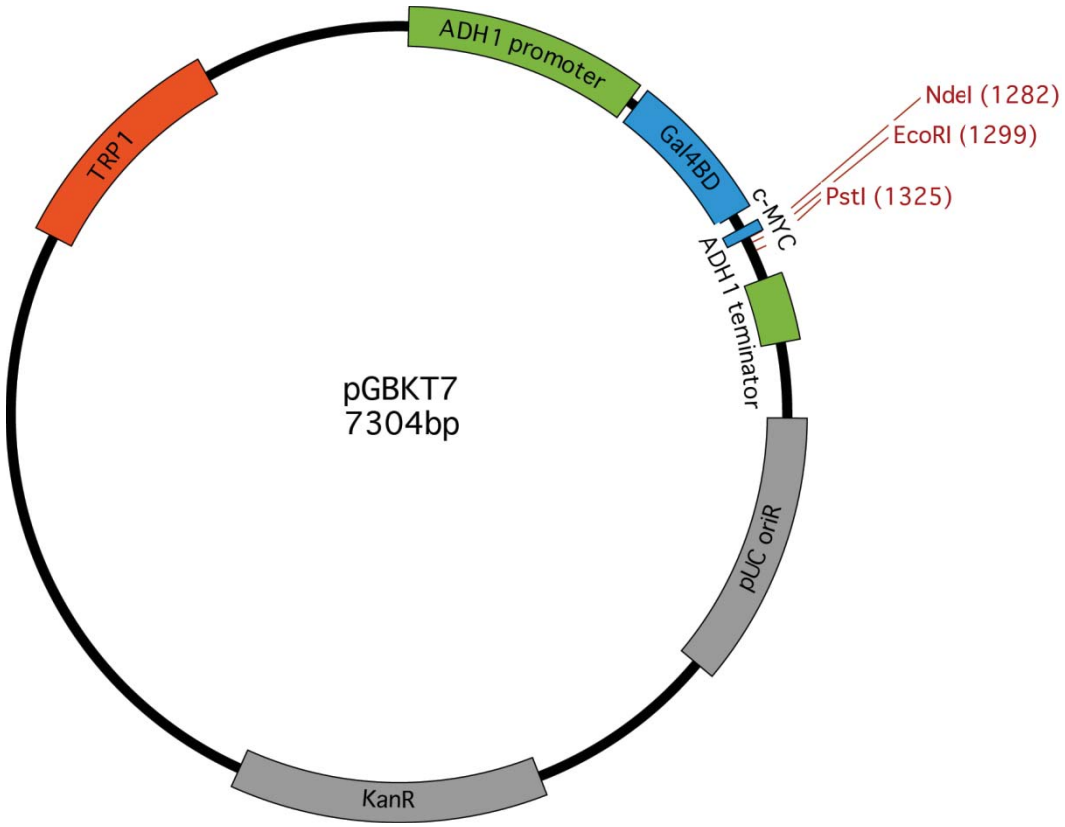

Figure 7.28 pKG24, pGBKT7 Yeast-2-hybrid vector fused to SymC C-terminus

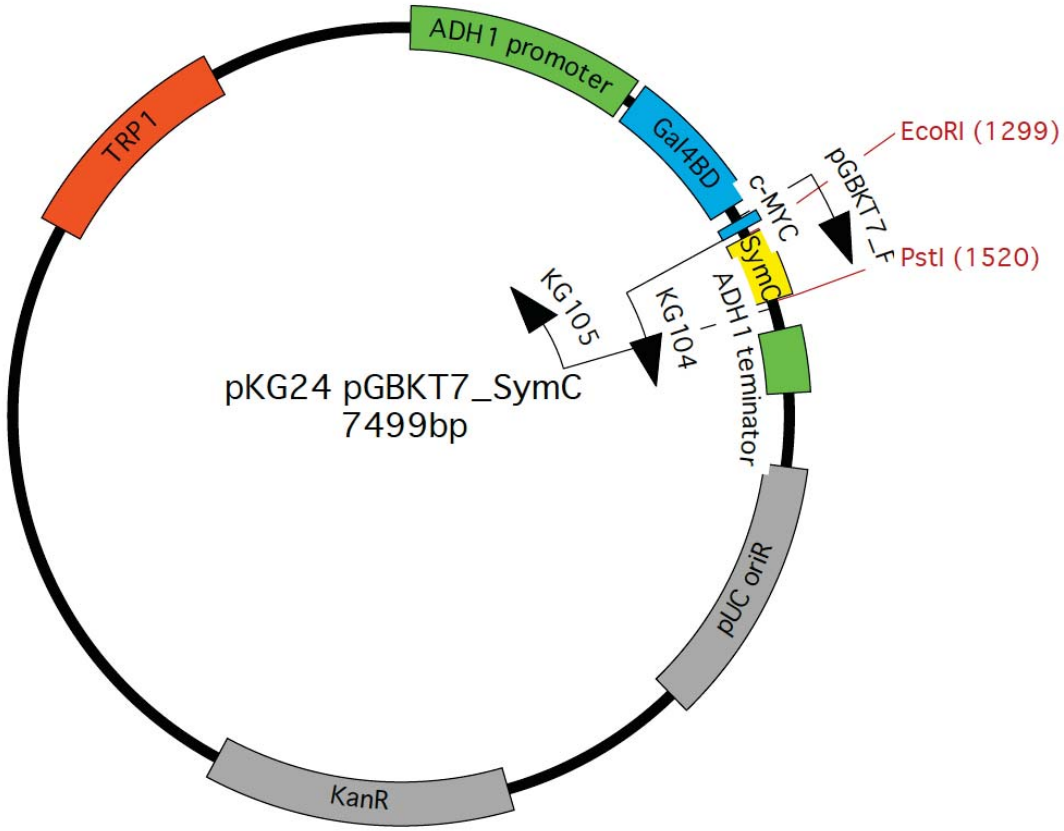

Figure 7.29 pKG25, pGADT7 Yeast-2-hybrid vector fused to *E. festucae* GpiA

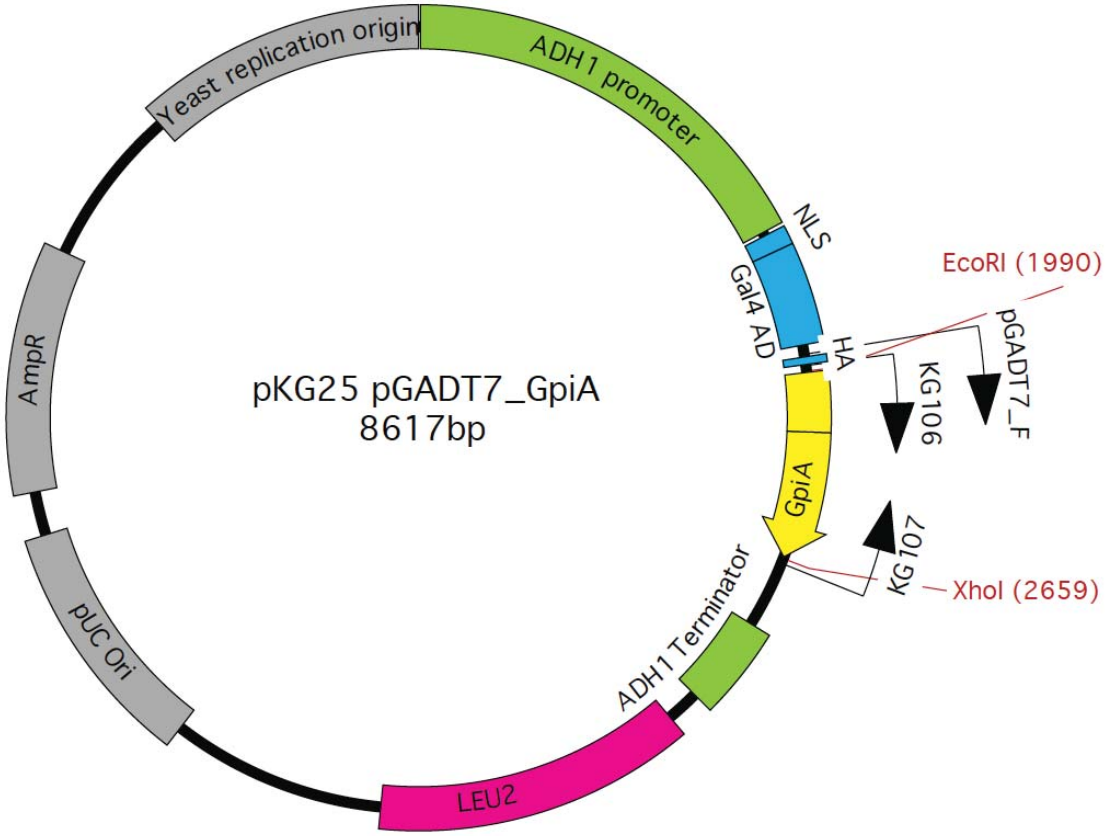

Figure 7.30 pKG26, pGADT7 Yeast-2-hybrid vector fused to *E. festucae* Arp3

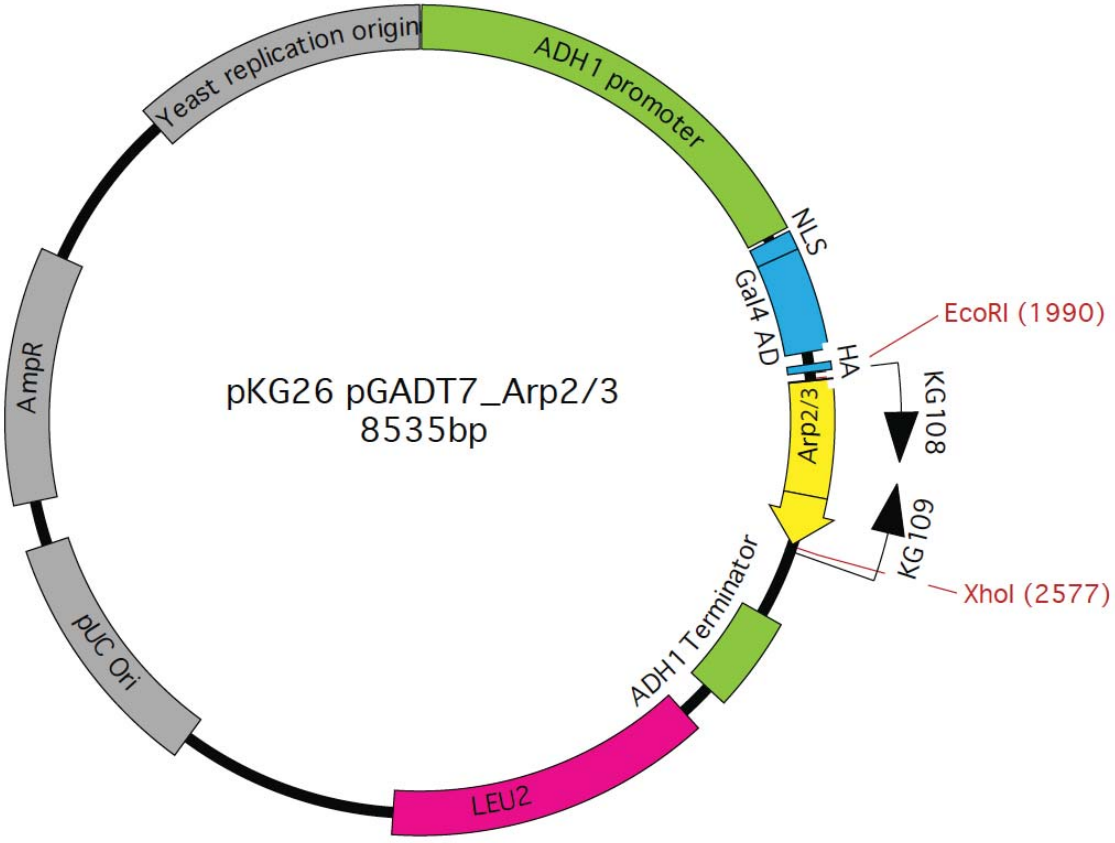

Figure 7.31 pKG27, pGADT7 Yeast-2-hybrid vector fused to *E. festucae* UthA

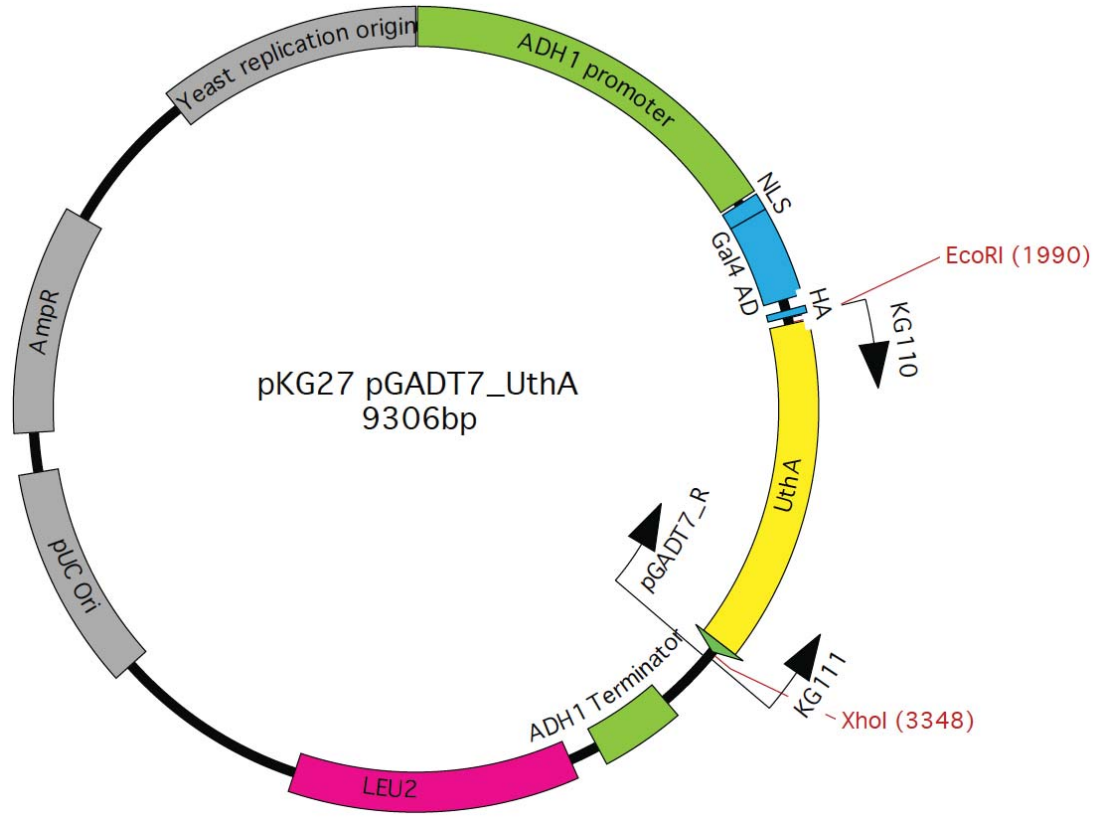

Figure 7.32 pKG28, pGADT7 Yeast-2-hybrid vector fused to *E. festucae* ErgM

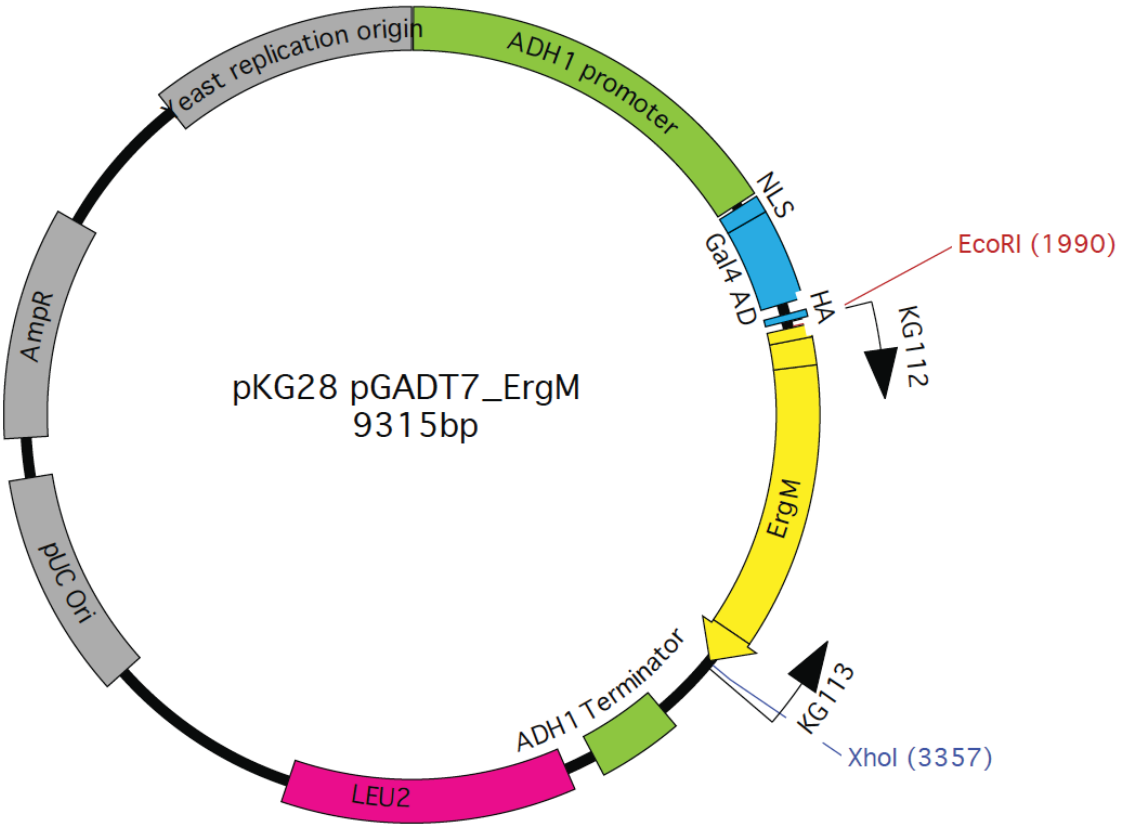

Figure 7.33 pGADT7-Rho1 DA, pGADT7 Yeast-2-hybrid vector fused to *N. crassa* Rho1

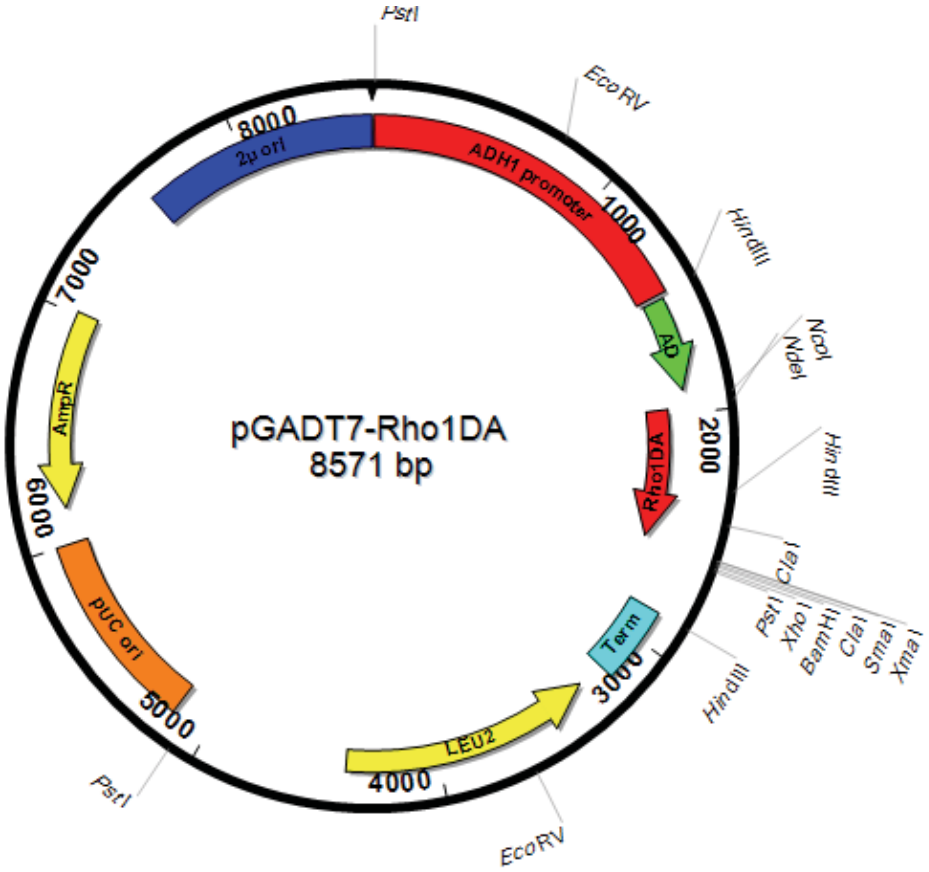

Figure 7.34 pGADT7-Rho1 DN, pGADT7 Yeast-2-hybrid vector fused to *N. crassa* RHO1

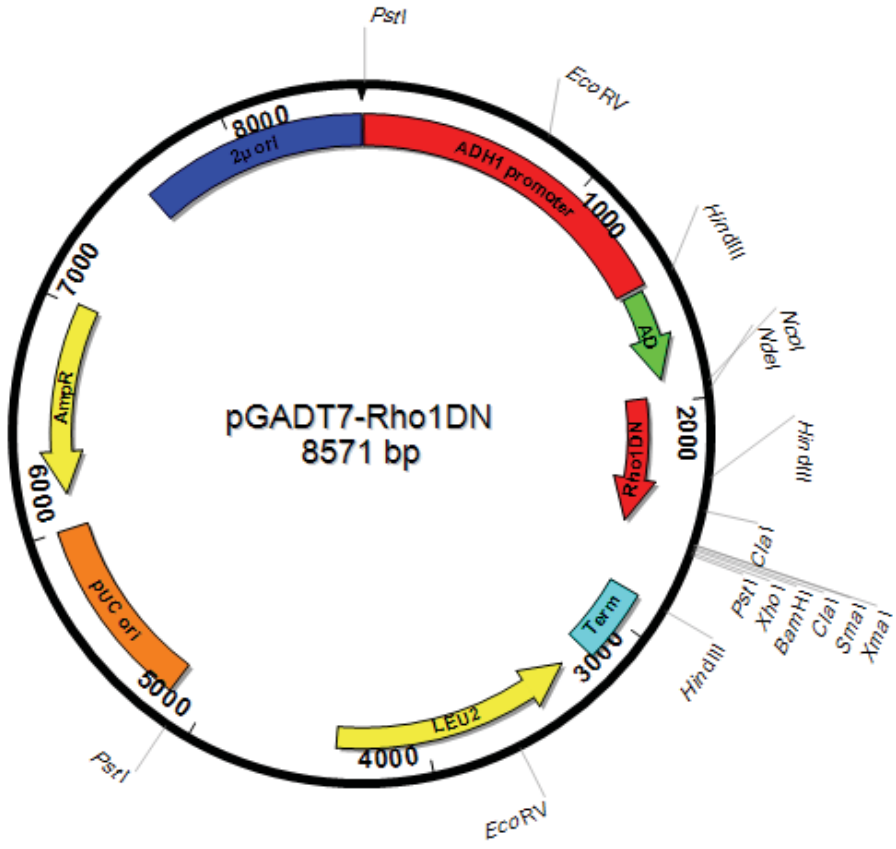

Figure 7.35 pGADT7-PKC1, pGADT7 Yeast-2-hybrid vector fused to *N. crassa* PCK1

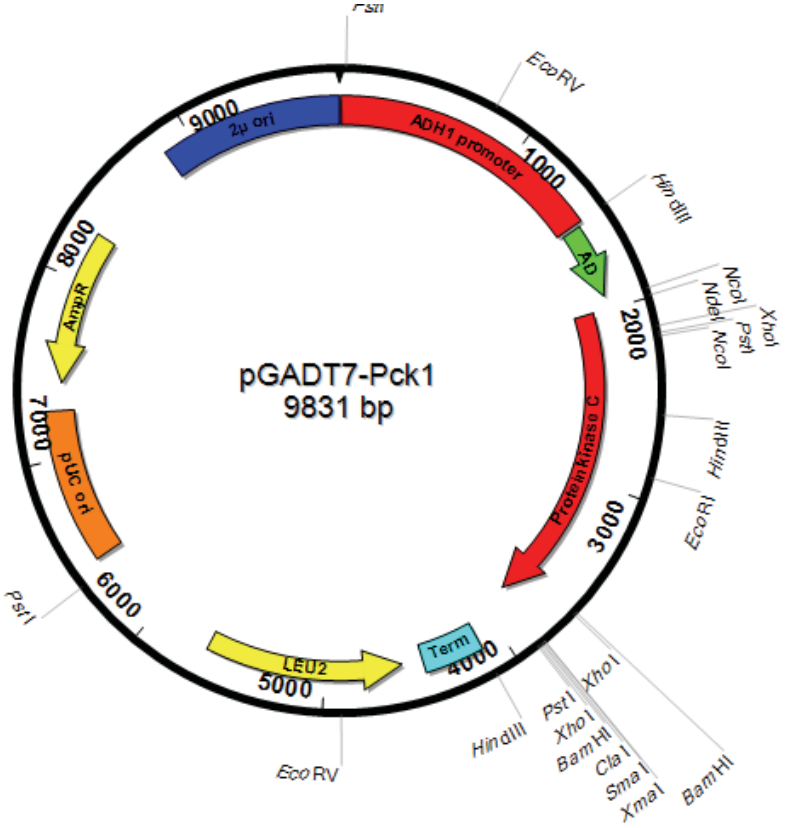

Figure 7.36 pGADT7-Mik1 13kb N-term, pGADT7 Yeast-2-hybrid vector fused to *N. crassa* MIK1

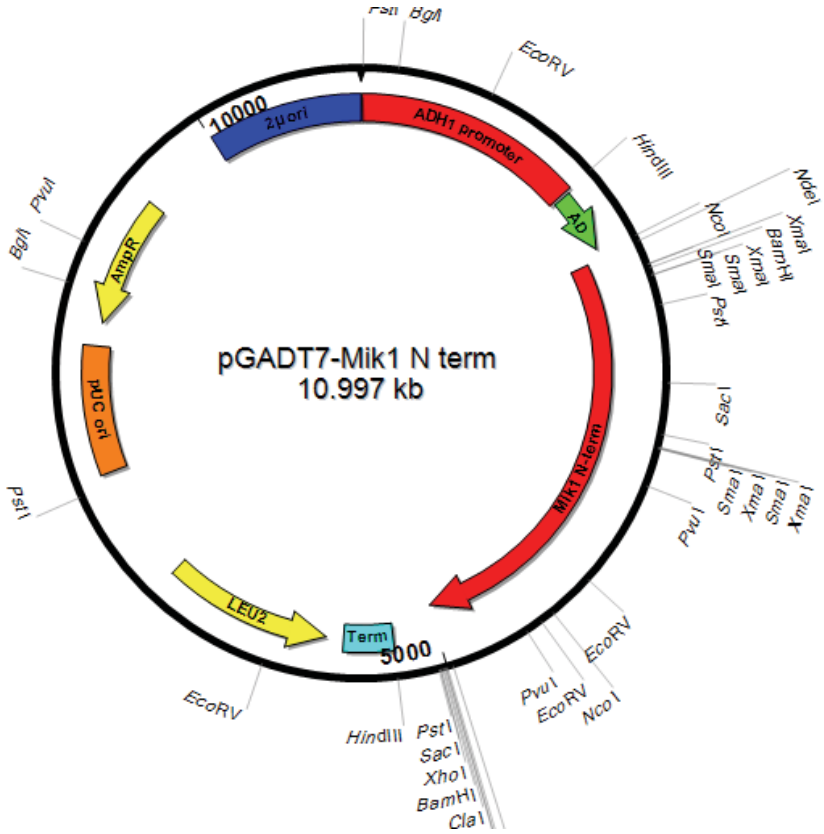

Figure 7.37 pGADT7-Mik1 13kb C-term, pGADT7 Yeast-2-hybrid vector fused to *N. crassa* MIK1

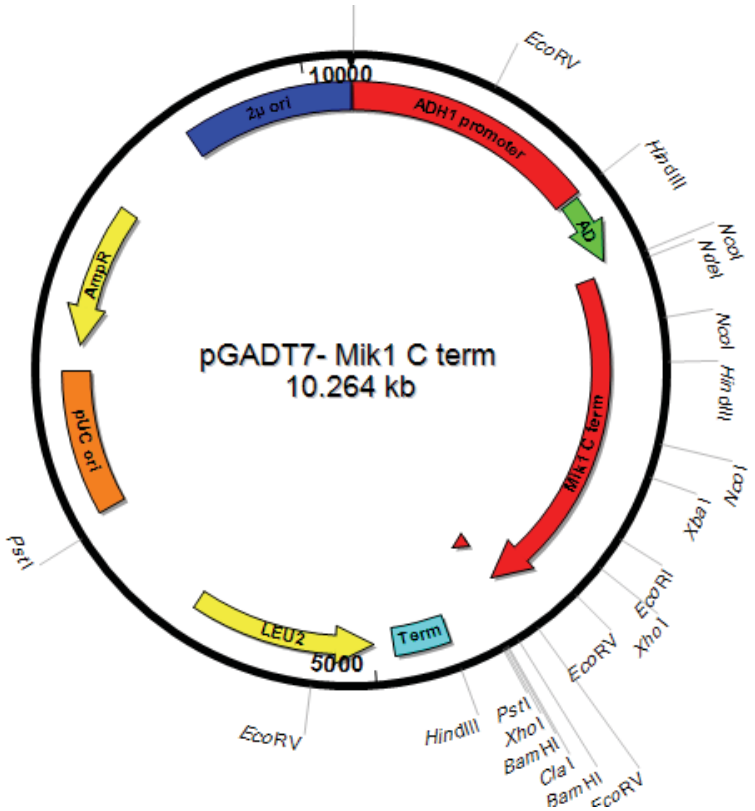

Figure 7.38 pGADT7-MEK-1, pGADT7 Yeast-2-hybrid vector fused to *N. crassa* MEK-1

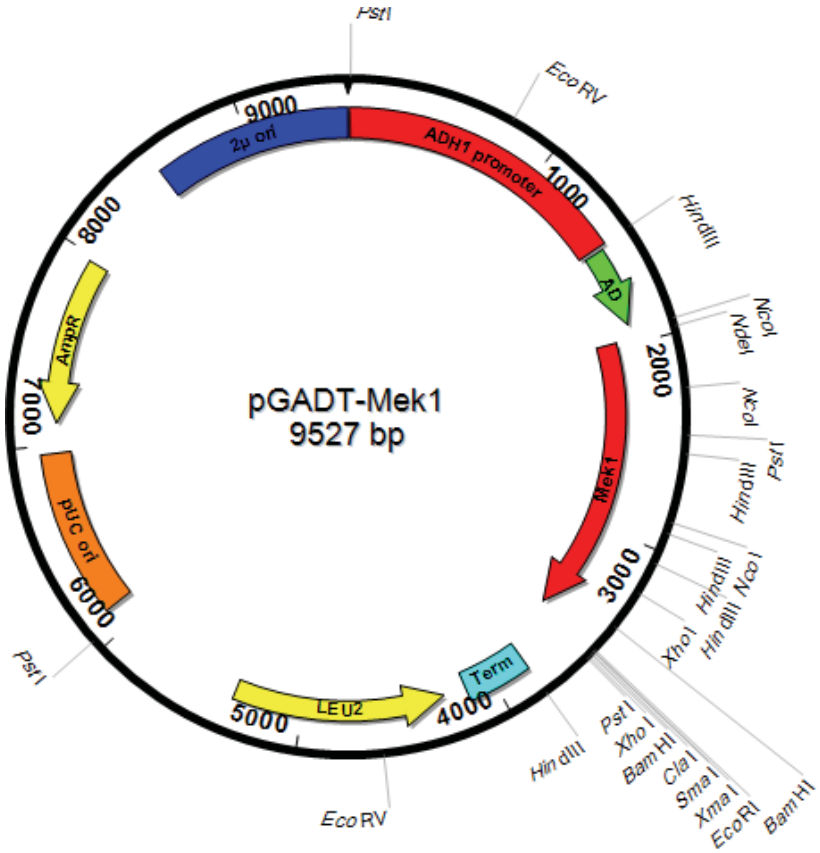

Figure 7.39 pGADT7- MEK-1 N-term, pGADT7 Yeast-2-hybrid vector fused to *N. crassa* MEK-1

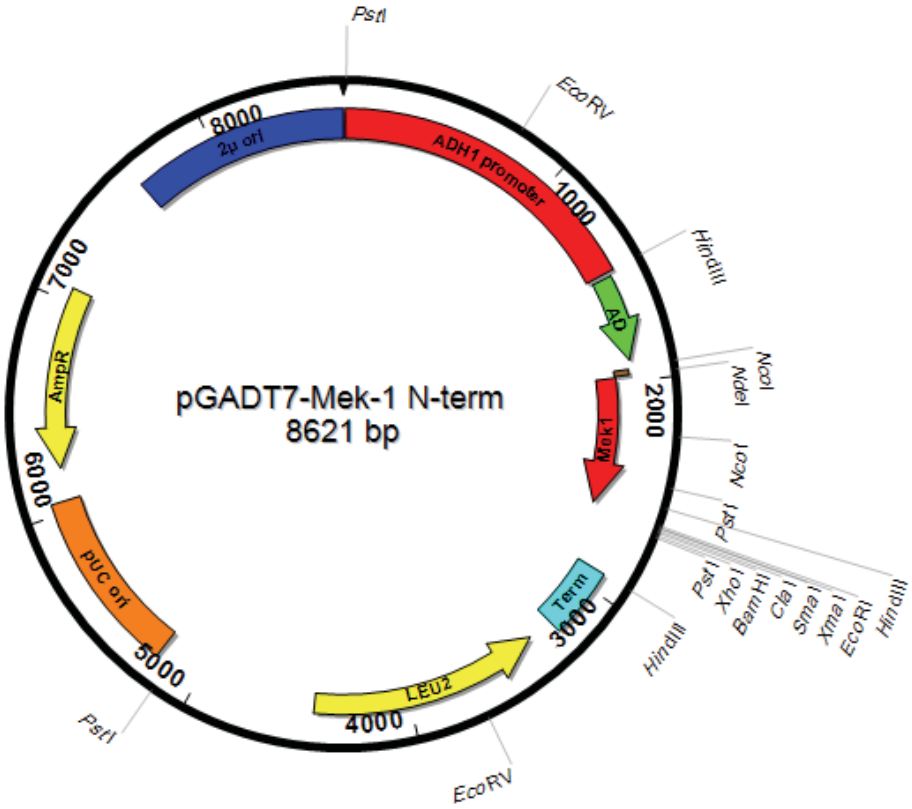

Figure 7.40 pGADT7- MEK-1 C-term, pGADT7 Yeast-2-hybrid vector fused to *N. crassa* MEK-1

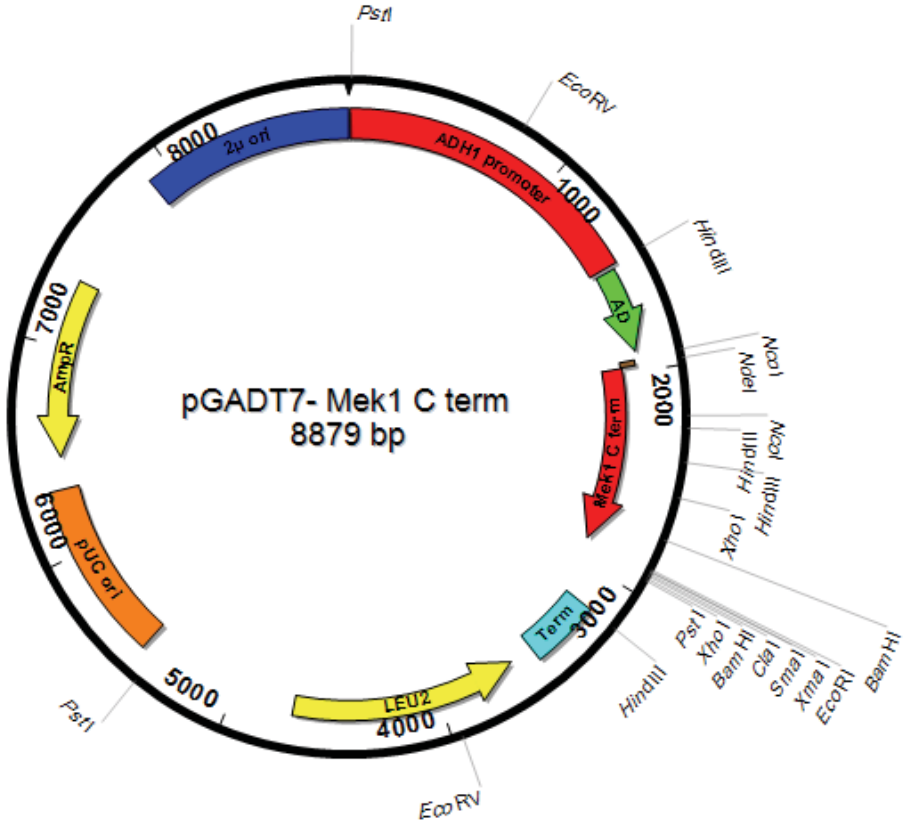

Figure 7.41 pGADT7-MAK-1, pGADT7 Yeast-2-hybrid vector fused to *N. crassa* MAK-1

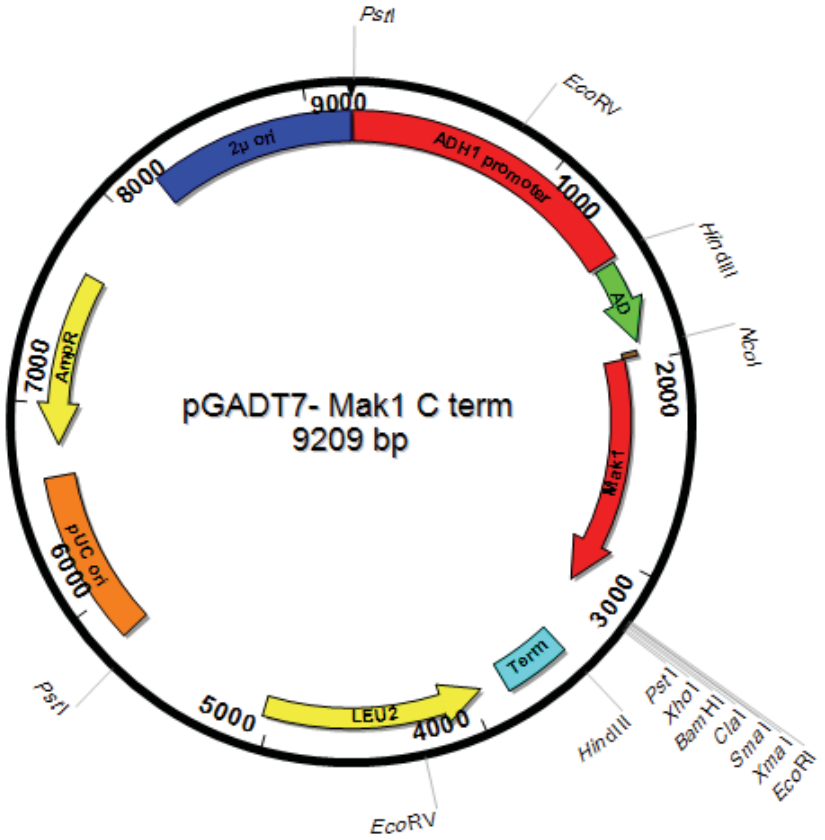

Figure 7.42 pGADT7-BEM-1, pGADT7 Yeast-2-hybrid vector fused to *N. crassa* BEM-1

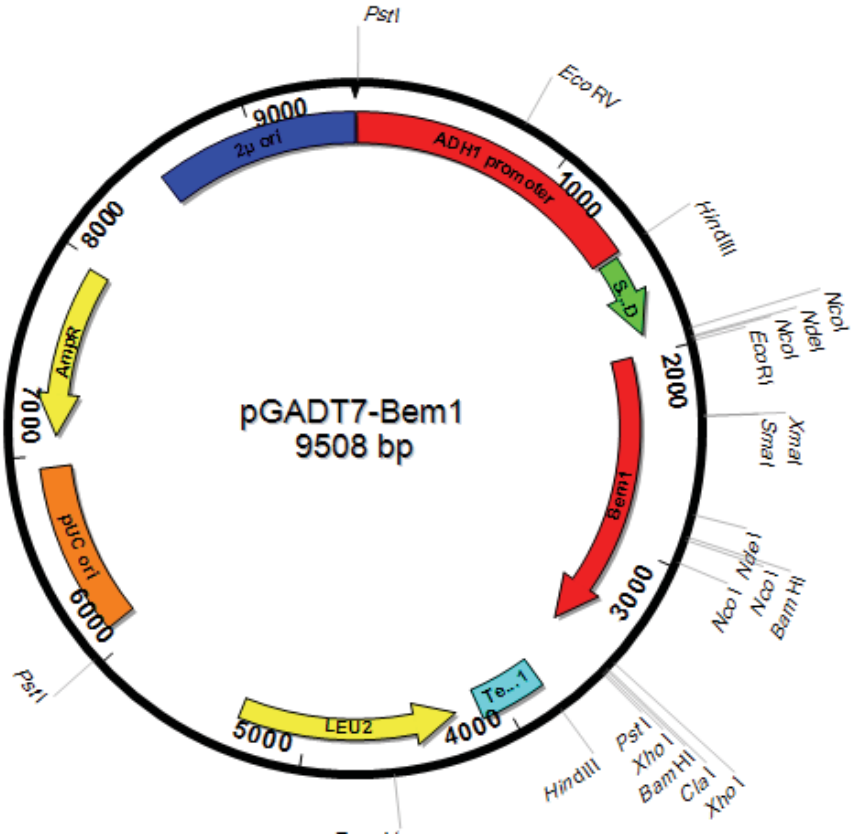

Figure 7.43 pGADT7-NOR-1, pGADT7 Yeast-2-hybrid vector fused to *N. crassa* NOR-1